Nikolay V. Baranovskiy
Geniy V. Kuznetsov

FOREST FIRE OCCURRENCES AND ECOLOGICAL IMPACT PREDICTION

MINISTRY OF EDUCATION AND SCIENCE OF THE RUSSIAN FEDERATION
TOMSK POLYTECHNIC UNIVERSITY

NIKOLAY V. BARANOVSKIY, GENIY V. KUZNETSOV

FOREST FIRE OCCURRENCES AND ECOLOGICAL IMPACT PREDICTION

Monograph

NOVOSIBIRSK
PUBLISHING HOUSE OF THE SIBERIAN BRANCH
OF THE RUSSIAN ACADEMY OF SCIENCES
2017

DOI 10.15372/FOREST2017BNV

Baranovskiy N.V. Forest fire occurrences and ecological impact prediction: monograph / N.V. Baranovskiy, G.V. Kuznetsov ; Ministry of education and science of the Russian Federation Tomsk polytechnic university. – Novosibirsk : Publishing House of the SB RAS, 2017. – 259 p.

The monograph presents the main results, obtained by domestic and foreign researchers in the area of forest fire occurrence and their environmental effects prediction. Data on the main processes and factors, influencing the forest fire occurrence, are given. Processes of forest fuel drying and inflammation are considered. Special attention is given to such important forest fire danger factors as weather conditions, anthropogenic load and thunderstorm activity. Foreign and domestic methods of forest fire danger prediction are described. Issues of pollutants emission and transfer, forest fires effects on biogeocenosis and population health are considered. Subjects of numerical weather forecast, high performance computing on supercomputers, geoinformation systems development are analyzed. Development prospects of approaches and technologies of forest fire danger prediction are discussed. The monograph is meant for experts in the area of forest fire protection, researchers, postgraduate students and senior students.

Reviewers:
Dr. Phys.-Mat. Sci, Professor Yu. N. Grigoryev
Dr.Eng., Professor A. S. Zavorin
Dr. Phys.-Mat. Sci, V. K. Smolyakov
Dr. Phys.-Mat. Sci, Professor, Honored Scientist of the RF
V. I. Terekhov

Approved for publication
By Academic Council of Tomsk Polytechnic University

This book was published with support in part of Russian Foundation for Basic Researches and administration of Tomsk region, project № 16-41-700831.

ISBN 978-5-7692-1538-4

CONTENTS

INTRODUCTION

Forest fires play an important role in forming and maintaining forest biogeocenoses [1]. Both positive and negative impact of fires on forests is known [2—4]. An ability to foresee the occurrence of forest fire spots is very important. Surface fires prediction is of the highest importance because more than 80% of all vegetation fires are surface fires [5]. Almost all crown fires develop from surface fires [5].

Climate warming leads to increase in forest fire danger among other matters. The prediction results for the year of 2030 [6—8], using global climate models and neurocalculator have shown that, for instance, the zonal identity of many Siberian weather stations is subject to change [9]. Climate changes are accompanied by extreme deviations in seasonal weather fluctuations, which may become the reason for large scale forest fires [10—12]. On the territory of Russia, the most important changes happen in the West Siberian region [13] that cannot but influence the increase in forest fire danger here in the future.

At present, a problem of most rational use of the funds donated for forest fire protection steps out. This implies creating new methods of predicting forest fires occurrence that must be based on mathematical models adequate to the real processes and corresponding to methodology and information support and computer software.

A group of forest fire danger prediction methods is widely known and practically applied. The Canadian [14], American [15, 16], several South European [17, 18] methods should be mentioned; among them stands a Russian development – the Nesterov's index [19]. The majority of approaches use meteorological data that characterize forest fire danger only in accordance with weather conditions. However, forest fire danger also depends on other factors (anthropogenic impact [20], thunderstorm activity [21], etc.).

The analysis of forest fire statistics in forestries has shown that the greater part of forest fires in suburban forestries occur due to people’s careless handling of fire. Moreover, the number of daily forest fire cases may even vary inside one forestry several times within a week [22].

Prediction modeling of forest fire danger may also be performed according to the forest site [23]. The research in this field by the members of the V. N. Sukachev Institute of Forest, Siberian Branch of the Russian Academy of Sciences (SB RAS), Krasnoyarsk, must be mentioned: flammable vegetation maps development [23, 24], experimental research in forest fuels and flammable vegetation drying [25], as well as field studies [26].

It is impossible to carry out field studies in large areas. Space monitoring enables to evaluate forest fire danger in accordance with meteorological conditions [27] and at present cannot be used to determine the probability of forest fire occurrence in relation to an anthropogenic impact and thunderstorm activity. Space image processing enables only identifying forest fire spots [28].

The spatial resolution of forest fire danger prediction method is of high importance. An approach that has a spatial resolution on the level of a minimal forest

mensuration unit (stratum) has already been developed. This system allows getting results in the forest district-quadrant system [29]. In Russia there are 1807 forestries, 7851 forest districts [30], each forest district has ca. 100 quadrants that consists of up to several dozens of strata [31].

Furthermore, it must be mentioned that the more time the prediction leaves for specific actions, the more valuable it is. It is essential that the time of acquiring the prediction be considerably less than the period of disaster induction [20]. There arises a necessity to apply multiprocessor computation systems [32] and a mathematical apparatus for parallelizing computations [33].

The low spatial resolution of the weather station network complicates forecast acquisition [34].

Within the forest fire danger prediction concept [35] it is suggested to be guided by the interactive communication of computer software that carries out forest fire prediction with computational complexes of numerical weather forecasting [36]. For example, a global model of the atmosphere is of interest [37].

A range of mathematical models for drying of forest fuels layer has been developed by now [38—40]. Due to large computation load the forest fire danger prediction system may provide calculations in real-time mode or in a mode that outruns the real time of process development by means of using multiprocessor computation systems of high productivity. At present, a simplified mathematical statement of the problem on forest fuels layer drying enables working on personal computers in this mode [41].

Forest fires pollute the atmosphere with products of pyrolysis and combustion of forest fuels. The scale of contamination and emission rates of main pollutants from forest fire spots may be evaluated, for instance, with the method [42] approved and circulated by Russia's Ministry of Ecology in 1997. The original composition of substances emitted and the scenario of atmosphere pollution with products of pyrolysis and combustion of forest fuels are of high importance. Moreover, information on the distribution of pollutants in the surrounding area, especially in populated areas, is relevant for predicting ecological consequences of forest fires. The mathematical model of impurity transport above the city area with regard to the formation of secondary pollutants [43] (for example, ozone as a result of photochemical reactions [44]) is numerically realized with the assistance of parallel calculation technology.

The evolution of modern information-computer technologies and the prediction methods of forest fire danger and their ecological consequences creates objective conditions for putting the science-based developments into practice of forest fire protection. The purpose of the present monograph is to form the reader's cohesive understanding regarding the modern evaluation methods of forest fire occurrence conditions and their ecological consequences. A practitioner will acquire information on the current methods of predicting such catastrophic events as forest fires. The researcher will be able to evaluate the current development level of the study in question and plan further scientific investigations.

REFERENCES

1. Forest fires management on ecoregional level. (2004) Materials of International research and practice seminar (Khabarovsk. Russia. 9—12 September 2003). M.: Aleks, 208 p. (In Russian)
2. Moore, P.D. (1982) Fire: catastrophic or creative? // Impact of Science of Society, 1, 3—13.
3. Sofronov M.A., Vakurov A.D. (1981) Fire in the forest. Novosibirsk: Nauka, Sib. branch, 128 p. (In Russian)
4. Panevin V.S., Danchenko A.M. (2002) Differentiated approach to forest fire fighting // Sopryazhennye zadachi mekhaniki, informatiki i ekologii: Materials of International conference. Tomsk: Izd-vo Tom. un-ta. P. 125—127. (In Russian)
5. Valendik E.N., Matveyev P.M., Sofronov M.A. (1979) Large forest fires. Moscow: Nauka, 198 p. (In Russian)
6. Budyko M.I. (1980) Climate of the past and the future. Leningrad: Gidrometeoizdat, 351 p. (In Russian)
7. Volokitina A.V., Sofronov M.A. (1996) Classification of flammable vegetation // Lesovedenie, 3, 38—44. (In Russian)
8. Volokitina A.V., Klimushin B.L., Sofronov M.A. (1995) Technology of flammable vegetation large-scale mapping: Practical recommendations / Institute of Forest SB RAS. Krasnoyarsk, 47 p. (In Russian)
9. Kondratyev K.Ya. (1996) New trends in global climate // Izv. RGO, 128(6), 47—54. (In Russian)
10. Nazimova D.I., Nozhenkova L.F., Pogrebnaya N.A. (1999) Application of neuronet technologies for classification and prediction of zonal conditions of landscapes by climate indications // Geografiya i prirodnye resursy, 2, 117—122. (In Russian)
11. Nozhenkova L.F. (1997) Intellectual support of forecasting and emergency management // Intellektualnye sistemy. Krasnoyarsk: Izd-vo KGTU, 83—99. (In Russian)
12. Nozhenkova L.F. (1997) Opportunities and experience of application of expert and geoinformation systems in AIUS RSCS // Works of Rus.Conf. “Problemy zascity naseleniya i territoriy ot chrezvychaynykh situatsiy”. Krasnoyarsk: Izd-vo KGTU, P. 32—35. (In Russian)
13. Lykosov V.N. (2002) Modeling and assessment of regional impact of global climate changes on environment // Program and thesis of International conference reports «ENVIROMIS-2002». Tomsk: Izd-vo Tomskogo CNTI, 88—89. (In Russian)
14. Stocks B.J., Alexander M.E., McAlpine R.S. et al. (1987) Canadian Forest Fire Danger Rating System. Canadian Forestry service. 500 p.
15. Kurbatskiy N.P., Kostyrina T.V. (1977) National system of fire danger calculation in the USA // Obnaruzhenie i analiz lesnykh pozharov / ILiD SB AS USSR. Krasnoyarsk, P. 38—90. (In Russian)
16. Deeming J.E., Burgan K.E., Cohen J.D. (1978) The National Fire-Danger Rating System. Ogden, Utah: USDA Forest Service, General Technical report. INT-39, 66 p.
17. Garcia Diez E.L., Rivas Soriano L., de Pablo F., Garcia Diez A. (1999) Prediction of the daily number of forest fires // Int. J. Wildland Fire, 9(3), 207—211.
18. Viegas D.X., Bovio G., Ferreira A. et al. (1999) Comparative study of various methods of fire danger evaluation in Southern Europe // Int. J. Wildland Fire, 10(4), 235—246.
19. Nesterov V.G. (1949) Forest fireability and methods of detection. Moscow; Leningrad: Goslesbumizdat, 76 p. (In Russian)
20. Grishin A.M. (2002) Disaster modeling and forecasting. Tomsk: Izd-vo Tom. un-ta, 122 p. (In Russian)
21. Azmetov R.R., Belyayev A.I., Moskovenko V.M. (2000) Prospects of establishment of the Russian system of thunderstorm electromagnetic monitoring for fire protection, power engineering, aviation, meteorology and disaster forecasting // Sopryazhennye zadachi mekhaniki, informatiki i ekologii: Materials of International conference. Tomsk: Izd-vo Tom. un-ta, P. 9—11. (In Russian)

22. Matsenko V.V., Sokolov A.Ya., Kalinin S.I. et al. (1999) General layout offire safety forest arrangement. V. 1. Explanation note. 5-99.14-17-PM / State Research Institute «Rosgiproles», Altai branch. Barnaul, 139 p. (In Russian)
23. Volokitina A.V., Nozhenkova L.F., Sofronov M.A., Nazimova D.I. (2000) Emergency forecast during vegetation fires near settlements // Sopryazhennye zadachi mekhaniki, informatiki i ekologii: Materials of International conference. Tomsk: Izd-vo Tom. un-ta, P. 39—48. (In Russian)
24. Volokitina A.V., Sofronov M.A. (2002) Classification and mapping of flammable vegetation. Novosibirsk: Izd-vo SB RAS, 314 p. (In Russian)
25. Zhukovskaja V.I. (1970) Humidification and drying of hydroscopic forest fuels // Voprosy lesnoy pirologii. ILiD SO AN USSR, Krasnoyarsk. P. 105—153. (In Russian)
26. Kurbatskiy N.P. (1970) Study of properties and amount of forest fire fuels // The same. P. 5—58. (In Russian)
27. Sukhinin A.I., Ponomarev E.I. (2003) Mapping and short-term fire danger prediction in forests of Eastern Siberis by satellite data // Sibirskij ekologicheskiy zhurnal, 6, 669—675. (In Russian)
28. Afonin S.V., Belov V.V., Gridnev Yu.V. (2000) Space monitoring system organization for in forest fires Tomsk region // Matematicheskoe i fizicheskoe modelirovanie sopryazhennyh zadach mekhaniki i ekologii: Selected reports of International Conference. Tomsk: Izd-vo Tom. un-ta, P. 22—36. (In Russian)
29. Abushenko I.A., Altyntsev D.A., Taschilin S.A., Tatarnikov A.V. (2002) Satellite system of efficient observations over forest fires in the territory of Siberia and Far East // Sopryazhennye zadachi mekhaniki, informatiki i ekologii: Materials of International conference. Tomsk: Izd-vo Tom. un-ta, P. 6. (In Russian)
30. Isayev A.S., Korovin G.N., Titov S.P. et al. (1995) Ecological problems of carbon dioxide absorption by means of reforestation in Russia: Analytical review. Moscow: Tsentr ekologicheskoy politiki, 156 p. (In Russian)
31. Project of forestry management and development of Timiryazevskiy forestry of Tomsk forestry territorial production association of the Ministry of RSFSR Forestry. V. III. Mensuraion description of Temiryazevo forestry. B. 3. Quarters 91-145. Inv. № 390 / Gosleskhoz USSR. Vsesoyuznoe obyedinenie “Lesproekt”. Zapadno-Sibirskoe lesoustroitelnoye predpriyatie. Tomsk, 1990. 400 p. (In Russian)
32. Korneyev V.V. (1998) Parallel computing systems. Moscow: Nolidzh, 320 p. (In Russian)
33. Malyshkin V.E. (1998) Basics of parallel computing: textbook. Novosibirsk: Izd-vo NGTU, 60 p. (In Russian)
34. Scientific-applied reference book on the USSR climate. Series 3. Multiyear data. Parts 1—6. Issue 20. (Tomsk, Novosibirsk, Kemerovo regions and Altai krai). SPb.: Gidrometeoizdat, 1993. 718 p. (In Russian)
35. Baranovskiy N.V. (2007) Forest fire danger prediction, based on a new concept // Materials of Intl. Conference “Rational Use and Reforestation in the Sustainable development System”. Gomel: In-t lesa NAN Belarusi, P. 129—132. (In Russian)
36. Baranovskiy N.V., Grishin A.M., Loskutnikova T.P. (2003) Inforemation-prognostic system of forest fire occurrence probability // Vychislitelnye tekhnologii, 2, 16—26. (In Russian)
37. Tolstykh M.A. (2001) Semi-Lagrangian atmospheric model with high resolution for a numerical weather forecast // Meteorologiya i gidrologiya, 4, 5—15. (In Russian)
38. Grishin A.M., Golovanov A.N., Kataeva L.Yu., Loboda E.L. (2001) Formulation and solution of the problem of drying of a layer of combustible forest materials // Combustion, Explosion and Shock Waves, 37(1), pp. 57-66.
39. Grishin A.M., Golovanov A.N., Kataeva L.Yu., Loboda E.L. (2001) Problem of drying of a layer of combustible forest materials // Inzhenerno-Fizicheskii Zhurnal, 74(4), pp. 58-64.
40. Loboda Ye.L. (2002) Physical-mathematical modeling of forest fire fuels layer drying and inflammation: Dissertation Phd. Phys.-Mat. Sci. Tomsk: TSU, 108 p. (In Russian)

41. Grishin A.M., Baranovskij N.V. (2003) Comparative analysis of simple models of drying of the layer of forest combustibles, including the data of experiments and natural observations // Inzhenerno-Fizicheskii Zhurnal, 76(5), pp. 166-169.
42. Grishin A.M. Dolgov A.A., Tsymbalyuk A.F. (1997) Method for pollutants detection and calculation from forest fires. M.: Minekologii RF, 26 p. (In Russian)
43. Belikov D.A. (2006) Parallel realization of mathematical model of atmospheric diffusion for research of distribution of primary and secondary air pollutants above urban territory: Avtoref. diss.. … Phd. Phys.-Mat. Sci. Tomsk: TSU, 20 p. (In Russian)
44. Belikov D.A., Starchenko A.V. (2005) Study secondary pollutants (ozone) generation in Tomsk air // Optika atmosfery i okeana, 18(5—6), 435—443. (In Russian)

CHAPTER 1
FACTORS OF FOREST FIRE DANGER

Abstract

The first paragraph gives information on forestry of the entire Russia and Tomsk Region, in particular. Regional situation with forest fires is described. Classifications of forest fuel accepted in Russia, the USA and Canada are considered. Such fire factors as thunderstorm and human activities are being discussed, as well as models of fuel-drying and fuel ignition. Information on numerical weather prediction and basics of bounder-layer theory are presented.

Keywords: lightning activity, anthropogenic load, weather prediction, forest fuel, drying, ignition

1.1. Forests and forestry in Russia

The forest ecological system of the Russian Federation occupies 1,2 billion hectares of its territory and contains ca. 25 % of the planet's forest resources [1]. The Russian forests are not only economic, but also a most important ecological resource due to the Russian Federation's providing annual carbon storage in an amount of 29 billion tons; its territory keeps 26% of world forests [1]. The global processes of regulating the environmental conditions, biodiversity, climate, river runoffs are largely affected by the Russian forests [1].

Forest ecological systems are of a very complex nature. The tasks of their sustainable management can only be solved in an integrated manner. At present, information support for the forest management system has an interdisciplinary basis. Land users, consumers of wood and non-wood resources and other concerned parties are engaged as partners to form information resources [2].

The main condition for effective forest management is the availability of reliable and comprehensive static and dynamic information on the state of the forest area. The institutional arrangements of forestry provide circulation of information flow regarding all questions on forestry, forest measurements, etc. (Table 1.1). Planned implementation of research and technology achievements, wide use of geoinformation systems and technologies, modeling and optimization techniques of forest management, development of information systems of various levels must secure intensive and integrated use of forest resources on retention of the ecological and genetic potential of the Russian forests [3].

The following forms of information are necessary in forest and forestry [4]:

Table 1.1. Information flow formation and movement in the Russian State Forest Enterprise [2]

Information source	Information content	Aggregation level	Approximate volume	Information's destination address
Forest district	Original documents on anthropogenic activities	Stratum, quadrant, forest district	15 MB	Forestry
Forestry	Cadastral survey, evaluations, forms, reporting, new mensuration descriptions, monitoring	Stratum, quadrant, forest district, forestry	100 MB	Forest management of the constituent entity of Russia, state forest management, forest district, authorized organizations
Forest management in a constituent entity of the Russian Federation	Cadastral survey, evaluations, forms, consolidated reporting, regional monitoring	Stratum, quadrant, forest district, forestry, constituent entity of Russia	500 MB	the Russian State Forest Enterprise, state forest management, authorized organizations
State forest management	Forest management materials, reports at requests of the Russian State Forest Enterprise	Stratum, quadrant, forest district, forestry, constituent entity of Russia, Russia	100—500 MB	Forest management, forestries, authorized organizations, the Russian State Forest Enterprise
Authorized organizations	Statistical reporting, forest inventory, forest monitoring, reports at requests	Forestry, constituent entity of Russia, region, Russia	0.1—1.5 GB	the Russian State Forest Enterprise, forest management, forestry
the Russian State Forest Enterprise	Statistical reporting, forest inventory, forest monitoring, reports at requests	Forestry, constituent entity of Russia, region, Russia	0.1—1.5 GB	the Russian Government

1) current — enters and gets accumulated as a result of the daily activities of the enterprise or management body not only on the basis of record keeping and reporting but also on the basis of monitoring data; it is conventional to take in account the changes of the last one or two years and partially of a forest inter-management cycle;

2) latest update — necessary in case of emergency situations, estimated in the natural habitat according to the remote sensing, compared to the current and monitoring information to estimate the occurring changes and take necessary measures;

3) forecasting — based on a retrospective analysis of the area condition together with the current information with an obligatory use of monitoring and mathematical modeling data.

The basis of the forestry's information system is a combined data base that allows using the potential of the mensuration data bases of a relational type and geoinformation systems most rationally [5] to input, store, process and issue materials of the planning and map-making support. The main block of the forestry's

information system is a stratum-type data bank. The input information for the stratum-type bank is provided by the materials for basic forest management updated at the load of the stratum-type bank in a forestry [1].

So far various forest managing companies and industry research centers have developed and put in use a range of program products for forest management and protection [4]. Figure 1.1 illustrates a general chart of the forecast and analysis system for the development of sustainable forest management projects on a forestry level.

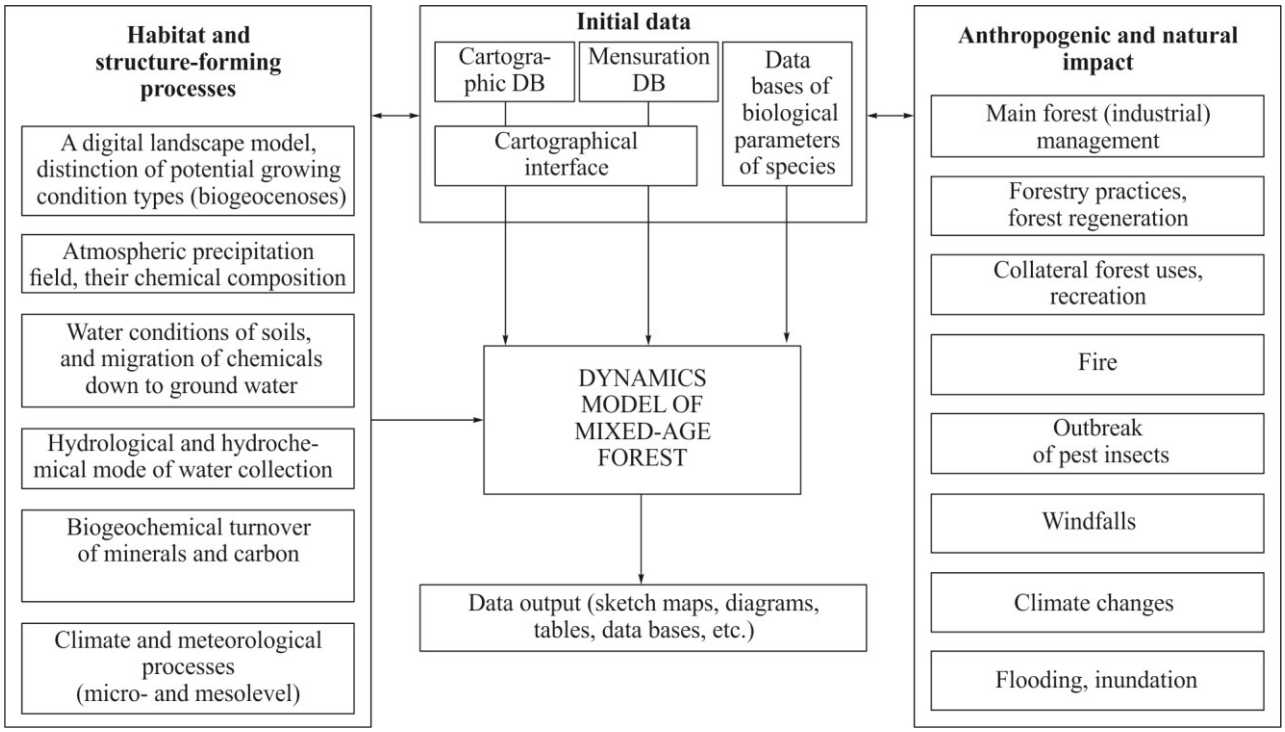

Figure. 1.1. A chart of the module and block structure of the forecast and analysis system for sustainable forestry designing [1]

1.2. Forests and forest management in the Tomsk Region

The Tomsk Region, its north in particular, is a fairly typical forested territory of a boreal zone. Its example may provide a quite general description of the conditions for fire occurrence. The region has vast forest resources. Forest areas cover 90.5 % of its total territory. There are 17 million hectares covered with woody species, including 9.9 million hectares covered with coniferous species [6].

The main landscape types within the Tomsk Region are interfluvial plains and river valleys along with old runoff plains [7]. Interfluvial plains are represented by positive and negative morphostructures. The geomorphological demarcation of the Tomsk Region is shown on Figure 1.2.

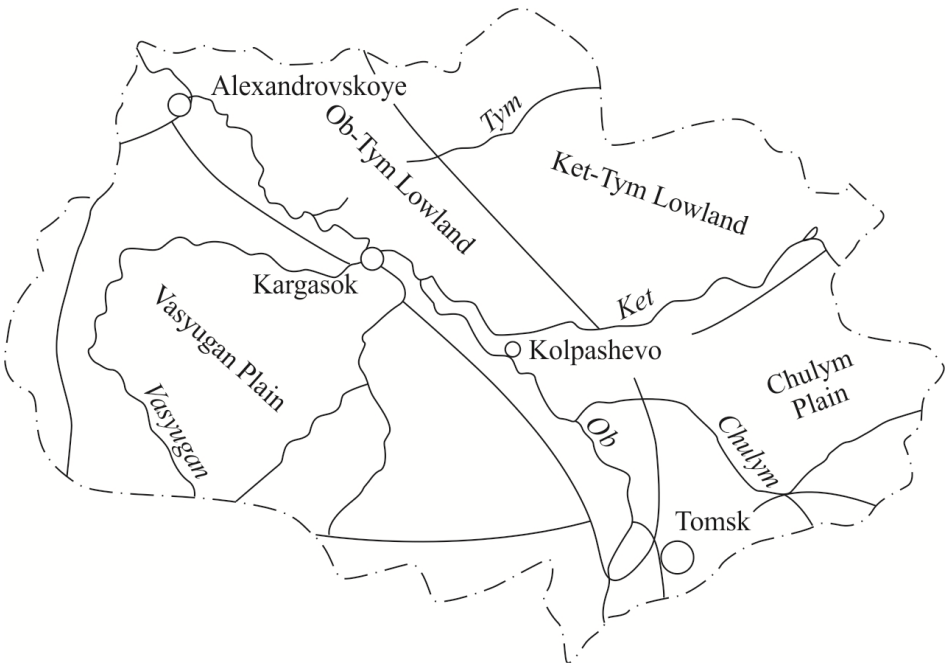

Figure. 1.2. Geomorphological demarcation of the Tomsk Region [7]

The region's forests are located in the Ob River basin on a plain territory with an excessive moistening of the territory and are essential in nature protection [6]. Relatively harsh weather conditions determine the rather limited species composition of forests. The prevailing forest-forming species are the common pine, Siberian stone pine, Siberian spruce, Siberian fir, silver birch and white birch, aspen and Siberian larch [6, 8]. The coniferous species, mainly the pine and the Siberian stone pine, form the basis of the region's forest raw material resources. Clear stands are more frequent in the region's north.

The domineering species in the Tomsk Region is the pine. The diversity of the physical characteristics of soils and the degree of their wetting gives a fairly wide range of forest types [8] that can be grouped in the following way: lichen, green moss, long-stem moss, sphagnum, grass marsh, mixed herbs [6]. It should be noted that the most significant changes in the species composition of stands, their age-class composition and density are brought by forest fires and outbreaks of pest insects [9—11].

Forest fire danger in the Tomsk Region is determined by the presence of a large proportion of coniferous forests, well-developed flammable ground vegetation and hot, dry summers. The climate of the Tomsk Region is boreal-type extreme continental [8]. Territories with continental climate create conditions especially favorable for forest fire occurrence [12]. In the region's forests, depending on the weather conditions, all three seasonal flammability peaks are registered: spring fire wave, constant summer and autumn fires [6].

According to the Tomsk Region's aviation forest protection data base, there were 2363 forest fire incidents recorded between 1993 and 2002 [8]. 55 to 350 fires occur in the region annually. Figure 1.3 presents the number of forest fires in administrative divisions of the region between 1993 and 2002.

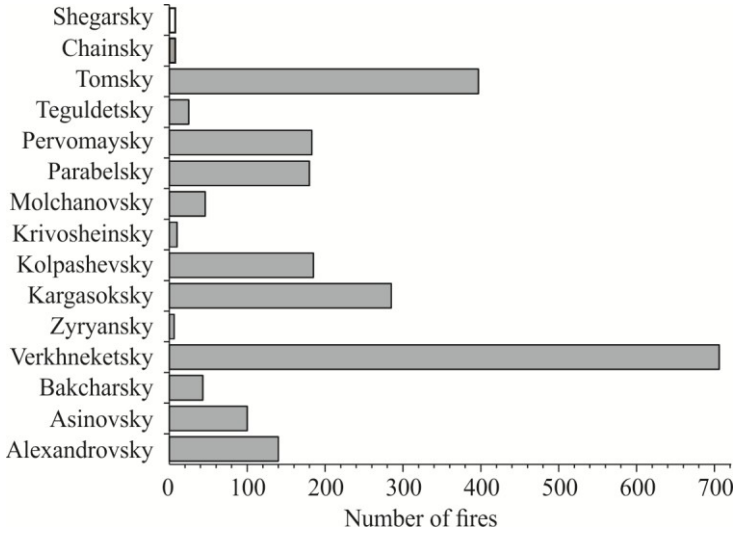

Figure. 1.3. The number of forest fires in the administrative districts of the Tomsk Region between 1993 and 2002 [8]

The index of the relative number of forest fire to the area of the region in question has a higher degree of informativeness. The highest level of flammability is characteristic of the Tomsk district (over 35 outbreaks of fire per 100 thousand hectares) (Figure 1.4). The degree of flammability of the district's forests is determined first of all by the seasonal activity of the local population and the properties of canopy cover [8]. This territory is distinguished by a high density of the rural population, its proximity to the region's center (the city of Tomsk) and richness in mushroom and berry lands. The districts of the next level in flammability are the Asinovsky, Verkhneketsky, Pervomaysky and (over 10 forest fire incidents per 100 thousand hectares). The forests of the (less populated) Parabelsky, Pervomaysky and Kargasok are prone to the largest fire disturbance. They are characterized by a low fire frequency, but large firing area. It is explained by the difficulties in detection and liquidation of fire spots on these districts' underdeveloped area [8].

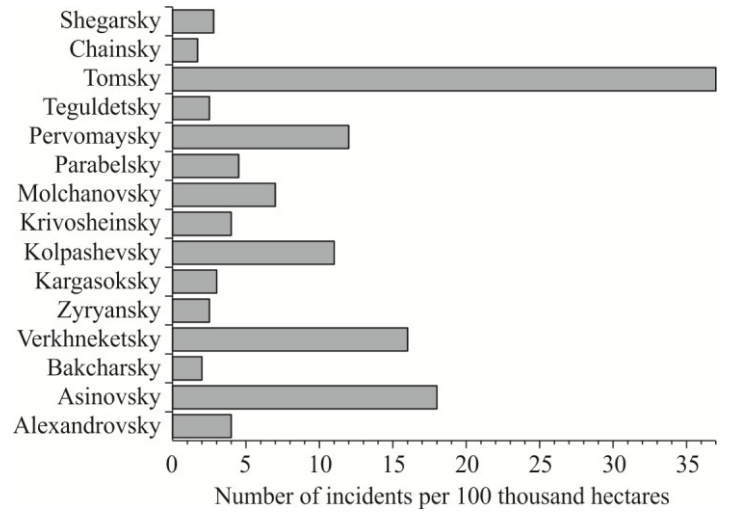

Figure. 1.4. The number of forest fires per an area of 100 thousand hectares in the administrative districts of the Tomsk Region [8]

A particular feature of the forests in the Tomsk Region is the availability of combustible material in all stands. Surface fires develop in the region predominantly (98,5 %), crown fires make 1,1 % of all incidents and 12,5 % of the firing area, peat fires occur more rarely [6]. The annual percentage of fires for anthropogenic reasons is fairly stable, and fires caused by storm discharge are cyclic. Periods of mass storms are changed to more quiet ones. The flammability of the region's forests is also changed substantially according to the fire hazardous season. The most 'flammable' months are June and July. The duration of the fire hazardous season according to the weather conditions varies between 137 and 161 days [6].

The reasons for forest fire occurrence in the Tomsk Region are quite different (Table 1.2).

Information recording about a specific reason for forest fire occurrence of an anthropogenic character will allow improving the existing methods of forest fire danger prediction. Specifying the reasons of forest fire occurrence may be the basis for new developments in the field of creating a system of assimilating data on the level of anthropogenic in controlled forested areas.

Table 1.2. Average area of forest fires in the Tomsk Region between 1993 and 2002 [8]

Fire cause	Number of fires	
	Number of incidents	%
Local population	1249	52.86
Storm	891	37.71
Timber procurer	12	0.51
Agricultural burning	3	0.13
High temperatures of air	1	0.04
Locomotive	9	0.38
Bonfire residue	1	0.04
Electric power transmission lines	1	0.04
Oil spill flaring	2	0.08
Gas exhaust into the air	1	0.04
Objects of forestry	8	0.34
Rocket stage drop	2	0.08
Expeditions	1	0.04
Undetermined	182	7.70

1.3. The classification of forest fuels

The most widespread forest fuels are united into complexes [13].

1. Fruticose lichens and mosses. They have a significant impact on fire occurrence and spreading in cases of their domineering in the plant community structure and determine the specificity of forest type. Their participation interest in complexes of many forest type fuels is high; they contain a higher water capacity in broad limits and hygroscopicity; they are able to dry quickly; they have a structure that stimulates spreading of burning on them.

2. subshrubs and herbs. The ground vegetation with a predomination of subshrubs and herbs is no less widespread in the taiga zone than lichen and moss crust. It is characteristic of non-forested areas (cuttings [14] and burnt areas). The cover with predomination of herbs in Siberia and the Far East is formed as a result of thinning of light coniferous forest under the influence of fires.

3. Auxiliary species and undergrowth. A dense storey that has an essential pyrological importance gets formed in many forest types. An increased fire danger of the common juniper auxiliary species is recorded. Its shrubs burn away with many sparks, i.e. fading needles, flying aside. The pyrological role of the auxiliary species is still understudied. In [13] the data on the dispersal of forests with auxiliary species are given, as well as the importance of the auxiliary species in fire occurrence based on the fire and burned area observation.

4. Litter. Litter arouses interest in fire nature studies as a constituent part of the fuel vegetation complex. The available total of the litter on the soil surface is determined by a proportion of its formation rate and its rate of conversion into ground litter. A wide variation of the litter quantity is recorded in literature.

5. Ground litter. In pedology [15], ground litter refers topsoil (A_0) that consists of dead plant parts with different degrees of decomposition and loss of natural structure. In the taiga zone, the higher the soil moisture, the thicker the ground litter. The ground litter moistened by rainfall remains wet for a long time and gradually passes moisture to the fuels on it. It dries layer-by-layer from the top.

6. Peat. As a natural burning object, peat is encountered as pedogenic horizon in wet peatland and boggy forests and as peat deposit formed by bog vegetation. Bog fires are substantially different from forest fires.

7. Deadfallen wood and stumps. Deadfallen wood refers to the tree trunks fallen on the soil surface that have died in the process of natural thinning of stands, as a result of windfall, windbreak or snowbreakage. Tree litter increases after fire and pest damage to the stands. Stumps as combustible material are characteristic of cuttings. In case of low surface fires the timber of isolated deadfallen wood and stumps does not burn down.

8. Stand’s canopy. In crown fires, mostly needles, leaves, living twigs bearing needles and thin (up to 7 mm)faded twigs burn in the stand’s canopy.

9. Tree trunks and limbs comprise a large part of the phytomass of forest biogeocenosis. However, in fires they burn down very rarely. Sometimes saplings burn in crown fires completely in dense pine sapling areas that developed on clear cuts that were much strewn with groundwood. In older stands, mosses and lichens burn on the trunks and limbs, the outer bark surface is scorched. Burning may occur in trunk caves with faulty wood. Stands perish in fires, but not burn down completely.

The properties of forest fuels are of high importance for forest fire danger prediction. The so-called fuel models are used for their description. There is a fairly detailed characteristic of forest fuels types that get involved in the surface forest fire process. Forest fuels are plants and their decomposition remains of different degrees that may burn in fire [16]. All plants, living or dead, and also litter, deadfallen wood, ground litter, humus and hystic horizons refer to fuels in forest biogeocenosis in practice.

The classification of forest fuels may contain three levels [17]:

a) the classification forest fuels elementary parts that include separate plants from ground vegetation, auxiliary species and undergrowth, lowly shrubs, morphological tree parts (limbs, branches, windfall), etc.;

b) classifications of simple complexes (forest fuel layers) inside biogeocenoses;

c) the classification of biogeocenoses as compound forest fuels complexes.

In the American national fire danger evaluation system (first NFDRS-72, then NFDRS-78) all forest fuels are divided into two main categories: living and dead. It is considered that the living plants are always able to support their high moisture content, whereas the moisture content of the dead forest fuels depends on the processes of their moistening and drying under the influence of weather conditions [18]. Such a division is just for the main US territory, since its forests almost lack the lichen and moss crust. In Russia's boreal zone lichen and moss crusts are quite widespread, so the American division for this territory is incorrect [17].

The dead forest fuels in the USA are divided into four classes: light, medium, heavy, and very heavy fuels, depending on the "time lag" value. A time lag is a period of time during which there is a loss of two thirds of moisture that can evaporate in the standard conditions of the air environment from this sample (layer) of forest fuels. It must be mentioned that the time lag is a constant value for the given forest fuels sample (layer) and does not depend on its moisture content. To Class One (1-hour time lag fuel) belong the forest fuels with an average time lag of 1 hour (0—2 hours). It is usually sphacelated herbaceous plants and dried wood particles with a diameter of 6 ммОбычно. Class Two (10-hour time lag fuel) contains forest fuels with an average time lag of 10 hours (from 2 to 20 hours). It is usually dead fallen branches with a diameter of 6 to 25 mm. The remaining fuel classes from the point of view of surface fire occurrence prediction are not the scope of our interest and we will not consider them in detail.

In this classification the living forest fuels exclude all the plants and their parts with a diameter of more than 6 mm. The living fuels able to actively burn and sustain their burning (needle-foliage Marsh Labrador tea, heather) must be distinguished.

The American system also classifies forest fuels ground layer in accordance with time lag. To Class One (1-hour time lag fuel) belongs the upper litter layer with a thickness of up to 6 mm; to Class Two (10-hour time lag fuel) belongs the litter (ground litter) layer in a depth of 6 to 25 mm; t Class Three (100-hour time lag fuel) belongs the ground litter layer in a depth of 25 to 100 mm; to Class Four (1000-hour time lag fuel) belong the layers of ground litter, peat, earth humus in a depth of 100 to 300 mm.

The drying rate of litter and ground litter layers depends on both the depth of their arrangement and their soil moisture regime. The American system does not mention moss and lichen layers.

The Canadian system of CFFDRS [19] chooses a three-layer complex of forest fuels as a standard for fire danger evaluation according to the weather conditions [20]; this complex corresponds to the ground vegetation consisting of green pinnate moss with pine needle litter at a fairly deep lower layer of the ground litter. The ground vegetation indicated is quite typical for the forests widespread in Canada. The

Canadian standard complex of forest fuels is similar to the one used for the development of the Russian forest fire indications of dryness [21, 22]. It is a cover of green mosses in pine forests on drained soils having three layers: 1) the upper moss layer with a thickness of 3—4 cm, 2) the lower moss layer with a thickness of 2—4 cm, 3) the ground litter layer with a thickness of 2,5—4,5 cm.

The layers of forest fuels are also classified in accordance with their spatial location in biogeocenoses [17]. Some Russian pyrologists distinguish three layers of which the middle layer is of interest for us (the layer that has mosses, lichens, small litter, sphacelated grass) since it is affected by fire sources. Meanwhile, [23] distinguishes nine full storeys in the forest area structure (including the atmosphere layer).

The Canadian classification divides the forest fuels into three large groups: 1) ground fuels, humus, peat, roots; 2) surface fuels, including foliage, needle and grass litter, small shrubs, large windfall; 3) crown fuels that contain limbs with needles and foliage and dead fallen branches [24]. In the USA, forest fuels are divided in accordance with both their location in biogeocenosis and the burning possibility and type of spreading on them [25].

In N. P. Kurbatskiy's classification [13, 26] it is not only the location in biogeocenosis that is considered when dividing all the forest fuel layers into groups, their function in fire is also viewed. All forest fuels are divided into three categories [13]: 1) burning conductors, 2) burning supporters, 3) burning suppressors.

Burning conductors are such forest fuels that form continuous layers on which burning may spread. It is mainly layers of mosses, lichens and small , plant debris (litter, dead grass, groundwood). They conduct flame combustion in surface fires.

Moreover, if the deposit of vegetating grass in an absolutely dry condition surpasses the deposit of dead grass, flame combustion is impossible [27]. The leading role in surface fire occurrence and spreading play forest fuels of Category I. This group is divided into 11 types of ground vegetation [28] in connection with geobotanical biomorphocycles. However, ground vegetation types, quite varying in geobotanical characteristics, may be homotypic in pyrological characteristics [17]. Later this classification was improved by dividing 10 pyrological types of lichen and moss and dead crusts [29]. Furthermore, classifications were offered by E. V. Konev [30], A. P. Yakovlev [31] and M. A. Sheshukov[32, 33].

For the physical-mathematical and predicting modeling of forest fire theory problems, including forest fire danger evaluation, thermophysical characteristics of the forest fuel layer are of a high importance, along with that thermokinetic constants of drying and pyrolysis processes of forest fuels must be considered [34]. There were attempts to develop a theoretically justified approach to the forest fuels classification [17] and count the data on the physical properties and calorific ability of different types of forest fuels [13]. Typical examples may be illustrated with the results of observing the fire maturation of the main burning conductors in the following regions — the Leningrad Region, Arkhangelsk Region, the European part of Russia, Tomsk Region [35], Gorny Altai, Krasnoyarsk Angara Region, Evenkiya, Western Syan and the crest of Tannu-Ola in Tyva, Krasnoyarsk forest steppe, the crest of

Khamar-Daban in Buryatia, Chita Region, South-West of Yakutia, South of the Khabarovsk Region.

For both evaluating the natural fire danger of biogeocenoses, and calculating the possible development of forest fires [17] the data on forest fuels deposits are necessary [13, 30, 36]. Using the maps of flammable vegetation, it is possible to predict forest fire prevention [37].

It is considered that a timely clean burn is the main method of facility protection from large forest fires. However, one should not forget of an emergency situation in Los Alamos (forests on an area over 20000 ha were perished, 500 houses in the city were burnt, the work of Los Alamos National Laboratory was practically stopped) [38]. The fire reason was preventive burning of the remains of dry previous year's vegetation. The technology of anticipatory clean burn should be used in connection with prediction modeling and evaluation of the condition of forest fuels and flammable vegetation at a particular moment.

Identifying the type of the main burning conductors may be carried out in three ways [39].

1. Defining types of the main burning conductors in strata through forest types in mensuration description. The accuracy of definition in this case is not high since all the enclosures referred to one forest type automatically acquire the typical (same) pyrological characteristic. However, "typical" enclosures are not frequent [39].

2. Defining types of the main burning conductors also through forest types recorded in the mensuration description. However the connection between the types of the main burning conductors and forest types is discovered as a result of special field research.

3. The characteristic of strata according to the types of the main burning conductors is made exactly at ground mensuration or at decoding air photographs.

The analysis of the pyrological evaluation in the Chunoyarskiy Forestry through the first two ways [39] has shown that the mensuration strata are not homogeneous in forest pyrolysis characteristics. Around 30 % of the strata areas do not correspond to the forest types pointed in mensuration descriptions of these strata according to the domineering species and around 40 % do not correspond according to the character of the ground vegetation, which is the basis in forest fire danger prediction.

At present, on the basis of the flammable vegetation maps, the maps of the natural fire danger are compiled that show the readiness to the burning of the strata in a given period at a given dryness class. Moreover, the maps of flammable vegetation may be used to predict the rate of fire spreading, intensity, and behavior and the choice of the optimal fire protection tactics [17]. The ultimate goal must be a complex software system whose development implies a combination of three different approaches [17]: computation and analysis algorithms, geoinformation system technologies [40] and expert system technologies [41]. The advantages of GIS-technologies for solving the problems on analysis of geographically bound information are well known. Applying the expert system technology is determined by, firstly, an orientation at forming recommendations for those who make decisions, and secondly, by the fact that the information on whose basis the decisions are made has a quality character in many instances. The values used have an indistinct diffuse semantics, and the methods that

use them are empirical or heuristic [37]. An expert system has been developed whose knowledge base and strategy of indistinct output are built on the method of evaluating and predicting fire danger with the use of flammable vegetation maps [42]. It must be mentioned that a part of forests surrounding settlements is often situated not on the territory of the State Forest Resource, but on the areas of former collective and state farms [37]. This fact complicates the compilation of flammable vegetation maps and forest fire danger prediction.

A new system of classifying the forest fuels has been recently developed in the USA [43]. The basis for the algorithm of the system operation is the following. 1. A prototype for a layer of fuel material is chosen. 2. The prototype is specified. 3. Characteristics of the layer of fuel material are calculated. 4. The final system classification has 192 formalized types of the fuel layer that differ in physical, chemical and structural properties. Each type is indexed in a certain three-dimensional space of attributes: 1) the index of potential spreading rate; 2) the crown index; 3) the index of fire impact (Figure 1.5).

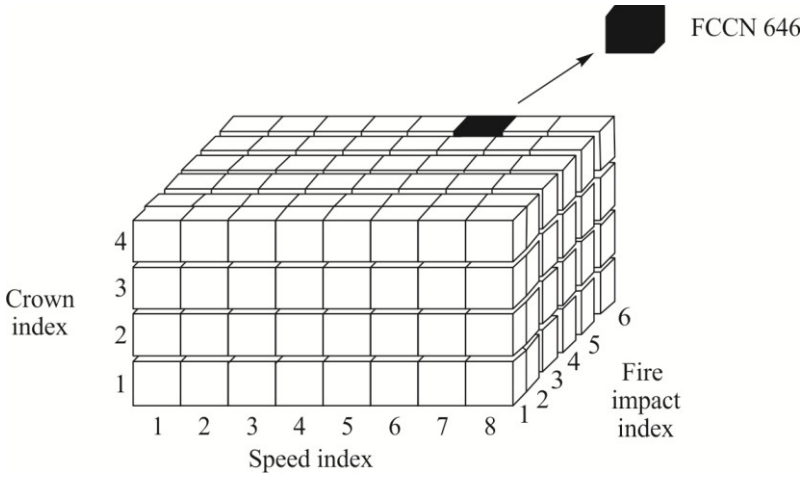

Figure 1.5. 192 formalized types of forest fuels grouped in a three-dimensional space of attributes [43].

The user's interface provides the following abilities for an access to forest fuels characteristics [43]:

а) the choice of forest fuels prototype that is based on general characteristics; and accepting the forest fuels characteristics given by default;

б) the choice of forest fuels prototype and its modification with the use of information on a certain area;

в) creating a user's type and user's data base on forest fuels;

г) search of the existing forest fuels type according to the criterion provided (for instance, the index of spreading rate).

As the result of system operation, the user-defined forest fuel layer will be bound to one of the formalized types. The FCC system prototype was available for beta-testing since the end of 2001 [43]. Figure 1.6 shows a screen shot of the FCC system operation.

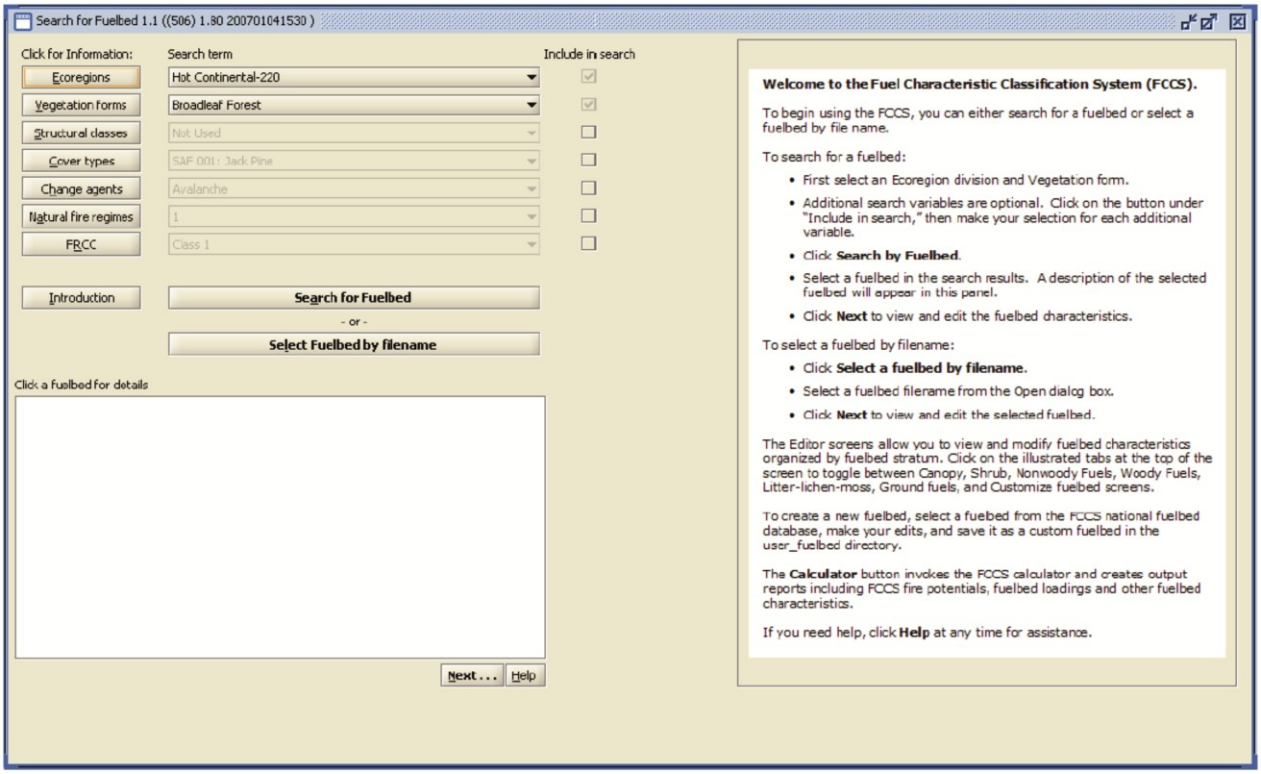

Figure 1.6. FCC system interface

1.4. Forest fire characteristics

An equation for describing the burning process of wood is known [44]; it counts the content of carbon, hydrogen, and oxygen in its material. In its output it was supposed that moisture does not participate in this process, and nitrogen affects the burning process moderately. Eventually, the following equation of a chemical reaction was formed [44]:

$$4C_6H_9O_4 + 25O_2 \rightarrow 18H_2O + 24CO_2 + 5{,}264{,}729\,\text{kJ}$$

The energy released as the result of this reaction is called *calorific capacity*.

The main statement of the physical model of forest fire occurrence and development stands in the so-called triangle of forest fuels – heat – oxygen access [45]. If any of these factors is absent, there will be no fire. The heat released as the result of burning of a forest fuels portion is transmitted by conduction, convection and radiance. [45] presents a three-stage process of a forest fire (Figure 1.7).

From the perspective of the mechanics of multiphase reacting environments, a forest fire is defined as an incident of uncontrolled multistage burning on an open space on a forested area within which there are interrelated processes of convective radiance energy transmission, warming, drying and pyrolysis of forest fuels, and also burning of gaseous and afterburning of condensed products of forest fuels pyrolysis [46].

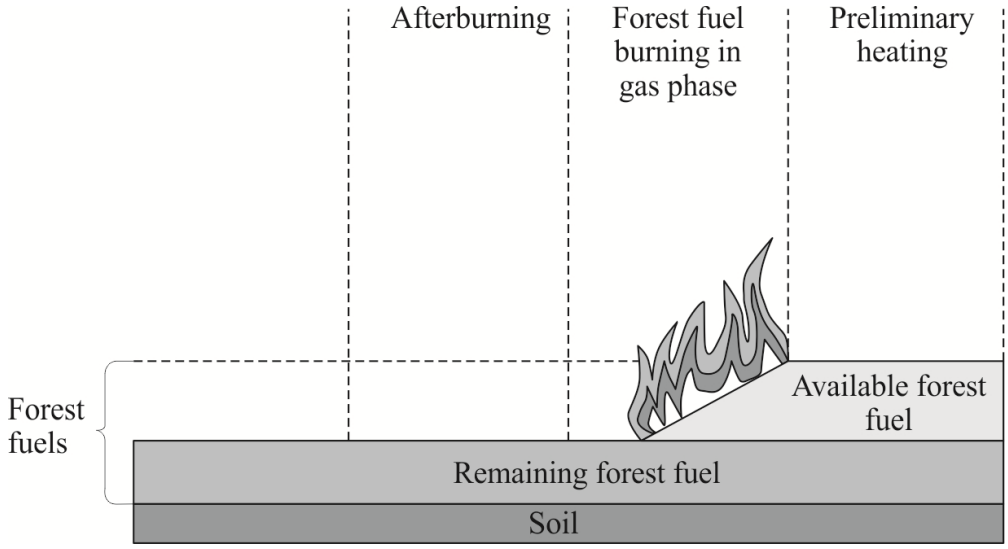

Figure 1.7. The process of forest fire development [45]
Stage One — preliminary warming, Stage Two — burning of forest fuels in the gas phase, Stage Three — afterburning or smoldering of forest fuels.

Forest fires are divided into surface, crown, top, underground (peat) and mass fires [23, 46]. In surface fires the ground vegetation is burnt. In crown fires, both the ground vegetation and tree crowns are burnt. In top fires only tree crowns are burnt. Underground fires are characterized by the presence of the burning spot in the thickness of the layer. Mass forest fires occur at a collisional catastrophe, air nuclear explosion, etc. [47].

At any moment on a forested territory there may be distinguished a quite large control environment volume — a fire zone in which the environment condition parameters (as the result of physical-chemical transformations induced by the forest fire) differ from the unperturbed values determined by the weather conditions and vegetation type [46]. The biggest change in the environment condition parameters occurs in the forest fire zone that is called a fire front. The front spreads with a certain rate on the forested area [46].

1.5. Thunderstorm activity

One of the reasons for forest fires is storm discharges. Lightning is an electric discharge conditioned by the division into positive and negative kinds in the clouds that leads to a difference in potentials of the range 10—100 mV[48]. In order for the division into kinds to happen, it is necessary that water be present in all three phases — solid, liquid and gas [49].

According to the development conditions, storms are divided into the air-mass and frontal ones. Air-mass storms over a continent occur as the result of the local air heating from the ground surface that leads to a development of rising flows of the local convection and a formation of heavy cumulonimbus clouds in it. The frontal storms

occur on the borders of warm and cold air masses [50]. There may be class kinds of cloud – cloud and cloud – ground. Around 90 % of cloud — ground classes are negative, and the nature of the remaining (positive) 10 % of classes is not fully clear [51]. The class types of cloud — ground, i.e. ground storm discharges [52]. The characteristics of the power of positive and negative ground storm discharges are different, and these differences are substantial from the point of view of inflaming the forest fuels. As the result of the vast majority of positive discharges, all the energy reaches the surface in one stroke, and the negative discharges are characterized by a multi-stroke [53].

Wide statistics on ground storm discharges has been collected within the functioning of the US National Lightning Detection Network [54]. This system may identify the majority of the ground storm discharges on the territories of the USA and Canada with the spatial resolution of several kilometers and an accuracy of determination in time of 1 msec. As the system operation result the data on the polarity, peak current and complexity of the stroke are archived (if it is a single or multi-stroke) [48].

Recent studies [55—59] of this problem were focused on the positive ground storm discharges that probably possess the most potent power on the planet [48]. As the large power of positive discharges, their high probability to generate a strong current at the stroke allows suggesting that positive discharges are a leading factor in forest fuels inflammation and forest fire occurrence. However, some scholars put this fact into question [60] and pay attention for many negative discharges with a continuing current effect.

Ground storm discharges are recorded in other countries as well. Between 1992 and 2001 a cycle of observing ground storm discharges was carries out in one of the regions in Spain [61]. The characteristics of $4{,}3 \cdot 10^6$ flashes were registered for the Iberian Peninsula during the first ten years of storm monitoring network operation: the yearly and daily cycle, polarity, complexity, peak current of the first strike. It was shown that the maximum thunderstorm activity is characteristic of the period from May to September. The maximum stroke frequency was 2,1 strokes/(km^2year). The maximum thunderstorm activity is associated with the mountainous landscape. The value of single strokes was 53,6 % and 89 % correspondingly for negative and positive ground storm discharges. The average current for the first stroke of the negative and positive discharges was 23,5 kA and 35,3 kA correspondingly. For the discharges of both fields the peak current is higher in the summer than that in the winter.

Figure 1.8 illustrates the spatial location of the storm monitoring network points in Spain. The location of sensors is marked with star signs. For the analysis of the geographical distribution of discharges the data on ground storm discharges were divided into blocks of 0,2° of longitude ×0.2° of latitude (368 km^2) [62]. For studying the temporal distribution of discharges, the intervals of year, month, hour, and integral were used on all the territory. The results consist of the ground storm discharge number according to the years of the studied period, an average daily variation of ground storm discharges [61] (Figure 1.9). The portion of positive ground storm discharges was around 9 %.

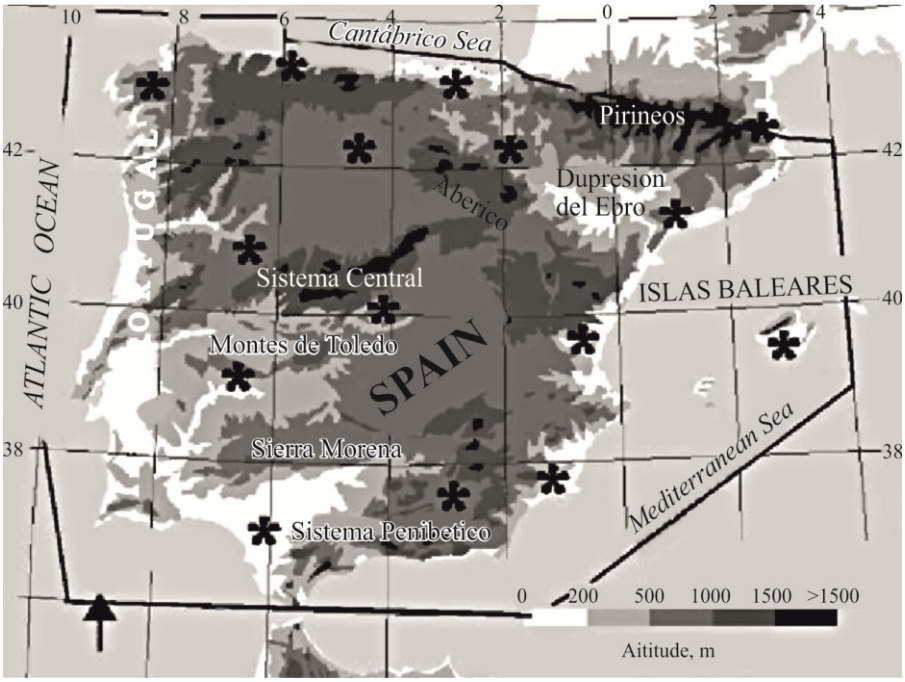

Figure 1.8. The spatial distribution of storm monitoring network points in Spain [61]

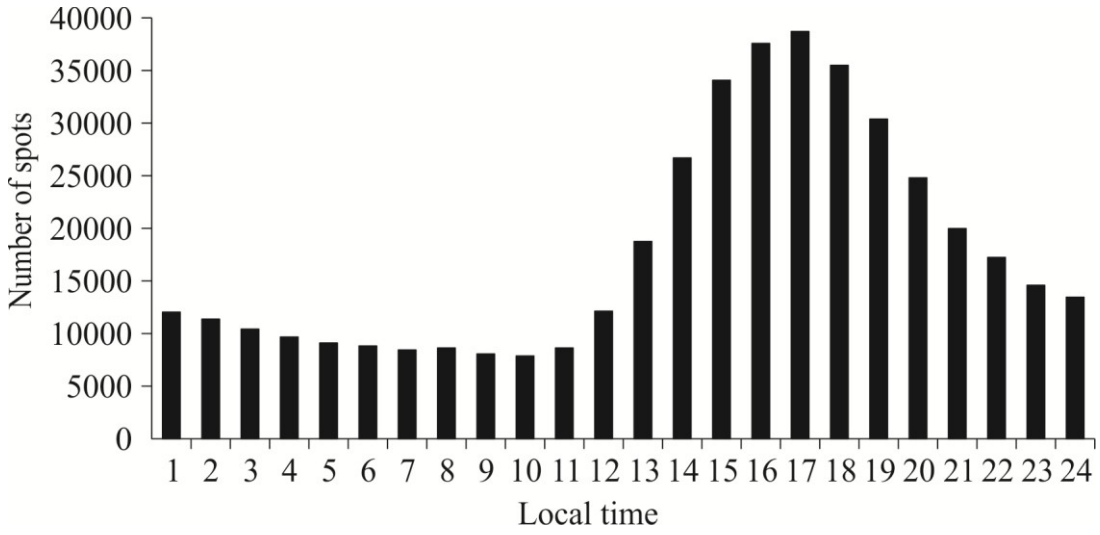

Figure 1.9. An average daily variation of the ground storm discharges in Spain between 1992 and 2001 [61]

The results of analyzing the ratio distribution (single or multi-stroke) of negative discharges in accordance with the years of the studied period, and also the daily variation of ground storm discharges are of interest [163]. Observations of storm discharges are also made in Japan [64, 65], France [66], Brazil [67—70], Italy [71], Russia[50].

For an effective operation of forest protection service it is necessary to know the dynamics of thunderstorm activity in the certain region. For example, the thunderstorm activity in the Krasnoyarsk Territory varies substantially within a day. Along with that, the highest degree of storm repetition is observed between 14 and 18 o'clock [72]. The average storm duration varies from 1,2 to 2.6 h. Within one day the biggest number of storms is recorded between 12 and 18 o'clock, local time [72]. Several factors influence storm-induced forest fire occurrence: 1) storm's passing, 2) presence of the cloud – ground discharge, 3) the amount of precipitation fallen in the storm, 4) the tree species and its physical state, 5) the presence of fuels, 6) soil conductivity. The biggest number of ground lightning discharge occurs at night or early morning [72]. Forest fuels inflammation occurs at night. Dew formation in the early morning creates unfavorable conditions for fire spreading in this period. Fires often occur only after a durable break in time after the storm [73].

In Russia, between 1992 and 2000 storm-induced forest fires equaled 37 to 53 % of the area on which fire had spread, with a relative number of 8.8—17.5 % [74]. Often dry storms, producing mass inflammations on a large space, create a very intense situation [72].

The analysis of the dependence of the forest fire number from the number of storms and population density in Finland is of interest [73]. The study was based on the data on storm-induced forest fires from 1985 to 1992 and from 1996 to 2001. The average population density in Finland is around 15 people per 1 km^2; it is more than in other Northern regions. Storm-induced forest fire spots that are unnoticed may lead to a large ecological damage. The formula for evaluating the proportion of the unnoticed forest fire spots to their total number has the following outline [73]

$$p_i = (1-B)\left(1-\frac{C}{a_i}\right)^{n_i},$$

where p_i — the proportion of forest fires caused by storm discharges in i municipality; B — the probability that a municipality non-resident will inform of the fire; C — the area on which one resident may notice the fire spot (is of the same importance for different municipalities, $C = 1000$ m^2 [110]), a_i — the area of i municipality, n_i — the number of individual representatives of the municipality.

It is also possible to estimate the number of lightning-induced forest fires registered in i municipality [73]:

$$e_i = \left(\sum_{j=1}^{k_i}\frac{r_{ij}}{(1-p_{ij})}\right)\frac{f_i}{\sum_{j=1}^{k_i} f_{ij}}(1-p)_i,$$

where k_i — the number of j municipalities; r_{ij} — the number of registered storm-induced fires in j municipality; p_{ij} — the probability that the forest fire in j municipality will be registered; f_i — the area of forested area in i municipality; f_{ij} — the area of forested area in j municipality[73].

The deviation of the estimated number of forest fires from the recorded one is determined by the formula [70]

$$D = \sum r_i \ln \frac{r_i}{e_i m},$$

where m — a modifying factor that is calculated as the relation of the sums of the registered and estimated storm-induced forest fires.

Other values that were determined are [73]: the distribution of the registered storm-induced forest fires according to the years of the period in question and their average, the number of the registered storm-induced forest fires for each day of the fire danger season during 14 years (Figures 1.10—1.12). The same densities of the storm-induced forest fires as in Sweden were acquired [75]. This result is predictable since the climate, vegetation, population density are similar in both countries.

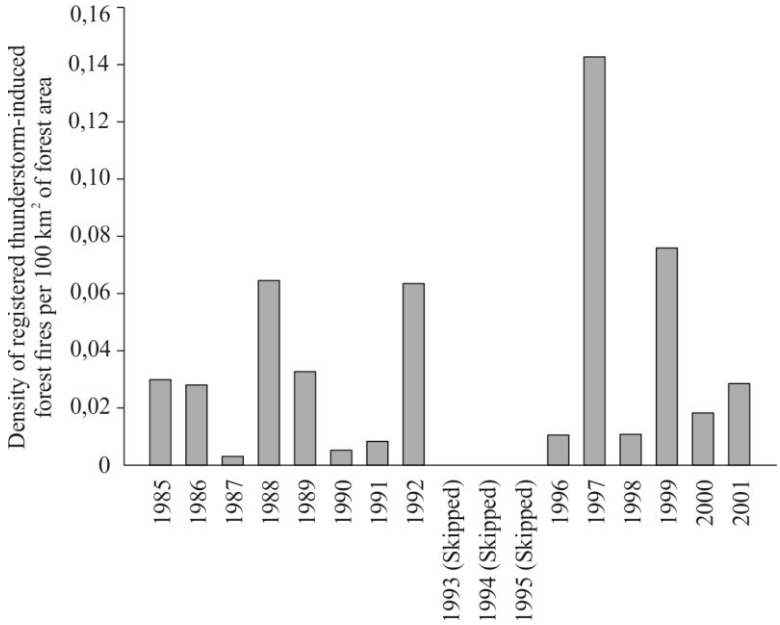

Figure 1.10. The density of the storm-induced forest fires on the forested area of Finland [73]

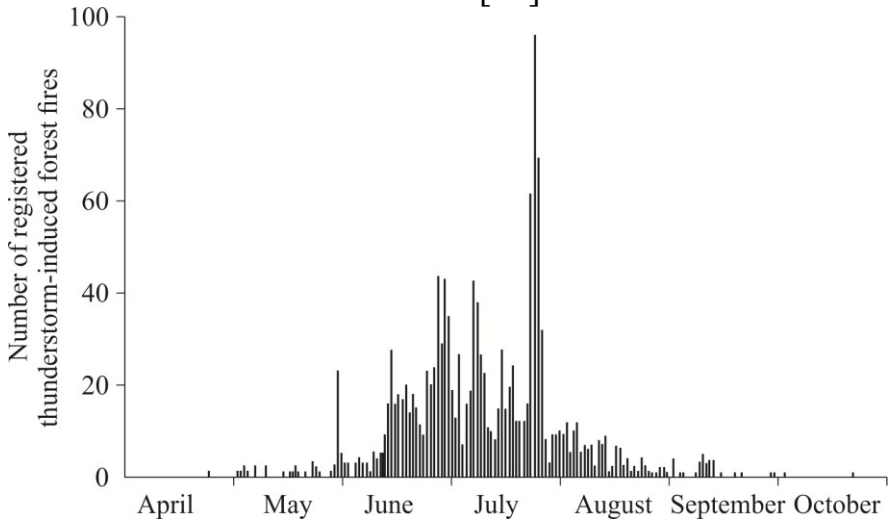

Figure 1.11. The number of the registered storm-induced forest fires for every day of the forest danger season during 14 years in Finland [73]

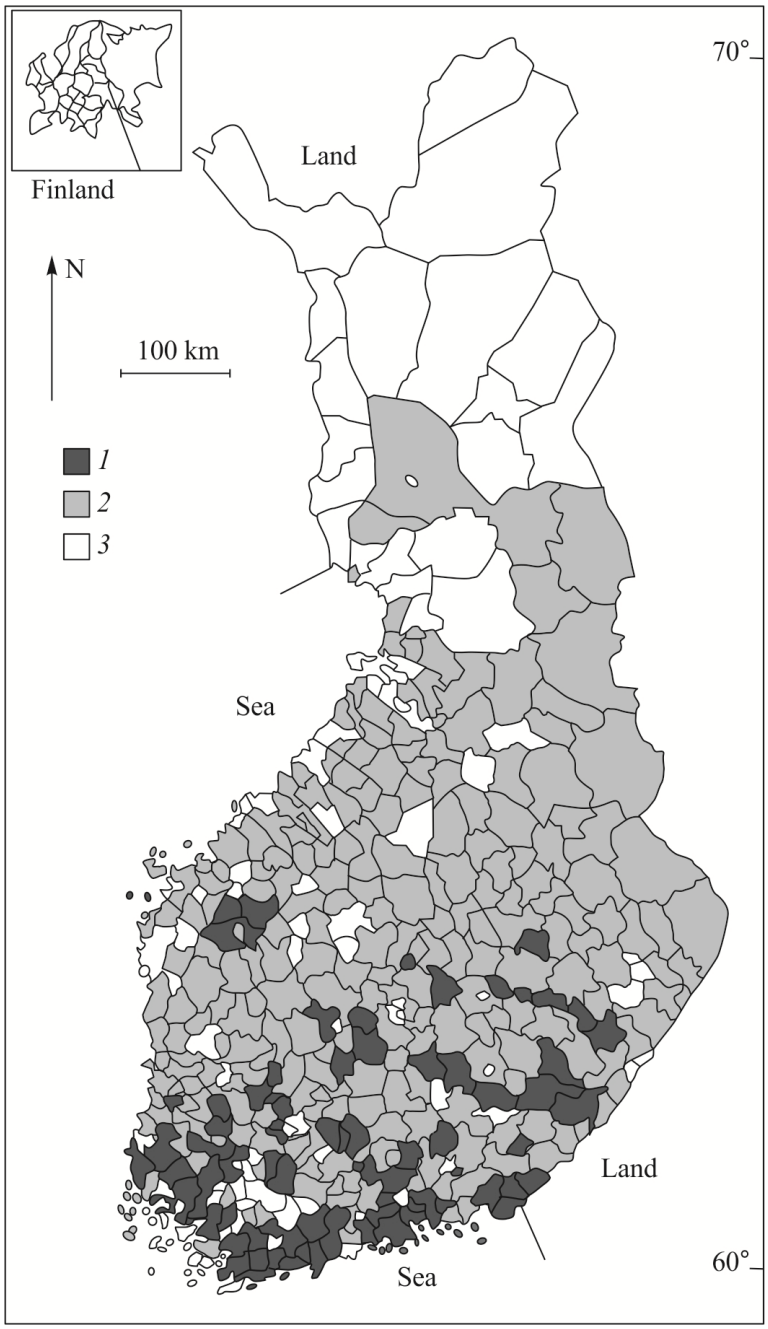

Figure 1.12. The average number of storm-induced forest fires registered annually per 100 km^2 of Finland's forested area [73]:
1 — 0.1—1.1; *2* — 0.01—0.1; *3* — 0—0.01.

In Northern Finland (higher than 65° of North latitude) the storm-induced forest fire was 6 times higher in the period from 1924 to 1927 than from 1985 to 1992 and from 1996 to 2001. [73]. It is possibly conditioned by the large variation of the forest fire incident numbers year by year [73]. For instance, the storm-induced forest fire density in Western Siberia varies from 0.05 to 0.1 piece/(year·100 km^2) [75]. This variation is the same or higher than that viewed in the corresponding latitudes of Finland [73]. The strong South-North gradient in the density of the registered storm-induced forest fires is conditioned by the natural reasons and does not depend on the effectiveness of their registration [73].

In the municipalities with a higher population density, a larger number (compared to the neighboring municipalities) of the registered storm-induced forest fires is recorded (Figure 1.13). The regressive linear model that describes this tendency has an outline of [73]

$$y = 0{,}11x + 0{,}037. \qquad (1.1)$$

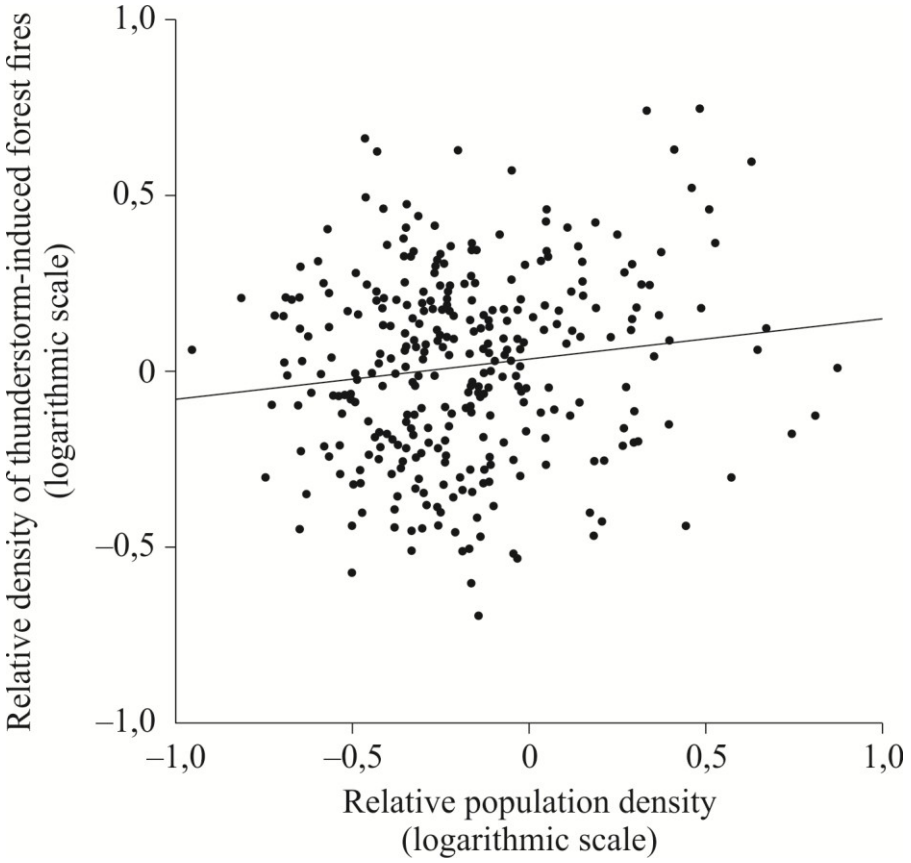

Figure 1.13. The dependency of the relative density of registered storm-induced forest fires on the relative population density (dots instead of the regressive curve of the first range). The horizontal axis counts the values of the relation of the population density of the municipality under study to the population density of the neighboring municipalities. The vertical axis counts the values of the relation of the registered storm-induced forest fires in the municipality under study to their number in the surrounding municipalities. The municipalities that did not register any fires (17 % total) are excluded from the analysis [73]

Only 16 % of the density variation of the registered storm-induced forest fires is explained by the dependence on the population density [75]. In practice, Model (1.1) may be used for calculating the maximum probability of evaluating the occurrence of non-registered storm-induced forest fires [75].

A study of the spatial distribution of storm-induced forest fires on the Ontario territory is exponential [76]. A fairly long period of time was analyzed: from 1976 to 1998.

Two areas were studied: a) the territory of all the Ontario Province and b) a rectangular region on the North-West of Ontario (a higher spatial resolution compared to the remaining territory). Storm-induced forest fires make 35 % of all the registered fires in Canada, moreover, the area on which fire was spread makes 85 % [77]. Each report on the registered forest fire incident contains: the fire location, the area burnt, forest type, weather conditions, the reason (storm or anthropogenic activity), and also information on fire liquidation. The total number of the forest fires analyzed was 40 000 (17 000 of which were storm-induced) [76]. The methods of spatial statistics (SPP-analysis) enables distinguishing clusters with the highest probability of storm-induced forest fire occurrence. Important measures in SPP are the space intensity (determined as the number of incidents per area unit) and NBS — nearest neighbour statistic (determines how close the incidents are one from the other) [76].

The set of incidents under study is fully spatially random, if the intensity is constant and the incidents are not united into clusters, not located with regular intervals. If both conditions are satisfied, then the events have a homogenous spatial distribution. There are two ways to avoid the random spatial location of the events. Clustering implies that the events are close to one another. In another case, their random spatial distribution is implied. Regularity implies a higher independence of the events.

NBS, that is called *K*-function, may be used for determining the type of event distribution — random, clustered, or regular [76]. $K(h)$ is determined as [76]

$$\lambda K(h) = E$$

(the number of events within the distance of h from a certain event),

where λ — the intensity of the average number of events per area unit, $E(\cdot)$ — expectation operator. If A is the size of the area under study, then the expected number of events in this area is λA. The expected number of the ordered pairs of events on the distance smaller than h is $\lambda A \times \lambda \hat{K}(h) = \lambda^2 A K(h)$. If d_{ij} is the distance between i and j events (firest) in A area and $I_h(d_{ij})$ is the indicator function функция (1, if $d_{ij} \le h$, otherwise 0), then the number of ordered pairs of events with a distance less than h in the area under study is $\sum_{i \neq j} \sum I_h(d_{ij})$.

Consequently, the evaluation $\hat{K}(h)$ is determined by the formula [76]

$$\hat{K}(h) = \frac{1}{\lambda^2} A \times \sum_{i \neq j} \sum I_h(d_{ij}).$$

Here $\lambda \approx \frac{n}{A}$, where n — the number of events[114].

The spatial intensity may also be calculated by using a kernel-evaluation [78]. For a random process $K(h) = \pi h^2$. A clusterized process will be at $K(h) > \pi h^2$. A regular process will be at $K(h) < \pi h^2$. Function [76] is used for visualization:

$$\hat{L}(h) = \sqrt{\frac{\hat{K}(h)}{\pi}}.$$

Figure 1.14 presents $\hat{L}(h)$ dependency for 1976 to 1998. The hypothesis on the random distribution of fire forests, according to [76], does not reflect the forest fire condition fully. There are two reasons to suppose both hypotheses — clustering and regularity. One of the reasons that storm-induced forest fires may be united into clusters is a spatial localization of storm events. The second reason for clustering is the spatial localization of vegetation, climate, and daily weather conditions (Figure 1.15).

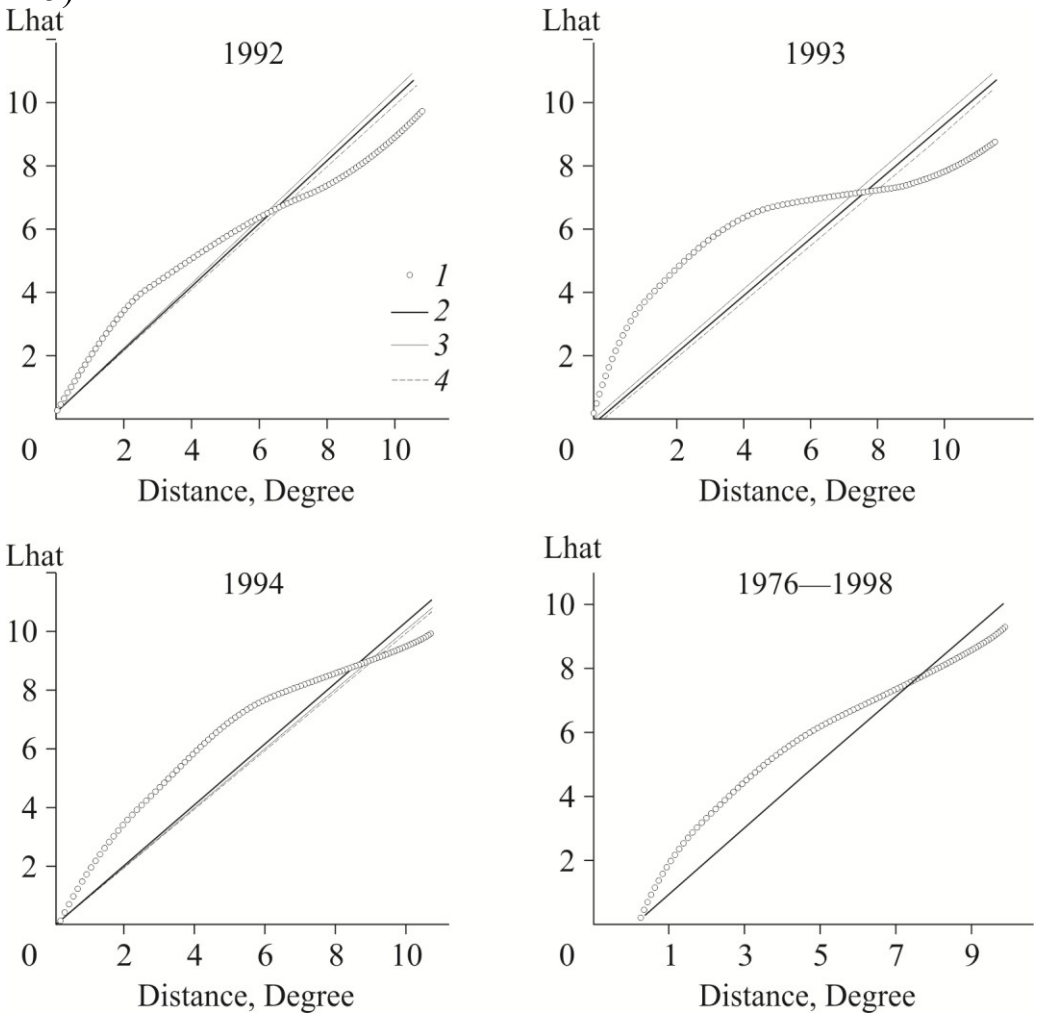

Figure 1.14. $\hat{L}(h)$ dependency on storms for forest fires on the Ontario territory in different years and on average within 1976 and 1998 [76]. The clustering peak is located around 3° and the regularity starts at 6°.

1 — Lhat, *2* — Average, *3* — Upper, *4* — Lower

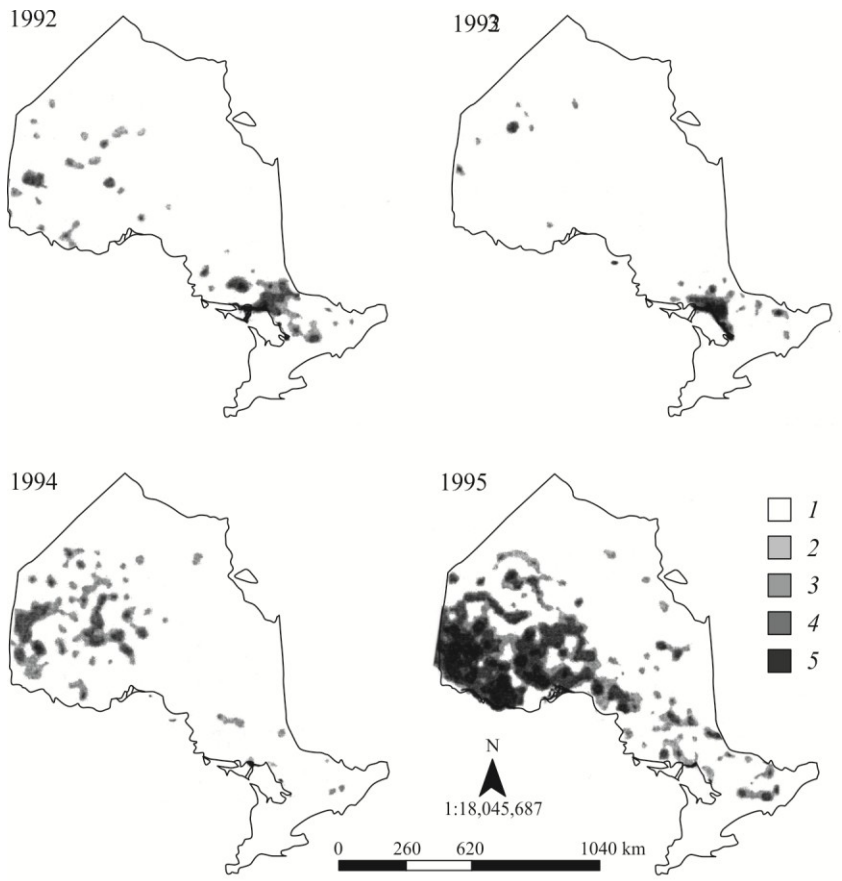

Figure 1.15. The spatial intensity of storm-induced forest fires on the Ontario Province territory in 1992—1995 [76].
The density of storm-induced forest fires, per 1 km^2: *1* — 0.001; *2* — 0.001—0.002; *3* — 0.002—0.004; *4* — 0.005—0.01; *5* — 0.01—0.025.

Clustering is revealed on the scales of 225—375 km. On larger distances there is regularity in forest fire distribution is revealed [76]. Moreover, an analysis of maps with spatial intensity of storm-induced forest fires, storm discharges was carried out for forest fire danger seasons of 1992—1998 in the North-East of the Ontario Province [76]. The analysis did not discover any obvious connection between the density of storm discharges and the density of forest fire incidents. The patterns for spatial intensity of storm discharges for the days when DMC > 20, are similar to the patterns of storm-induced forest fires [76]. Therefore, localized conditions of dry weather and storms are the leading factors of spatial clustering of storm-induced forest fires [76].

The estimation of storm-induced forest fire occurrence probability in Central Spain is exponential [79]. Only 4 % of forest fires in Spain occur due to storm discharges, primarily in remote regions. [79] analysis is a part of the FIREMAP project research whose goal is to develop a fire danger evaluation index. Time and space interaction of storm-induced forest fires and templates of topography, vegetation and weather were studied.

To estimate the occurrence of storm-induced forest fires on the basis of the data on moisture content and dead forest fuels, it is potentially productive to use the Canadian and American sub-systems.

Storm-induced forest fires create a big problem in the Alps region [80]. Here storm-induced forest fires are characteristic from May to October. Their number reaches its peak in July-August (78 % of all forest fire incidents). This problem, in connection with the climate's global warming and the increase in dry season, is of great importance [80].

An opinion has been formed so far that fire fighters, especially managers, should learn the history of fire incidents in order to understand and model the spatial distribution of inflammations [81]. As a rule, fire atlases register the so-called dot, but not area, information on fires. Technologies of spatial forest fire mapping, especially of storm-induced fires, that use dot information on their occurrence are perspective [81].

For forest fires that occurred in the autonomous region of Aragon (in the North-East of Spain), it is known of the fire location, area burnt, vegetation type, weather conditions, reasons (storm, anthropogenic activity, unidentified), and also information on fire liquidation. 3131 human-induced and 2637 storm-induced forest fire incidents were considered. 1855 forest fires occurred as a result of unidentified reasons. The same hypotheses as with forest fire analysis in the Ontario Province (Canada) were accepted as the reasons for storm-induced forest fire clustering [76]. Figure 1.16 shows fire incident patterns. The vertical axis enables counting the density of inflammation spots, their number per 1 km^2. The blue color points storm-induced forest fires, while the red color points the human-induced forest fires. The patterns of forest fires with anthropogenic reasons are more widespread in space that those of storm-induced fires (Figure 1.17). The occurrence of a large number of "hot" dots on the territory under study is possible [81]. Big fragmentation of spatial distribution of forest fires is observed around mountainous regions. "Hot" dots of anthropogenically induced forest fires are concentrated in more fragmented regions and borders of forest/non-forest territories (Figure 1.18).

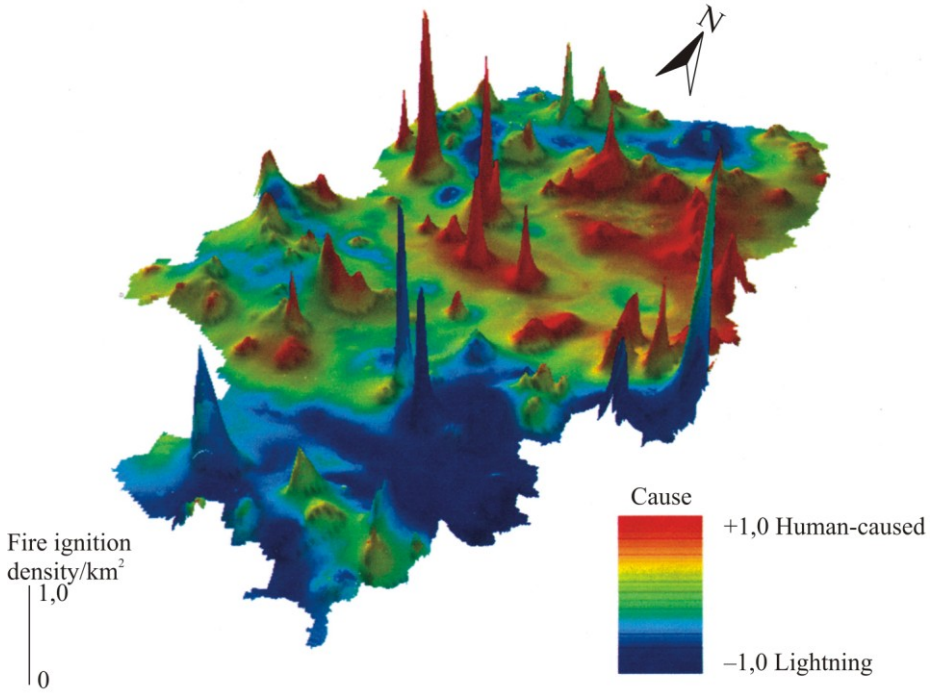

Figure 1.16. Spatial patterns of forest fire events in the Aragon's autonomy (Spain) [81]

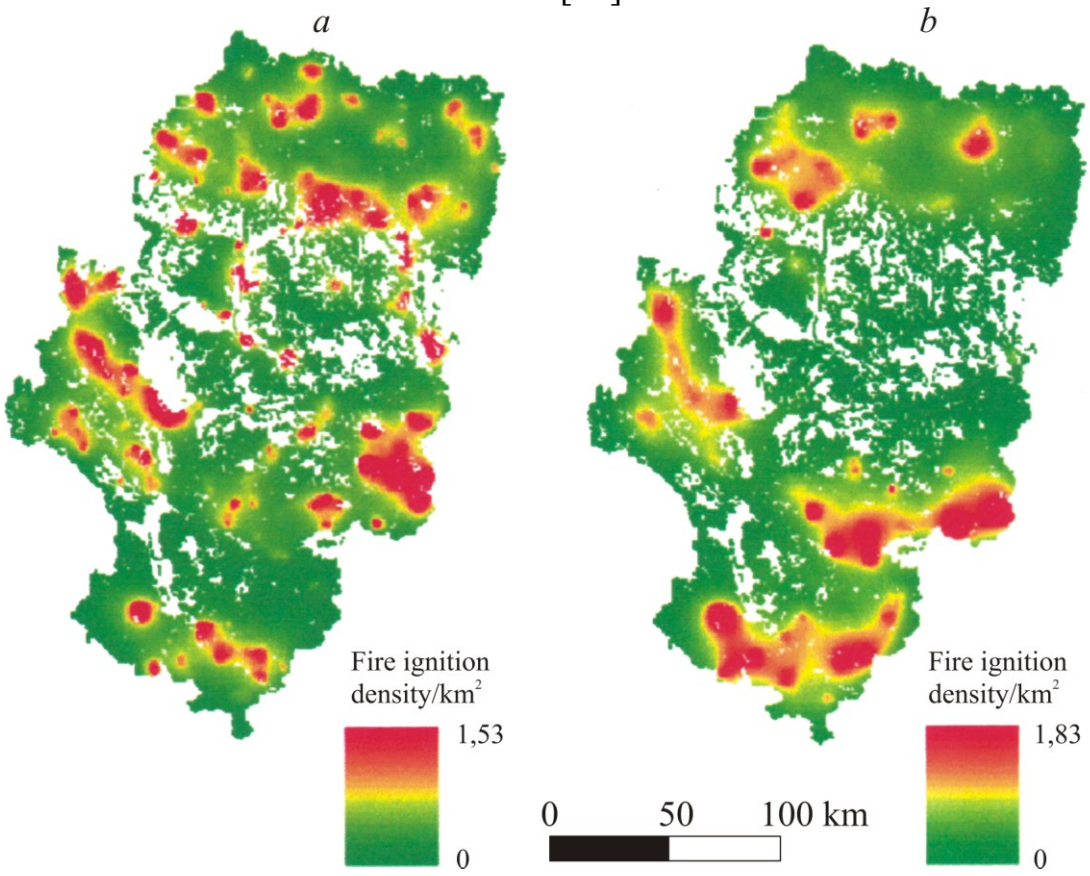

Figure 1.17. Spatial patterns of human caused (a) and lightning (b) activities in the Aragon's autonomy (Spain) [81]

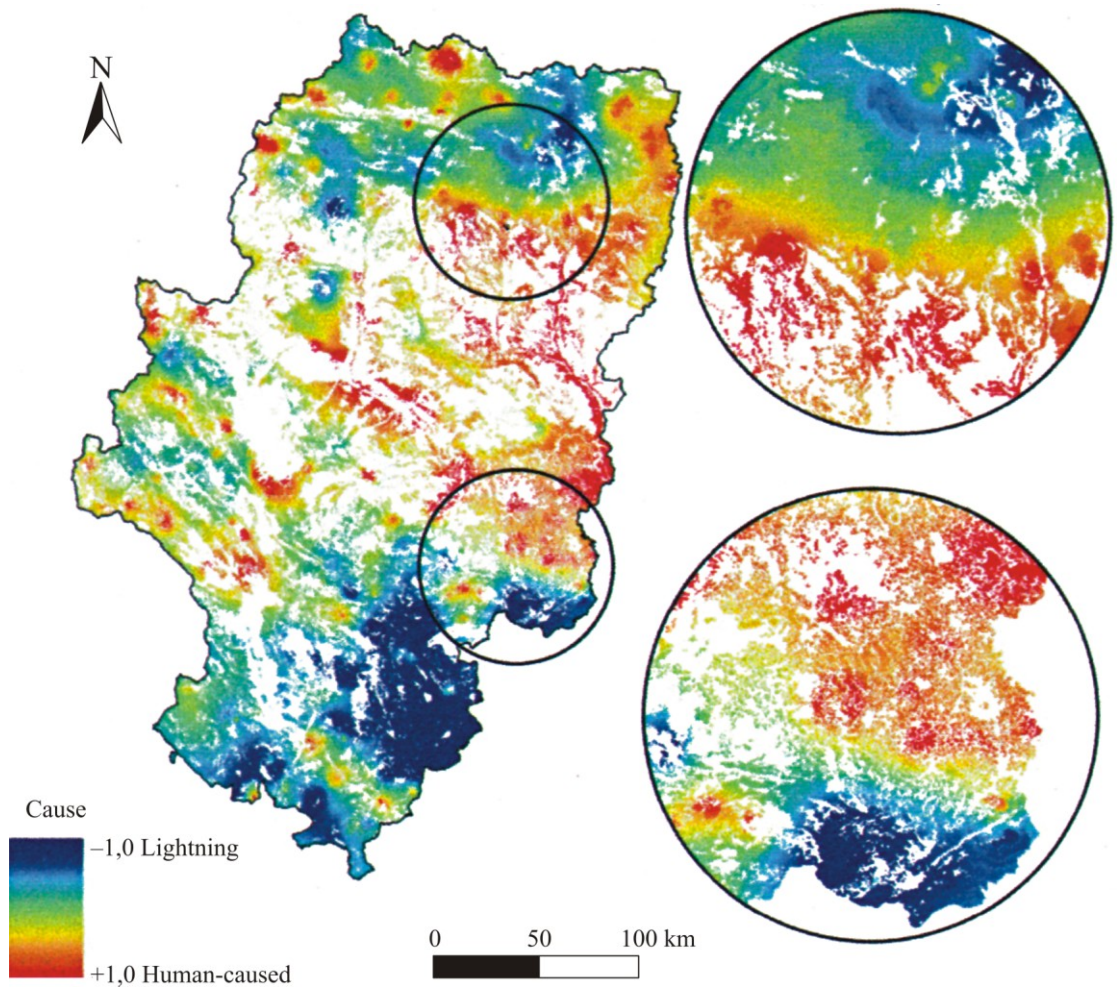

Figure 1.18. Spatial patterns of forest-covered territories in in the Aragon's autonomy (Spain) [81]

Storm-induced forest fires may occur in any forested area independent from the closeness of sources with anthropogenic load, including in poorly habitable regions. Often forest fire sources are found several days after storm. In Russia, it is only in a few regions that storm discharge registration systems operate [74].

In Russia, the statistics of storm-induced forest fires was analyzed [82, 83]. An increase in natural sources (lightnings) is predicted in connection with climate warming [84, 85]. There are examples of forest area classifications in accordance with the degree of fire danger with the use of satellite data to estimate the forest fire danger from storms [86]. The region under study included the Evenk Autonomous District, Krasnoyarsk Territory, the republics of Tyva and Khakassia [86]. Landscape characteristics, climate conditions and thunderstorm activity are known quite entirely for this territory (Table 1.3).

Due to the fact that in the Siberia's central regions 30 % of average annual forest fires occur as a result of storms, a system of lightning discharge registration was launched in 1997 [74]. To monitor storm-induced forest fires it is necessary to know the number of lightning discharges that come onto 1 km^2 of the earth surface, the distribution of the lightning discharge current, the intensity of thunderstorm activity (the number of stormy days per year).

In order to predict the inflammation of forest fuels by an electric discharge it is important to evaluate the possibility of lightning discharge occurrence under the conditions of storm front formation and passage. It is considered that the reason for storm-induced forest fires is the low air humidity when air masses are much heated and rising flows occur that stimulates the formation of stormy clouds [87, 88].

The mechanism for storm-induced forest fire occurrence and development is the following (Figure 1.19). In the zone of lightning current spreading it is divided into sparks that form spark sources of inflammation having a high temperature in a certain time interval (above 5000 °C) at which vegetation particles are decomposed with a formation of gaseous products. With a sufficient thickness of forest fuel layer a cumulative decomposition of vegetation particle takes place that is accompanied by the formation of a necessary amount of gaseous products that are able of composing a flammable mixture that may get inflamed. If the surrounding forest fuels have a low moisture content, the burning spot occurs. Later the fire spreads around the burning spot if the surrounding forest fuels have a moisture content below the critical level, and the amount of precipitation of the fallen rain is not enough to extinguish the burning. Further spreading of fire on the forest area leads to a fire.

Table 1.3. An average storm duration and the number of stormy days in Middle Siberia [86]

Weather station	Average storm duration, h								The number of annual stormy days
	IV	V	VI	VII	VIII	IX	X	Год	
Podkamennaya Tunguska	–	2.0	8.7	15.7	9.0	0.7	–	36.1	19
Yartsevo	0.06	3.0	10.9	17.3	10.7	1.0	0.04	43.0	25
Kezhma	0.01	1.3	6.9	13.5	6.5	0.7	0.02	28.9	17
Yenisseysk	0.1	3.0	8.5	11.9	7.4	0.9	0.06	31.9	21
Boguchany	0.02	2.2	8.8	19.3	10.0	0.6	–	40.9	23
Strelka	0.05	4.8	12.3	24.6	11.6	1.1	0.05	54.5	26
Kazachinskoye	0.01	2.8	7.8	12.7	7.9	1.3	–	32.5	23
Pirovskoye	–	4.9	12.8	23.6	12.4	1.1	0.04	54.8	26
Pokhtet	0.04	5.3	14.8	24.6	13.6	1.6	–	59.9	27
Achinsk	0.05	2.9	10.0	15.0	10.1	0.8	–	38.8	22
Kansk	0.06	2.0	7.4	14.8	7.2	1.0	0.01	32.5	17
Krasnoyarsk	0.05	3.0	7.5	14.8	8.4	0.7	–	35.5	23
Uzhur	–	5.1	11.6	25.4	15.0	1.3	–	58.4	20
Shira	–	1.2	9.4	17.9	11.7	1.3	–	41.5	19
Minusinsk	0.1	1.3	5.7	9.8	5.8	0.7	0.03	23.4	20
Tashtyp	0.01	2.8	10.0	18.0	10.6	1.0	0.06	42.5	25
Olenya Rechka	0.2	2.2	17.7	34.7	26.2	3.4	0.02	59.8	25
Nizhneye Usinsk	0.1	2.2	17.7	34.7	26.2	3.4	0.02	84.3	37
Chada	0.01	0.9	10.2	27.3	22.9	3.2	–	64.5	31
Erzin	0.04	1.0	8.6	25.7	15.7	1.1	–	52.1	25

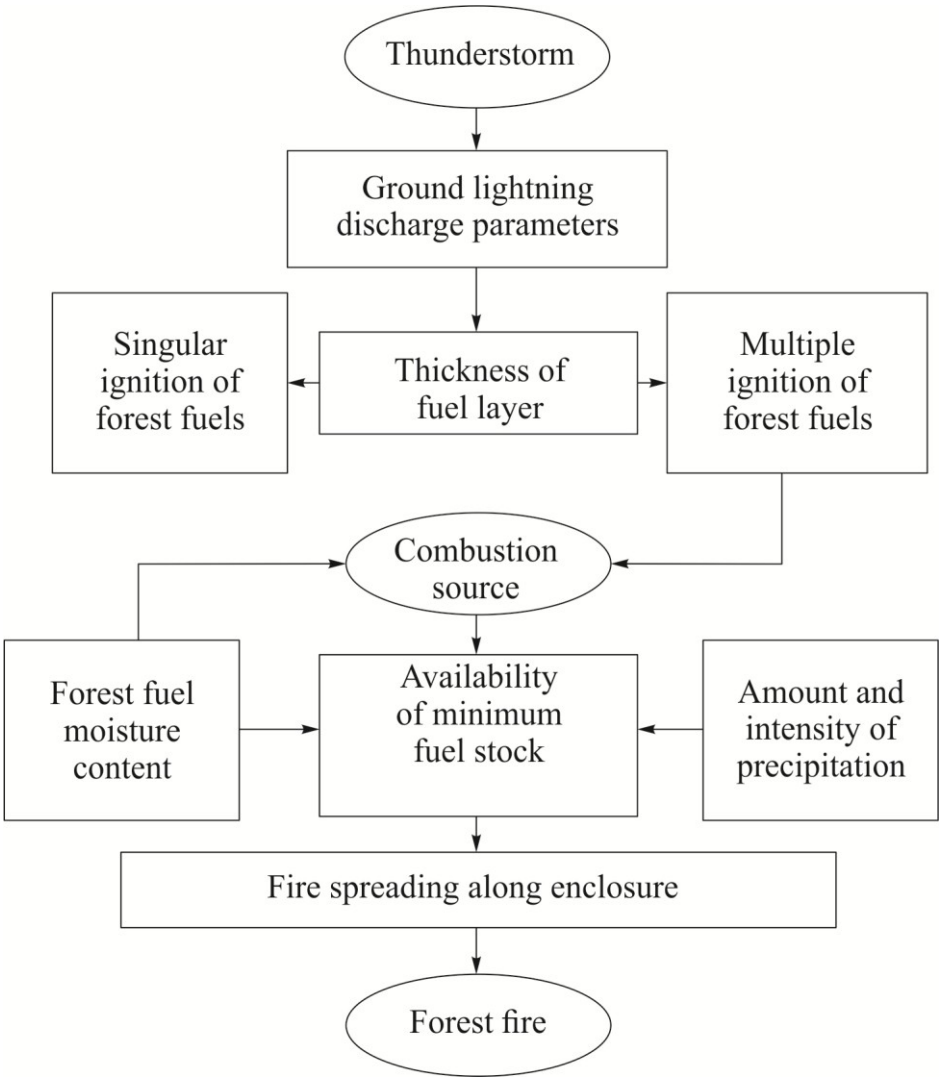

Figure 1.19. A chart of storm-induced forest fire occurrence [86]

The most informative characteristic of lightning discharge occurrence is the difference between the particle's temperature raised moist-adiabatically from the level of 850 to 500 hPa, and the real air temperature on a top level [86]. The use of this regularity enables to record the so-called storm index. This index determines the possibility for realizing such weather conditions in which storm electric discharge is possible.

A mathematical model of the storm index may be presented in a form of a sum [86]:

$$K = \mu \sum a_i X_i, \qquad (1.2)$$

where X_i — information fields (of temperature), a_i — weight coefficients, $\mu = 1/(1 + b \cdot T_з)$ — normalization coefficient that reflects the value of air temperature in the surface layer ($T_з$). The coefficient of correlation with the statistical data was chosen as the significant criterion of authenticity. The (1.2) relation took the outline of [89] after optimization:

$$K = \frac{1}{1-0,8T_з}(2,3T_{850} + 2,1T_{500} - 1,8D_{850} - 2,3D_{700}),$$

where T and D — the air and dew point temperature on the corresponding levels acquired from the TOVS radiosonde.

The method of evaluating the storm index [86, 89] is based on the sounding data from the atmosphere acquired by the TOVS appliance (Figure 1.20) that can be recorded up to four times a day from a non-regulated dot network with an interval from 17 to 100 km. The parameters of the lower atmosphere may be interpolated at a radius of up to 200 km. Information layer that allows classifications of the territory on the basis of the storm index, along with the outline map of fire danger in accordance with the weather conditions [90] provides an opportunity to evaluate forest fire danger on the basis of natural factors.

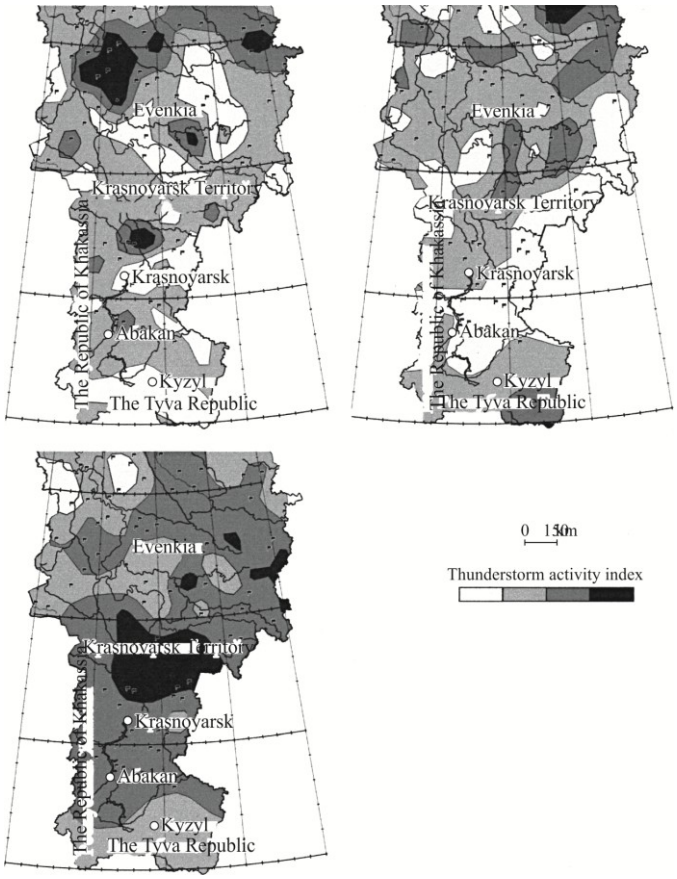

Figure 1.20. The dynamics of storm index on the Middle Siberian territory in different observation periods according to TOVS appliance from American satellites NOAA, 2001 [89]

The sounding locations of the atmosphere are marked with checkboxes. Black color corresponds to the storm index's maximum.

1.6. Anthropogenic Load

A necessity to use the data on the presence of fire sources for evaluating forest fire danger was already recorded by I. S. Melekhov [91]. An increase in urbanization level, recreational load lead to changes in forest ecosystems, also in the results of forest fire effect. An analysis of social and psychological aspects of the recreational visits to the forests and forest fire occurrence was made [92]. It was estimated that the higher the distance from the settlement is, the fewer are the visits to the forest and the number of forest fires [93, 94] in accordance with Rayleigh and Poisson distributions [95]. One of the main components of the anthropogenic load is recreation (leisure) on forested areas. Predicting the value of recreational loads on the forest, the time and specific places of visitation will allow solving some questions not only regarding planning and organizing mass leisure of the population, but also regarding preventing forest fire occurrence, the increase in promptness of their discovery and extinguishing [92]. In geographical studies on population migration, different mathematical models are used. Some of them were tested for the description of forest fires in relation with rural settlements [96]. It turned out that functions of density probabilities of logarithmically normal distribution and the Pareto type function may be also be used with this purpose. Studies for forest fire distribution are mainly connected with seasonal regularities of their occurrence. Fire distribution according to week days is far less studied. In the regions of mass tourism and leisure, 51% of disturbance of the preventive fire-fighting regulations occur in forests [97] on holidays and weekends , whereas 36—41 % such disturbances [98, 99] occur in the regions of industrial forest land use. A typical distribution of fires according to the week days (in the Timiryazevskoye forestry) is given on Figure 1.21.

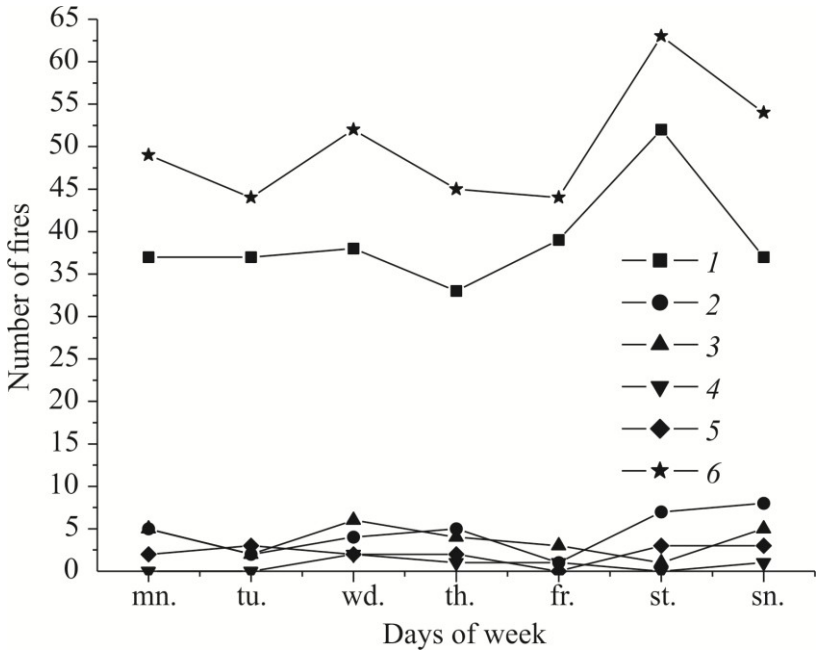

Figure 1.21. The distribution of fires according to week days in the Timiryazevskoye forestry, Tomsk Region, between 1994—1998 [22]. Forestries: *1* — Timiryazevskoye, *2* — Moryakovskoye, *3* — Bogorodskoye, *4* — Kireyevskoye, *5* — Zhukovskoye, *6* — total of all forestries

The biggest number of fires occur on Saturdays. More fires are discovered in the second half of the day (2-4 p.m.) — 25 %, fewer — in the night and early morning.

The results of sociological surveys sometimes explain some data on fires that occurred in a specific region [92].

The process of evaluating the information and decision making on visits to the forest depends on many factors, among which the following are distinguished: the social and natural environment where the one who will make a decision on visiting the forest is found; the impact of psychological laws of behavior. The process of decision making on the whole may be illustrated with a chart (Figure 1.22).

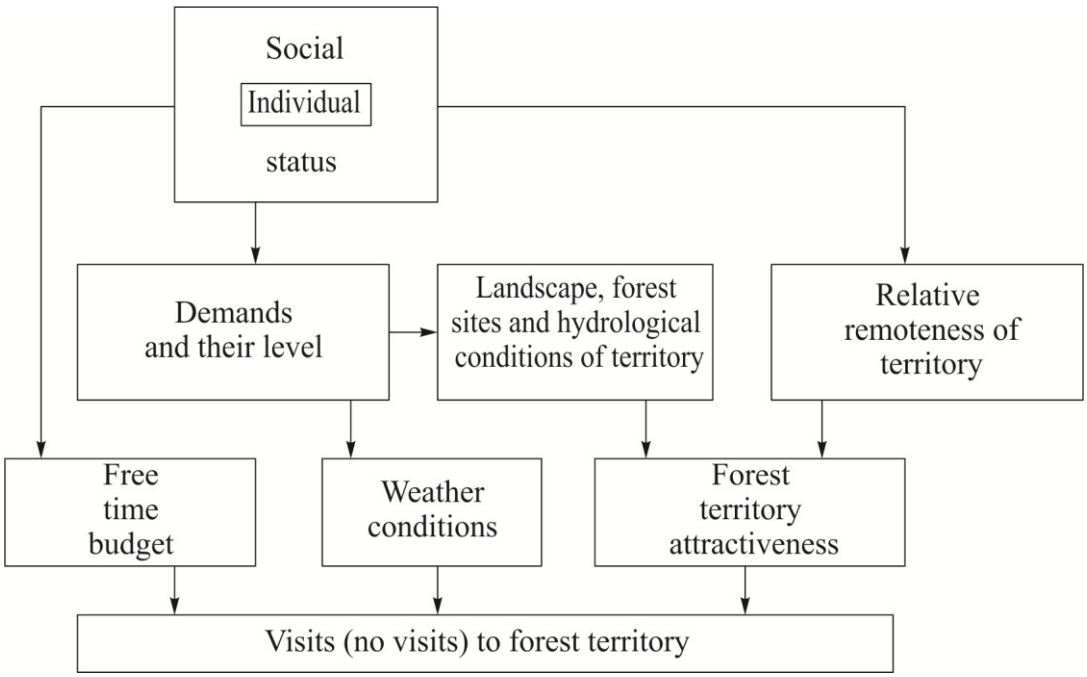

Figure 1.22. A chart of the process of a subject's evaluating the information and making a decision on visiting a forest territory [92]

With an increase of the number of dwellers, a probability of fire occurring near settlements also increases. The coefficient of fire danger visitations shows the frequency of visits (per 1000 residents per day) leading to the occurrence of one fire. An settlement's fire danger visitation index may be acquired from here [92]. The distribution of fire sources on the territory and in time is similar to the distribution of forest fires and is annually reproduced with only a slight deviation from the multiannual average [100].

Careless handling of fire serves a reason for 81.85 % of fires. Unidentified reasons may also be counted as careless handling of fire. All the other reasons are less than 10 %. A storm discharge (1.4 %) and an incendiary crime (1.4 %) are the weightiest of them [101].

The main anthropogenic sources for inflammation are single warmed to high temperatures metal and non-metal particles [102]. Such particles are formed and travel at a distance from several tens of centimeters to tens of meters as a result of

being blown by the wind of not extinguished bonfires, transport of burning particles form fire front, welding and or metal arc cutting. Social factors affect the occurrence of forest fires. For instance, 93 % of all the fires in the national forests of Minnesota, Wisconsin and Michigan occurred due to human fault in 1986 [103]. During the factor s under question such questions as state characteristics, the density of car and rail roads, the distance to a territory not covered with forests, distance to a city, population density, etc. [103]. On forest areas with a higher degree of population density, car and rail roads, the level of fire danger is higher. An increase in human access to a forested are increases the probability of forest fires.

GIS-analysis of time and space models of forest fires of the 1950—1992 seasons that were caused by anthropogenic reasons in the forests of Vancouver island (Canada) is demonstrative (Figure 1.23).

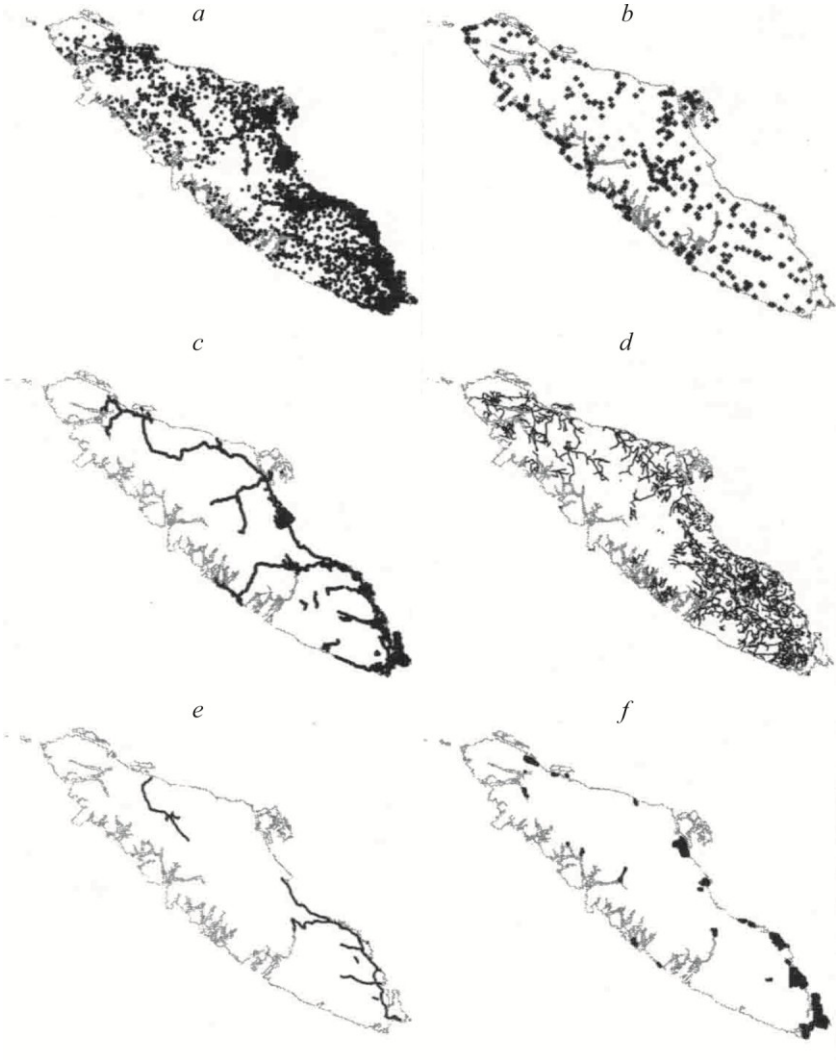

Figure 1.23. An interconnection of forest fires and infrastructure by the example of Vancouver Island[104].

a — human-induced forest fires, *b* — camping sites and camps, *c* — pave ways, *d* — country roads, *e* — rail roads, *f* — municipalities.

6329 forest fire inflammations were analyzed (Table 1.4, Figure 1.24, 1.25). Arc/Info and Arc View GIS software was used. The investigation area was divided into 36050 cells. A logical regressive model was developed [104]:

$$P_i = \frac{1}{1+e^{-z}},$$

$$z = \beta_0 + \beta_1 X_1 + \beta_2 X_2 + ... + \beta_\rho X_\rho,$$

where P_i — the probability of forest fire occurrence in i cell, z — the linear combination of independent variables with weight coefficients of β, X_i — the value of the independent variable for a certain cell. The following factors are used as independent variables: an average amount of summer precipitation, the average temperature of July, the distance from the middle of each cell to the closest object of infrastructure. The model coefficients are acquired with the regressive analysis.

Table 1.4. The reasons for forest fire occurrence from an anthropogenic load on Vancouver Island [104]

Fire cause	The number of fires	Area burnt, ha	
		Total	Average (per fire)
Mixed	2567	17370	6.8
Recreation	1809	4462	2.5
Logging	1021	20927	20.5
Soil clean-up	512	966	1.9
Rail road	189	276	1.5
Other industrial sources	120	954	8.0
Tracks	104	2650	25.5
Not identified	7	8	1.2
Total	6329	47613	7.5

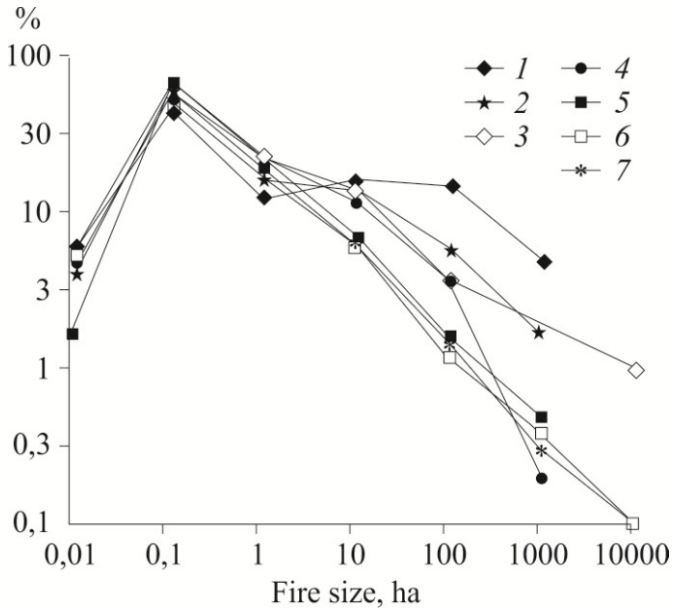

Fig. 1.24. Distribution of forest fires of different size occurring for various anthropogenic reasons [104].

1 — logging; *2* — other industrial sources; *3* — tracks; *4* — soil clean-up; *5* — rail road; *6* — recreation; *7* — mixed reasons.

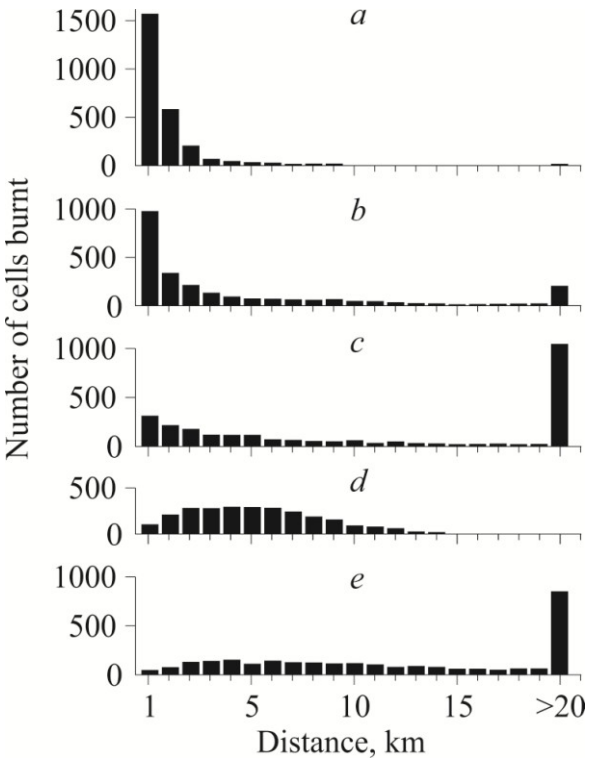

Figure 1.25. The number of burnt cells of the forested are of Vancouver Island in dependence from the distance to the infrastructure objects [104]

See explanations in text.

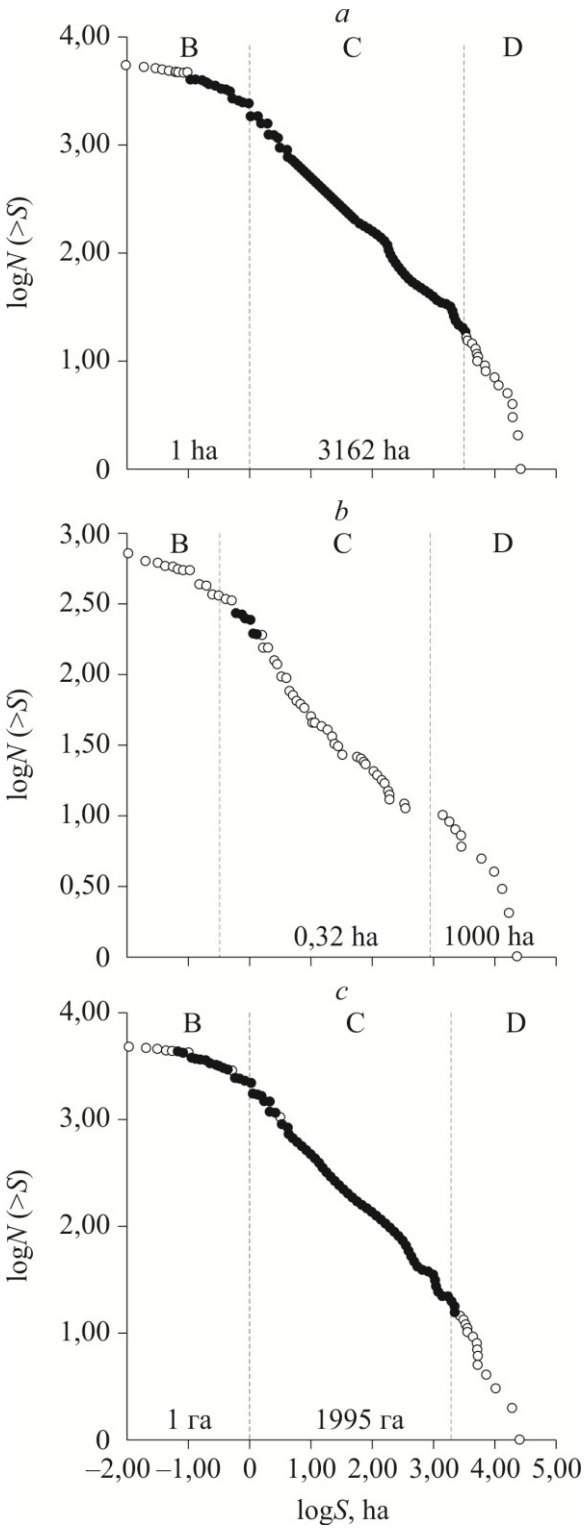

Figure 1.26. The dependency of the logarithm of the N fire number with an area over S ($N > S$) of S area [106]

The number of the burnt cells is closely connected with the closeness of country roads, paved roads and rail roads and decreases with the increase of the distance from them (especially from country roads) (see Figure 1.25, *a*). The number of burnt cells increases with a distance from camps and camping sites reaching is maximum at a distance of 5 km from their location, but it decreases with the following distancing (see Picture 1.25, *d*). A big number (the difference with the nearby territories is by one order and more) of cells burn down at a distance of more than 20 km from paved and rail roads, of Vancouver municipalities (see Figure 1.25, *b*, *c*, *e*).

The frequency and reasons for fires are mainly conditioned by the level of urbanization of the territory and, consequently, the level of the anthropogenic load. The anthropogenic load onto a forested area is determined by the number of settlements and their population [105]. With an increase in population density, the forest flammability in relative values increases [12] (Table 1.5). This connection for the total of the European countries is characterized by the correlation coefficient of 0,84 and is expressed by the equation [12]

$$Y_1 = 3 + 0,128X,$$

where X — number of people per 1 km^2, and Y_1 — the annual number of fires per 100 thousand hectares of the forest area.

The number of campers and hunters increases the summer maximum of fires that is connected with the distance to the settlements and transportation ways [12].

Forest fire distribution connected with the remoteness from the transportation ways is described by the exemplifying function [95]

$$P_{N_0}(x) = \lambda e^{-\lambda x},$$

where N_0 — the number of forest fires, $P_{N_0}(x)$ — the density of distributional probability of N_0 per x (x — distance), and with remoteness from settlements— by the laws of Rayleigh [95]

$$P_{N_0}(x) = 2\pi\lambda x e^{-\pi\lambda x^2}$$

and Poisson

$$P_{N_0}(x) = \frac{[M(x)]^x}{x!} e^{-M(x)},$$

where $M(x)$ — the mathematical expectation of the distribution, that corresponds to the average remoteness of fires from settlementsв. In order to evaluate the fire distribution from a settlement, it is important to know, how many fires are caused by its dwellers. The connection between the number of fires N and the number of dwellers in a separate settlement P, thousand people, is expressed with the equation [96]

$$N = 0,28P + 3,46. \qquad (1.3)$$

The interconnection between the N number of forest fires on the x distance from forestry location and the n number of settlements on this very distance is expressed with an equation [96]

$$N = 2,53n + 2,31. \qquad (1.4)$$

It follows from the reason analysis that the countries with a smaller population density the number of fires increases in the process of territory development. The more distant from settlements and transportation ways, the lower the fire number; their average size increases logically.

The number of forest fires along with other factors may be determined not only by the population density in the region, but also its territorial distribution (Table 1.5). In regions with the same population density, the same area and other equal conditions, but different number of settlements, the number of fires will be different [96]. By uniting the equations (1.3) and (1.4) another equation is produced that describes the dependence of the fire number on the numbers of dwellers and settlements [96]:

$$N = 2,6\sqrt{(n+0,91)(n+0,08\Sigma P)}.$$

Large scale effects of forest fire occurrence induced by the anthropogenic load (and example of the Mediterranean part of the Iberian Peninsula between 1989 and 2003) are possible [106] (Figure 1.26).

Table 1.5. Forest flammability (1952—1954) in some countries in connection with the population density [12]

Country	Population per 1 km^2 (1949—1956)	Number of fires per 100000 ha	Average fire area, ha	Relative flammability, %
Finland	14	1.3	15.5	0.015
Sweden	18	3.3	1.1	0.004
Ireland	43	18.1	10.2	0.173
Spain	55	3.4	13.0	0.063
France	77	15.7	12.3	0.233
Austria	83	4.4	1.3	0.003
Portugal	89	29.8	15.9	0.058
Italy	155	11.7	9.9	0.213
Federal Republic of Germany	196	23.7	1.3	0.033
Britain	207	27.3	1.6	0.045
Belgium	284	23.0	2.2	0.062
Netherlands	317	55.9	1.3	0.080
Turkey	31	9.6	35.7	0.306
Israel	73	32.4	23.4	0.518
USA	20	48.3	14.3	0.678
Australia (New South Wales)	42	17.0	316.7	3.55
Canada	2	0.3	78.4	0.025

The Mediterranean part of the Iberian Peninsula. B corresponds to minor fires (0—1 ha), C — medium (1—2000 ha), D — large forest fires (over 2000 ha). *a* — information on all the forest fire number; *b, c* — for human-induced forest fires and natural reasons correspondingly.

1.7. Weather conditions and the models of numerical weather forecasting

Meteorological parameters are an important factor of forest fire danger [107]. The main parameters include: temperature, humidity, pressure and atmospheric density, the rate and direction of wind, radiative flows of energy, the amount and intensity of precipitation, the temperature and moisture of soil, etc. [108].

As a rule, for forest fire danger prediction the data of meteorological parameter registration stations are used [109] or the data of TOVS satellite sounding [90]. For scenario modeling [110] reference information is used [111].

It must be mentioned that the weather station network in Siberia, the North and Far East is underdeveloped. However, in the recent years quite developed mathematical models of the atmosphere [112] and climate [113] have been introduced. The physical-mathematical approach gains a higher degree of importance in meteorology at present. Mathematical methods enable creating complicated models and predict further development of atmosphere processes; they are widely used now in the practice of real-time weather forecast [108]. The forecast success rate of short-term forecast is high and approaches 90 %. The accuracy of long-term forecasts is supposed to be increased when using the hydrodynamic method and creating on its basis complex models of general atmospheric circulation [108].

An important factor in weather forecast is the ability of the models to interpret the local conditions. Deviations in the output data of the numerical weather forecast may appear due to various reasons like incorrect calculation of subgrid parameters. To correct the output data of the numerical prediction model with a use of these observations, the regressive method is used [114].

In meteorology, probability methods are also used [114]. The *probability* term was already used in the early studies in meteorology between 1900 and 1925. [115]. The second wave of interest to probability prediction arouse in 1940—1955. [116]. The Bayes hierarchy approach enables combining information of the long-term and short-term periods of observation (for example, for the recently opened weather stations) [117].

For medium-term weather forecast models the semi-Lagrangian approach is widely used [111]. The model of shallow water in the isobaric system of coordinates [118], i.e. σ-level with a preset value of pressure is recorded and equations in the system of coordinates are considered (λ, φ). A two-dimensional model may be extended for a three-dimensional case with the use of a vertical σ coordinate ($\sigma = p/p_s$, p — air pressure, p_s — ground-level pressure) and a matched network of direct backward transforming the standard isobaric levels into values of virtual temperature [119] on σ levels and surface pressure [120]. The arrangement within the limits of the shallow water model is formed the following way [118].

Equation of vorticity potential:

$$\frac{d}{dt}\left(\frac{\varsigma + f}{\Phi - \Phi_s}\right) = 0.$$

Equation of momentum:

$$\left(\frac{d\mathbf{V}}{dt}\right)_H = -\nabla\Phi - f\,\mathbf{k}\times\mathbf{V}.$$

Equation of nonseparability:

$$\frac{d(\Phi-\Phi_s)}{dt} = -(\Phi-\Phi_s)D,$$

where ς — relative vorticity; Φ — atmospheric density; f — Coriolis parameter; D — divergence, d/dt — Lagrangian derivative, H — index of side view; $\nabla = \frac{i}{a\cos\varphi}\frac{\partial}{\partial\lambda} + \frac{j}{a}\frac{\partial}{\partial\varphi}$ — gradient operator on a sphere; λ — longitude; φ — latitude; $\mathbf{V}$ — vector of horizontal velocity with u and v components in the directions of λ and φ correspondingly, a — the radius of the Earth, $\mathbf{k}$ — unit vector in the vertical direction. The model problem (Fig. 1.27—1.29) considers a 48-hour interval.

The three-dimensional model is formed the following way [118].

Equation of full vorticity:

$$\frac{d}{dt}(\varsigma+f) = -(\varsigma+f)D - \frac{R_d}{a^2\cos\varphi}\left(\frac{\partial T_v}{\partial\lambda}\frac{\partial \ln p_s}{\partial\varphi} - \frac{\partial T_v}{\partial\varphi}\frac{\partial \ln p_s}{\partial\lambda}\right) -$$

$$-\frac{1}{a\cos\varphi}\left(\frac{\partial\dot{\sigma}}{\partial\lambda}\frac{\partial v}{\partial\sigma} - \cos\varphi\frac{\partial\dot{\sigma}}{\partial\varphi}\frac{\partial u}{\partial\sigma}\right) + F_\varsigma. \quad , \qquad (1.5)$$

Equation of momentum:

$$\left(\frac{d\mathbf{V}}{dt}\right)_H = -\nabla\Phi - R_d T_v \nabla \ln p_s - f\,\mathbf{k}\times\mathbf{V} + \mathbf{F}_V. \qquad (1.6)$$

Hydrostatic equation:

$$\frac{\partial\Phi}{\partial \ln\sigma} = -R_d T_v. \qquad (1.7)$$

Equation of nonseparability:

$$\frac{d \ln p_s}{dt} + D + \frac{\partial\dot{\sigma}}{\partial\sigma} = \upsilon. \qquad (1.8)$$

Equation of power:

$$\frac{dT}{dt} - \frac{R_d T_v}{c_{pd}[1+(\delta-1)q]}\left(\frac{\dot{\sigma}}{\sigma} + \frac{\quad}{dt}\right) = F_T. \qquad (1.9)$$

Equation to determine specific humidity:

$$\frac{dq}{dt} = F_q, \tag{1.10}$$

where p — pressure; p_s — pressure at the underlying surface; D — divergence on σ level; R_d — gas constant for dry gas; T — temperature; q — specific humidity; T_v — virtual temperature ($T_v = T(1 + 0{,}61q)$); $k = R_d/c_{pd}$, c_{pd} — specific heat capacity of dry air at constant pressure; δ — the relation of specific heat capacities of humid and dry air, σ_T — the value of σ on the upper border of a model atmosphere and F_ζ, F_V, F_T, F_q describe the sources and vorticity flowoffs, momentum, heat and humidity that are conditioned by the corresponding subgrid processes.

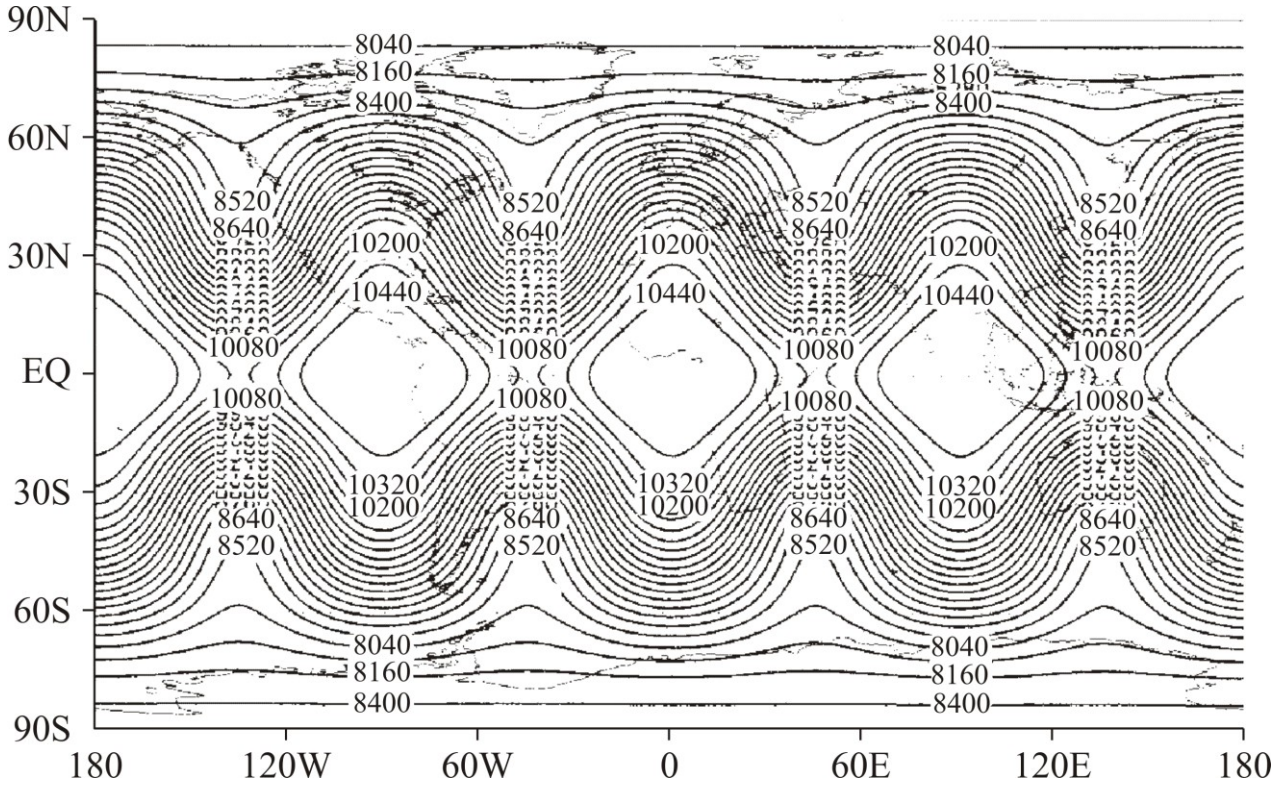

Fig. 1.27. A model problem. The initial state for the shallow water model: Rossby-Haurwitz wave [118]

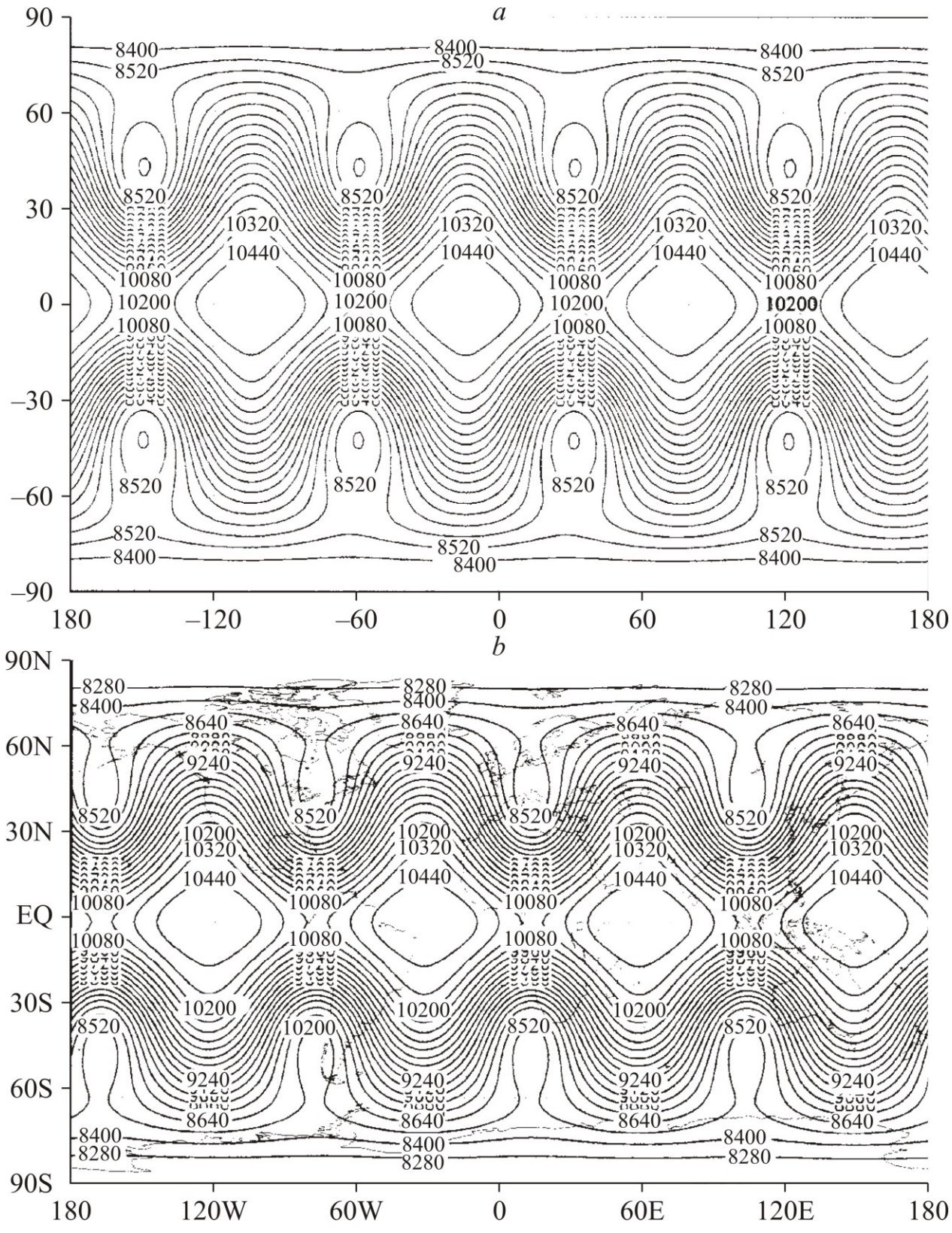

Fig. 1.28. A model problem. The evolution of Rossby-Haurwitz waveon Day 7 (*a*) and 14 (*b*) [118]

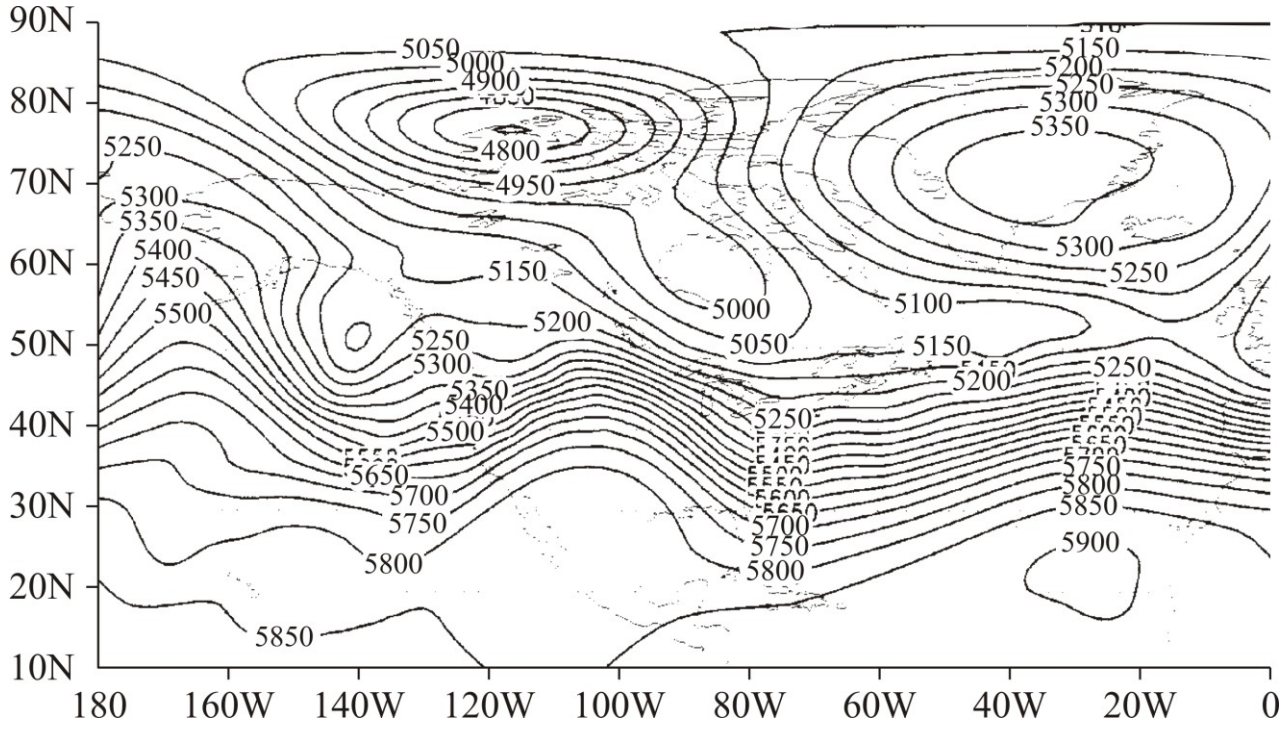

Fig. 1.29. A model problem. Geopotential prediction for 48 hours according to the initial data of 12 February 1979 (including orography) [118]

The system of equations (1.5) — (1.10) is closed by periodically boundary conditions according to the longitude and boundary conditions on the upper and lower boundary:

$$\dot{\sigma} = \sigma_T, \sigma = 1,$$

where $\sigma = p/p_s$.

The model includes a full set of process parameterizations of a subgrid scale (short- and long-wave radiation, deep and shallow convection, planetary boundary level, slowdown of gravitational waves), developed in Météo-France that is used in the French model of ARPEGE/IFS real-time forecast [121]. So far this atmosphere model version has been improved [112]. Instead of (1.6), (1.8), (1.9) equations it contains the following equations [112]

$$\left(\frac{d(\overline{V} + 2\overline{\Omega} \times \overline{r}}{dt} \right)_H = -\nabla\Phi - R_d T_v \nabla \ln p_s + \overline{F}_V,$$

$$\frac{d\left[\ln p_s + \frac{\Phi_s}{R_d T} \right]}{dt} + D + \frac{\partial \dot{\sigma}}{\partial \sigma} = \frac{1}{R_d T} \overline{V} \cdot \nabla \Phi_s,$$

$$\frac{dT}{dt} - \frac{R_{\mathrm{d}} T_v}{c_{p\mathrm{d}}[1+(\delta-1)q]}\left(\frac{\dot{\sigma}}{\sigma} + \frac{d\left[\ln p_{\mathrm{s}} + \frac{\Phi_s}{R_{\mathrm{d}} T}\right]}{dt}\right) = -\frac{1}{c_{p\mathrm{d}}}\overline{V}\cdot\nabla\Phi_{\mathrm{s}} + F_T,$$

where Φ — geopotential, Φ_{s} — ground geopotential.

This global atmosphere model is tested on a set of 12 five-day forecasts [112, 118]. The initial data were non-initialized results of the analysis on *p* levels of the European Centre for Medium-Range Weather Forecasts, cut to spectral reduction T119. To interpolate these data vertically on model σ levels, a one-dimensional variation algorithm was used [119]. The model was tested at a horizontal resolution of 1.5° in longitude and latitude and 20 staggered σ levels vertically; time step of 36 min. In the experimental data the vertices of the model system of coordinates coincide with the geographical poles. The system of parallel architecture CRAY YMP-8E of the Russian Meteorological Office was used as a numerator [112]. Figure 1.30 illustrates the analyzed and predicted pressure distribution on the sea level on 24 December 1978.

The spatial resolution of global mathematical atmosphere models is usually quite rough (ca. 40 km) [112]. One of the ways to model the regional atmosphere circulation is to use variable resolution according to the latitude and pole rotation of a spherical system of coordinates [122]. Moreover, there are no barriers to use a rough solution acquired via a global atmosphere model as the initial and boundary conditions for non-hydrostatic model of the regional atmosphere [123]. In connection with the methods of restoring the detailed structure of weather parameter fields on the city and regional levels in accordance with the predicted large-scale values of meteorological fields [124] this may provide an opportunity (for a specific territory) to acquire weather data with a higher spatial resolution than the existing weather station network allows (especially for the regions with an underdeveloped weather station network).

In the majority of the numerical weather forecast models the variables on a height of 2 m are not prediction variable models. The values of these variables are interpolation between the values of the ground variables on the lowest model level. To improve the prediction of temperature ($T_{2\mathrm{м}}$) and relative humidity ($RH_{2\mathrm{м}}$) on a height of 2 m in the semi-Lagrangian model of numerical weather forecast (PLAV-2005) [112], a parameterization of heat and moisture exchange on the land surface [125] with vegetation taken into account [126, 127] was realized.

Experiments [128] based on 72-hour predictions were made to evaluate the importance of the accuracy in problem setting on the initial data on the moisture content and temperature of soil with a use of this parameterization of the surface; these experiments have shown that an error in the initial data may lead to fairly big changes in temperature forecast and the relative humidity on a height of 2 m. A necessary step to improve the quality of predicting these weather parameters is the realizing the setting pattern of the initial data for pedological variables [129].

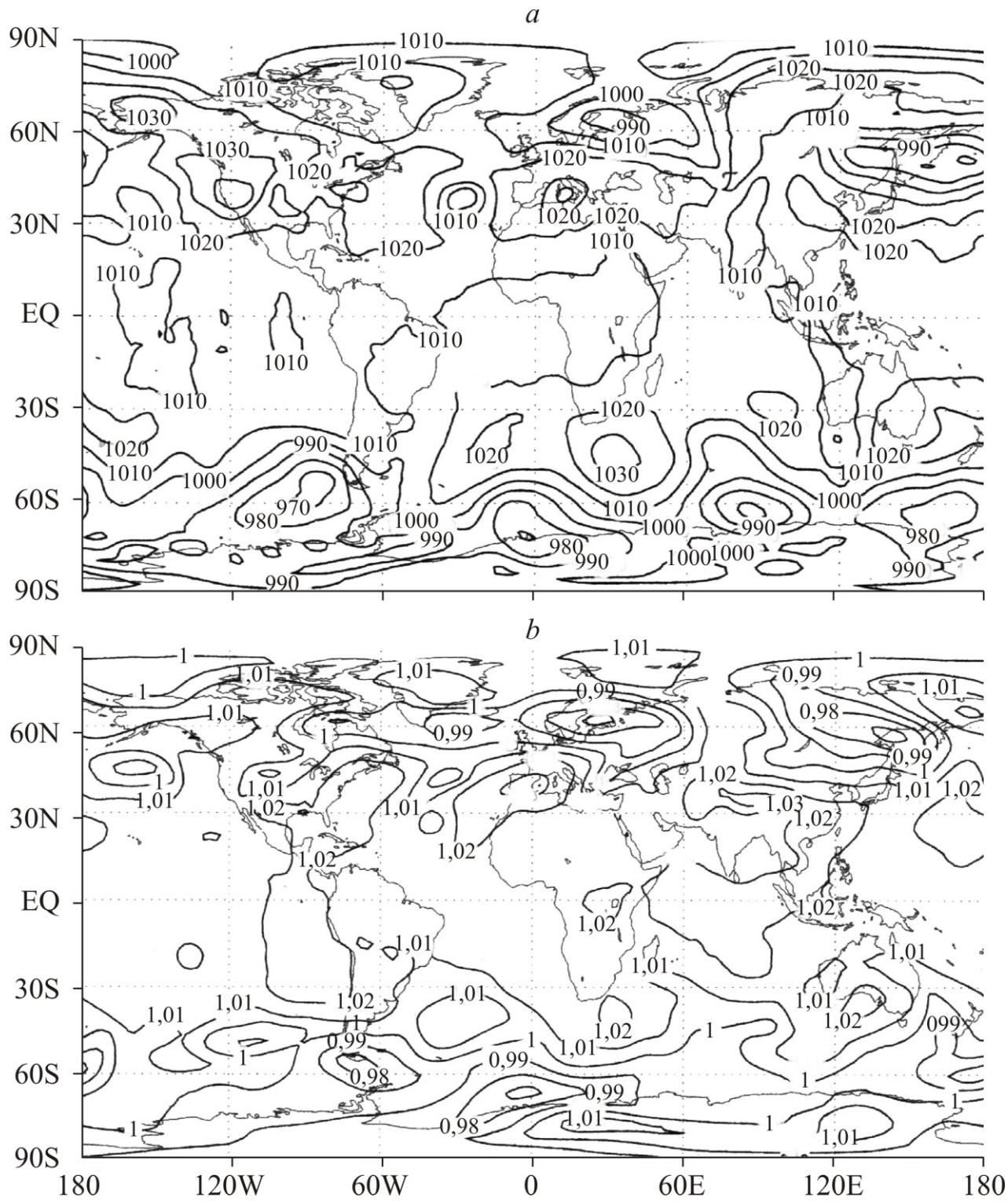

Fig. 1.30. The analysis (*а*) and prediction (*б*) of atmospheric pressure distribution on the sea level on 24 December 1978 [118]

Chart [129] initialized the following variable models: T_s surface temperature of soil, T_p temperature of the deep soil layer, ω_s moisture content of the near-surface soil layer and ω_p moisture content of the deep soil layer. The method of soil temperature

correction is based on calculating the increment of the temperature analysis at a height of 2 m in each point of the grid [125]:

$$\Delta T_{\text{s}} = \Delta T_{2\text{м}}, \;\; \Delta T_{\text{p}} = \Delta T_{2\text{м}} / 2\pi,$$

where Δ denotes the increment, i.e. analysis values minus prediction values. Correction is always made. Full or partial soil temperature correction deactivation leads to an obvious prediction impairment [129].

To correct the calculated value of moisture content of the surface or primary soil layers Method [130] is used, however, with coefficients patterned at parameterization, ISBA [125]:

$$\Delta\omega_{\text{s}} = \alpha_{\text{s}}^{T}\Delta T_{2\text{м}} + \alpha_{\text{s}}^{H}\Delta H_{2\text{м}},$$
$$\Delta\omega_{\text{p}} = \alpha_{\text{p}}^{T}\Delta T_{2\text{м}} + \alpha_{\text{p}}^{H}\Delta H_{2\text{м}}.$$

Coefficients $\alpha_{\text{s}}^{T}, \alpha_{\text{s}}^{H}, \alpha_{\text{p}}^{T}, \alpha_{\text{s}}^{H}$ depend on the soil structure, local solar time and are characteristic of the underlying surface. Analytic expressions for these coefficients are known [129]:

$$\alpha_{\text{s}}^{T} = f(txt)(1-\text{veg})\left[a_0^{T}(t^*) + a_1^{T}(t^*)\text{veg} + a_2^{T}(t^*)\text{veg}^2\right],$$

$$\alpha_{\text{s}}^{H} = f(txt)(1-\text{veg})\left[a_0^{H}(t^*) + a_1^{H}(t^*)\text{veg} + a_2^{H}(t^*)\text{veg}^2\right],$$

$$\alpha_{\text{p}}^{T} = f(txt)\left\{(1-\text{veg})\left[b_0^{T}(t^*) + b_1^{T}(t^*)\text{veg} + b_2^{T}(t^*)\text{veg}^2\right] + \right.$$
$$\left. + \text{veg}\frac{\text{LAI}}{R_{s\min}}\left[c_0^{T}(t^*) + c_1^{T}(t^*)\text{veg}\right]\right\}, \qquad (1.11)$$

$$\alpha_{\text{p}}^{H} = f(txt)\left\{(1-\text{veg})\left[b_0^{H}(t^*) + b_1^{H}(t^*)\text{veg} + b_2^{H}(t^*)\text{veg}^2\right] + \right.$$
$$\left. + \text{veg}\frac{\text{LAI}}{R_{s\min}}\left[c_0^{H}(t^*) + c_1^{H}(t^*)\text{veg}\right]\right\},$$

where veg — a fraction of grid cell covered with vegetation; LAI — leaf-area index, $R_{\text{s min}}$ — minimum surface resistance. The t^*local solar time is expressed in hours and is an integral function that depends on the наклона солнца and absolute solar time (i.e. date, longitude and latitude).

$$f(txt) = \frac{(\omega_{\text{fc}} - \omega_{\text{wilt}})_{txt}}{(\omega_{\text{fc}} - \omega_{\text{wilt}})_{\text{loam}}},$$

where ω_{wilt} — wilting point, ω_{fc} — field capacity for various soil structures (*txt*).

Analytic functions for expression of coefficients (1.11) that also depend on the local solar time have the following outline [129]

$$x(t^*) = x_s \sin\left(\frac{2\pi t^*}{24}\right) + x_c \cos\left(\frac{2\pi t^*}{24}\right) + x_m,$$

where $x = a_i^T, a_i^H, b_i^T, b_i^H, c_i^T, c_i^H$. [129] contains a detailed coefficient output and their numerical values.

The Russian Meteorological Office uses the following pattern [125]:

$$\Delta T_{\text{s}} = 0,5\Delta T_{2\text{м}}, \quad \Delta T_p = 0, \quad \Delta\omega_s = 0, \quad \Delta\omega_{\text{p}} = 0,$$

i.e. correction of soil moisture content and soil deep layer temperature is not made.

The first use experience has shown that in case of applying a new analysis pattern of soil variables the quality of predicting the temperature and relative humidity at a height of 2 m in plain regions is improved [125].

Apart from global models, there are regional numerical weather forecast models, for example, ALADIN model [131]. This model is created by an international team of scholars under supervision of Météo-France. ALADIN is a three-dimensional barocline system of primary equations that uses a two-level in time, a semi-Lagrangian semi-implicit numerical integration scheme [131]. The parameterization complex of physical phenomena includes [132, 133], for instance, the parameterization of the vertical diffusion and planetary boundary level. At present, the MM5 weather forecast model is widespread [134]. It is a mesoscale regional non-hydrostatic model of numerical weather forecast with the use of σ coordinate. The model was developed for predicting atmosphere circulation. WRF system has been recently developed extensively [135]. The application area of regional models is extremely wide, in a scale from several meters to thousands of kilometers.

1.8. Drying and ignition of combustible material

The process of forest fuel layer drying under the impact of outer conditions is important for evaluating forest fire danger on a controlled territory. In the recent years a range of physical and mathematical models for forest fuel layer drying has been developed [136, 137, 138, 139].

The most complete of them [136] uses basic notions and methods of и continuous multiphase medium mechanics [140], as well as methods of solving conjugate problems of heat-and-mass transfer [141] in accordance with the general mathematical model of forest fires [142]. Conjugate setting and boundary level model are used (streamline conditions of the constant flow are considered). The model is set out by a system of equations that reflect the mass conservation laws, momentum, quantity of energy (two-temperature model), and also includes equations of components' mass state and conservation in the gaseous phase. The gaseous phase is considered to be transparent; diffuse approximation is used for radiation transfer in heterogeneous environment [142]. Sun radiation and water evaporation in states free from or bound with forest fuels by Hertz-Knudsen law is also taken into consideration.

At a certain choice of heat transfer coefficient, theoretical values of forest fuels mass loss differ not more than by 5 % from experimental data, and calculations in conjugate and partite settings are in good agreement (Fig. 1.31).

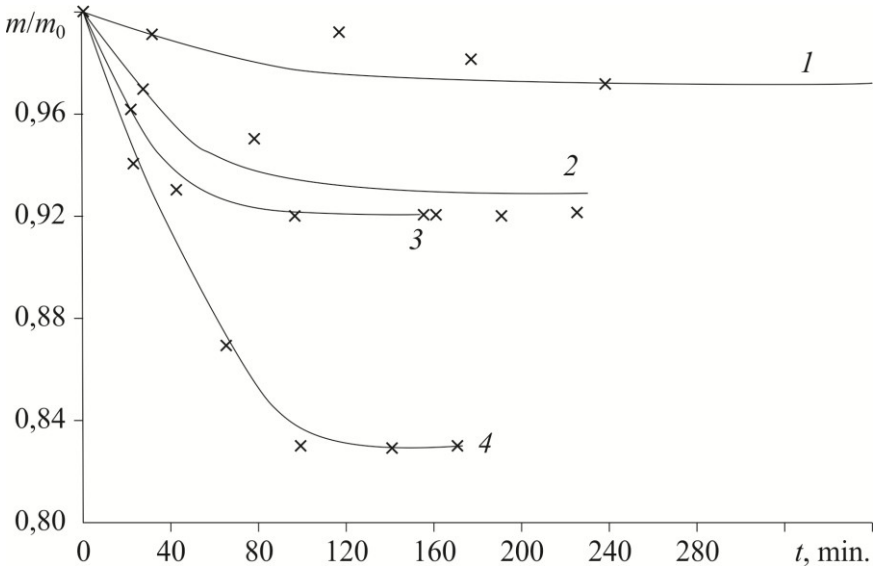

Fig. 1.31. A decrease in pine needles mass from time [38]: at $T = 30$ (*1*), 52 (*2*), 70 (*3*), 96 °C (*4*), line — calculation, dots — experiment

Mathematical modeling of forest fuel layer drying in natural conditions is possible for three scenarios: catastrophic, medium and low fire danger [143, 144], as well as in different soil types (sandy and clayey soil). With a catastrophic scenario, fire danger starts already in May. On sandy soils the process of forest fuels drying is quicker than that on clayey soils.

The analysis of the connection between the moisture content of the forest fuel layer and the number of forest fires in the Tomsk Region in the recent years is demonstrative [144]. The moisture content of the forest fuel layer determines the fire danger period and correlates with the number of forest fires [144].

A one-dimensional mathematical model on the basis of the following hypotheses is a model simplification [136]: 1) convective heat transfer between the forest fuel layer and surface layer of the atmosphere is described through the boundary conditions of third kind with the known coefficient of convective heat transfer; 2) P pressure, T temperature and ρ density of gaseous phase in the forest fuel layer coincide with the corresponding meteorological data (P_e, T_e and ρ_e) for a specific time period and location under study; 3) emission in the forest fuel layer is governed by Buger-Lambert law; 4) evaporation of the inherent water and droplets of water stuck to forest fuels elements is described by Hertz-Knudsen law.

Energy equation and equations for the volume ratio of dry organic matter and volumetric moisture content have the following outline [138]

$$\sum_{i=1}^{2}\rho_i\varphi_i C_{pi}\frac{\partial T_s}{\partial t}=\frac{\partial}{\partial z}\left(\lambda_s\frac{\partial T_s}{\partial z}\right)+\frac{\partial q_{R_z}}{\partial z}-$$

$$-q_2\frac{k'_{02}\rho_2\varphi_2}{\sqrt{T_s}}\exp\left(-\frac{E}{RT_s}\right)-\alpha_v\left(T_s-T_e\right),$$

$$\rho_1\frac{\partial\varphi_1}{\partial t}=0,$$

$$\frac{d\varphi_2}{dt}=-\frac{k'_{02}\varphi_2}{\sqrt{T_s}}\exp\left(-\frac{E}{RT_s}\right).$$

Boundary conditions on the upper and lower boundary of the forest fuel layer [138]:

$$-\lambda_s\frac{\partial T_s}{\partial z}\bigg|_{z=h}=\alpha_e(T_{sw}-T_e)+q_2R_{2w}-\varphi_{sw}q_{R_w},$$

$$\lambda_s\frac{\partial T_s}{\partial z}\bigg|_{z=0}=\alpha_0\left(T_{s0}-T_0\right)+q_{R_w}\left(1-\varphi_{sw}\right)\exp\left(-k_1\rho_1 h\right).$$

The initial conditions for the temperature, volume ratio of the organic matter and volumetric moisture content are [138]:

$$T_s(z)\big|_{t=0}=T_{s\text{н}}(z),\ \ \varphi_1(z)\big|_{t=0}=\varphi_{1\text{н}}\left(z\right),\ \ \varphi_2(z)\big|_{t=0}=\varphi_{2\text{н}}(z),$$

where z — coordinate calculated from soil surface perpendicular to the underlying surface; t — time; T_s — temperature of the condensed phase; λ_s — coefficient of thermal conductivity of the condensed phase in the forest fuel layer; α_e and α_0 — coefficients of heat transfer on the upper and lower boundaries correspondingly; T_0 — soil temperature; T_e — temperature of the surrounding air; φ_1 — volume ratio of dry organic matter; φ_2 — volumetric moisture content of the forest fuel layer; $\alpha_v = \alpha_e S$ — coefficient of volumetric convective heat transfer; S — surface area of macropores; ρ_i, C_{pi}, φ_i — densities, heating capacities and volume ratios of dry organic matter ($i = 1$) bound with the dry organic matter of water ($i = 2$); k'_{02} and E — preexponential factor and activation energy characterizing the evaporation of gravity water; R — universal gas constant; φ_{sw} — volume ration of condensed phase on the upper boundary of forest fuels; q_{R_w} and q_{R_z} — densities of built-up radiation flux, on the interface of environment and radiation flux that penetrate the forest fuel layer; q_2 — heat evaporation of water mass unit; R_2 — mass rate of moisture evaporation; k_1 — coefficient of radiation damping in the forest fuel layer; h — layer thickness of forest fuels; w and $н$ indices are ascribed to state parameters at $z = h$ and $t = 0$ correspondingly.

As the result of transition to non-dimensional variables and of forest fuel layer thickness averaging, a simplified zero-dimensional statement of the problem of forest fuel layer drying is acquired in the shape of ordinary differential equation for the

θ_s dimensionless temperature average according to the forest fuel layer and non-dimensional volumetric moisture content of the layer φ_2 [137, 139]:

$$\left(1+a\varphi_2\right)\frac{d\theta_s}{d\tau}=\frac{1}{\delta^2}\left\{-\mathrm{Bi}\left(\theta_s-\theta_e\right)-\frac{b\varphi_2}{\sqrt{1+\beta\theta_s}}\left[1-\pi_e\exp\left(-\frac{\theta_s}{1+\beta\theta_s}\right)\right]\times\right.$$

$$\times\exp\frac{\theta_s}{1+\beta\theta_s}+\left(\varphi_{1\text{н}}+\varphi_2\right)\left[c-d\left(1+\beta\theta_s\right)^4\right]-\mathrm{Bi}_0\left(\theta_s-\theta_0\right)-\left(\varphi_{1\text{н}}+\varphi_2\right)\times$$

$$\left.\times\left[c_0-d_0\left(1+\beta\theta_s\right)^4\right]\right\}+\frac{q_{R_w}}{\bar{k}_1}\left(1-\exp\left(-\bar{k}_1\right)\right)-\bar{\alpha}_V\left(\theta_s-\theta_e\right)-\frac{\varphi_2}{\sqrt{1+\beta\theta_s}}\times$$

$$\times\left[1-\pi_e\exp\left(-\frac{\theta_s}{1+\beta\theta_s}\right)\right]\exp\frac{\theta_s}{1+\beta\theta_s},\quad(1.12)$$

$$\frac{d\varphi_2}{\partial\tau}=-\frac{\gamma\varphi_2}{\sqrt{1+\beta\theta_S}}\left[1-\pi_e\exp\left(-\frac{\theta_s}{1+\beta\theta_s}\right)\right]\exp\frac{\theta_s}{1+\beta\theta_s},\qquad(1.13)$$

$$\varphi_2\big|_{\tau=0}=\varphi_{2\text{н}},\quad\theta_s\big|_{\tau=0}=0,\qquad(1.14)$$

где $\theta_s=\dfrac{(T_s-T_{s\text{н}})E}{RT_{s\text{н}}{}^2}$ — dimensionless temperature of the forest fuel layer; $\theta_0=\dfrac{(T_0-T_{s\text{н}})E}{RT_{s\text{н}}{}^2}$ — dimensionless soil temperature; $\theta_e=\dfrac{(T_e-T_{s\text{н}})E}{RT_{s\text{н}}{}^2}$ — dimensionless temperature of the surrounding environment; $\tau=\dfrac{tq_2k'_{02}\rho_2E}{\rho_1\varphi_{1\text{н}}C_{p1}RT_{s\text{н}}^2\sqrt{T_{s\text{н}}}}\times\times\exp\left(-\dfrac{E}{RT_{s\text{н}}}\right)$ — dimensionless time; $\delta^2=\dfrac{q_2k'_{02}\rho_2h^2E}{\lambda_1\varphi_{1\text{н}}\sqrt{T_{s\text{н}}}\;\;RT_{s\text{н}}^2}\exp\left(-\dfrac{E}{RT_{s\text{н}}}\right)$ — dimensionless criterion (analogy of Frank-Kamenetskiy criterion [145]); $\beta=RT_{s\text{н}}/E$ — dimensionless value, the opposite of activation energy; $\gamma=\dfrac{\rho_1\varphi_{1\text{н}}C_{p1}RT_{s\text{н}}{}^2}{\rho_2q_2E}$ — dimensionless criterion of conformity that characterized the drying rate of forest fuel layer; $\mathrm{Bi}=\dfrac{\alpha_eh}{\lambda_1\varphi_{1\text{н}}}$ — Biot number that characterizes the heat transfer intensity of the forest fuel layer and atmospheric boundary level; $\mathrm{Bi}_0=\dfrac{\alpha_0h}{\lambda_1\varphi_{1\text{н}}}$ — Biot number that characterizes the heat transfer

intensity of the forest fuel layer and soil; $a = \frac{\rho_2 C_{p2}}{\rho_1 C_{p1} \varphi_{1н}}$, $b =$ $= \frac{E \quad q_2 k'_{02} \rho_2 h}{R T_{sн}^2 \sqrt{T_{sн}} \lambda_1 \varphi_{1н}} \exp\left(-\frac{E}{R T_{sн}}\right)$, $c = \frac{E \quad h\left[(1-A) q_R(h) + J_w\right] \cos\alpha}{\lambda_1 \varphi_{1н} R T_{sн}^2}$, $d =$ $= \frac{\varepsilon_s \sigma T_{sн}^2 h E}{R \lambda_1 \varphi_{1н}}$ — dimensionless values that characterize the volumetric heat capacity of water, thermal effect of water evaporation, radiation energy influx and the layer's emissivity factor; $c_0 = c \exp(-\bar{k}_1)$, $d_0 =$ $= d \exp(-\bar{k}_1)$ — dimensionless values; $\bar{\alpha}_v = \frac{\alpha_v R T_{sн}^2 \sqrt{T_{sн}}}{q_2 k'_{02} \rho_2 E} \exp\left(\frac{E}{R T_{sн}}\right)$, $\bar{q}_{R_w} = \frac{q_{Rw} k_1 \rho_1 \sqrt{T_{sн}}}{q_2 k'_{02} \rho_2 E} \exp\left(\frac{E}{R T_{sн}}\right)$, $\bar{k}_1 = k_1 \rho_1 h$ — dimensionless values of the volumetric coefficient of heat transfer, radiative heat flux and the coefficient of radiation damping; π_e — relative air humidity. The results of numerical modeling of the forest fuel layer drying in one-dimensional and zero-dimensional statements are in good agreement (ratio error does not exceed 10—15 %) [146].

With the use of the method of partial separation of variables [147], as a consequence of integration (1.12)—(1.13) with consideration of the first condition (1.14), a formula can be introduced [139]

$$\varphi_2 = \varphi_{2н} \exp\left(I(\tau)\right),$$

where $I(\tau) = -\gamma \int_0^\tau \frac{\left[1 - \pi_e \exp\left(-\frac{\theta_s}{1+\beta\theta_s}\right)\right]}{\sqrt{1+\beta\theta_s}} \exp\left(\frac{\theta_s}{1+\beta\theta_s}\right) d\tau.$

For the approximate calculation of $I(\tau)$ integral, expansion into series in accordance with τ in the neighborhood of $\tau = 0.$ is used. This allows finding the τ_c. non-dimensional time of layer drying. If two members of Taylor expansion are preserved for the subintegral function, then as the result of calculations there will be the following formula for τ_c 33 non-dimensional time of drying in the second order [139]:

$$\tau_c = \frac{\sqrt{\left(1-\pi_{e0}\right)^2 + 2\left\{\theta'_{s0} - \pi_{e0}\right\} \frac{1}{\gamma} \ln \frac{\varphi_{2н}}{\varphi_{2*}}} - \left(1-\pi_{e0}\right)}{\left\{\theta'_{s0} - \pi'_{e0}\right\}},$$

where $\pi'_{e0} = \left.\frac{d\pi_e(\tau)}{d\tau}\right|_{\tau=0}$, $\theta'_{s0} = \left.\frac{d\theta_s(\tau)}{d\tau}\right|_{\tau=0}$, φ_{2*} — critical volumetric moisture content of the forest fuel layer. Numerical calculations and experimental data for the process of drying the forest fuel layer correspond [148] (Figure 1.32).

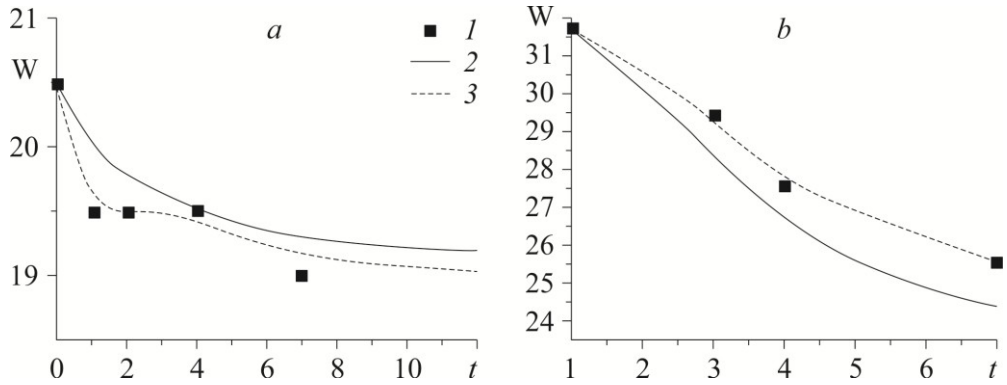

Fig. 1.32. The dependence of the forest fuel layer moisture content on time. *1* — experimental data, *2* — numerical solution, *3* — spline approximation of the experimental data. *а* — pine needles, T_e = 273 K, $w_н$ = 20,5 %, π_e = 80 % [137], *б* — small reed, T_e = 293 K, $w_н$ = 31,8 %, π_e = 80 % [148]

The use of a simplified mathematical model of forest fuel layer drying recorded in the conditions of neglecting the value of water vapor partial pressure [138]. It must be mentioned that with drying at low temperatures, water vapor partial pressure must be considered [149].

An experimental research of liquid droplet evaporation from the surfaces of typical forest fuel elements (needles of pine, cedar, spruce; Fig. 1.33) and drying of forest fuels is demonstrative in the statement of a problem analogous to [136]. Dependences of droplet evaporation rate $(\rho v)_w$ from the moisture content of needles w, and surface roughness R_z were acquired [150].

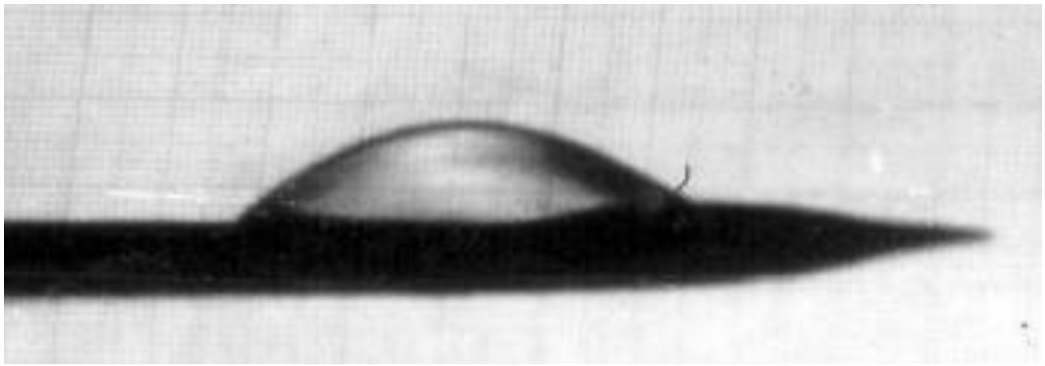

Fig. 1.33. A droplet on a pine needle [150]

To realize the mathematical models [136, 137, 138, 139] thermokinetic constant values for unbalanced drying of forest fuels E_2/R, k_2 are necessary, where E_2 — effective heat of moisture evaporation (the analogy of activation energy in chemical kinetics), R — universal gaseous constant, k_2 — preexponential factor. For high temperatures realized in the forest fire front, water loss in the forest fuel layer obeys the law [23]

$$\frac{dm}{d\tau} = \frac{A(m-m_1)SM}{\sqrt{2\pi MRT}}\left[p_0 \exp\left(-\frac{E_2}{RT}\right) - p_e \right], \quad (1.15)$$

where m — mass of forest fuels; m_1 — mass of dried needles; τ — time; A — empirical coefficient; S — effective surface area; M — molecular water mass; T — absolute temperature; p_0 — thermal water pressure [151]; p_e — partial water-vapor pressure. At high temperatures (from 333 to 423 K) saturated vapor pressure is [149]

$$p_n = p_0 \exp\left(-\frac{E_2}{RT}\right) >> p_e, \quad (1.16)$$

therefore in the numerical simulation of forest fire spreading [23] p_e was not considered in (1.15).

For low temperatures $T < 333$ K and high relative humidity $\varphi = p_e / p_n$, the equation (1.16) may not be realized and to find E_2/R, k_2 an equation must be used [149]:

$$\frac{dm}{d\tau} = -\frac{A(m-m_1)SM(1-\varphi)}{\sqrt{2\pi MRT}} p_n, \quad (1.17)$$

where φ — relative humidity, p_n — saturated vapor pressure.

The experimental investigation of the process of forest fuel drying was carried out in isothermal conditions at temperatures of $T = 303$, 325, 345, 369 K with needle samples of the pine, cedar, and spruce inserted in a drying cabinet. Relative air humidity in the drying cabinet, temperature and air pressure were controlled in experiments.

Thermokinetic constants E_2/R and $k_2 = \frac{ASM(1-\varphi)}{\sqrt{2\pi MR}}$ were found from Equation (1.17) by the Freeman-Carroll method of rectification [152]. Table 1.6 shows the values of E_2/R and k_2 for living needles.

Table 1.6. Thermokinetic constants of forest fuel (needle) drying [149]

E_2/R, K^{-1}	k_2, K$^{1/2}$ c^{-1}	T, K	Source
4373	18.32	303—369	[149]
5247	$1.487 \cdot 10^5$	369	[23]
4560	2.3	443—770	[153]
5956	$6.03 \cdot 10^5$	333—403	[154]

A significant scatter in values of E_2/R and k_2 in Table 1.6 is caused by various conditions of experiment conduct, and the implemented methods of measurement result processing.

In order to check the validation of calculation results with Model [136] of forest fuel drying, a range of experiments in an aerodynamic tunnel was carried out [149].

The targets of research were forest fuel samples: needles of pine, spruce and cedar. Forest fuel elements located horizontally were surrounded by laminar air flow

generated by the MT-324 type of a subsonic wind tunnel. Storage density of forest fuels with chaotic needle orientation varied — $\rho = (44{,}5—110{,}6)$ kg/m^3. The angle of a plane with forest fuel elements on it and air vector of $\alpha = (0—20)°$ changed with a special coordinate spacer. The airflow rate is $V_e = (0—0{,}695)$ m/s (was estimated by the Pitot-Prandtl tube, a MMN-240 micromanometer and thermal anemometer), forest fuel moisture content is $W = (m - m_0)/m_0$, where m, m_0 — the values of mass and oven-dry mass of forest fuels, $W =$ $= (0{,}0539—0{,}7036)$ %, surrounding air temperature is $T = (18—29)$ °C. Air pressure $P = (748—764)$ mmHg was controlled with a BAMM-1 aneroid barometer, relative air humidity $\varphi = (32—77)$ % was controlled with a MB-4M aspiration hygrometer, m needle mass loss in length of t time that was measured on a Class 2 ADV-200M analytical balance with an accuracy to 10^{-4} g. The m/m_0 non-dimensional sample mass loss (where m_0 — initial mass) characterized the amount of water evaporated from the surface of the material under study within the drying period. The t drying period varied within 90—300 min. The net inaccuracy of parameter choice did not exceed $\delta V_e \le 4{,}2$ %, $\delta m \le 2{,}1$ %, $\delta T \le 5{,}3$ %, $\delta P \le 6{,}0$ %, $\delta\varphi \le 7{,}9$ %. The confidence intervals were calculated by results of three-five dimensions with a probability belief of 0.95.

The conditions for the air flow to surround forest fuel samples, the meteorological parameters of the atmosphere, and storage density [149] corresponded their full-scale values. The h layer height was chosen so that forest fuel samples be in the boundary layer [149]:

$$h < \delta = \sqrt{\mathrm{Re}}, \qquad (1.18)$$

where δ — the thickness of the boundary layer, Re — the Reynolds number. Satisfying the inequality (1.18), according to the supposition [149], corresponds to the natural conditions. Fig. 1.34 illustrates the facility to test flows in the forest fuel layer and estimate the boundary conditions for ignition.

The storage density in the pointed measurement range acquired naturally is an unessential factor. The initial moisture content of forest fuels, environmental temperature, air pressure and relative air humidity have a stronger impact on forest fuel drying intensity. The impact of the angle of a plane is inappreciable [149].

Water may be bound to a material in a chemical, physical and chemical, and physical and mechanical way in a droplet form [151]. The regularities for evaporation of water droplets located on a rough shape surface and, as a limiting case, on the surface of separate needles of pine, cedar, spruce differ [149].

The evaporation of great water droplets ($r > 5 \cdot 10^{-3}$ m) is described by Hertz-Knudsen law [149]:

$$(\rho v)_w = \frac{AM(p_* - p_e)}{\sqrt{2\pi MRT}},$$

where A — accommodation coefficient; M — molar mass; R — universal gaseous constant, in the value of $A \approx 1{,}8A_o$ (A_o — accommodation coefficient for water evaporating from the free surface). The evaporation rate $(\rho v)_w$ of great droplets

changes loosely depending on R_z. To describe the evaporation of small droplets, the following linear connection may be used [149]

$$\frac{m}{m_0} = (1 - 1,08 \cdot 10^{-5} R_z) 0,273 d_0^{-1,426} t,$$

where m_0, d_0 — the initial mass values (kg), and droplet diameter (m), t — time, min.

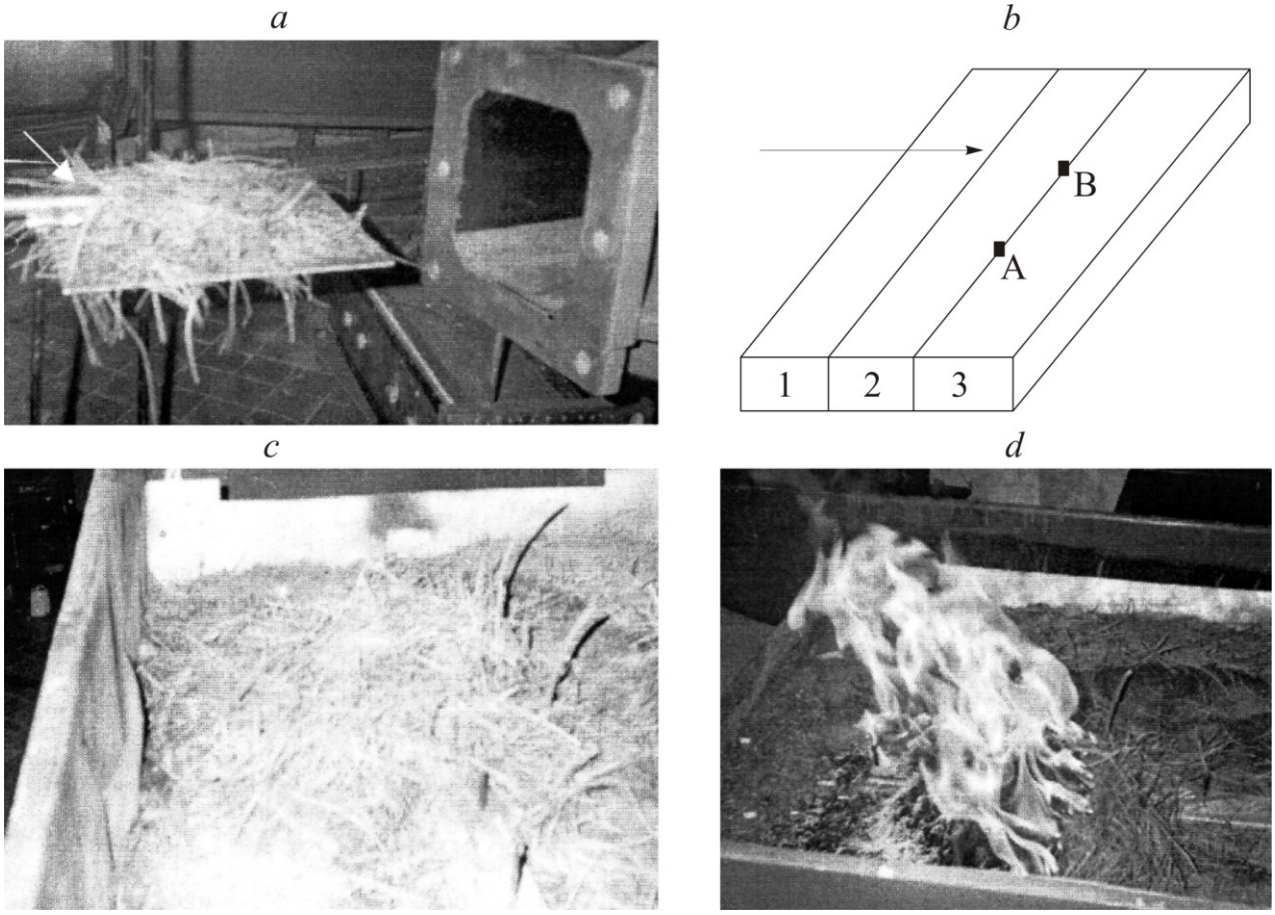

Fig. 1.34. The facility to study the air flow in the forest fuel layer (*a*). The arrow points at the Pitot-Prandtl tube. The trial arrangement to estimate the boundary conditions for ignition (*b*). A и B — places to install a heat flow probe and thermocouple. The facility to estimate the boundary conditions for ignition (*c*). Fire spreading along the surface (*d*) [143]

There is no mass transfer between dry needles and water as a liquid spray [149]. The 'living' needles absorbs droplet moisture. The rate of droplet evaporation located on the living needles is higher than that of the droplet on dry needles. Visualization of midsection cut of the living and dead needles with a 20-time zooming has shown that mass transfer between the droplet and needles occurs through air pores. The air pores of dry needles are atrophied and moisture does not transfer from the droplet to the needles [149].

The needles may be viewed as a colloidal and capillary-porous material [155]. The characteristics of forest fuel mass transfer may be estimated with the moisture transfer potential. The water capacity and moisture conductivity coefficients of some forest fuels are known. Desorption is accompanied by shrinkage of pine needles, and adsorption – by their swell. Inside the forest fuel elements complex processes occur (desorption, adsorption, osmosis) that are connected with changes of the thin needle structure in the process of its drying [155].

The ignition is one of the important processes that influence the forest fire danger level. At present, the theory of ignition is a separate branch of chemical physics. In its full setting the ignition model of the condensed system includes stages of matter heating, quick response in the surface layer with formation of pyrolysis products, self-acceleration of chemical reactions at the burning rate yielding to a stationary mode [156].

Depending on the matter type and heat transmission method, cases are realized when a so-called leading exothermal reaction may be distinguished that determines the main regularities of ignition process. In accordance with the leading reaction localization, a range of ignition models were named solidphase, heterogeneous and gas-phase. For many substances able to react exothermically in the condensed and gas phases, it is impossible to create such an idealization. Therefore, the problem on ignition should be solved with consideration of the interaction of several individual mechanisms.

To ignite a condensed matter (k), an outer heat impulse is necessary that leads to heating the surface layers of k-matter and accelerating the exothermal reactions [156]. Ignition happens when the intensity of heat sink equals or becomes smaller than the intensity of the source in the chemical reaction zone [157—159].

A simple problem is the ignition of k-matter with a hot body at an impulsive thermal input. The unbounded plate of k-matter is considered whose length and width are large compared to its thickness. Due to the supposition that temperature change occurs only in x direction, the derivatives of temperature on y and z equal zero. As a result of this hypothesis, a solid phase ignition model was formed [160]:

$$\frac{\partial T}{\partial t} = \chi \frac{\partial^2 T}{\partial x^2} + \frac{Qz}{c} \exp\left(-\frac{E}{RT_s} \right), \qquad (1.19)$$

$$T(x,0) = T_i$$

$$T(0,t) = T_s \text{ at } 0 < t < t_1,$$

$$\frac{\partial T(0,t)}{\partial x} = 0 \text{ at } t > t_1, \qquad (1.20)$$

$$\frac{\partial T(L,t)}{\partial x} = 0 \text{ at } t > 0,$$

where T — temperature, K; χ — temperature conductivity, cm^2/s; Q — thermal effect of condensed phase reaction that is related to mass unit, kal/g; z — pre-exponential factor, 1/s; c — heat capacity per unit mass, kal/(g·K); E — activation energy, kal/mole; t — time, c; x — orthogonal coordinate, cm; L — plate thickness, cm; t_1 — operating time of heat impulse, s; T_s — hot body temperature, K; T_i — initial temperature, K.

Model (1.19)—(1.20) does not consider firing effect, which is just for special cases: the reactions of the condensed phase progress, following order zero in concentration, or the time of ignition is so small that in this period only an insignificant part of k-matter burns out [156]. The model may be recorded in a non-dimensional way with the use of the linear connection[160]

$$\Theta = \frac{E}{RT_*^2(T - T_*)},$$

where Θ — dimensionless temperature. T_* — corresponds the temperature in which the chemical reaction is the most substantial. In the problem under study it is the temperature of the heating element.

The ignition of some k-matter (carbon, polymers, etc.) is conditioned by the heterogeneous exothermal chemical reaction that progresses on the k-matter surface [156]. An oxidation element is delivered to the k-matter surface by diffusion. Kinetic (reaction rate depends on the outer parameters, concentration and temperature in the Arrhenius law) and diffusional (process rate is determined by diffusion rate) mechanisms of heterogeneous reaction depending on the outer parameters are possible. The simplest heterogeneous ignition model is known [156]:

$$c\rho\frac{\partial T}{\partial t} = \lambda\frac{\partial^2 T}{\partial x^2},$$

$$T(0, x) = T_i$$

$$T(0, \infty) = T_i$$

$$-\lambda\frac{\partial T(t, 0)}{\partial x} = q_s + B_g \exp\left(-\frac{E_g}{RT}\right),$$

where c, ρ, λ — heating capacity, density and thermal conductivity of the igniting k-matter, T — temperature, K; t — time, c; x — orthogonal coordinate, cm; q_s — the outer heat of constant intensity; E_g — activation energy of the heterogeneous reaction; $B_g = Q_g k_g$, Q_g — thermal effect of the heterogeneous reaction; k_g depends on the concentration of the oxidation element. A solution of this problem is also possible in non-dimensional variables. The T_* scaling temperature is in the solution result and obtains a meaning of 'ignition rate' if the method of its experimental determination is possible to prove [156].

For some substances the ignition process is limited by the gaseous phase [161, 162]. K-phase is a heat runoff and the supplier of gaseous products of combustion

and oxidation agent. The gas phase model of k-matter ignition in the oxygen atmosphere or inert environment is also known [156]. The physical setting of the problem is based on the following hypotheses:

1) k-phase of the solid matter is the source of gaseous products of the oxidation agent and fuel that form as a result of thermal pyrolysis and heat sink. Possible exothermal reactions in the volume of k-phase are not counted;

2) the content of the firing environment that is under a fixed p pressure includes only the oxidation agent, or inert gar, or a mixture of the oxidation agent and inert gas;

3) ignition occurs in the gaseous phase as a result of heat emission from the reaction of fuel vapors and oxygen.

In accordance with such a physical model of ignition, the system of the initial differential equations of the mathematical model has the following outline.

Equation of oxidation vapor diffusion:

$$\rho_1 \frac{\partial X}{\partial t} = \frac{\partial}{\partial x}\left(\rho_1 D \frac{\partial X}{\partial x}\right) - \Phi(X, Y, T). \quad (1.21)$$

Equation of fuel vapor diffusion:

$$\rho_1 \frac{\partial Y}{\partial t} = \frac{\partial}{\partial x}\left(\rho_1 D \frac{\partial Y}{\partial x}\right) - \Phi(X, Y, T). \quad (1.22)$$

Equation of energy in the gaseous phase:

$$c_1\rho_1 \frac{\partial T}{\partial t} = \frac{\partial}{\partial x}\left(\lambda_1 \frac{\partial T}{\partial x}\right) - Q\Phi(X, Y, T). \quad (1.23)$$

Equation of energy for k-phase matter:

$$c_2\rho_2 \frac{\partial T}{\partial t} = \frac{\partial}{\partial x}\left(\lambda_2 \frac{\partial T}{\partial x}\right), \quad (1.24)$$

where x — coordinate; t — time; X, Y — mass fractions of the oxidation agent and fuel; ρ — density; c — heat capacity at constant pressure; λ — coefficient of thermal conductivity; D — diffusion coefficient; Q — thermal effect of the reaction in the gaseous phase; $\Phi(X, Y, T)$ — the rate of chemical reactions; indices 1 and 2 refer to gas and k-matter correspondingly. For system closure, the initial and boundary conditions are necessary that will be estimated by the specificity of the problem.

In the ignition period, the thermal and diffusive relaxation lengths are over several orders more than the convective one [156]. Therefore System (1.21)—(1.24) does not consider the convective heat and matter transfer.

Mathematical settings of ignition problems are systems of non-stationary non-linear equations of mathematical physics and they require the use of numerical modeling apparatus and corresponding numerical methods [163—166]. However, analytical methods of solving ignition problems also find their place.

A crosslink method has been developed that implies two stages of ignition process development: Stage 1 when process of sample heating may be neglected owing to the chemical reaction, and Stage 2 when its own heat emission is counted only [156]. The method owes its name to a procedure of solution conjugation for both stages that is performed for the functions and their derivatives in time. The last achievement is the use of the method of matched asymptotic expansions [167, 168]. In this case, conjugation is performed in accordance with the coordinate.

The next mechanism for forming a fire spot and spreading its front over forest fuels is known [23]. A forest fuel portion is heated that, with the rise of temperature, is accompanied by evaporation of moisture free and bound with forest fuels, and pyrolysis of forest fuels. As the result of thermal decomposition gaseous and condensed products of pyrolysis are formed. Combustible gaseous pyrolysis products are mainly CO, H_2, CH_4, C_2H_6. Combustible gaseous pyrolysis components are oxidized by the oxygen from the air, with the formation of combustion products (CO_2 и H_2O). Apart from that, a heterogeneous reaction of breeze coke oxidation occurs in the fire spot (mainly on the stage of afterburning of carbon residue).

When modeling chemical kinetics of many combustion processes, either overall reactions of chemical components, or the concept of elementary reactions may be used [169]. An elementary reaction on a molecular level flows exactly in accordance with the equation of this reaction [170]. For instance, the reaction of hydroxyl radical (OH) with molecular hydrogen (H_2) with formation of water molecule and hydrogen atom is the following [169]:

$$OH + H_2 \rightarrow H_2O + H.$$

As the result of molecular movement in the gaseous phase, collision of the hydroxyl radical with hydrogen molecule occurs. In the case of recreational collisions, the molecules react with forming combustion products. The reaction below

$$2H_2 + O_2 \rightarrow 2H_2O$$

is not elementary. It is known that the water molecule is not formed as the result of a single collision between these reacting molecules. The overall reactions are a sequence of a large number of reactions.

The reaction of hydrogen oxidation has been well studied [171]. For the set of H_2, O_2, OH, H, O, HO_2, H_2O, H_2O_2 components, the maximum full mechanism of burning is known [171—174] (Table 1.7).

Table 1.7. The maximum chart, mechanism and thermokinetic parameters of reactions [171—174]

Reaction	A^+	n^+	E^+	A^-	n^-	E^-
$H_2 + O_2 \leftrightarrow 2OH$	$2.81 \cdot 10^{10}$	0	38.90	$6.24 \cdot 10^{8}$	0	20.38
$H_2 + OH \leftrightarrow H_2O + H$	$8.65 \cdot 10^{10}$	0	5.4	$3.21 \cdot 10^{11}$	0	20.82
$O_2 + H \leftrightarrow OH + O$	$4.42 \cdot 10^{11}$	0	17.60	$2.20 \cdot 10^{10}$	0	0.98
$H_2 + O \leftrightarrow OH + H$	$7.07 \cdot 10^{7}$	1	8.95	$3.15 \cdot 10^{8}$	1	7.05
$H_2O + O \leftrightarrow 2OH$	$8.00 \cdot 10^{10}$	0	18.80	$9.63 \cdot 10^{9}$	0	1.47
$H + H + M \leftrightarrow H_2 + M$	$2.00 \cdot 10^{8}$	0	0	$2.20 \cdot 10^{16}$	–1	103.26
$O + O + M \leftrightarrow O_2 + M$	$4.53 \cdot 10^{8}$	0	0.53	$4.37 \cdot 10^{17}$	–1	118.50
$H + OH + M \leftrightarrow H_2O + M$	$1.27 \cdot 10^{16}$	–2	0	$1.81 \cdot 10^{16}$	0	118.20
$OH + OH + M \leftrightarrow H_2O_2 + M$	$9.10 \cdot 10^{8}$	0	0	$9.53 \cdot 10^{15}$	0	51.06
$OH + O + M \leftrightarrow HO_2 + M$	$8.50 \cdot 10^{10}$	0	6.69	$1.11 \cdot 10^{17}$	0	73.50
$H + O_2 + M \leftrightarrow HO_2 + M$	$3.78 \cdot 10^{9}$	0	–1.89	$2.48 \cdot 10^{14}$	0	48.30
$H_2 + HO_2 \leftrightarrow H_2O_2 + H$	$9.50 \cdot 10^{8}$	0	21.80	$3.38 \cdot 10^{9}$	0	4.15
$H_2 + HO_2 \leftrightarrow H_2O + OH$	$1.50 \cdot 10^{8}$	0	24.80	$9.71 \cdot 10^{5}$	0.5	77.94
$H_2O + HO_2 \leftrightarrow H_2O_2 + OH$	$4.00 \cdot 10^{10}$	0	34.00	$3.83 \cdot 10^{10}$	0	4.08
$HO_2 + HO_2 \leftrightarrow H_2O_2 + O_2$	$4.00 \cdot 10^{9}$	0	0	$1.11 \cdot 10^{9}$	0.5	41.70
$H + HO_2 \leftrightarrow OH + OH$	$8.90 \cdot 10^{9}$	0	2.58	$4.28 \cdot 10^{8}$	0	37.13
$H + HO_2 \leftrightarrow H_2O + O$	$2.00 \cdot 10^{10}$	0	3.58	$7.99 \cdot 10^{9}$	0	58.62
$H + HO_2 \leftrightarrow H_2 + O_2$	$5.00 \cdot 10^{9}$	0	1.20	$1.08 \cdot 10^{10}$	0	54.27
$O + HO_2 \leftrightarrow OH + O_2$	$6.00 \cdot 10^{10}$	0	0	$5.86 \cdot 10^{10}$	0	51.17
$H + H_2O_2 \leftrightarrow H_2O + OH$	$1.30 \cdot 10^{12}$	0	11.90	$6.52 \cdot 10^{11}$	0	79.53
$O + H_2O_2 \leftrightarrow OH + HO_2$	$4.00 \cdot 10^{10}$	0	1.30	$5.02 \cdot 10^{10}$	0	13.89
$H_2 + O_2 \leftrightarrow H_2O + O$	$8.00 \cdot 10^{10}$	0	57.62	$4.00 \cdot 10^{10}$	0	61.28
$H_2 + O_2 + M \leftrightarrow H_2O_2 + M$	$5.00 \cdot 10^{6}$	0	21.90	$1.16 \cdot 10^{12}$	0	54.44
$OH + M \leftrightarrow O + H + M$	$4.00 \cdot 10^{13}$	0	105.3	$6.31 \cdot 10^{8}$	0	3.94
$HO_2 + OH \leftrightarrow H_2O + O_2$	$3.00 \cdot 10^{10}$	0	0.6	$8.75 \cdot 10^{9}$	0.5	69.97
$H_2 + O + M \leftrightarrow H_2O + M$	$5.00 \cdot 10^{8}$	0	0	$1.17 \cdot 10^{14}$	0	116.78
$H_2O + O + M \leftrightarrow H_2O_2 + M$	$9.00 \cdot 10^{7}$	0	13.00	$1.13 \cdot 10^{14}$	0	46.73
$H_2O_2 + O \leftrightarrow H_2O + O_2$	$2.00 \cdot 10^{8}$	0	29.00	$2.01 \cdot 10^{8}$	0	113.24
$H_2O_2 + H_2 \leftrightarrow 2H_2O$	$2.00 \cdot 10^{10}$	0	22.00	$3.72 \cdot 10^{9}$	0	105.06
$HO_2 + H + M \leftrightarrow H_2O_2 + M$	$3.00 \cdot 10^{8}$	0	1.50	$1.51 \cdot 10^{14}$	0	87.11
$OH + wall \leftrightarrow OH_s$	30.4	0	0	0.1	0	0
$H + wall \leftrightarrow H_s$	10.5	0	0	0.1	0	0
$O + wall \leftrightarrow O_s$	29.5	0	0	0.1	0	0
$HO_2 + wall \leftrightarrow HO_{2s}$	46.4	0	0	0.1	0	0

Note. A — pre-exponential factor in l/(mole s) for bimolecular and in l/(mole^2·s) for triolecular reactions; n — temperature degree factor; E — activation energy, kkal/mole; the '+' index marks parameters for the straight reaction, the '–' index – for counter reaction.

There exist more complicated burning mechanisms (like that of hydrogen). In [169], a chart with a consideration of 38 elementary reactions is viewed, in [175], the chart contains 42 reactions. Simplified charts are also known. For example, for the conditions of the experiment [176] a rather simple chart was acquired [174]:

$H_2 + O_2 \leftrightarrow 2OH.$

$H_2 + OH \leftrightarrow H_2O + H.$

$O_2 + H \leftrightarrow OH + O.$

$H_2 + O \leftrightarrow OH + H.$

$H + OH + M \rightarrow H_2O + M.$

$O_2 + H + M \rightarrow HO_2 + M.$

$H + HO_2 \rightarrow 2OH.$

$H \rightarrow wall.$

The simplified mechanism [174] has been studied with the help of a program complex that realizes the method of thermodynamic analysis [177]. Elementary reactions with CH_4, C_2H_6 are known[169].

Porous carbon particles, being one of the sources for fire occurrence [102], can burn themselves in the process of forest fuel layer ignition [178]. During burning of a carbon particle in the oxygen, the main reactions are [179]:

$$C + O_2 = CO_2,$$
$$2C + O_2 = 2CO,$$
$$C + CO_2 = 2CO,$$
$$2CO + O_2 = 2CO_2.$$

The first three reactions are heterogeneous and may occur inside the porous part of carbon. The fourth reaction is homogeneous and may occur either inside the porous particle, or in the gas. Model [179] describes the burning of a porous carbon particle with a radius of a in clean oxygen in an oven with a temperature of the walls and gas of T_w by means of equations for preserving carbon and oxygen atoms, as well as heat [179]:

$$\mathrm{div}\sum \frac{m_j I_j}{\mu_j} = \frac{W_s}{\mu_C}, \qquad (1.25)$$

$$\mathrm{div}\sum \frac{n_j I_j}{\mu_j} = 0, \qquad (1.26)$$

$$\mathrm{div}\left(\sum I_j h_j + I_h\right) = sWh_C - I_R\delta(r-a), \qquad (1.27)$$

where j = 1, 2 and 3 correspond to CO_2, CO and O_2; m_j, n_j — the number of carbon and oxygen atoms in the molecule of the substance under study ($C_{m_j}O_{n_j}$;) I_j — substance flow j, kg/(m^2·s); I_h — heat flow, kJ/(m^2·s); μ_j — the molecular mass of the gaseous substance j, kg/mole; h_C — enthalpy of solid carbon formation, kJ/(kg·K); I_R — heat flow with an emission from the particle to oven walls; $\delta(r - a)$ — delta function; r — radial coordinate, m. The full rate of consuming carbon inside the porous particle at the process of heterogeneous reactions equals the product of W rate per the value of s specific inner surface.

Equation of nonseparability for the gas [179]:

$$\mathrm{div}U = sW, \qquad (1.28)$$

where $U = \varepsilon\rho u$, U — mass gas flow through the surface unit; ε — porosity; ρ — gas density; u — Stefan flow.

Changes in pressure inside the particle are descried by Darcy's law:

$$\varepsilon u = -\frac{k}{\mu}\mathrm{grad}p, \qquad (1.29)$$

where k — penetrability coefficient of the porous particle; p — pressure, atm.; μ — gas viscosity. It is considered that inside the porous particle there is the molecular

mode of gas flow, and the parameters of the porous environment do not change in the process of the particle burning [179].

Equation of oxygen diffusion [179]:

$$\mathrm{div}I_3 = -\left(\frac{\mu_3}{\mu_C}W_{O1}s + \frac{\mu_3}{2\mu_C}W_{O2}s + \frac{\mu_3}{2\mu_1}\varepsilon W_g\right), \quad (1.30)$$

where W_{O1} W_{O2} — rate of reactions of carbon with oxygen, kg/(m^2·s), in which carbon dioxide and carbon monoxide is formed correspondingly, W_g — the rate of homogeneous reaction, kg/(m^2·s).

The formula for the substance and heat flows [179]:

$$I_j = Uz_j - \varepsilon\rho D\mathrm{grad}z_j,$$
$$I_h = UcT - [\varepsilon\lambda_g + (1-\varepsilon)\lambda_C]\mathrm{grad}T, \quad (1.31)$$

where z_j — relative mass concentration of j substance, D — diffusion coefficient, c — heat capacity per unit mass (per 1 kg of matter), λ_g and λ_C — thermal conductivity coefficients of gas and solid carbon correspondingly.

The boundary conditions for equations (1.25)—(1.31) have an outline [179]

$$r = 0: U = 0, I_j = 0, I_h = 0, \frac{dp}{dr} = 0,$$

$$r = \infty: z_j = z_j^{\infty}, T = T_w, p = p_0,$$

where z_j^{∞} — relative mass concentration of j substance in the environment.

For a complete modeling of a carbon particle burning, it is necessary to also investigate the processes in the gas above the particle surface [179].

Forest fuels may also be ignited as a result of ground storm discharge [180]. However, not all the attempts to ignite forest fuels will lead to the intended effect [45]. If ignition from lightning is considered, this process must occur under the fulfillment of four conditions [18]: 1) there must be a contact of the lightning channel and forest fuels, 2) moisture must be removed from forest fuels, 3) the temperature of forest fuels must reach the temperature pyrolysis 4) the products of pyrolysis must be heated to a certain temperature. This means that the ignition probability of forest fuels depends on many factors.

The possibility of igniting forest fuels with an electric arc was determined [86]. The facility [181] allowed creating an electric with a voltage of 100000 V with a duration of up to 5 min. The minimum energy to ignite forest fuels was determined by a test method in two steps. At Step One, electrodes were deep inside the sample. The electrodes were drawn apart, and so the distance at which inflammation of the whole sample being in a completely dry state occurred. The voltage on the discharge gap was maintained equal to the breakdown voltage. At Step Two samples with different moisture content were tested. The energy necessary for ignition was calculated with the formula [86]

$$W = UIt,$$

where W — the amount of heat, J; U — breakdown electric voltage, V; I — current intensity, A; t — the exposure time of the arc, s.

Table 1.8 illustrates minimum ignition energies of different forest fuels by the electric arc [86].

Table 1.8. Minimum energy of forest fuel ignition by the electric arc [86]

Forest fuel type	Critical moisture content, %				Time of exposure by the arc, s				Ignition energy, J
	X	$\pm m$	V	P	X	$\pm m$	V	P	$X \pm m$
Dead grass	10.1	0.2	7.4	2.4	1.0	0.2	6.7	2.1	90.0 ± 0.5
Foliage litter	8.4	0.2	8.4	2.6	1.0	0.3	11.7	3.4	90.0 ± 0.9
Decay of coniferous species	6.4	0.3	14.9	4.5	1.0	0.5	16.9	5.1	90.3 ± 0.6
Ground litter	7.5	0.3	11.9	4.2	1.0	0.5	16.8	5.0	90.5 ± 1.3
Schreiber's moss	9.1	0.2	5.6	1.8	1.0	0.4	14.0	4.5	90.5 ± 1.4
Cladonia lichen	10.9	0.3	7.8	2.5	1.2	0.5	16.0	4.6	107.5 ± 0.9
Pine needle litter	9.2	0.3	9.1	2.8	1.3	0.6	15.6	4.7	116.9 ± 0.5
Sphagnum	9.3	0.3	11.8	3.7	1.5	0.6	18.0	5.4	135.2 ± 1.1

Note. X — arithmetical average; m — error of mean; V — coefficient of variation, %; P — measure of inaccuracy, %.

An important factor at forest fuel lightning-induced ignition is the specific resistivity of the soil [86] that determines the way lightning current spreads in the soil and on its surface. The specific soil resistivity was measured in different forest types with the use of [182, 183] methods. Moreover, measurements of the specific resistivity of the network of tree roots were also made.

A forest fuel may ignite at a lightning effect with two scenarios [86]: 1) direct contact of the forest fuel layer and the lightning channel (it is in principle enough for inflammation of any combustible environment); 2) secondary effect of lightning (the appearance of spark discharges) [184].

The ignition of condensed substances by a single particle heated to high temperatures is possible [185, 186]. In general, the real scenario is the fallout of metal, metal oxide and non-metal particles on the surface. Probabilities of fallout of different carbonaceous formations that represent compounds of carbon with different combustion products of both special igniting mixtures and customary combustible materials (wood, coal). As a rule, real particles have a form of irregular polyhedron and are in a solid condition at precipitation. Counting the real configuration of particles precipitating on the fuel surface is certainly not possible. However, particles similar to a sphere or cylinder are quite frequent [187, 188]. In the hypothesis that a particle has a form of a low height cylinder, the mathematical statement of a problem on the solidphase ignition of a condensed matter has the following outline [185]

$$c_1\rho_1 \frac{\partial T_1}{\partial t} = \lambda_1 \left(\frac{\partial^2 T_1}{\partial r^2} + \frac{1}{r}\frac{\partial T_1}{\partial r} + \frac{\partial^2 T_1}{\partial z^2} \right) + Qk_0 \exp\left(-\frac{E}{RT_1} \right), \quad 0 \le r \le r_1,\ h \le z \le H + h, \tag{1.32}$$

$$c_2\rho_2 \frac{\partial T_2}{\partial t} = \lambda_2 \left(\frac{\partial^2 T_2}{\partial r^2} + \frac{1}{r}\frac{\partial T_2}{\partial r} + \frac{\partial^2 T_{21}}{\partial z^2} \right), \quad 0 \le r \le r_2, 0 \le z \le h, \tag{1.33}$$

where T — temperature; c — specific heat capacity; ρ — density, λ — thermal conductivity; t — time; r, z — cylindrical coordinates; H — cylinder height of the condensed matter emitted in the plate; E — activation energy; R — universal gas constant; k_0 — pre-exponential factor; Q — reaction heat, Index 1 and 2 correspond to the condensed matter and particle. It is accepted that axes of symmetry of the particle and cylindrical matter emitted in the plate coincide.

The boundary and initial conditions for the problem stated have an outline of

$$-\lambda_1 \frac{\partial T_1(r, h, t)}{\partial z} = \alpha(T_g - T_1) + \varepsilon\sigma(T_g^4 - T_1^4), \quad r_2 < r < r_1, 0 < t < t_1, \tag{1.34}$$

$$-\lambda_1 \frac{\partial T_1(r, h+H, t)}{\partial z} = 0, \quad 0 < r < r_1, 0 < t < t_1, \tag{1.35}$$

$$-\lambda_1 \frac{\partial T_1(0, z, t)}{\partial r} = 0, \quad h \le z \le H + h, 0 < t < t_1, \tag{1.36}$$

$$-\lambda_1 \frac{\partial T_1(r_1, z, t)}{\partial r} = 0, \quad h \le z \le H + h, 0 < t < t_1, \tag{1.37}$$

$$-\lambda_1 \frac{\partial T_1(r, h, t)}{\partial z} = -\lambda_2 \frac{\partial T_2(r, h, t)}{\partial z}, \quad T_1 = T_2, 0 < r < r_2, 0 < t < t_1, \tag{1.38}$$

$$-\lambda \frac{\partial T_2(r, 0, t)}{\partial z} = \alpha(T_g - T_2) + \varepsilon\sigma(T_g^4 - T_2^4), \quad 0 \le r \le r_2, 0 < t < t_1, \tag{1.39}$$

$$-\lambda_2 \frac{\partial T_2(0, z, t)}{\partial r} = 0, \quad 0 \le z \le h, 0 < t < t_1, \tag{1.40}$$

$$-\lambda_2 \frac{\partial T_2(r_2, z, t)}{\partial r} = \alpha(T_g - T_2) + \varepsilon\sigma(T_g^4 - T_2^4),$$
$$0 \le z \le h,\ 0 < t < t_1, \qquad (1.41)$$

$$T_2(r, z, 0) = T_g = T_{p,0} = \text{const},$$
$$0 < r < r_2,\ 0 \le z < h, \qquad (1.42)$$

$$T_1(r, z, 0) = T_{s,0} = \text{const},$$
$$0 < r < r_1,\ h < z < H + h, \qquad (1.43)$$

where α — coefficient of heat transfer on all open areas of the particle surface and k-matter; σ — Stefan-Boltzmann constant; T_g — temperature of the outer gas flow; $T_{p,0}$ — temperature of the particle at the start time; ε — given emissivity factor; $T_{s,0}$ — temperature of k-matter at the start time.

For typical materials [185] — polyvinylnitrate and carbonaceous particles it is determined that at relatively low temperatures the inflammation modes of the condensed matter are adequate in inflammation delay time to heating modes of the condensed matter by the gas flow without particles, and at high temperatures – to heating modes by a metal plate with a fixed temperature (Fig. 1.35).

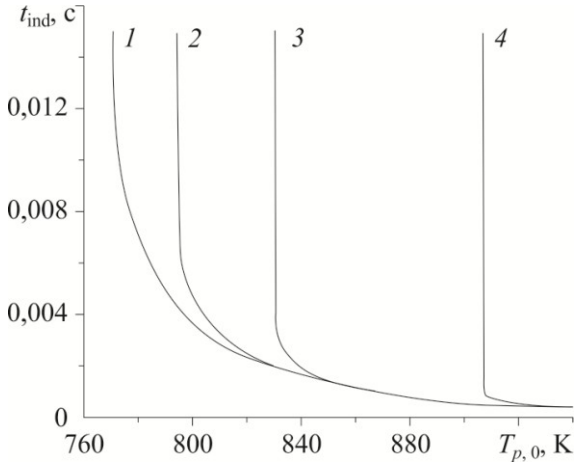

Fig. 1.35. Dependencies of inflammation delay time of the condensed matter for particles of different sizes [185]. r_2, micron: *1* — 200; 2 — 150; *3* — 100; *4* — 50.

It is of interest that the ignition specificity directly by a particle is revealed only in a fairly narrow temperature variation range. However, the boundaries for each of the three characteristic modes of ignition by a particle may be stated only as a result of solving the problem (1.32)—(1.43).

Temperature distribution along the z axis of the system particle-k-matter ($r = 0$) at the inflammation moment with different initial temperatures of the external environment and the particle [185] show (Table 1.9) that with an increase of $T_{p,0}$ the

cooling rate of the particle decreases substantially, and the temperature gradient value in the near-surface layers of the particle and matter increases.

Table 1.9. Temperature distribution in z axis of the system системы particle—k-matter ($r = 0$) at the inflammation moment at different initial temperatures of the environment and particle [185]

z_i, 10^{-3} m		$T_{0,z}$ at $T_g = T_{p,0}$, K			
		600	700	800	900
Particle	0	488.24	497.94	504.09	899.16
	0.025	487.74	496.87	502.38	895.35
	0.050	487.37	495.91	500.53	869.5
	0.075	487.19	494.98	498.47	783.57
	0.100	1983.76	1990.3	2001.03	2000.1
Condensed matter	0.225	480.35	475.98	474.42	300
	0.350	472.38	466.09	458.12	300
	0.475	461.98	453.64	444.81	300
	0.600	454.40	445.04	435.01	300
	0.725	447.39	436.51	427.92	300
	0.850	445.43	434.28	423.12	300
	0.975	443.37	431.78	420.31	300
	1.100	442.72	431.01	419.41	300

Model [186] changes from Statement [185] fundamentally. Inside the unbounded reactive matter, an inert hot body with a spherical form is considered. The ignition model describes this process in the supposition that the particle has an infinite large stock of energy. The hot body's heat is transferred to k-matter, as the result of which ignition takes place. The mathematical model for this is the following:

$$\frac{\partial \Theta}{\partial \tau} = \frac{1}{(d+\xi)^2}\frac{\partial}{\partial \xi}\left[(d+\xi)^2\frac{\partial \Theta}{\partial \xi}\right] + (1-\eta)^m \exp\left[\frac{\Theta}{1+\beta\Theta}\right],$$

$$\frac{\partial \eta}{\partial \tau} = \frac{Le}{(d+\xi)^2}\frac{\partial}{\partial \xi}\left[(d+\xi)^2\frac{\partial \eta}{\partial \xi}\right] + \gamma(1-\eta)^m \exp\left[\frac{\Theta}{1+\beta\Theta}\right],$$

$$K_{c\rho}\frac{d}{3}\left[1+N_\phi\delta(\Theta_1-\Theta_\phi)\right]\frac{\partial \Theta_1}{\partial \tau} = \frac{\partial \Theta(0,\tau)}{\partial \xi},$$

$$\Theta_1(0) = 0, \quad \Theta(\xi, 0) = -\Theta_0, \quad \eta(\xi, 0) = 0,$$

$$\Theta(0,\tau) = \Theta_1(\tau), \quad \frac{\partial \eta(0,\tau)}{\partial \xi} = 0,$$

$$\frac{\partial \Theta(\infty,\tau)}{\partial \xi} = \frac{\partial \eta(\infty,\tau)}{\partial \xi} = 0,$$

где $K_{c\rho} = \frac{c_1\rho_1}{c\rho}$, $Le = \frac{Dc\rho}{\lambda}$, $N_\phi = \frac{q_\phi E}{c_1 RT_0}$, $\gamma = \frac{cRT_0^2}{a_0 EQ}$, $\beta = \frac{RT_0}{E}$,

$t_a = \frac{cRT_0^2}{EQz}\exp\left(\frac{E}{RT_0}\right)$, $x_a = \sqrt{\frac{\lambda}{c\rho}t_a}$, $d = \frac{r_0}{x_a}$, $\xi = \frac{r - r_0}{x_a}$, $\tau = \frac{t}{t_a}$, $\eta = \frac{a_0 - a}{a_0}$,

$\Theta = \frac{E}{RT_0^2}(T - T_0)$, $\Theta_0 = \frac{E}{RT_0^2}(T_0 - T_н)$, Θ — dimensionless temperature; η — burnout; m — reaction order; ξ — dimensionless spatial coordinate; r — spatial coordinate; τ — dimensionless time; t — time; c, c_1 — heat capacity of the condensed matter and particle correspondingly; ρ, ρ_1 — density of the condensed matter and particle correspondingly; λ — thermal conductivity of the condensed matter; q_ϕ — thermal effect of the phase change; D — diffusion coefficient; E — activation energy; R — universal gas constant; Q — thermal effect of the combustion reaction of the condensed matter; z — pre-exponential factor; T_0, $T_н$ — the initial temperatures of the particle and condensed matter correspondingly; t_a, x_a — characteristic time and size correspondingly.

Non-dimensionalizing of the system of equations was implemented according to [156]. Fig. 1.36 illustrates the change in the particle temperature in time.

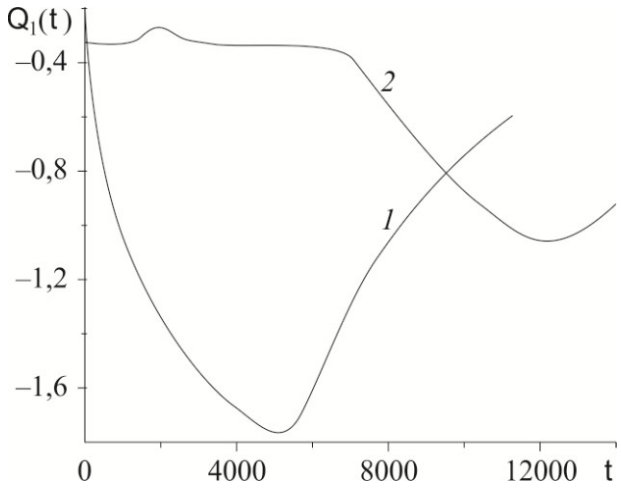

Fig. 1.36. Changes in the particle temperature in time [186].
1 — without consideration of the phase transition; *2* — with consideration of the phase transition

It is clearly visible that phase transformations in the inert hot body influence the ignition process of the reactive matter substantially.

The ignition of forest fuels at natural or technological disasters [47, 189—190] is possible under the influence of a radiative flow of energy. Experimental research in the ignition of litter layers of cedar, spruce, fir needles, birch leaves, and also *Cladonia* lichens and Schreiber's moss by the radiative flow of energy [191] have shown that moss is ignited much faster than other forest fuels. The time for ignition of needle litter of different trees at the same moisture content is identical within the experimental data accuracy, and for birch leaf litter it is slightly lower than for the

litter of coniferous species. The observed differences are connected with the peculiarities of interaction between the radiative flow with the needle and foliage litter layers. The density of the heat current necessary for igniting the forest fuels [192] increases with the growth of moisture content and density of the forest fuel layer and decreases with the spot diameter growth. Herewith, the critical density of the flow (for instance, laser emission) surpasses the corresponding values of the flow from an incandescent light bulb [192]. These results enable a conclusion that there is a direct influence of the process heat transfer in forest fuels onto the ignition character [192].

Inflammation of forest fuels depends, in [193, 194] terminology, on the pyrological features of forest fuels:

a) heat content as a measure of heat energy that may be released as the result of forest fuel burning [195, 196];

b) ash content [197, 198];

c) density and thermal conductivity.

For example, for the domineering types of vegetation in the Mediterranean region heat and ash content are known (Table 1.10—1.13). These data are used in the development of a pyrological classification of forest fuels of this region [199, 200].

Table 1.10. Thermal content of the domineering vegetation types of the Mediterranean region [199]

Type	Average value of heat content, kJ/kg
Erica arborea (foliage)	23.586
Arbutus unedo (foliage)	21.467
Cupressus sempervirens (foliage)	20.996
Quercus ilex (foliage)	20.690
Pinus brutia (needles)	20.625
Pistacia lentiscus (foliage)	20.264
Calicotome vilosa (thorns, caules)	20.019
Genista acanthoclada (thorns, caules)	19.852
Quercus ilex (limbs)	19.568
Erica arborea (limbs)	19.343
Pinus brutia (limbs)	19.283
Quercus coccifera (limbs)	19.253
Phlomis fruticosa (limbs)	19.250
Phlomis fruticosa (foliage)	19.233
Arbutus unedo (limbs)	19.07
Sarcopoterium spinosum (thorns, limbs)	19.054
Cistus salvaefolius (limbs)	19.046
Pistacia lentiscus (limbs)	18.916
Cupressus sempervirens (limbs)	18.861
Thymus capitatus (thorns, foliage)	18.773
Cistus salvaefolius (foliage)	18.654
Querqus coccifera (limbs)	18.582

It is of interest that the foliage (needles) mainly has a higher ash content than the branches of the same species (see Table 1.11). The relation of surface area to volume is much larger for the foliage (needles) than for the twigs of the same species (see Table 1.12). However, the spread of this parameter for needles of different pine types is minor as opposed to oak species.

The results of a quantitative analysis of the pyrological features of some forest fuels most frequent for the center of the Krasnoyarsk Territory are noteworthy [201]. The research of the ignition and burning of plants (Table 1.14), and also dry pills made of them [201] enables to evaluate the fire danger for each typical forest fuel met in Siberia fairly simply.

Table 1.11. Ash content of some vegetation types in the Mediterranean region [199]

Type	Ash content, % of mass in a dry condition
Phlomis fruticosa (foliage)	8.00
Cistus salvaefolius (foliage)	7.41
Querqus coccifera (foliage)	5.56
Cupressus sempervirens (foliage)	5.32
Pistacia lentiscus (foliage)	5.06
Querqus coccifera (limbs)	4.25
Phlomis fruticosa (limbs)	4.16
Arbutus unedo (foliage)	3.81
Pistacia lentiscus (limbs)	3.66
Pinus brutia (limbs)	3.30
Pinus brutia (needles)	3.18
Quercus ilex (foliage)	3.15
Cupressus sempervirens (limbs)	3.14
Sarcopoterium spinosum (thorns, limbs)	2.85
Cistus salvaefolius (limbs)	2.58
Thymus capitatus (thorns, foliage)	2.53
Erica arborea (foliage)	2.51
Quercus ilex (limbs)	2.50
Arbutus unedo (limbs)	2.35
Erica arborea (limbs)	1.63
Calycotome vilosa (thorns, caules)	1.51
Genista acanthoclada (thorns, caules)	1.47

The time of inflammation delay time for different forest fuel types in a muffle furnace may be used as such a factor [30]. For example, at a temperature of the environment at 560 °C, the delay time of the inflammation of Schreiber's moss at a humidity of 88 % is from 7 to 15 s; of aspen foliage at a humidity of 63 % – around 5 s. The big variation in determining this parameter of ignition shows that it is not only humidity that influences the ignition induction period. It is obvious that in experiments [30] some other characteristics of the moss or external conditions were not controlled; deviations of these parameters have led to large inaccuracies in determining the delay time. It is also important to note that dry forest fuel samples inflame almost instantly. However, depending on the forest fuel type the inflammation period and amount of the minimum ignition energy vary in a wide range. Dead grass, fruticose lichens have the lowest value of these factors, while needle litter and sphagnum have the highest. Lichens ignite faster with a higher moisture content and smaller ignition energy compared to other forest fuels because its ash content is rather small, and the content of hemicellulose is rather high [86]. Hemicelluloses are thermally unstable, their decomposition starts already at 200 °C [202]. Such forest fuels as needles and mosses are dominated by cellulose that is thermally more stable.

Table 1.12. The relation of surface area to volume for domineering vegetation types in the Mediterranean region [199]

Size and type of forest fuels	Type	Relation of surface area to volume, cm^{-1}
1	2	3
Foliage and needles	*Quercus ilex*	87.82
	Arbutus unedo	65.82
	Pinus halepensis	62.49
	Pinus brutia	55.54
	Cistus salvaefolius	44.49
	Querqus coccifera	41.41
	Pistacia lentiscus	35.32
	Phlomis fruticosa	24.46
Limbs thinner than 0,6 cm	*Cistus salvaefolius* (dead)	23.46
	Cistus salvaefolius (living)	23.01
	Quercus ilex (dead)	17.76
	Querqus coccifera (living)	16.56
	Quercus ilex (living)	16.04
	Phlomis fruticosa (dead)	14.37
	Querqus coccifera (dead)	14.23
	Pistacia lentiscus (dead)	12.79
	Arbutus unedo (living)	11.8
	Pistacia lentiscus (living)	11.58
	Phlomis fruticosa (living)	11.15
	Arbutus unedo (dead)	11.11
Limbs with a diameter of 0,6—2,5 cm	*Cistus salvaefolius* (living)	8.09
	Querqus coccifera (dead)	4.47
	Phlomis fruticosa (living)	4.38
	Arbutus unedo (dead)	3.7
	Pistacia lentiscus (dead)	3.61
	Pistacia lentiscus (living)	3.31
	Arbutus unedo (living)	3.2
	Querqus coccifera (living)	2.91
	Quercus ilex (living)	2.66
Limbs with a diameter of 2,5—7,6 cm	*Quercus ilex* (living)	1.63
	Arbutus unedo (dead)	1.43
	Querqus coccifera (living)	1.34
	Arbutus unedo (living)	1.27
	Pistacia lentiscus (living)	1.13

Table 1.13. The density of some vegetation types in the Mediterranean region [200]

Вид	Density, kg/m^3
Cistus salvaefolius (foliage)	310
Cistus salvaefolius (limbs)	620
Pistacia lentiscus (foliage)	540
Pistacia lentiscus (limbs)	740
Quercus ilex (foliage)	450
Querqus coccifera (foliage)	450
Querqus coccifera (limbs)	670
Phlomis fruticosa (foliage)	210
Phlomis fruticosa (limbs)	590
Arbutus unedo (foliage)	570
Arbutus unedo (limbs)	630
Pinus brutia (needles)	310
Pinus halepensis (needles)	290

Table 1.14. The results of experimental research of the vegetation ignition and burning [201]

Plant	Mass of the element, g	Temperature in the furnace, ±20 K	Time period, s			Humidity, %	Density, g/cm^3
			before combustion	of flame combustion	of smoldering		
Labrador tea	0.3	843	5 ± 1	10 ± 2	24 ± 10	–	–
Cowberry	0.6 ± 0.3	831	8 ± 2	5.3 ± 1.5	17 ± 5	52	0.78
Stone bramble	0.33 ± 0.06	836	6 ± 2	2.0 ± 0.7	14	72	0.72
Hawksbeard	1.7 ± 0.3	844	9 ± 1	3.6 ± 1.0	32 ± 5	79	0.62
Aspen (foliage)	0.4 ± 0.1	833	5.5 ± 0.5	2.0 ± 0.5	12 ± 3	63	0.93
Carex	0.14 ± 0.02	839	6 ± 1	1.7 ± 1	5 ± 2	–	–
Scouring horsetail	0.8 ± 0.1	838	33 ± 1	8 ± 3	54 ± 16	61	0.79
Vicia unijuga	0.59 ± 0.3	834	4.4±1.5	4±3	8 ± 1	73	0.86
Meadow horsetail	1.52 ± 0.49	824	8.56 ± 1.4	4.1 ± 0.9	40 ± 5	77	0.70
Schreber's moss	2.6	834	11.6±4.5	short term	38 ± 9	88	0.99
Vicia cracca	0.40	842	5.6	–	13	72	0.82
Wood geranium	0.70 ± 0.2	837	7.6±1.7	–	26 ± 3	74	0.86
Fern	0.22±0.07	829	6.5 ± 1.4	–	16 ± 2	68	0.79
Field horsetail	1.7 ± 0.3	816	5.4 ± 1.8	–	57 ± 10	74	0.60
Cat's foot	0.61	837	6.5 ± 1.4	–	41 ± 9	74	0.65
Yarrow	0.4 ± 0.2	830	4 ± 1	–	14 ± 5	79	0.87
Plantains	0.8 ± 0.2	835	8 ± 1	–	19 ± 5	82	0.88
Siberian chrysanthemum	1.1 ± 0.2	830	7.4 ± 1.6	–	44 ± 1	85	0.72
Hop-clover	0.89 ± 0.28	832	6.18 ± 0.09	–	25 ± 2	80	–

Note. Dash — not available.

1.9. Elements of boundary layer theory

To solve the tasks of drying [23, 136] and pyrolysis of the forest fuel layer in the conjugate setting it is most rational to use the boundary layer model, but not solve the Navier-Stokes equations. The injection process of chemically reacting gases is an important mechanism element of gas-phase combustion characteristic of many liquid and solid matters [203]. From the point of view of forest fire theory, it is reasonable to use the boundary layer model. The combustion process of forest fuels has a lot in common with the flow in the boundary layer at the injection of a flammable gas through the porous surface [203]. It is possible, for instance, to create a physical and mathematical model of forest fuel burning with a consideration of the injection of gaseous flammable products of forest fuel thermal decomposition to a wall-adjacent area through the porous layer.

Certain physical suppositions allow to describe the aerodynamic trail flows after bodies with systems of non-linear parabolic type equations. Such equations are called boundary-layer equations [204]. The main supposition of the boundary layer theory is that when a body moves in liquid or gas with a fairly big rate, all the flow may be conventionally divided into two areas: 1) the area of a small thickness near the body that is called the boundary layer (the impact of viscous forces is comparable to the

impact of inertial forces), and 2) the area of the so-called outer (with respect to the boundary layer) flow where the impact of viscous forces is negligible, and inertial forces prevail.

The boundary layer equations are usually acquired from the basic equations that describe the movement of viscous liquids. In the plane motion of an incompressible viscous liquid with constant properties and without any outer forces, the main system of equations consists of two equations of motion (Navier-Stokes equations) and an equation of continuity [204]:

$$\frac{\partial u}{\partial t}+u\frac{\partial u}{\partial x}+v\frac{\partial u}{\partial y}=-\frac{1}{\rho}\frac{\partial p}{\partial x}+\nu\left(\frac{\partial^2 u}{\partial x^2}+\frac{\partial^2 u}{\partial y^2}\right), \quad (1.44)$$

$$\frac{\partial v}{\partial t}+u\frac{\partial v}{\partial x}+v\frac{\partial v}{\partial y}=-\frac{1}{\rho}\frac{\partial p}{\partial y}+\nu\left(\frac{\partial^2 v}{\partial x^2}+\frac{\partial^2 v}{\partial y^2}\right), \quad (1.45)$$

$$\frac{\partial u}{\partial x}+\frac{\partial v}{\partial y}=0, \quad (1.46)$$

where t — time; x and y — independent orthogonal spatial variables; u and v — velocity components in x and y directions correspondingly; p — pressure; ρ — liquid density, ν — coefficient of kinematic viscosity.

In order to get boundary layer equations, (1.44)—(1.46) system is brought to a dimensionless form and Reynolds number is introduced. If the Re number is fairly big, then the $\varepsilon=\frac{1}{\sqrt{\mathrm{Re}}}$ value may be considered small.

It is possible to get a system of equations for the null approximation by presenting the desired functions in a factorization form according to the rates of this parameter. If we turn to dimensional variables again and omit the 0 index, then we will have a system of equations of incompressible viscous liquid plane motion in the boundary layer that bears the name of L. Prandtl [204]:

$$\frac{\partial u}{\partial t}+u\frac{\partial u}{\partial x}+v\frac{\partial u}{\partial y}=-\frac{1}{\rho}\frac{\partial p}{\partial x}+\nu\frac{\partial^2 u}{\partial y^2}, \quad (1.47)$$

$$\frac{\partial p}{\partial y}=0, \quad (1.48)$$

$$\frac{\partial u}{\partial x}+\frac{\partial v}{\partial y}=0. \quad (1.49)$$

Equation (1.48) shows that the pressure , что across the boundary layer in each cross section is constant and is the function of the x coordinate and time. The pressure distribution on the outer edge of the boundary level coincides with the one that would be on the body surface if there was no boundary level. Pressure distribution is supposed to be taken from the solution of the corresponding problem on the flow of

perfect liquid around the body directly on its surface. If the value of the longitudinal velocity at the flow of perfect liquid around the body is denoted through $U = U(x, y)$ and the condition of no fluid loss through the surface is considered ($v = 0$), then U and p on the body surface must satisfy the equation [204]

$$\frac{\partial U}{\partial t} + U\frac{\partial U}{\partial x} = -\frac{1}{\rho}\frac{\partial p}{\partial x}. \qquad (1.50)$$

Therefore, the pressure gradient $\frac{\partial p}{\partial x}$ on the outer edge of the boundary layer may be acquired from the equation (1.50), if the U velocity distribution along the surface at the perfect liquid flow around it is known.

The boundary conditions for the system (1.47)—(1.49) are usually recorded the following way [204]:

$$u = v = 0 \text{ with } y = 0, \qquad (1.51)$$

$$u \to U \text{ with } y \to \infty. \qquad (1.52)$$

Condition (1.51) is usually called the condition of *adhesion*, and (1.52) reflects the asymptotic tendency of the longitudinal velocity to the velocity on the outer edge of the boundary layer. Apart from the boundary conditions for the system (1.47)—(1.49), initial conditions at a value of $x = x_0$ must be set up:

$$u = \overline{u}(t, x_0, y), \quad v = \overline{v}(t, x_0, y), \qquad (1.53)$$

and the initial conditions at $t = 0$:

$$u = u(x, y), \quad v = v(x, y) \text{ for } x \geq x_0, \qquad (1.54)$$

concordant at $x = x_0$ with (1.53).

The burning processes in the boundary layers are quite hard and are conditioned by the impact of a big number of gas-dynamic and thermal parameters [203] that requires a common solution of the dynamic, thermal and diffusional problems with a consideration of the chemical kinetics, variability of thermophysical properties, many-component diffusion and other factors [203].

The flows in the boundary level may be realized in streamline and turbulent conditions [203]. The main condition for forming the dynamic streamline boundary layers is the low viscosity of the liquid, in particular, the large value of Re number that, however, does not reach the critical value at which the flow mode in the boundary level becomes turbulent [205]. In analogy, for temperature layers, such a condition becomes the Péclet number's (Pe) reaching big values; and for concentration layers — the Péclet diffusion number's (Pe_d) reaching big values.

At the growth of Re number in the flows of real liquid in tubes and channels, as well as in the boundary layer, a well-defined transition from a streamline to a turbulent flow form takes place on the streamlined body. This transition, also called the emergence of turbulence, is of fundamental importance [206]. In turbulent flows,

the main flow is superimposed by the oscillatory, as the result of which a mixture of liquid portions occurs.

The asymptotic theory of the boundary layer is one of the most simple and effective models of turbulent heat and mass transfer [203, 207—209]. The use of this approach in solving the problem on the boundary level with a burning front allows analyzing the impact of different factors on the main characteristics of transfer processes [203].

Mathematical modeling of the turbulent flow in the boundary layers with phase and chemical transformations is a rather intricate problem [203]. Various modifications of k—ε-models of turbulence have become widespread [210—213]. The equations for the kinetic energy of turbulence and its dissipation rate in the simplest setting have the following outline [203]

$$\rho U\frac{\partial k}{\partial x}+\rho V\frac{\partial k}{\partial y}=\frac{\partial}{\partial y}\left(\left[\mu+\frac{\mu_t}{\sigma_k}\right]\frac{\partial k}{\partial y}\right)+\mu_{\mathrm{t}}\left(\frac{\partial U}{\partial y}\right)^2-\rho\varepsilon+F_1, \quad (1.55)$$

$$\rho U\frac{\partial \varepsilon}{\partial x}+\rho V\frac{\partial \varepsilon}{\partial y}=\frac{\partial}{\partial y}\left(\left[\mu+\frac{\mu_t}{\sigma_\varepsilon}\right]\frac{\partial \varepsilon}{\partial y}\right)+C_1\frac{\varepsilon}{k}\mu_{\mathrm{t}}\left(\frac{\partial U}{\partial y}\right)^2-C_2\rho\frac{\varepsilon^2}{k}+F_2. \quad (1.56)$$

Equations (1.55), (1.56) are solved along with the system of differential equations of the boundary layer. Here U, V — longitudinal and transverse components of velocity; $\mu_{\mathrm{t}}=C_\mu\dfrac{\rho k^2}{\varepsilon}$ — turbulent viscosity; k — turbulent kinetic energy; ε — its dissipation rate, C_1, C_2, C_μ, σ_k, σ_ε, F_1, F_2 — constants and functions of the turbulence model. The constants of this model may depend on the local Reynolds turbulent number $\mathrm{Re_t}=\dfrac{\rho k^2}{\mu\varepsilon}$ and the distance to the wall (the so-called models for low Reynolds numbers) [203]. Within the framework of models of this type it is possible to consider the initial streamline current area, the impact of buoyancy force on the turbulent characteristics and the impact of turbulent fluctuations on the chemical reactions rate [203].

Experimental research of the boundary layer structure with the burning front [214—216] which uses ethanol as a fuel creates a foundation for developing models of forest fire occurrence and spreading as a result of the initial inflammation of foreign fuels. In the reality, such situations may occur, for instance, after accidents at petroleum refining, petroleum chemistry and chemistry sites [217—220], road accidents with the means of fire hazardous substance and material transportation [221], and in incendiary forest fires.

Experimental research in blowing of a foreign substance without burning [222], with consideration of evaporation [223] and steam-flue gas mixture condensation [224] create the basis for development of more sophisticated models of forest fire condition of the forest fuel layer.

REFERENCES

1. Kuznetsov V.I., Kozlov N.I., Khomyakov P.M. (2005) Mathematical modeling of forest evolution for forestry management. Moscow: LENAND, 232 p. (In Russian)
2. Concept of the Russian Federation forestries informatization. M.: Rosleskhoz, 1995. 98 p. (In Russian)
3. Concept of forestry development in Russian for 2003—2010 years. Moscow: MPR, Rosleskhoz, 2003. 12 p. (In Russian)
4. Chernykh V.L., Sysuyev V.V. (2000) Information technologies in forestry: textbook / Min.of Educ. of the RF; Mariy Min. Tech. Univ. Yoshkar-Ola, 377 p. (In Russian)
5. Trifonova T.A., Mischenko N.V., Krasnoschekov A.N. (2005) Geoinformation systems and remote sensing in ecological surveys: textbook for higher schools. M: Akademicheskiy proekt, 352 p. (In Russian)
6. Panevin V.R. (2006) Forests and forestry of Tomsk region: textbook. Tomsk: Izd-vo Tom. un-ta, 126 p. (In Russian)
7. Yevseyeva I.S., Zemtsov A.A. (1990) Relief generation in forest-swamp area of West-Siberian Plain. Tomsk: Izd-vo Tom. un-ta, 242 p. (In Russian)
8. Yanko I.V. (2005) Pyrological evaluation of Tomsk region territory. Dissertation … Phd.Geogr.Sci. Tomsk: Tomsk state Pedagogical University, 174 p. (In Russian)
9. Sukhinin A.I., Pavlichenko E.A. (2002) Fires in taiga location of silkworm // Annex to Siberian ecological journal, 1, 13—16. (In Russian)
10. Grodnitskiy D.L., Ovchinnikova T.M., Soldatov V.V. Raznobarskiy V.G. (2002) Massive reproduction of Monochamus sutor in taiga location of // Same. 17—21. (In Russian)
11. Belov A.N., Belov A.A. (2003) Dynamics of gypsy moth reproduction in in Saratov region oak forest // Lesnoye khozyaystvo, 3, 41—42. (In Russian)
12. Kurbatskiy N.P. (1964) Fires in taiga, laws of occurrence and development: Autoref. thes. … DSci / ILiD SO AN USSR. Krasnoyarsk, 38 p. (In Russian)
13. Kurbatskiy N.P. (1970) Study of properties and amount of forest fire fuels // Voprosy lesnoy pirologii. ILiD SO AN USSR, Krasnoyarsk, P. 5—58. (In Russian)
14. Valendik E.N., Kisilyakhov E.K., Verhovets S.V. (2003) Fire danger in fellings in dark coniferous forest of Krasnoyarsk krai // Lesnoye khozyaystvo, 3, 36—38. (In Russian)
15. Dobrovolskiy V.V. (2001) Geography of soil with basics of soil studies: textbook for higher institutions. Moscow: Gumanit. izd. centr. VLADOS, 384 p. (In Russian)
16. Kurbatskiy N.P. (1972) Terminology of forest pyrology // Voprosy lesnoy pi-rologii / ILiD SO AN USSR. Krasnoyarsk, 171—231. (In Russian)
17. Volokitina A.V., Sofronov M.A. (2002) Classification and mapping of flammable vegetation. Novosibirsk: Izd-vo SB RAS, 314 p. (In Russian)
18. Deeming J.E., Burgan K.E., Cohen J.D. (1978) The National Fire-Danger Rating System. Ogden, Utah: USDA Forest Service, General Technical report. INT-39, 66 p.
19. Stocks B.J., Alexander M.E., McAlpine R.S. et al. (1987) Canadian Forest Fire Danger Rating System. Canadian Forestry service, 500 p.
20. Van Wagner C.E. (1987) Development and structure of the Canadian Forest Fire Weather Index System / Petawawa. Canadian Forest Service. Technical report 35. Ontario, 37 p.
21. Nesterov V.G. (1949) Forest fireability and methods of detection. Moscow; Leningrad: Goslesbumizdat, 76 p. (In Russian)
22. Vonskiy R.M., Zhdanko V.A. (1976) Principles of meteorological factors development of forest fire danger (methodical recommendations) / LenNIILH. Leningrad, 47 p. (In Russian)
23. Grishin A.M. (1992) Mathematical modeling of forest fires and new methods of fighting them ними. Novosibirsk: Nauka, Sib.branch, 408 p. (In Russian)
24. Alexander M.E., Lawson B.D., Stocks B.J., Van Wagner C.E. (1984) User guide to the Canadian Forest Fire Behaviour Prediction System: rate of spread relationships / Canadian Forest Service Fire Danger Group, 73 p.

25. Burgan R.E., Rothermel R.C. (1984) Behave: fire behaviour prediction and fuel modeling system — fuel subsystem / USDA Forest Service. General Technical Report INT-167. 126 p.
26. Kurbatskiy N.P. (1962) Technique and tactics of forest fires fighting. Moscow: Goslesbumizdat, 154 p. (In Russian)
27. Baranov N.M. (1979) Influence of grass seasonal development on forest ripening of forest area in Khama-Daban mountains // Modelirovanie v okhrane lesov ot pozharov / ILiD SO AN USSR. Krasnoyarsk, P. 86—89. (In Russian)
28. Sofronov M.A. (1970) Forest fires in the Altai Mountains // Voprosy lesnoy pirologii / ILiD SO AN, USSR. Krasnoyarsk, P. 241—272. (In Russian)
29. Valendik E.N., Matveyev P.M., Sofronov M.A. (1979) Large forest fires. Moscow: Nauka, 198 p. (In Russian)
30. Konev E.V. (1977) Physical basics of vegetation burning. Novosibirsk: Nauka, Sib.branch, 239 p. (In Russian)
31. Yakovlev A.P. (1979) Fire danger of pine and larch forests // Forest fires in Yakutia and their impact on forest nature. Novosibirsk: Nauka, Sib.branch, P. 195—213. (In Russian)
32. Sheshukov M.A., Neshatayev V.V., Naykrug I.B. (1973) Some principles of fire-fighting palnning // Lesnoye khozyaystvo, 6, 48—53. (In Russian)
33. Sheshukov M.A. (1988) Bioecological and zonal-geographical basics of forest fire protection in the Far East. Autoref. thes. … DSci. Krasnoyarsk. (In Russian)
34. Grishin A.M. Sinitsyn R.P., Akimova I.V. (1991) Comparative analysis of thermokinetic constants of drying and pyrolysis of forest fire fuels // Fizika goreniya i vzryva, 27(6), 17—24.
35. Furyayev V.V. (1970) Fires in taiga of Ket-Chulym interfluve // Voprosy lesnoy pirologii / ILiD SO AN, USSR. Krasnoyarsk, P. 273—320. (In Russian)
36. Dichenkov N.A. (1992) Geographicity of forest fire fuels stock // Lesokhozyaystvennaya informatsiya, 257, 156—160. (In Russian)
37. Volokitina A.V., Nozhenkova L.F., Sofronov M.A., Nazimova D.I. (2000) Emergency forecast during vegetation fires near settlements // Sopryazhennye zadachi mekhaniki, informatiki i ekologii: Materials of International conference. Tomsk: Izd-vo Tom. un-ta, P. 39—48. (In Russian)
38. Grishin A.M. (2000) Modeling and prediction of technogenic and ecological disasters // Matematicheskoe i fizicheskoe modelirovanie sopryazhennyh zadach mekhaniki i ekologii: Selected reports of International Conference. Tomsk: Izd-vo Tom. un-ta, P. 64—87. (In Russian)
39. Volokitina A.V. (1987) Pyrological evaluation of forest type of Krasnoyarsk region near Angara river // Lesnye pozhary i borba s nimi / VNIILM. M., P. 104—116. (In Russian)
40. Nozhenkova L.F. (2001) Technology of expert geoinformation systems development for decision making for emergency prevention and elimination: Autoref. thes. … Dr.Eng. Krasnoyarsk, 41 p. (In Russian)
41. Gavrilova T.A., Khoroshevskiy V.F. (2001) Knowledge bases of intellectual systems: textbook. SPb. and other.: Piter, 382 p. (In Russian)
42. Tereshkov V.I., Vilchik R.I., Nozhenkova L.F. (1995) Krasnoyarsk region's integrated information-expert system of emergencies // Problemy bezopasnosti pri chrezvychaynykh situatsiyakh, 11, 77—83. (In Russian)
43. Sandberg D.V., Ottmar R.D., Cushon G.H. (2001) Characterizing fuels in the 21st century // Inter. J. Wildland Fire, 10(3—4), 381—387.
44. Byram G.M. (1959) Combustion of forest fuels // Forest fire control and use / Ed. K. P. Davis. N. Y.: McGraw-Hill, P. 61—89.
45. Wagtendonk J.W. Van. (2006) Fire as a physical process // Fire in California's ecosystems / Eds. N. G. Sugihara et al. Berkeley: University of California Press, P. 38—57.
46. Grishin A.M. Filkov A.I. (2005) Prediction of forest fires occurrence and distribution. Kemerovo: Praktika, 202 p. (In Russian)

47. Pinayev V.S., Scherbakov V.A. (1996) Fires, caused by nuclear explosions and ther results // Fizika goreniya i vzryva, 32(5), 116—121.
48. Latham D., Williams E. (2001) Lightning and forest fires // Forest Fires: Behavior and Ecological Effects. Amsterdam: Elsevier, P. 375—418.
49. Williams E.R. (1989) The tripole structure of thunderstorms // J. Geophys. Res, 94, 13151—13167.
50. Kozlov V.I., Mullayarov V.A. (2004) Thunderstorm activity in Yakutia. Yakutsk: YaF Izd-va SB RAS, 104 p. (In Russian)
51. Latham D.J. (1991) Lightning flashes from a prescribed fire-induced cloud // J. Geophyics Res, 96, 17151—17157.
52. Ivanov V.A. (1996) Forest fires from thunderstorms in the Yenisei Plain: Autoref. thes. … DSci. Krasnoyarsk, 23 p. (In Russian)
53. Uman M.A. (1969) Lightning. N. Y.: McGraw-Hill. 320 p.
54. Cummins K.L., Murphy M.J., Bardo E.A. et al. (1998) A combined TOA/MDF technology upgrade of the U.S. national lightning detection network // J. Geophys. Res, 103, 9035—9044.
55. Lyons W.A., Nelson T.E., Williams E.R. et al. (1998) Enhanced positive cloud-to-ground lightning in thunderstorms ingesting smoke from fires // Science, 282, 77—80.
56. Boccippio D.J., Williams E.R., Heckman S.J. et al. (1995) ELF transients, and positive ground strokes // Science, 269, 1088—1091.
57. Burke C.P., Jones D.L. (1996) On the polarity and continuing current in unusually large lightning flashes deduced from ELF events // J. Atmosp. and Solar-Terres. Phys, 58, 531—548.
58. Cummer S.A., Inan U.S. (1996) Sprite-producing lightning using ELF radio atmospherics // Geophys. Res. Letters, 24, 1731—1734.
59. Huang E., Williams E., Boldi R. et al. (1999) Criteria for sprites and elves based on Schumann resonance measurements // J. Geophys. Res, 104, 1693—1694.
60. Flannigan M.D., Wotton B.M. (1991) Lightning-ignited fires in northwestern Ontario // Can. J. Forest Res, 21, 277—287.
61. Soriano L.R., De Pablo F., Tomas C. (2005) Ten-year study of cloud-to-ground lightning activity in the Iberian Peninsula // J. Atmosp. and Solar-Terrestr. Phys, 67(16), 1632—1639.
62. Orville R.E., Huffines G.R. (2001) Cloud-to-ground lightning in the United States: NLDN results in the first decade, 1989—98 // Monthly Weather Review, 129, 1179 — 1193.
63. Ateitio J., Ezcurra A., Herrero I. (2001) Cloud-to-ground lightning characteristics in the Spanish Bascue Country area during the period 1992—1996 // J. Atmos. and Solar-Terrest. Phys, 63(10), 1005—1015.
64. Mardiana R., Kawasaki Z.-I., Morimoto T. (2002) Three-dimensional lightning observations of cloud-to-ground flashes using broadband interferometers // J. Atmos. and Solar-Terrest. Phys, 64(1), 91—103.
65. Tantisattayakul T., Masugata K., Kitamura I., Kontani K. (2005) Broadband VHF sources locating system using arrival-time differences for mapping of lighting discharge process // J. Atmos. and Solar-Terrest. Phys, 67(11), 1039—1039.
66. Seity Y., Soula S., Sauvageot H. (2000) Radar observation and lightning detection in coastal thunderstorms // Phys. and Chem. of the Earth. Part B: Hydrology, oceans and atmosphere, 25(10—12), 1107—1110.
67. Pinto O. Jr., Pinto I.R.C.A., Naccarato K.P. (2007) Maximum cloud-to-ground lightning flash densities observed by lightning location systems in the tropical region: A review // Atmosph. Res, 84(3), 189—200.
68. Campos L.Z.S., Saba M.M.F., Pinto O. Jr., Ballarotti M.G. (2007) Waveshapes of continuing currents and properties of M-components in natural negative cloud-to-ground lightning from high-speed video observations // Atmosph. Res, 84(9), 302—310.
69. Pinto I.R.C.A., Pinto O. Jr. (2003) Cloud-to-ground lightning distribution in Brazil // J. Atmosp. and Solar-Terrest. Phys., 65(6), 733—737.

70. Pinto O. Jr., Pinto I.R.C.A., Diniz J.H. et al. (2003) A seven-year study about the negative cloud-to-ground lighting flash characteristics in Southeastern Brazil // J. Atmosp. and Solar-Terrest. Phys., 65(6), 739—748.
71. Bernardi M., Ferrari D. (2004) Evaluation of the LLS efficiency effects on the ground flash density, using the Italian lightning detection system SIRF // J. Electrostatics, 60(2—4), 131—140.
72. Ivanov V.A. (1987) Thunderstorm activity and forest fires // Lesnye pozhary i borba s nimi / VNIILM. Moscow, P. 208—217. (In Russian)
73. Larjavaara M., Kuuluvainen T., Rita H. (2005) Spatial distribution of lightning-ignited fires in Finland // Forest Ecology and Management, 208(1—3), 177—188.
74. Azmetov R.R., Belyayev A.I., Moskovenko V.M. (2000) Prospects of establishment of the Russian system of thunderstorm electromagnetic monitoring for fire protection, power engineering, aviation, meteorology and disaster forecasting // Sopryazhennye zadachi mekhaniki, informatiki i ekologii: Materials of International conference. Tomsk: Izd-vo Tom. un-ta, P. 9—11. (In Russian)
75. Granstrom A. (1993) Spatial and temporal variation in lightning ignitions in Sweden // J. Vegetation Science, 4, 737—744.
76. Podur J., Martell D.L., Csilagg F. (2003) Spatial patterns lightning-caused forest fires in Ontario 1976—1998 // Ecological Modelling, 164(1), 1—20.
77. Weber M.G., Stocks B.J. (1998) Forest fires and sustainability in the boreal forests of Canada // Ambio, 27, 545—550.
78. Bailey T.C., Gatrell A.C. (1995) Interactive spatial data analysis. Essex: Longman Group Limited, 413 p.
79. Nieto H., Aguado I., Chuvieco E. (2006) Estimation of lightning-caused fires occurrence probability in Central Spain // Forest Ecology and Management, 234, Suppl. 1. P. S67.
80. Conedera M., Cesti G., Pezzatti G.B. et al. (2006) Lightning-induced fires in the Alpine region: An increasing problem // Forest Ecology and Management, 234, Suppl. 1. P. S68.
81. Amatulli G., Perez-Cabello F., Du la Riva J. (2007) Mapping lightning/human-caused wildfires occurrence under ignition point location uncertainty // Ecological Modelling, 200(3—4), 321—333.
82. Chirvinskiy P.N. (1950) Trees and lightnings // Priroda, 10, 28—33. (In Russian)
83. Stolyarchuk L.V., Belaya A.Yu. (1981) Criteria of storm fire danger // Lesnoye khozyaystvo, 7, 48—49. (In Russian)
84. Pavlov I.N. (2003) Global changes of arboreal plants habitat. Krasnoyarsk: SibGTU, 170 p. (In Russian)
85. Kasischke E.S., Christensen N.L., Stocks B.J. (1995) Fire, global warming and the carbon balance of boreal forests // Ecological Applications, 5, 437—451.
86. Ivanov V.A. (2006) Methodological basics of forest classification of Middle Siberia by degree of theunderstorm fire danger. Dissertation. … DSci. Krasnoyarsk: SibGTU, 350 p. (In Russian)
87. Gribanov L.N. (1953) Forest fire fighting, caused by lightning discharges // Lesnoye khozyaystvo, 4, 64-64. (In Russian)
88. Gribanov L.N. (1955) Thunderstorms phenomena and forest fires // Botan. zhurn. 40(3), 429—432. (In Russian)
89. Ponomarev Ye.I., Ivanov V.A., Korshunov N.A. (2006) Satellite data TOVS for prediction of storm fire danger in the forest // Geografiya i prir. Resursy, 1, 147—150. (In Russian)
90. Sukhinin A.I., Ponomarev E.I. (2003) Mapping and short-term fire danger prediction in forests of Eastern Siberis by satellite data // Sibirskij ekologicheskiy zhurnal, 6, 669—675. (In Russian)
91. Melekhov I.R. (1947) Forest nature and forest fires. Arkhangelsk, 60 p. (In Russian)
92. Andreev Yu.A., Larchenko G.F. (1987) Social and psychological aspects of recreational visits to forests and fire occurrence // Lesnye pozhary i borba s nimi / VNIILM. Moscow, P. 251—263. (In Russian)

93. Kurbatskiy N.P. (1964) Problem of forest fires // Vozniknovenie lesnykh pozharov. Moscow: Nauka, P. 5—60. (In Russian)
94. Melluma A.Zh., Rungule R.Kh., Yemsis I.V. (1982) Recreation in nature as environmental protection problem. Riga: Zinatne, 144 p. (In Russian)
95. Telitsyn G.P. (1984) Study of relation of forest trips and fire occurrence // Lesovedenie, 1, 59—63. (In Russian)
96. Andreev Yu.A. (1986) Laws of forest fires distribution // Metody i sredstva borby s lesnymi pozharami / VNIILM. Moscow, P. 43—52. (In Russian)
97. Kolezhuk V.K., Savchenko A.G. (1976) About forest fire safety violations // Lesnoye khozyaystvo, 7, 58—59. (In Russian)
98. Andreev Yu.A., Domrachev A.A. (1998) Social and demographic aspects of forest fires occurrence // Mater. of 7-th Intl.Conf. “Sistemy bezopasnosti”—SB-98. Moscow: Izd-vo MIPB, P. 158—160. (In Russian)
99. Telitsyin G.P. (1983) Influence of forest trips on forest fires rate // Povyshenie produktivnosti lesov Dalnego Vostoka / DalNIILH. Khabarovsk, 380 p. (In Russian)
100. Telitsyin G.P. (1987) Method for fire danger determining in the forest territory // Lesnye pozhary i borba s nimi / VNIILM. Moscow, P. 13—28. (In Russian)
101. Matsenko V.V., Sokolov A.Ya., Kalinin S.I. et al. (1999) General layout offire safety forest arrangement. V. 1. Explanation note. 5-99.14-17-PM / State Research Institute «Rosgiproles», Altai branch. Barnaul, 139 p. (In Russian)
102. Romanenkov I.G., Levites F.A. (1991) Fire protection of construction structures. Moscow: Stroyizdat, 320 p. (In Russian)
103. Cardille J.A., Ventura S.J., Turner M.G. (2001) Environmental and social factors influencing wildfires in the Upper Midwest, United States // Ecological Applications, 11(1), 111—127.
104. Pew K.L., Larsen C.P.S. (2001) GIS analysis of spatial and temporal patterns of human-caused wildfires in the temperate rain forest of Vancouver Island, Canada // Forest Ecology and Management, 140(1), 1—18.
105. Andreev Yu.A. (2003) Influence of anthropogenic and natural factors on forest fire occurrence and in settlements. Autoref. thes. … Dr.Eng. Moscow: FGU VNIIPO MChS Rossii, 45 p. (In Russian)
106. Benavent-Corai J., Rojo C., Suarez-Torres J., Velasco-Garcia L. (2007) Scaling properties in forest fire sequences: The human role in the order of nature // Ecological Modelling, 205(3—4), 336—342.
107. Grishin A.M. (2002) Disaster modeling and forecasting. Tomsk: Izd-vo Tom. un-ta, 122 p. (In Russian)
108. Kosarev V.P., Andryuschenko T.T. (2007) Forest meteorology with basics of climatology: Uchebnoe posobie. 2-e izd., ispr. i dop. / Pod red. B. V. Babikova. SPb.: Lan, 288 p. (In Russian)
109. Filkov A.I. (2005) Determintate-probability system of forest fire danger prediction. Dissertation … PhD.Phys.Math.Sci. Tomsk: TSU, 163 p. (In Russian)
110. Baranovskiy N.V. Mathematical modeling of the most probable scenarios and conditions of forest fires occurrence. Dissertation … PhD.Phys.Math.Sci. Tomsk: TSU, 153 p. (In Russian)
111. Scientific-applied reference book on the USSR climate. Series 3. Multiyear data. Parts 1—6. Issue 20. (Tomsk, Novosibirsk, Kemerovo regions and Altai krai). SPb.: Gidrometeoizdat, 1993. 718 p. (In Russian)
112. Tolstykh M.A. (2001) Semi-Lagrangian atmospheric model with high resolution for a numerical weather forecast // Meteorologiya i gidrologiya, 4, 5—15. (In Russian)
113. Dymnikov V.P., Lykosov V.N., Volodin E.M. et al. (2005) Modeling of climate and its changes // Sovremennye problemy vychislitelnoy matematiki i matematicheskogo modelirovaniya. In two volumes. V. 2. Moscow: Nauka, P. 38—175. (In Russian)

114. Murphy A.H., Winkler R.L. (1984) Probability forecasting in meteorology // J. American Statistical Association, 79(387), 489—500.
115. Hallenbeck C. (1920) Forecasting precipitation in percentages of probability // Monthly Weather Review, 48, 645—647.
116. Brier G.W. (1944) Verification of a Forecaster's Confidence and the use of probability statements in weather forecasting / US Weather Bureau. Research Paper N 16. Washington, D.C.
117. Nott D.J., Dunsmuir W.T.M., Kohn R., Woodcock F. (2001) Statistical correction of a deterministic numerical weather prediction model // Journal of American Statistical Association, 96(455), 794—804.
118. Tolstykh M.A. (1997) Global semi-Lagrangian atmospheric model based on compact finite-differences and its implementation on a parallel computer: INRIA Research Report #3080, Theme 4 / INRIA. Domaine de Voluceau, Rocquencourt, France, 25 p.
119. Vazhnik A.I. (1996) Scheme of vertical interpolation for a discrete four-dimensional system of observation data acquisition // Meteorologiya i gidrologiya, 10, 15—28. (In Russian)
120. Kristjansson J.E. (1992) Initialization of cloud water in a numerical weather prediction model // Meteorology and Atmospheric Physics, 50(1—3), 21—30. (In Russian)
121. Geleyn J.F., Bazile E., Bougeault P. et al. (1995) Atmospheric parameterization schemes in Meteo-France's ARPEGE N.W.P. model // Parameterization of Subgrid-Scale Physical Processes. ECMWF Seminar 1994. Reading, UK, P. 385—402.
122. Tolstykh M.A. (2002) Numerical modeling of regional atmospheric circulation using a global model with variable resolution // Program and reports of international conference «ENVIROMIS-2002». Tomsk: Izd-vo Tomskogo CNTI, P. 57—57. (In Russian)
123. Yesaulov A.O., Starchenko A.V. (2002) Realization of mesoscale model of air impurity transfer on supercomputers // Program and reports of international conference «ENVIROMIS-2002». Tomsk: Izd-vo Tomskogo CNTI, P. 64-64. (In Russian)
124. Chavro A.I., Dmitriev E.V. (2002) Method for restoration of a detailed structure of meteoparameters field on urban and regional scale by their integral features // Same. P. 89—90. (In Russian)
125. Bogoslovskiy N.N., Tolstykh M.A. (2006) Realization of an assimilation scheme for soil variables in a global semi-Lagrangian model of weather forecast // Vychislitelnye tekhnologii, 11, Spec. Issue, P. 20—24. (In Russian)
126. Noilhan J., Plantos S. (1989) A simple parameterization of land surface processes for meteorological models // Monthly Weather Review, 117, 536—549.
127. Noilhan J., Mahfouf J.-F. (1996) The ISBA land surface parameterization scheme // Global and Planetary. Change, 13, 145—149.
128. Giard D., Bazile E. (1996) Assimilation of soil temperature and water content with ISBA in arpege: Some new developments and tests // HIRLAM Newsl. Swedish Meteorological and Hydrological Institute, 24, 10—12.
129. Giard D., Bazile E. (2000) Implementation of a new assimilation scheme for soil and surface variables in a global NWP model // Monthly Weather Review. 128, 997—1015.
130. Mahfouf J.-F. (1991) Analysis of soil moisture from near surface parameters: a feasibility study // J. Appl. Meteorology, 30, 1534—1547.
131. Huth R., Mladek R., Metelka L. et al. (2003) On the integrability of limited-area numerical weather prediction model ALADIN over extended time periods // Studia Geophysica et Geodaetica, 47(4), 863— 873.
132. Bubnová R., Hello G., Bénard P., Geleyn J.F. (1995) Integration of the fully-elastic equations cast in the hydrostatic pressure terrain-following coordinate in the framework of the ARPEGE/ALADIN NWP system // Monthly Weather Review, 123, 515—535.
133. Váňa F. (1998) Physical parametrizations in the ALADIN model // Meteorol. Zpr, 51, 33—44. (in Czech).

134. Lixiang Z., Xiaoshan Z., Yongzuo L., Jinggui W. (2000) Case study on tropical cyclone track prediction with MM5 // J. Nanjing Institute of Meteorology, 23(1), 73—80.
135. Michalakes J., Chen S., Dudhia J. et al. (2001) Development of a next generation regional weather research and forecast model // Developments in Teracomputing: Proceedings of the Ninth ECMWF Workshop on the Use of High Performance Computing in Meteorology / Eds. W. Zwieflhofer, N. Kreitz. Singapore. World Scientific, P. 269—276.
136. Grishin A.M., Golovanov A.N., Kataeva L.Yu., Loboda E.L. (2001) Formulation and solution of the problem of drying of a layer of combustible forest materials // Combustion, Explosion and Shock Waves, 37(1), pp. 57-66.
137. Grishin A.M., Baranovskij N.V. (2003) Comparative analysis of simple models of drying of the layer of forest combustibles, including the data of experiments and natural observations // Inzhenerno-Fizicheskii Zhurnal, 76(5), pp. 166-169.
138. Grishin A.M. Kataeva L.Yu., Loboda Ye.L. (2001) Mathematical modeling of forest fire fuels layer drying // Vychislitelnye tekhnologii, 6(2), 140—144. (In Russian)
139. Grishin A.M. Baranovskiy N.V., Meynert I.V., Pavshuk Yu.Yu. (2001) Analytical and numerical solution of a problem of forest fire fuels layer drying // Lesnye i stepnye pozhary: vozniknovenie, rasprostranenie, tushenie i ekologicheskie posledstviya: Mater. of the 4-t international conference. Tomsk: Izd-vo TSU, P. 47—50. (In Russian)
140. Nigmatulin R.I. (1987) Dynamics of multiphase media. P. 1. Moscow: Nauka, 464 p. (In Russian)
141. Grishin A.M. Fomin V.M. (1984) Adjacent and non-stationary tasks of reacting media mechanics. Novosibirsk: Nauka, Sib.branch, 318 p. (In Russian)
142. Grishin A.M. (1997) Mathematical modeling of forest fire and new methods of fighting them. Russia. Tomsk: Publishing House of the Tomsk State University, 390 p. (In Russian)
143. Loboda Ye.L. (2002) Physical-mathematical modeling of forest fire fuels layer drying and inflammation: Dissertation … Phd. Phys.-Mat. Sci. Tomsk: TSU, 108 p. (In Russian)
144. Kataeva L.Yu. (2000) Application of methods and notions of gas and fluid mechanics for mathematical modeling of some urgent ecological problems. Dissertation … PhD.Phys.Math.Sci. Tomsk: TSU, 180 p. (In Russian)
145. Frank-Kamenetskiy D.A. (1987) Diffusion and heat transfer in chemical kinetics. Moscow: Nauka, 492 p. (In Russian)
146. Loboda E.L., Grishin A.M. Kataeva L.Yu., Baranovskiy N.V. (2001) Mathematical modeling of forest fire fuels layer drying // Lesnye i stepnye pozhary: vozniknovenie, rasprostranenie, tushenie i ekologicheskie posledstviya: Mater. of the 4-t international conference. Tomsk: Izd-vo TSU, P. 120 — 129. (In Russian)
147. Volpert A.I., Khudyaev S.I. (1975) Analysis in classes of discontinuous finctions and equations of mathematical physics. Moscow: Nauka, 396 p. (In Russian)
148. Baranovskiy N.V. (2007) Mathematical provision of steppe fire danger prediction // Ekologicheskie sistemy i pribory, 2, 41—45. (In Russian)
149. Grishin A.M., Golovanov A.N., Rusakov R.V. (2001) About moisture evaporation in the layer of forest fire fuels // Lesnye i stepnye pozhary: vozniknovenie, rasprostranenie, tushenie i ekologicheskie posledstviya: Mater. of the 4-t international conference. Tomsk: Izd-vo TSU, P. 51—51. (In Russian)
150. Grishin A.M., Golovanov A.N., Dolgov A.A. et al. (2002) Experimental and theoretical research of forest fire fuels drying // Izvestiya TPU, 305(2), 31 — 43. (In Russian)
151. Teylor Kh.R. (1935) Physical chemistry. Leningrad: ONTI, 832 p. (In Russian)
152. Freeman E.C., Carroll B. (1958) // J. Physical Chemistry, 62, 394—402.
153. Koshlin V.B., Sinitsyn R.P. (1989) Determining of effective kinetic constants of pine needles pyrolysis // Mekhanika reagiruyuschikh sred i yeyo prilozheniya. Novosibirsk: Nauka, Sib.branch, P. 49—57. (In Russian)

154. Grishin A.M., Abaltusov V.E., Zverev V.G. et al. (1981) Kinetics of uneven drying of some forest fire fuels // Fizika goreniya i metody yeyo issledovaniya/ ChGU. Cheboksary, P. 129—139. (In Russian)
155. Grishin A.M., Golovanov A.N. (2001) Determining of mass transfer characteristics in some forest fuels // Inzh.-fiz. Zhurn, 74(4), 53—57.
156. Vilyunov V.N. (1984) Theory of condensed matters ignition. Novosibirsk: Nauka, Sib.branch, 187 p. (In Russian)
157. Vant-Goff Ya.G. (1936) Essay on chemical dynamics. Leningrad: ONTI, 178 p. (In Russian)
158. Semenov N.N. (1934) Chain reactions. Leningrad: Goshimizdat, 555 p. (In Russian)
159. Semenov N.N. (1928) To the theory of burning processes // Zhurn. russkogo fiz.-khim. obschestva. Fizika, 60(3), 241—250. (In Russian)
160. Frank-Kamenetskiy D.A. (1967) Diffusion and heat transfer in chemical kinetics. Moscow: Nauka, 491 p. (In Russian)
161. McAlevy R.F. III, Cowan P.L., Summerfield M. (1960) The mechanism of ignition of composite propellants by hot gases // APS Progress in Astronautics and Rocketry: Solid Propellant Rocket Research. V. 1. N.Y.: Academic Press, P. 623—652.
162. Beyer R.B., Fishman N. (1960) Solid propellant ignition studies with high flux radiant energy as a thermal source // Ibid. P. 673—692.
163. Samarskiy A.A. (1983) Theory of difference schemes. Moscow: Nauka, P. 33—36. (In Russian)
164. Samarskiy A.A., Nikolaev E.R. (1978) Methods of grid equations solving. Moscow: Nauka, 590 p. (In Russian)
165. Samarskiy A. A., Vabischevich P. N. (2001) Additive schemes for mathematical physics problems. M.: Nauka, 320 p.
166. Samarskiy A.A., Vabischevich P.N. (2003) Computational heat transfer. Moscow: Editorial URSS, 784 p. (In Russian)
167. Burkina R.S., Vilunov V.N. (1982) Asymptotic problems of the burning theory. Tomsk: Izd-vo TSU, 100 p. (In Russian)
168. Burkina R.S. (1995) Ignition of porous body by a radiation beam // Fizika goreniya i vzryva, 31(6), 5—13.
169. Warnatz J., Maas U., Dibbl R.W. (2006) Combustion. Physical and chemical fundamentals, modeling and simulation, experiments, pollutant formation / Transl. from Eng. G. L. Agafonova. Rev. P. A. Vlasova. Moscow: Fizmatlit, 352 p. (In Russian)
170. Homann K.H. (1975) Reaktionskinetik. Darmstadt: Steinkopff, 154 P.
171. Lewis B., Elbe G. (1968) Combusion, flame and explosion of gases. Moscow: Mir, 592 p. (In Russian)
172. Dimitrov V.I., Azatyan V.V. (1975) Maximum kinetic mechanism of H_2 oxidation // Voprosy gazodinamiki / ITPM, SO AN USSR. Novosibirsk, P. 69—73. (In Russian)
173. Dimitrov V.I. (1977) The maximum kinetic mechanism rate konstants in the H_2—O_2 mixtures // React. Kinetic Catal. Lett., 7(1), 81—86.
174. Matveyev V.G. (2001) Reducing of hydrogen combustion mechnism // Fizika goreniya i vzryva, 37(1), 3—5.
175. Maas U., Pope S.B. (1992) Simplifying chemical kinetics: Intristic low-dimensional manifolds in composition space // Combustion and Flame, 88(2), 239—264.
176. Kovalski A.A. (1933) // Phys. Z. Sow. Bd. 4. P. 723.
177. Dimitrov V.I. (1982) Simple kinetics. Novosibirsk: Nauka, Sib.branch, 383 p. (In Russian)
178. Zvyailskaya A. I., Subbotin A. N. (1996) Influence of moisture content and heat and mass exchange with the environment on the critical conditions of low fire initiation // Fizika goreniya i vzryva, 32(5), 99—106.

179. Gremyachkin V.M. (2006) Kinetics of heterogeneous reactions of carbon and oxygen during combustion of porous carbon particles in oxygen // Combustion, Explosion and Shock Waves. 42, 254—263.
180. Plummer F.G. (1912) Lightning in relation to forest fires // Bulletin 111. USDA Forest Service. Washington, DC: Government Printing Office, 39 p.
181. Popov B.G., Verevkin V.N., Bondarev V.A. (1977) Static electricity in chemical industry. Moscow: Khimiya, 200 p. (In Russian)
182. Khmelevskiy V.K. (1984) Electrical survey. Rev. 2-nd. Moscow: Izd-vo MGU, 422 p. (In Russian)
183. Pozdnyakov A.I. (2001) Field electrophysics of soil. Moscow: MAIK Nauka, Interperiodika, 187 p. (In Russian)
184. Latham D.J., Schlieter J.A. (1989) Ignition probabilities of wildland fuels based on simulated lightning discharges / USDA Forest Service Res. Pap. INT-411. 16 p.
185. Kuznetsov G.V., Mamontov G.Ya., Taratushkina G.V. (2004) Numerical Simulation of Ignition of a Condensed Substance by a Particle Heated to High Temperatures // Combustion, Explosion and Shock Waves, 40(1), pp. 70-76.
186. Burkina R.S., Mikova E.A. (2006) Peculiarities of condensed matter ignition by a hot particle with final storage of heat with phase transition in it // Fundamentalnye i prikladnye problemy sovremennoy mekhaniki: Mater. konf-cii. Tomsk: Izd-vo TGU, P. 86—87. (In Russian)
187. Kunakov G.A., Chulkov A.Z. (1975) Characteristics of combustion products of metal-containing fuels // Rocket fuels. Moscow: Mir, P. 74—96. (In Russian)
188. Bakirov F.T., Zakharov V.M., Poleschuk I.Z. et al. (1989) Generation and burning out of ashes during hydrocarbon burning. Moscow: Mashinostroenie, 128 p. (In Russian)
189. Kurbatskiy N.P. (1975) About forest fire occurrence in the area of falling Tungus meteorite // Problemy meteoritiki. Novosibirsk: Nauka, Sib.branch, P. 69—71. (In Russian)
190. Grishin A.M., Perminov V.A. (1996) Ignition of forest massifs by a high-altitude radiant energy source // Fizika Goreniya i Vzryva, 32(5), pp. 107-115.
191. Grishin A.M., Zima V.P., Kuznetsov V.T., Skorik A.I. (2002) Ignition of combustible forest materials by a radiant energy flux // Combustion, Explosion and Shock Waves, 38(1), pp. 24-29.
192. Grishin A.M., Golovanov A.N., Medvedev V.V. (1999) Ignition of a forest fuel layer under heat radiation // Fizika Goreniya i Vzryva, 35(6), pp. 22-25.
193. Anderson H.E. (1970) Forest fuel ignitability // Fire Technology, 6(4), 312—319.
194. Rundel P.W. (1981) Structural and chemical components of flammability // Proceedings of the conference on fire regimes and ecosystem properties / Eds H. A. Mooney, T. M. Bonnicksen, N. L. Christenson, J. E. Lotan, W. A. Reiners. USDA Forest Service Gen. Tech. Rep. WO-26. P. 183—207.
195. Sussot R., DeGroot W.F., Shafizadeh F. (1975) Heat content of natural fuels // Fire and Flammability, 6, 311—325.
196. Shafizadeh F., Chin P. S., DeGroot W.F. (1977) Effective heat content of green forest fuels // Forest Science, 23, 81—89.
197. Mutch R.W., Philpot C.W. (1970) Relation of silica content to flammability in grasses // Forest Science, 16, 64—65.
198. Philpot C.W. (1970) Influence of mineral content on the pyrolysis of plant material // Forest Science, 16, 461—471.
199. Dimitrakopoulos A.P., Panov P.I. (2001) Pyric properties of some dominant Mediterranean vegetation species // Int. J. Wildland Fire, 10(1), 23—27.
200. Dimitrakopoulos A.P. (2001) A statistical classification of Mediterranean species based on their flammability components // Ibid, 10(2), 113—118.

201. Mitrofanov D.P. (1972) Comparison of pyrologial features of some forest fire fuels // Voprosy lesnoy pirologii / ILiD SO AN, USSR. Krasnoyarsk, P. 52—76. (In Russian)
202. Rodygina G.L., Sosnovskaya E.N. (1974) About chemical composition and thermic resistance of some forest fire fuels // Voprosy lesnoy pirologii / ILiD SO AN, USSR. Krasnoyarsk, P. 7—40. (In Russian)
203. Volchkov E.P., Terekhov V.I., Terekhov V.V. (2004) Flow structure, heat- and mass-transfer in the boundary layers with injection of chemically reactive matters (review) // Fizika Goreniya i Vzryva, 40(1), pp. 3-20.
204. Paskonov V.M., Polezhaev V.I., Chudov L.A. (1984) Numerical modeling of heat and mass exchange. Moscow: Nauka, 285 p. (In Russian)
205. Loytsyanskiy L.G. (2003) Mechanics of fluid and gas: textbook for higher institutions. 7-th edition, Rev. Moscow: Drofa, 840 p. (In Russian)
206. Shlikhting G. (1974) Theory of boundary layer. Moscow: Nauka, 711 p. (In Russian)
207. Spalding D.B. (1978) A general theory of turbulent combustion // J. Energy. 2, 16—23.
208. Boyarshinov B.F., Volchkov E.P., Terekhov V.I., Shutov R.A. (1981) Turbulent boundary layer with blowing of reacting substance // Fizika goreniya i vzryva, 17(6), 21—28. (In Russian)
209. Volchkov E.P., Terekhov V.I. (1982) Turbulent heat and mass transfer in the boundary layer with chemical reactions involved // Protsessy perenosa v vy-sokotemperaturnyh i khimicheski reagiruyuschikh potokakh / IT SO AN USSR. Novosibirsk, P. 13—39. (In Russian)
210. Volchkov E.P., Dvornikov N.A., Perepechko L.N. (1998) Mathematical modeling ща turbulent hydrogen burning in the boundary layer. // Inzh.-fiz. zhurn., 71(1), 86—91. (In Russian)
211. Perepechko L.N. (1998) Modeling of heat and mass transfer processes in the boundary layer with phase and chemical transformations. Dissertation … PhD.Phys.Math.Sci. Novosibirsk. (In Russian)
212. Volchkov E.P., Terekhov V.V., Terekhov V.I. (2002) Modeling of joint effect of blowing and burning on friction resistance and heat exchange in the boundary layer // Trudy XXVI Sibirskogo teplofizicheskogo seminara / IT SB RAS. Novosibirsk, CD-ROM. 26 p. (In Russian)
213. Volchkov E.P., Terekhov V.V., Terekhov V.I. (2002) Structure of a boundary layer with hydrogen combustion at different blow-in intensities // Fizika Goreniya i Vzryva, 38(3), pp. 20-29.
214. Boyarshinov B.F., Volchkov E.P., Terekhov V.I. (1992) Structure of a boundary layer with injection and combustion of ethanol // Combustion, Explosion, and Shock Waves, 28(3), pp. 235-242.
215. Boyarshinov B.F. (2007) Boundary layer with large-scale structures, with evaporation and burning: Dissertation … DSci. Novosibirsk: IT SB RAS, 381 p. (In Russian)
216. Boyarshinov B.F., Volchkov E.P., Terekhov V.I. (1991) Flow structure and heat and mass transfer in boundary layer with ethanol combustion // Flame Structure. V. 1. Novosibirsk: Nauka, JB, P. 141—146. (In Russian)
217. Romanov V.I. (2006) Applied aspects of emergency emissions in the atmosphere. Reference book. Moscow: Fizmatkniga, 368 p. (In Russian)
218. Method for evaluation of emergency consequences in fire and explosion dangerous facilities. Moscow: MChS, 1994. 42 p. (In Russian)
219. Safonov V.R., Odishariya G.E., Shvyryaev A.A. (1996) Theory and Practice of risk analysis in gas industry. Moscow: NUMC Minprirody Rossii, 208 p. (In Russian)
220. Kirillova E.B., Popkov V.F., Khusniyarov M.Kh. (2004) Impact on oil refining, petrochemical and chemical facilities: Textbook. Ufa: Izd-vo UGNTU, 61 p. (In Russian)
221. Kolodkin V.M., Murin A.V., Petrov A.K., Gorskiy V.G. (2001) Quantitative assessment of chemical accident risk / Rev. V.M. Kolodkina. Izhevsk: ID «Udmurtskiy universitet», 228 p. (In Russian)

222. Perepechko L.N. (2000) Investigation of heat and mass transfer processes in the boundary layer with injection // Arch. Thermodynamics, 21(3—4), 41—54.
223. Volchkov E.P., Lukashov V.V., Terekhov V.V. (1999) About similarity of heat and mass transfer processes with extrinsic blowing // Problemy gazodinamiki i teplo-massoobmena v energeticheskikh ustanovkakh: Sb. M.: Izd-vo MEI, P. 11—16. (In Russian)
224. Volchkov E. P., Terekhov V.V., Terekhov V.I. (2000) Heat and mass transfer in the boundary layer with humid air flow and vapor condensation on surface // Teplofizika i aeromehanika, 7(2), 257—266. (In Russian)

CHAPTER 2
METHODS OF FOREST FIRE DANGER PREDICTION

Abstract

The second paragraph describes different Russian and foreign methods of forest fire prediction. A new concept of forest fire hazard prediction is introduced.

Keywords: forest fire danger, prediction, evaluation, probability, concept

2.1. The Canadian and American methods of forest fire danger prediction

Canadian Forest Service has an over 75-year-old history of scientific studies [1]. Forest fires are an important factor for Canada's forest ecosystem formation. Ca. 10000 fires occur in this country annually. Forest areas on a territory of 2.5 million hectares burn down. The number of fires and the burnt area varies year to year (Fig. 2.1).

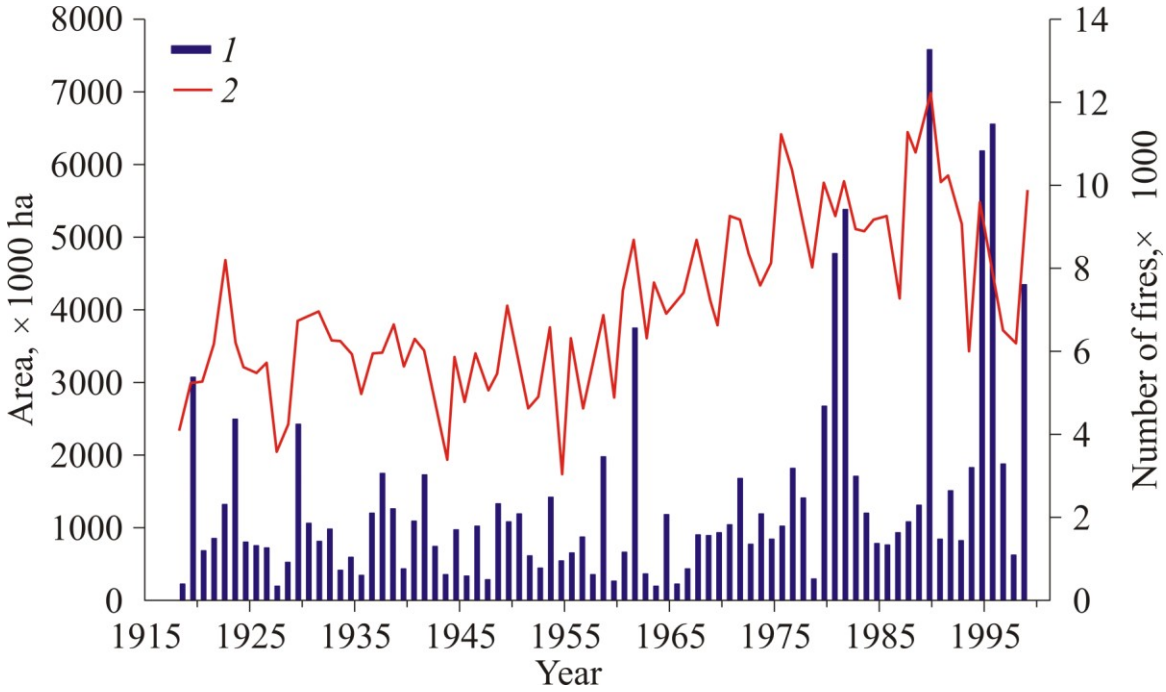

Fig. 2.1. Annual number of fires (1) and the area burned (2) in Canada [1]

Canadian Forest Fire Danger Rating System (CFFDRS) has two main sub-systems (modules) — Canadian Forest Fire Weather Index (FWI) System and Canadian Forest Fire Behavior Prediction (FBP) System (рис. 2.2, 2.3). Two other elements (Fuel Moisture System и Canadian Forest Fire Occurrence Prediction (FOP) System) are not developed for the whole country but there are regional versions of these systems [1].

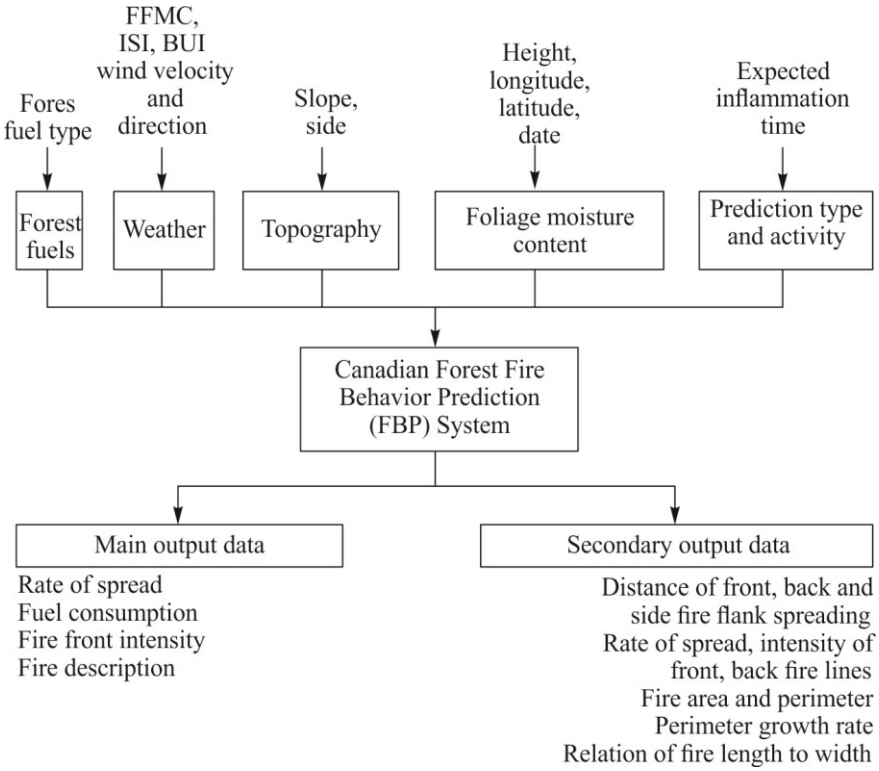

Fig. 2.2. The structure of CFFDRS [1]

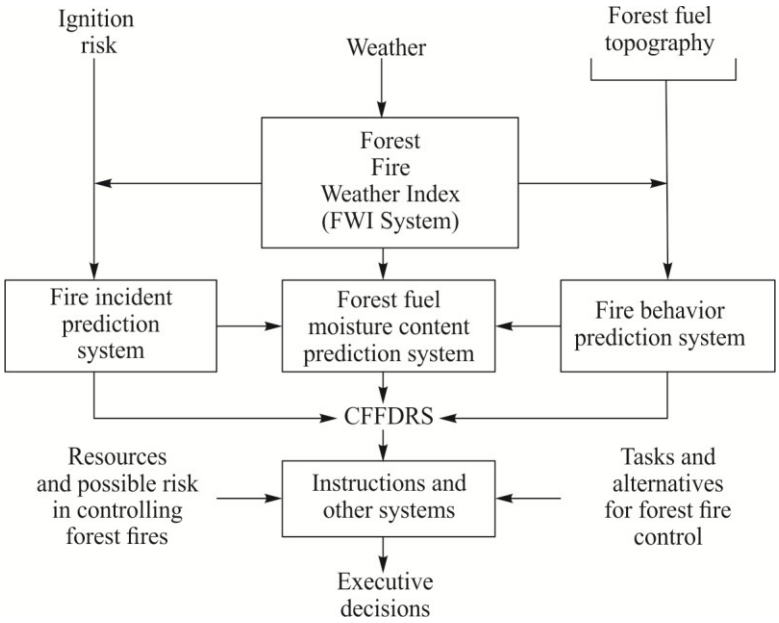

Fig. 2.3. The structure FBP [1]
See explanations in the text.

The Canadian method of forest fire danger prediction [2] is formed on a basis analyzing a large number of statistical data according to which tables of fire danger dependence on different factors are formed. Within the FWI sub-system the moisture content of forest fuels is predicted depending on weather conditions; whereas within FBP forest spot's behavior for different forest plant communities. The full structure of forest fire danger prediction system is shown on Fig. 2.4 [2].

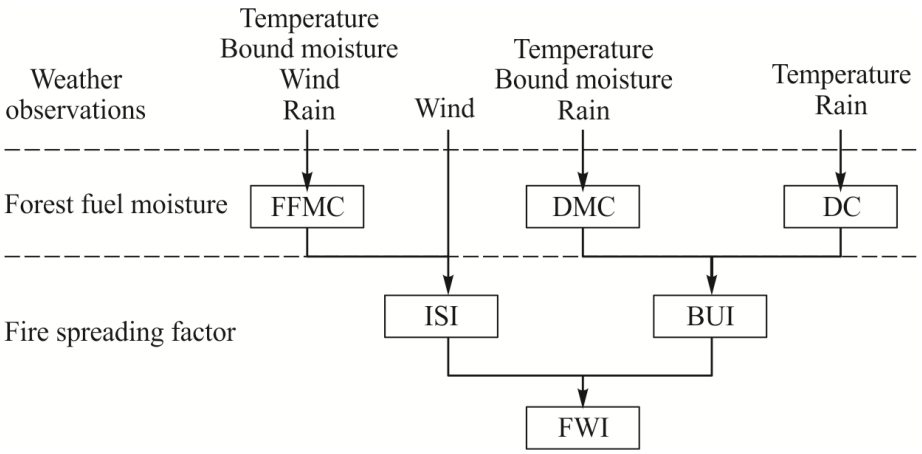

Fig. 2.4. A chart of the Canadian fire danger prediction system [2]

The following characteristics are used in prediction.

FFMC (Fine Fuel Moisture Code) — a numerical value characterizing the corresponding moisture of ground litter and forest fuels deposit.

DMC (Duff Moisture Code) — a numerical value characterizing the average organic layer's moisture loss on the mean depth. This characteristic indicates water discharge in the middle layer of forest fuels and wood-based materials of medium size.

DC (Drought Code) — a numerical value characterizing the corresponding average moisture of the deeply and densely packed organic layer. This indication is an important characteristic of effects of forest fuels seasonal drying and smouldering in the forest fuels layer depth and big logs.

ISI — a numerical value, characterizing the expected fire spreading speed. It unites the wind action and FFMC parameter per fire spreading speed excluding the impact of forest fuels quantity.

BUI — a numerical value of the total quantity forest fuels feasible for burning that unites DMC and DC.

FWI — a numerical value of fire intensity that is a total of ISI and BUI. This characteristic is used as a general fire danger index in the Canadian forests.

The value of FWI is calculated through FFMC, DMC, DC in accordance with Fig. 2.4 with the following formulae [2]:

$$m_0 = 147.2\left(101 - F_0\right)/\left(59.5 + F_0\right),$$

$$r_f = r_0 - 0,5,\ r_0 > 0,5.$$

If $m_0 \le 150$, then

$$m_r = m_0 + 42,5 r_f \exp\left(-100/\left(251 - m_0\right)\right)\left(1 - \exp\left(-6,93/r_f\right)\right).$$

If $m_0 > 150$, then

$$m_r = m_0 + 42,5 r_f \exp\left(-100/\left(251 - m_0\right)\right)\left(1 - \exp\left(-6,93/r_f\right)\right) +$$

$$+ 0,0015\left(m_0 - 150\right)^2 r_f^{0,5}.$$

The next step is choosing a new value $m_0 = m_r$:

$$E_d = 0,942H^{0,679} + 11\exp\big((H-100)/10\big) + \\ + 0,18\big(21,1-T\big)\big(1-\exp(-0,115H)\big),$$

$$E_w = 0,618H^{0,753} + 10\exp\big((H-100)/10\big) + \\ + 0,18\big(21,1-T\big)\big(1-\exp(-0,115H)\big),$$

If $m_0 > E_d$, then k_d is determined with the following formulae (2.1), (2.2), after which we calculate m from (2.5).

$$k_0 = 0,424\Big(1-\big(H/100\big)^{1,7}\Big) + 0,0694W^{0,5}\Big(1-\big(H/100\big)^{8}\Big), \quad (2.1)$$

$$k_d = k_0 \times 0,581\exp(0,0365T). \quad (2.2)$$

If $m_0 < E_w$, then we calculate k_w from (2.3) and (2.4), after which m is estimated from (2.5):

$$k_l = 0,424\left[1-\left(\frac{100-H}{100}\right)^{1,7}\right] + 0,0694W^{0,5}\left[1-\left(\frac{100-H}{100}\right)^{8}\right], \quad (2.3)$$

$$k_w = k_l \times 0,581\exp(0,0365T), \quad (2.4)$$

$$\begin{cases} m = E_d + (m_0 - E_d)\times 10^{-k_d}, \\ m = E_w - (E_w - m_0)\times 10^{-k_w}. \end{cases} \quad (2.5)$$

If $E_d \geq m_0 \geq E_w$, then $m = m_0$. Then F is calculated:

$$F = 59,5\big(250-m\big)/\big(147,2+m\big).$$

Here m_0 is the forest fuels moisture on the preceding day; m_r is forest fuels moisture after rainfall, m is the forest fuels moisture after drying; F is FFMC; F_0 is the previous value of FFMC; T is the day temperature (°C); H is the relative air humidity (%); r_0 is the amount of precipitation (mm), r_f is the effective amount of precipitation.

DMC is calculated analogically [2]:

$$r_e = 0,92r_0 - 1,27,\ r_0 > 1,5,$$

$$M_0 = 20 + \exp(5,6348 - P_o/43,43),$$

$$b = 100/(0,5+0,3P_0),\ P_0 \leq 33,$$

$$b = 14 - 1,3\ln P_0,\ 33 < P_0 \leq 65,$$

$$b = 6,2\ln P_0 - 17,2,\ P_0 > 65,$$

$$M_r = M_0 + 1000 r_e / (48,77 + b r_e),$$

$$P_r = 244,72 - 43,43 \ln(M_r - 20),$$

$$K = 1,894(T + 1,1)(100 - H) L_e \times 10^{-6},$$

$$P = P_0 (\text{или } P_r) + 100 \text{ K}.$$

Here r_e is the effective amount of precipitation; P_0 is the value DMC on the preceding day; P_r is the value of DMC after rainfall; L_e is the effective day duration (hour); P is the value of DMC.

DC is calculated analogically [2]:

$$r_d = 0,83 r_0 - 1,27,\ r_0 > 2,8,$$

$$Q_0 = 800 \exp(-D_0 / 400),$$

$$Q_r = Q_0 + 3,937 r_d,$$

$$D_r = 400 \ln(800 / Q_r),$$

$$V = 0,36(T + 2,8) + L_f,$$

$$D = D_0 (or D_r) + 0,5V$$

Here r_d is the effective amount of precipitation; D_0 is the previous value of DC; D_r is the value of DC after rainfall; D is the current value DC; L_f is the day duration coordinated with DC.

$$f(W) = \exp(0,05039 W),$$

$$f(F) = 91,9 \exp(-0,1386 m)\left(1 + m^{5,31} / (4,93 \cdot 10^7)\right),$$

$$R = 0,208 f(W) f(F).$$

Здесь R is the value of ISI; $f(W)$ is the wind function; $f(F)$ is the forest fuels moisture function.

$$U = 0,8 PD / (P + 0,4D),\ P \le 0,4D,$$

$$U = P - \left[1 - 0,8D / \left(P + 0,4D\right)\right]\left[0,92 + (0,0114P)^{1,7}\right],\ P > 0,4D.$$

Here U is the value of BUI.

$$f(D) = 0,626 U^{0,809} + 2,\ U \le 80,$$

$$f(D) = 1000 / \left(25 + 108,64 \exp(-0,023U)\right),\ U > 80,$$

$$B = 0,1 R f(D),$$

$$\ln S = 2,72(0,434 \ln B)^{0,647}, \ B > 1,$$

$$S = B, \ B \le 1.$$

Здесь $f(D)$ is the function of forest fuels layer moisture; B is the intermediate value of FWI; S is the final value of FWI.

Fire danger index value is calculated with the following formula [2]

$$DSR = 0,0272\left(FWI\right)^{1,77}.$$

The system characterizes fire danger on the whole on a calculated area, i.e. tens and hundreds of thousand hectares. This method predicts fire danger fairly accurately because it is based on the statistical data on forest fires of over 20-year period.

Markov's chain apparatus has been used to describe the daily variation of fire danger index recently [3]. Markov's first order chain with m states may be characterized with the matrix of P state transition probability. P_{ij} is the probability that the system will be in j state tomorrow if it is i state today. Markov's chain of r order is a chain for which the conditional probability distribution of system states tomorrow depends on the system states within the r preceding days. There exist all-around statistical analysis results of Markov's model use reliability [4] for a system of fire danger evaluation based on a 26-year chronological weather data sequence observed on Ontario's 15 weather stations [3] (Fig. 2.5).

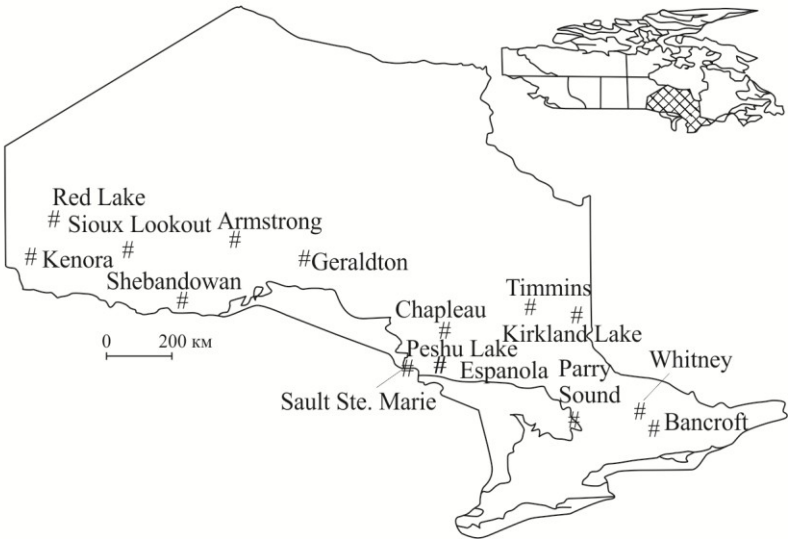

Fig. 2.5. Ontario's weather station network [3]

The results of a statistical test [3] may be summarized in the following way:

A. Spring: The test results show that it is rational to use Markov's first order chain on all 15 weather stations or Markov's first order chain for 14 of 15 stations and Markov's second order chain for Red Lake Station.

B. Early summer: The test results show that it is possible to use Markov's first order chain on 14 of 15 weather stations and Markov's second order chain for Parry Sound Station.

C. Summer: The test results show that it is reasonable to use Markov's first order chain on 13 of 15 weather stations and Markov's second order chain for Chapleau and Kenora Stations or Markov's first order chain for 12 of 15 stations and Markov's second order chain for Chapleau, Kenora Geraldton Stations.

Consequently, it is possible to model the daily variations in FWI within each sub-season as Markov's first order chain.

A method of fire danger estimation for different forested areas was developed in the USA in 1972 [5, 6]. This system was successfully tested from Florida to Alaska and from Maine to California.

A logical structure of the system [5, 6] represents an abstract model of the impact of different factors and conditions on the process of fire occurrence and spreading. The system chart has the following outline (Fig. 2.6) [5].

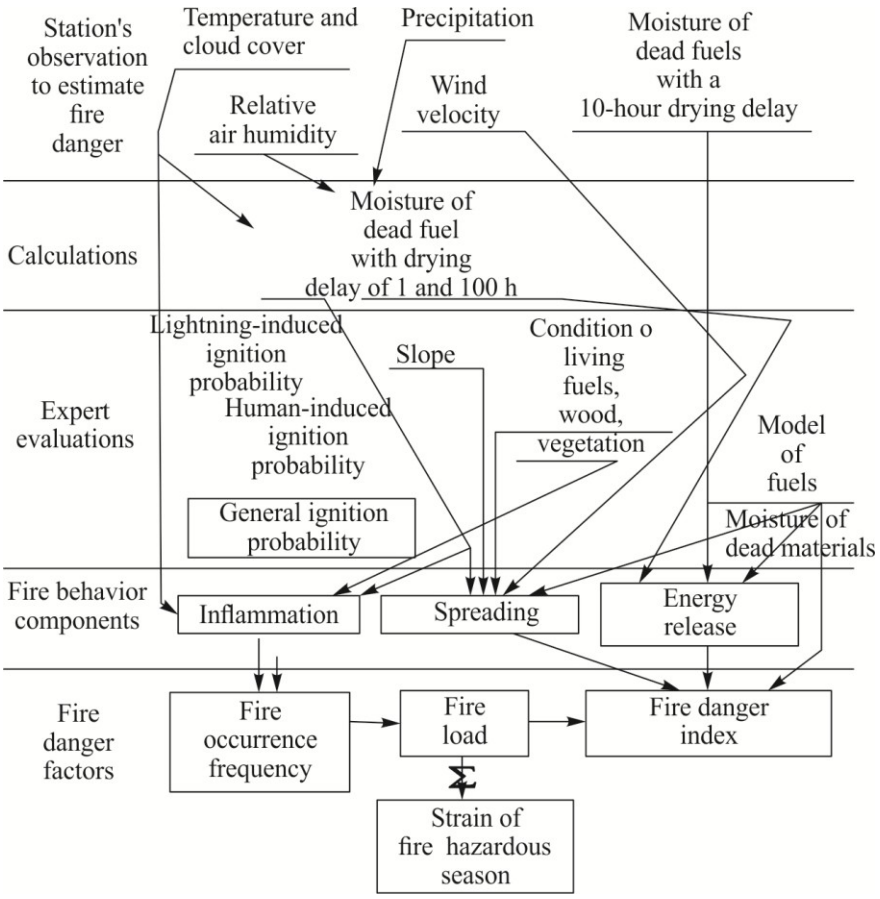

Fig. 2.6. A logical chart of the national fire danger estimation system in the forests of the USA [5]

All forest fuels are divided into nine typical models. The system suggests dividing the separately protected areas into physically and geographically homogeneous parts each of which must be correlated with one of nine models. A fire danger evaluation is prepared for each considered area separately. The final fire danger evaluation uses many tables and corrections according to data acquired empirically.

It is known that the current forest fuels moisture content of all classes is closely related to forest fuels moisture content of the second class. It is estimated either with special standard lump woods or with meteorological observation tables. For example, the weather condition, temperature and relative air humidity at 1 p.m. (design time station) are estimated preliminarily. Weather evaluation coding is presented in Table 2.1 [5]. Then moisture content of the second class forest fuels is estimated in accordance with a special table. The next step is assessing the moisture content of the first and third class forest fuels. It is also carried out with tables differentiated for forest fuels models. As the input parameters it is necessary to have a coded evaluation of weather condition, temperature and relative air humidity. It must be mentioned that the correction system enables counting not only forest fuels drying but also moistening.

*Table 2.1.*The coded evaluation of weather condition [5]

Weather condition	Code
Clear (cloud cover under 0,1)	0
Scattered clouds (cloud cover from 0.1 to 0.5)	1
Ragged clouds (cloud cover from 0.6 to 0.9)	2
Lowering sky (cloud cover over 0.9)	3
Foggy	4
Drizzle (precipitation in drops)	5
Rain	6
Snow with rain or snow	7
Shower	8
Approaching thunder storm	9

Stage Two - with account for a weather pattern - is closely related to the First stage. Stage Three of fire danger calculation is an expert evaluation of fire occurrence probability and a range of other characteristics of fire danger. Table 2.2 unites the actual lightning activity level of the preceding day and the expertly predicted level for the current day; this table is used for evaluating the occurrence of lightning-induced fires.

*Table 2.2.*Lightning-induced fire danger [5]

Lightning activity level observed	Lightning activity level predicted				
	1	2	3	4	5
1	0	10	20	40	80
2	3	13	23	43	83
3	5	15	25	45	85
4	10	20	30	50	90
5	20	30	40	60	100

The man-induced fire occurrence danger is predicted according to three characteristics: the seasonal danger class, a special indication of danger sources, the level of day activity and danger sources [5].

The seasonal danger class [5] is a comparative evaluation of fire danger on a calculated area opposed to the danger on the neighboring areas. It is evaluated according to the fire data of the last 5 to 10 years with a consideration of their maximum number in the separate months. It is numerically displayed in dimensionless units from 0 to 10.

A special indication of danger source [5] is the estimation of source value in the general total of human-induced fire sources. It is calculated as a part of this month's total forest fires number that suits the danger source under consideration.

The source's day activity level [5] is estimated daily as an expert evaluation on a five-point scale. It is possible to count the receptivity of forest fuels to this source at the current moment. The activity characteristic indicates the weekly, monthly and seasonal imbalance of separate danger source occurrence on the calculated area (non-working days, vacation period, cutting remnants burning season) [5].

A special danger source indication (%) and its day activity (point) are used to estimate the partial danger factor in a 100-point scale. The sum of these factors for each danger source gives a non-standardized human-induced fire occurrence danger. Human-induced fire occurrence danger is estimated according to this characteristic and seasonal danger class according to Table 2.3 in a 100-point scale.

Table 2.3. Estimation of man-induced fire danger [5]

Man-induced non-standardized danger	Seasonal danger class									
	1	2	3	4	5	6	7	8	9	10
0—5	1	1	1	1	2	2	2	2	3	3
6—10	1	2	2	3	4	5	6	7	7	8
11—15	1	3	4	5	7	8	9	11	12	13
16—20	1	4	6	7	9	11	13	15	17	18
21—25	2	5	7	9	12	14	16	19	21	23
26—30	3	6	9	11	14	17	20	23	26	29
31—35	3	7	10	13	17	20	24	27	30	34
36—40	4	8	12	16	19	23	27	31	35	39
41—45	4	9	13	18	22	26	31	35	39	44
46—50	5	10	15	20	24	29	34	39	44	49
51—55	5	11	16	22	27	32	38	43	49	54
56—60	6	12	18	24	30	36	41	47	53	59
61—65	6	13	19	26	32	39	45	51	57	64
66—70	7	14	21	28	35	42	49	56	62	69
71—75	7	15	22	30	37	45	52	60	67	74
76—80	8	16	24	32	40	48	56	64	72	80
81—85	8	17	25	34	42	51	59	68	76	85
86—90	9	18	27	36	45	54	63	72	81	90
91—95	9	19	28	38	47	57	66	76	85	95
96—100	10	20	30	40	50	60	70	80	90	100

The total danger is evaluated as a sum of lightning and human-induced danger indications. The system suggests accepting 100 points for all the cases when the sum of indications exceeds 100 points [5]. The question regarding the danger source occurrence imbalance in time is solved. For the detailed fire danger evaluation it is also important to know the most probable daily territorial distribution of danger sources. At Stage Four indications of inflammation, fire margin spreading speed, energy release [5] are evaluated in the system. At Stage Five the fire occurrence frequency characteristic (in a 100-point scale) is evaluated through the total danger and inflammation indication.

The fire occurrence frequency indication allows evaluating the fire occurrence danger level without specifying the number. The fire danger index unites the fire spreading and energy release indications (it is estimated according to the table, characterizes the efforts necessary for fire suppression in the circumstances of this particular forest fuels model; it is measured from 0 to 12 units) [5].

The fire load indication characterizes total efforts necessary for suppressing all fires that occur on the theoretical area during design time period [5].

The system application is also possible outside the USA in conditions similar in climate and vegetation. The fire danger indications are characterized in dimensionless values. The dimensionless units are built on scales of different ratios (100-/12-/5-point scales). For some models the 100-point scale is used only partially, i.e. less than 80 %.

The Canadian and American methods are similar in structure, approaches and fire danger index formation principles. For this reason, both have similar advantages and disadvantages.

2.2. The method of the Leningrad Institute of Forestry Management and Nesterov's Index

In the forest pyrology a term *forest fire maturity* [7] is used that implies a condition in which the burning process may spread over all of the forest area. This condition is determined empirically by bonfire making from 1 kg of relatively dry forest fuels and the following observation of the surface forest fire burning from the catching fire center. It is obvious that the forest fire maturity of a district is determined not only by forest fuels moisture content, but also by the environment condition parameters (temperature and air humidity), and also by wind speed.

The fire danger degree conditioned by the enclosure's fire maturity is determined in forest pyrology with Nesterov's fire danger index (a complex meteorological characteristic) [8]:

$$\Gamma_j = \Gamma_{j-1}\xi_j + T_j(T_j - T_{pj}).$$

Here Γ_j is a complex meteorological factor of fire danger, which dimension is K^2; T_j, T_{pj} are the air and dew point temperatures at 1-3 p.m. of the local time for the current day, K; ξ is the precipitation record coefficient that equals zero if the total of the preceding day's precipitation $f_j > 3$ mm, or 1, if $f_j < 3$ mm; j index corresponds the current day of the fire danger season [8, 9]. As the research has shown [10], the probability of forest fire occurrence and its intensity increase with an increase of Γ_j complex indication.

The method [8] is currently used in the entire territory of Russia as an officially accepted regulatory document. In 1999 the State Standard P 22.1.09-99 *Monitoring and forest fire prediction. General requirements* [11] that have been used till present.

The Leningrad Institute of Forestry Management has developed a method of forest fire danger prediction that uses a notion of *inflammation* and the total number of fire sources [10]. The forest fuels inflammation is determined through moisture content and temperature of combustion conductors, whereas the total number of fire

sources is determined through the structure and activity level of these sources. The prediction of forest fire number, which is a random variable, is carried out by means of distributional function generation for a fixed period with certain humidity limits of combustion conductors and a relative number of fire sources.

In [10], as distinct from Nesterov's method, the moisture content of forest fuels layer is chosen to be the main physical parameter for forest fire danger prediction. Equations for the drying of the forest fuels layer are used [10]:

$$\frac{dW}{dt} = -k(W - W_{\text{p}}), \quad \frac{d(W - W_{\text{p}})}{dt} = -k(W - W_{\text{p}}), \quad (2.6)$$

where t is the time; k is the drying coefficient (logarithmic speed of drying); W_{p} is the balanced moisture content.

The first equation (2.6) is recommended to be used at constant daily and seasonal temperatures and air humidity, and the second – on the contrary, when W_{p} changes with time.

Except equations (2.6), an analogous [10] for the moisture content of the forest fuels layer at the fallout of precipitation:

$$\frac{dR}{dr} = k_{\text{в}}(R^* - R),$$

where R is the current amount of water detained by forest fuels layer; R is the layer's moisture limit; r is the amount of precipitation that has reached forest fuels layer; $k_{\text{в}}$ is the constant water saturation coefficient.

Method [10] also counts the humidifying effect of forest fuels with atmosphere precipitation. However, the canopy cover is differentiated into several layers: tree and shrub layer, upper ground vegetation layer (upper moss and lichen layer with a depth of 3-4 cm), lower ground vegetation layer, upper ground litter and peat layer (2 cm).

The amount of precipitation reaching the certain layer (n) of forest fuels (q_n) and the amount of precipitation detained by this layer (R) are estimated with the following recurrent formulae [10]:

$$q_n = q_{n-1} - R_{n-1}(q_{n-1}),$$

$$R_n(q_n) = R_n^* - (R_n^* - R_n^0)e^{-\rho_n q_n},$$

where R_n^* is the moisture capacity of the forest fuels n-layer; R_n^0 is the initial moisture content of the n-layer; ρ_n is the constant coefficient characterizing the precipitation detaining intensity of the forest fuels n-layer.

The amount of precipitation detained by the tree and shrub layer is determined from the relation [10]

$$R_0(q_0) = R_0^* - (R_0^* - R_0^0)e^{-\rho_0 q_0},$$

где R_0^* is the maximum water capacity of the stand's canopy; q_0 is the amount of the fallen precipitation; ρ_0 is the precipitation detaining intensity of the stand's canopy.

2.3. G. A. Dorrer's and S. P. Yakimov's Method

The equation of moisture balance in forest fuels layer has the following outline [12]:

$$\frac{dW}{dt} = q_{\text{ик}} + q_{\text{ил}} + q_{\text{с}} + q_{\text{ос}} + q_{\text{п}}.$$

Here on the left is the layer's moisture content change speed; $q_{\text{ик}}$ is the speed of moisture content evaporation due to convective heat transfer with air, kg/(kg·s); $q_{\text{ил}}$ is the speed of moisture evaporation due to radiation effect, kg/(kg·s); $q_{\text{с}}$ is the speed of moisture income into the forest fuels layer due to sorption from air, kg/(kg·s); $q_{\text{ос}}$ is the speed of moisture income with precipitation, kg/(kg·s); $q_{\text{п}}$ is the speed of moisture outflow into the soil, kg/(kg·s).

The probability determination [13] of the term *fire danger* is of interest. "Fire probability is a probability of fire occurrence on the protected area calculated on the emergence of factors that are conditioning to it". The fire danger determination as fire occurrence probability requires defining a set of functions $P_n(\tau, \Psi)$, $n = 0, 1, ...$ that determine the occurrence probability on the Ψ area within the τ time period exactly n fires, where

$$\sum_{n=0}^{\infty} P_n(\tau, \Psi) = 1.$$

Hence, the occurrence probability at least one fire equals

$$P_{n>0}(\tau, \Psi) = \sum_{n=1}^{\infty} P_n(\tau, \Psi) = 1 - P_0(\tau, \Psi),$$

where $P_0(\tau, \Psi)$ is the probability that on the Ψ area within the τ time period no fire occurs.

2.4. The Spanish Method of Predicting The Forest Fires Number

The index of Daily Fire Risk (DFR) has been developed in Spain [14] that is expressed qualitatively in *day type* categories (Table 2.4). Two meteorological parameters (stability and humidity) are used in a certain local atmospheric column.

Table 2.4. Day type classification [14]

Characteristic	*e*, kJ/kg	*D*, kJ/kg	Day type
Not consistently dry	$\leq$6	$\geq$12	I
Not consistently wet	$\leq$6	<12	II
Consistently dry	>6	$\geq$12	III
Consistently wet	>6	<12	IV

The stability of the atmospheric column (e). If the level of 850—700 hPa is accepted as the lower level of the atmospheric column (orography effects are neglected), then $e = S_{700}—S_{850}$, where $S = C_pT + gH$ is the Montgomery potential, S is the stability profile. The high (low) value of e is associated with a strong (weak) stability. C_p, g, T, H equal the dry air heating capacity at constant pressure, free fall acceleration, temperature and geopotential height correspondingly. With ascension to a height the value of gravity force acceleration decreases. This sophisticates the calculations. To determine the temperature correctly a notion of geopotential height is introduced. Its essence is that the Earth is accepted as an ideal sphere, meanwhile the gravity force is directed exactly into the center. In this case it is not necessary to take the changes of g acceleration into account. For the start point of the geopotential height, similar to the geometric, the average sea level is accepted. H geopotential height and h geometric height are described with equations

$$H = \frac{rh}{r+h}, \quad h = \frac{rH}{r-H},$$

where r is the Earth radius.

D humidity is expressed through $D = (h^* - h)_{850}$, where $h^* = S + Lq^*$, $h = S + Lq$, in total $D = L(q^* - q)_{850}$. Here L, q, q^* is the hidden evaporation heat, specific humidity and saturated specific humidity correspondingly. The values (e, D) may be acquired immediately at 00.00 o'clock with the radiosonde data use [14].

The territory of Galicia is viewed as a test one [14], data from La Coruna station are used. For this station the average values e and D are 6 and 12 kJ/kg. For various data collected within 1981—1985 (July, August, September) it was acquired [15] that $DFR_I >$
$> DFR_{III} > DFR_{IV} > DFR_{II}$, where DFR_i = (fire number/ day number) for i = I, II, III, IV. Correspondingly, fire danger will be "very high, I", "high, III", "low, IV", "very low, II".

The number of fires registered within a specific day depends on the previous weather conditions (some conditions may predominate within a long period of time like drought or strong local downfall) and from daily weather conditions that may be described in terms of e, D. The number of fires per day NF(d) may be expressed NF(d) = PW(d)W(d) where PW(d) is the input of previous weather conditions, W(d) is the input of daily conditions.

From the point of view of forest science [6], fire incidents depend on two factors: danger and natural calamities. Danger is a factor that can be associated with daily meteorological conditions W(d) (for instance, DFR) [14]. A natural calamity (for example, drought) depends on the previous weather PW(d). Correspondingly, the predicted number of fires for days d and $d-1$ will be determined through PNF(d) = PW(d)W(d), PNF($d-1$) = PW($d-1$)W($d-1$). If RNF($d-1$) is the number of fires recorded in a day ($d-1$), and it is supposed that the prediction was true then PNF($d-1$) =
= RNF($d-1$) и PW($d-1$) = RNF($d-1$)/W($d-1$). Since meteorological changes that characterize the previous weather PW(d) in total have a timely scale of more than two days, the supposition PW($d-1$) = PW(d) is true, consequently [14]

$$\mathrm{PNF}(d) = \frac{\mathrm{RNF}(d-1)\mathrm{W}(d)}{\mathrm{W}(d-1)}.$$

The dimensionless normalized index DFR (NDFR) for each day type is determined as [14]

$$\mathrm{NDFR}_i = \frac{\mathrm{DFR}_i}{\mathrm{DFR_I} + \mathrm{DFR_{II}} + \mathrm{DFR_{III}} + \mathrm{DFR_{IV}}} \quad \text{for } i = \text{I, II, III, IV.}$$

The average value is acquired from a set of data within different periods. $\mathrm{NDFR_I} = 0{,}4$; $\mathrm{NDFR_{II}} = 0{,}1$; $\mathrm{NDFR_{III}} = 0{,}3$; $\mathrm{NDFR_{IV}} = 0{,}2$. $\mathrm{W}(d) = a\mathrm{NDFR}(d)$, where a is the coefficient of proportionality. The awareness of a is not obligatory, since this coefficient decreases eventually and we get [14]

$$\mathrm{PNF}(d) = \frac{\mathrm{RNF}(d-1)\mathrm{NDFR}(d)}{\mathrm{NDFR}(d-1)}.$$

To eliminate possible radiosonde data errors in the number of fires, one more day may also be counted [14, 16]:

$$\mathrm{PNF}(d) = \left(0.3\frac{\mathrm{RNF}(d-2)}{\mathrm{NDFR}(d-2)} + 0.7\frac{\mathrm{RNF}(d-1)}{\mathrm{NDFR}(d-1)}\right)\mathrm{NDFR}(d).$$

The prediction acquired at 00.00 o'clock provides around 15 h for operational management in preparing the staff and means for fire extinguishing. The input data are easily accessible from standard meteoroligal sondes.

The Spanish method [14, 16] has been modified to acquire medium-range prediction [17]. There has been developed a system of equations that will enable predicting the fire number not only for the following day, but also for the next 5 days. The model has been verified in Galicia, Spain with the use of statistics on forest fires in 1993. Fig. 2.7 illustrated the predicted and recorded number of forest fires per day for July, August and September 1993.

The medium-range prediction is carried out with equations [17] listed in Table 2.5. For acquiring the prediction information on predicted, but not recorded number of forest fires is used on the second day already. Fig. 2.8 illustrates the results of the medium-range prediction.

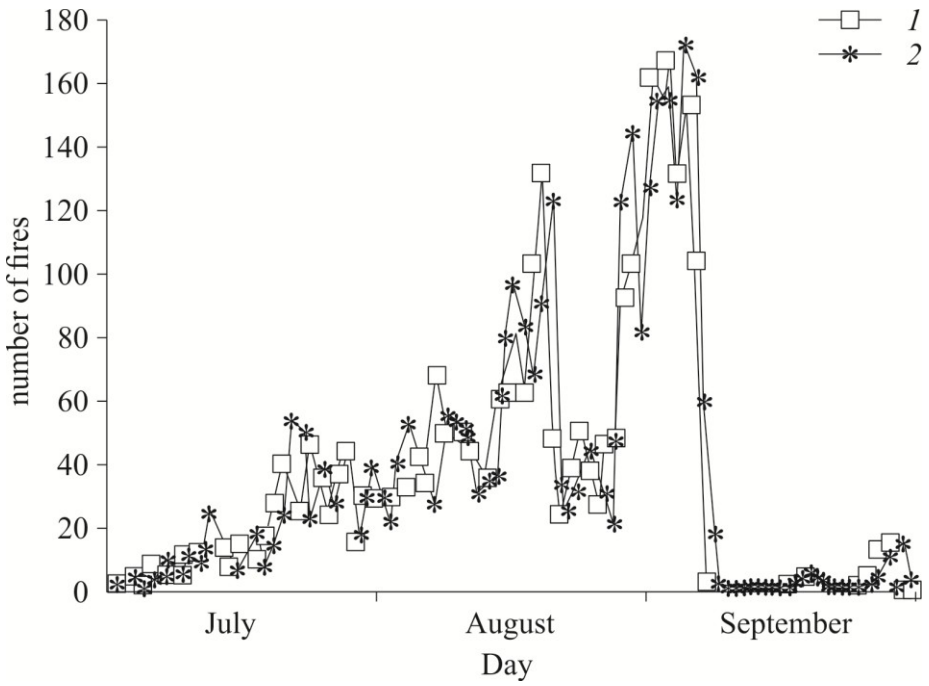

Fig. 2.7. Predicted (*1*) and recorded (*2*) number of forest fires per day for July, August and September 1993 in Galicia [17]

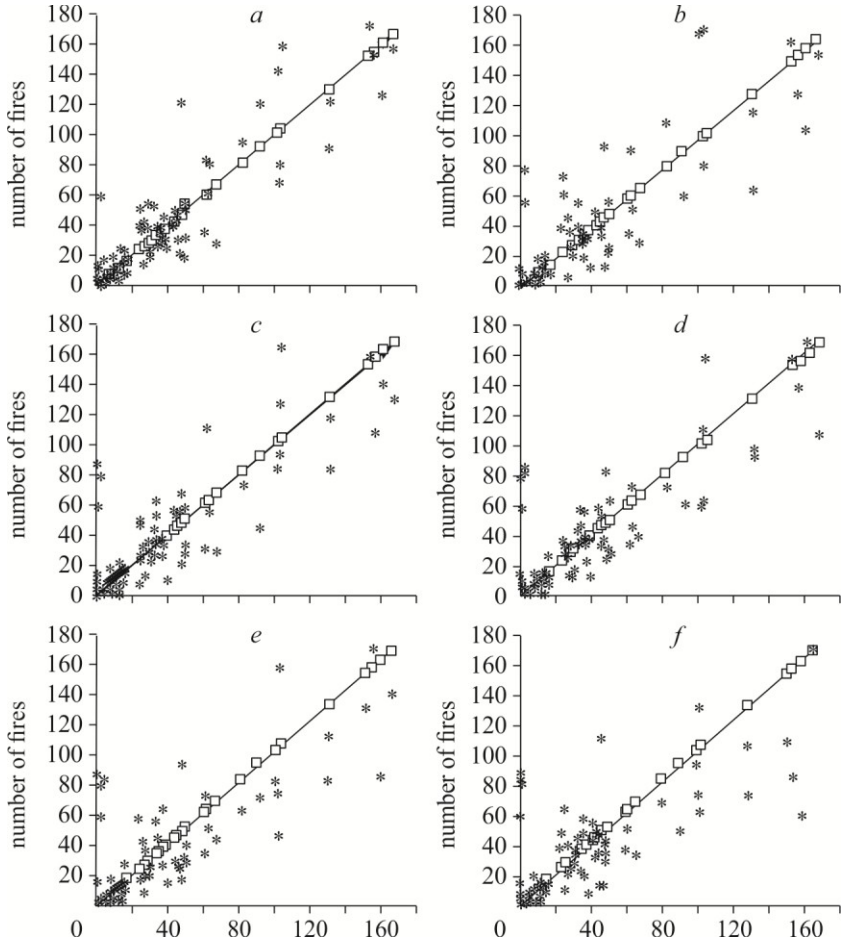

Fig. 2.8. Medium-range prediction [17]. Recorded (*1*, PNF) and predicted (*2*, PNF) number of forest fires.

a — PNF(*d*), *b* — PNF(*d* + 1), *c* — PNF(*d* + 2), *d* — PNF(*d* + 3), *e* — PNF(*d* + 4), *f* — PNF(*d* + 5).

Table 2.5. Formulae for medium-range prediction [17]

Equation	Range, h
$\mathrm{PNF}(d)=\left[0,3\frac{\mathrm{RNF}(d-2)}{\mathrm{DFR}(d-2)}+0,7\frac{\mathrm{RNF}(d-1)}{\mathrm{DFR}(d-1)}\right]\mathrm{DFR}(d)$	0—24
$\mathrm{PNF}(d+1)=\left[0,3\frac{\mathrm{RNF}(d-1)}{\mathrm{DFR}(d-1)}+0,7\frac{\mathrm{RNF}(d)}{\mathrm{DFR}(d)}\right]\mathrm{DFR}(d+1)$	24—48
$\mathrm{PNF}(d+2)=\left[0,3\frac{\mathrm{RNF}(d)}{\mathrm{DFR}(d)}+0,7\frac{RNF(d+1)}{DFR(d+1)}\right]\mathrm{DFR}(d+2)$	48—72
$\mathrm{PNF}(d+3)=\left[0,3\frac{\mathrm{RNF}(d+1)}{\mathrm{DFR}(d+1)}+0,7\frac{\mathrm{RNF}(d+2)}{\mathrm{DFR}(d+2)}\right]\mathrm{DFR}(d+3)$	72—96
$\mathrm{PNF}(d+4)=\left[0,3\frac{\mathrm{RNF}(d+2)}{\mathrm{DFR}(d+2)}+0,7\frac{\mathrm{RNF}(d+3)}{\mathrm{DFR}(d+3)}\right]\mathrm{DFR}(d+4)$	96—120
$\mathrm{PNF}(d+5)=\left[0,3\frac{\mathrm{RNF}(d+3)}{\mathrm{DFR}(d+3)}+0,7\frac{\mathrm{RNF}(d+4)}{\mathrm{DFR}(d+4)}\right]\mathrm{DFR}(d+5)$	120—144

The correspondence analysis of the predicted and real fires shows that the Spanish method describes the real analyzed process rather well. For the practical use of this method, information from rawinsounding stations is necessary [16]. The Spanish method [14, 16] may be used in other geographical zones. NDFR for each specific territory must be identified. It is possible to use this method together with other forest fire danger prediction systems.

For the medium-range prediction of the forest fire number, information on the temperature and air humidity, geopotential height on the levels of 700 and 850 hPa is necessary. One must be oriented at the medium-range weather forecast. Even in case of errors, it will not always lead to errors in the forest fire number prediction since weather conditions are contained in the model through defining the day type. Statistical tests [17] have shown that the day type specified according to the radiosounding data enables a reasonable description of current weather W(d).

2.5. The European System of Forest Fire Danger Prediction

On the territory of several South-European countries different methods for forest fire danger prediction are used [18].

The French method is known as Numerical Risk. Daily indications of air temperature, relative humidity, cloud cover, wind speed and the initial value of soil moisture content are required for calculations.

The Italian method IREPI requires daily average values of air temperature, relative humidity, wind speed, the amount of precipitation and sun illumination.

The Portuguese method is a modified version of Nesterov's index. This index is formed from the daily index and the total index that is a weighted sum of daily indices of the preceding days. Everything depends on the amount of precipitation. The air temperature and relative humidity at 12:00 o'clock are required for the

evaluation. The wind speed and direction is taken into account at the final stage of the classification in accordance with the local conditions.

All the methods represent a numerical index that increases with the increase in the conditions of danger. In the majority of cases this number is transferred to a fire danger scale with three-five levels for practical purposes. The fire danger evaluation methods presented above [18] based on meteorological factors have been testes with the use of the statistical data of 3-9 years for the daily number of fires in the burnt area. Apart from the methods accepted in France, Italy, Portugal and Spain, the Canadian method has been included into the comparative analysis [18]. Each research study team worked with statistical and meteorological data from their countries. For each area there were daily values of fires and burnt area. However, these indications depend not only on meteorological, but also other, especially of anthropogenic load, factors; consequently, it was considered that these extra factors did not impose mutual impact [18].

For the results acquired by different methods to be comparable, a general danger index scale was used. This scale within the limits from 0 до 100 was accepted in all methods with the use of the following equation [18]

$$I'_x = 100\left(I_x - I_{\min}\right)/\left(I_{\max} - I_{\min}\right), \qquad (2.7)$$

where I'_x is the normalized value of the I_x index; $I_{\min}$ is the minimal index value in a specific area during the analysis period; $I_{\max}$ is the maximum index value in a certain region during the analysis period.

Using Equation (2.7), the values of modified and standard danger indices were grouped into 10 classes limited correspondingly 0—10, 10—20, …, 90—100, as all other parameters connected.

The analysis of the results has shown [18] that the Canadian method has the best functional performance in the summer conditions, except for Savona region. Though the Spanish method has a strong effect in determining both the number of fires and the area burnt, it goes the second in separating the days with fires from the days without fires. The Portuguese method operates well in the winter time and fairly well in the summer time in all the regions. The French and Italian methods produce good results in the summer time, but both of them give an excessive number of days with extremely high fire danger values. It is interesting that the Spanish method has given comparatively good results in the winter conditions, but very weak results in the summer conditions. The Italian method, though developed for winter conditions, has shown good results in Savona and fairly modest results in other cases. The French method has given the worst results in the winter conditions. Therefore, the Canadian method and Nesterov's modified method have shown the best general functional performance.

Considering the tests carried out, a so-called European system, European Forest Fire Risk Forecasting System (EFFRFS), was developed that was used on the South-European area. The system basis was formed by methods developed in Italy, France, Spain, Portugal [18] and Canada[2]. The methods known previously are used in total. Each index is illustrated with maps for all Southern Europe. At present a modification of the European system is used that additionally records the satellite data and is called

European Forest Fire Information System (EFFIS) [19]; its center is formed by the mentioned above methods of Southern Europe and the Canadian index. All the indices are adapted to a 100-point scale for comparison. In the recent years the system was put into use in Germany and other West European countries, along with Bulgaria.

2.6. The methods of Tomsk State University

A determinate-probability method for forest fire occurrence probability prediction with account of anthropogenic load and thunderstorm activity has been developed at Tomsk State University [20, 21]. To determine the probability the following formula is suggested:

$$P_j = \sum_{i=1}^{N} \left[P_{ij}(A) P_{ij}(FF/A) + P_{ij}(L) P_{ij}(FF/L) \right] P_{ij}(C)$$

Here P_j is the forest fire occurrence probability for j interval on a in controlled forest area; N is the total strata number on F area; P_{ij}(A) is the probability of anthropogenic load; $P_{ij}(FF/\text{A})$ is the probability of fire occurrence resulting from the anthropogenic load on the F_i stratum territory; P_{ij}(L) is the probability of dry storm occurrence on the F_i stratum territory; P_{ij} (FF/L) is the probability of forest fire occurrence from lightning provided that dry storms may appear on the F_i stratum territory; P_{ij}(C) is the probability of fire occurrence due to weather conditions of forest fire maturation; j index corresponds to the fire danger season day. To calculate the probability of forest fire occurrence one must calculate moisture content of the forest fuels layer in mathematical models of forest fuels layer drying model and determine the probability members through the frequency of events.

Tomsk State University has also developed a method to evaluate the territory's susceptibility to forest fire occurrence with meteorological factors [267]. The territory of the Tomsk Region was taken for illustrations. The following equation is offered for fire danger evaluation [22]:

$$Y = 2.87 + 0.07T - 0.06F + 0.08Q, \qquad (2.8)$$

where Y is the predicted fire danger, dimensionless value, T is the maximum air temperature (°C), F is the minimal air humidity (%), *and* Q is the amount of precipitation per day (mm). Fig. 2.9 illustrates the demarcation of the Tomsk Region according to the degree of its weather and climate susceptibility to forest fire occurrence, Fig. 2.10 contains the predicted value Y (according to Model (2.8)) and the real number of forest fires on the Tomsk Region territory. Moreover, as a result of the regressive analysis, the dependance of the predicted fire danger (daily advance time) on complex meteorological characteristic (Nesterov's index) и KBDI (Keetch-Byram Drought Index) was acquired [22]:

$$Y = 0.0005 \cdot \text{КМП} + 0.009 \cdot \text{KBDI} - 16. \qquad (2.9)$$

Fig. 2.11 presents the *Y* predicted value (with Model (2.9)) and real number of forest fires on the Tomsk Region territory.

Fig. 2.9. Zoning of Tomsk Region, according to the degree of weather and climate predisposition (*1* — low, *2* — moderate, *3* — high) to forest fire occurrence [22]

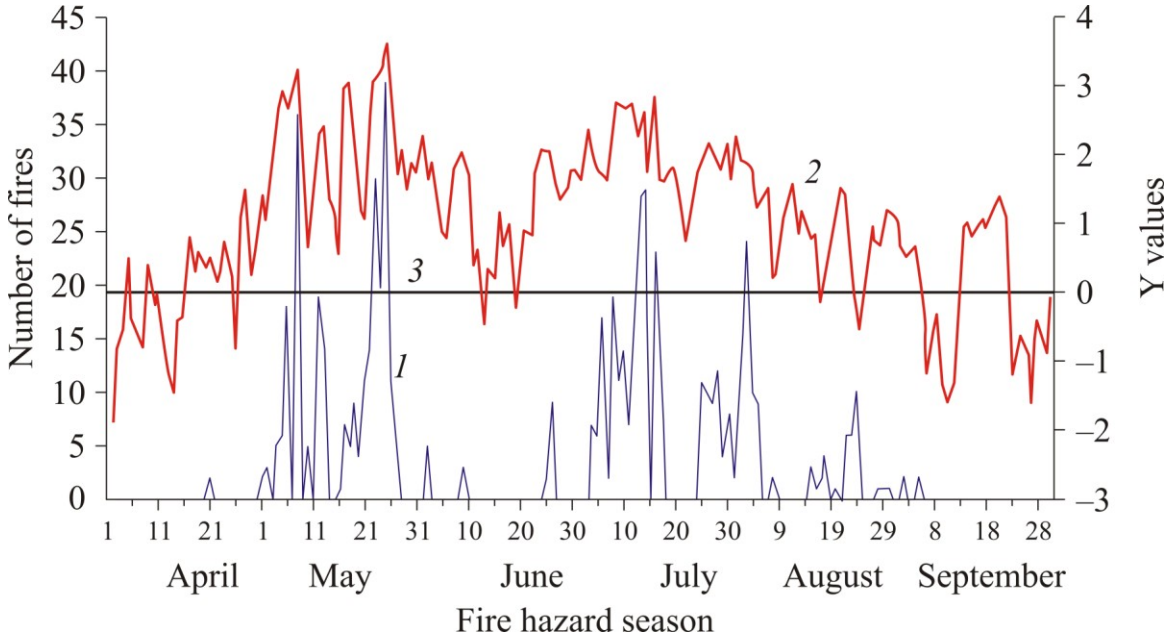

Fig. 2.10. Predicted Y value and actual number of forest fires in Tomsk region according to model (2.8) [22]
1 — actual forest fires; 2 — Y values; 3 — boundary of the minimal fire danger.

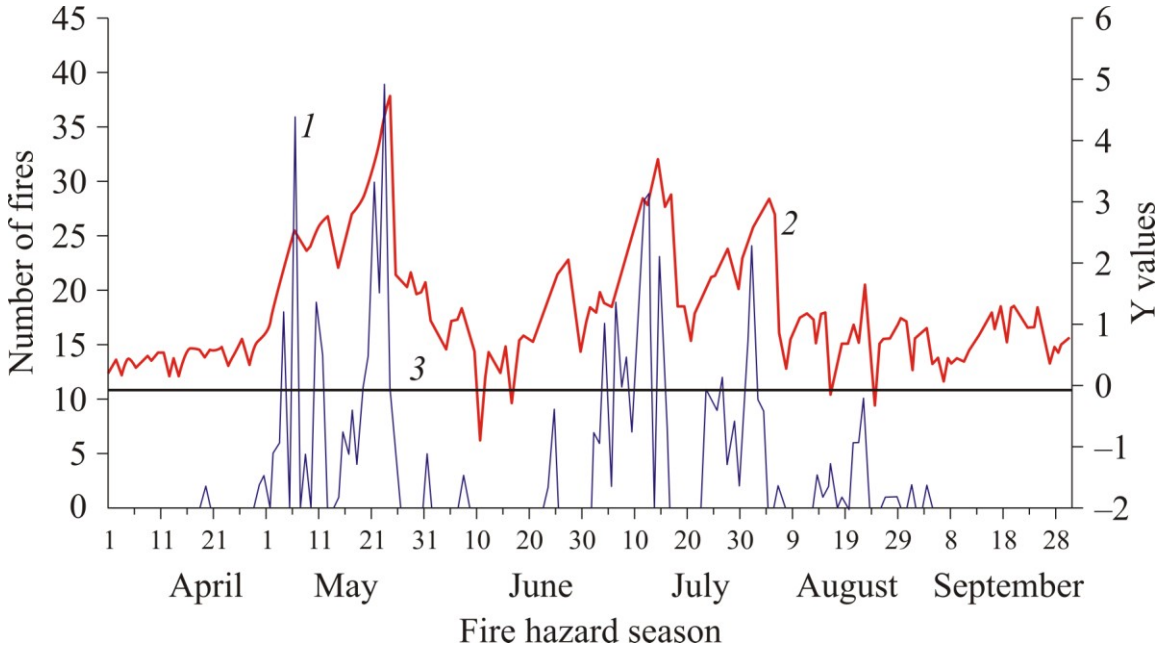

Fig. 2.11. Predicted Y value and actual number of forest fires in Tomsk region according to model (2.9) [22]
1 — actual forest fires; 2 — Y values; 3 — boundary of the minimal fire danger.

The prediction importance of the complex model (2.9) proved to be high [22]: the correlation coefficient is $R = 0{,}45$—$0{,}56$ (depending on the selection) and it was much higher than in the case of prediction according to the fire danger class and KBDI separately. It is possible to say that with the Y value of over two units a high forest fire danger is predicted. When Y is less or equals zero, fire danger is at minimum [22]. Nevertheless, using Model (2.9) is hindered by the fact that it is necessary to know the values of the fire danger class of the preceding days. Therefore, Model (2.8) uses daily values of atmospheric precipitation, temperature and air humidity as predictors. The significant coefficient of the $R = 0{,}42$ correlation is acquired [22]. The use of short- and medium-term forecast of meteorological parameters enables predicting forest fire danger for a period up to 11 days [22].

To detect the anthropogenic constituent of forest fire occurrence reasons, the data on the population size in the Tomsk Region and the regressive analysis method were used [23]. The equation of constraints of the forest fire number and the population density has the following outline [22]

$$Y = 1{,}323 + 0{,}189 \cdot X, \qquad (2.10)$$

where Y is the number of forest fires per day during the fire danger season; X is the population density (people/km^2). Equation (2.10) may be used to preliminarily evaluate the anthropogenic constituent of the territory's fire danger.

2.7. The method of Moscow State Forest University

[24] suggests evaluating the forest area's fire danger by using the Bayes model. For the increase in reliability, a priori and a posteriori data are used. Forest fire danger prediction is based on fire statistics of the previous years on a certain territory

and experimental data from sample areas. Two hypotheses are put forward: $S1$: fire occurrence is possible on the protected area, $S2$: fire is impossible on the protected area. A priori probabilities of these hypotheses $P(S1)$ and $P(S2)$ is determined by the data from forest protection subdivisions of a long period. Information on weather conditions and current forest fires enters the forest protection subdivisions daily. The a priori probabilities of $P(A/S1)$ and $P(A/S2)$ hypotheses are determined by using this information and some additional data on forest fuels condition [24]

$$P(A) = \frac{P(S1) \cdot P(A/S1)}{P(S1) \cdot P(A/S1) + P(S2) \cdot P(A/S2)}.$$

2.8. The Method of Moscow State University

Landscape science offers a range of approaches for monitoring and information support of decision making on forest fire management [25]. A method to evaluate the current fire danger has been developed on the basis of the pyrological properties of the Southern and Middle Sikhote-Alin landscapes in their close interaction with forest fires. The information on around 1000 forest fires from 1971 to 1977 has been analyzed. A map of up-to-date fire incidents has been acquired that demonstrates the relative fire area in a season for a certain landscape per 100 thousand hectares and the frequency of fire occurrence, i.e. the number of fires per 100 thousand hectares in a season. The landscapes are also classified according to the moistening level. An evaluation of the probability (in fact the numerical index in percent) of forest's 1 ha in different conditions (for instance, spring, late spring, summer, etc.) for different landscapes is offered.

2.9. The Method of Storm-Induced Forest Fire Prediction (Canada)

For practitioners the evaluation of the probability that the ground storm discharge may lead to fire occurrence that will be discovered arouses interest [26]. The relevance and necessity of this method development may be explained with the fact that storms are the main cause or forest fire occurrence in Canada [26]. If the fire spot is too small or away from the observation systems, it will not be counted in the prediction. Model [26] is realized in a software program form. The system evaluates the probability of forest fire incident and its probable location according to the daily data on storm activity, weather conditions and forest management inventory data.

The processes involved in the storm-induced forest fire occurrence may be divided into three separate stages. During the first stage the ground storm discharge inflames the forest fuels. Then the smouldering stage comes that may last several days. At the final stage the fire outbreak spot transforms into the flame combustion phase and forest fire occurs. The probability model is outlined below [26]:

$$P_{\text{fire}}(t) = P_{\text{LCC}} P_{\text{ign}} P_{\text{sur}}(t) P_{\text{arr}},$$

where $P_{\text{fire}}(t)$ is the probability of storm-induced forest fire occurrence at a certain time; P_{LCC} is the probability of lightning impact with sustainable current activity; P_{ign} is the probability of inflammation from lightning current; P_{sur} is the probability of

smoldering till t moment in time; P_{arr} is the probability of transformation from smouldering to flame combustion.

The total number of possible ground storm discharges is determined as [26]

$$N_{flash} = \frac{1}{P_{DE}},$$

where P_{DE} is the probability of detecting the individual ground storm discharge within the storm monitoring network.

The probability that among all the discharges there is no discharge with sustainable current activity is determined as [26]

$$q_{LCC} = (1 - p_{\%LCC})^{\frac{1}{P_{DE}}},$$

where $p_{\%LCC}$ is the probability of discharge of a certain polarity with sustainable current activity,

$$P_{LCC} = 1 - q_{LCC} = 1 - (1 - p_{\%LCC})^{\frac{1}{P_{DE}}}.$$

The probability of forest fuels inflammation with the ground storm discharge is calculated with equations acquired as a result of experimental data processing in inflammation of different forest fuels types with an electric arc [27]. For example, the probability of *Pinus ponderosa* inflammation is determined from equations for the negative and positive ground storm discharge [27]:

$$P_{ign} = 1,04 \exp(-0,054mc),$$

$$P_{ign} = 0,92 \exp(-0,087mc),$$

where mc is the moisture content.

Regressive analysis methods determine the burning probability of, for instance, peat in the smouldering mode [28]:

$$P_{н} = 1/[1 + \exp(-19,329 + 17,047R_{м} + 1,7170R_{I} + 23,059\rho_{I})],$$

where ρ_I is the concentration of non-organic matters, $R_м$ and R are the humidity and mass of non-organic matters corresponding to the organic. The P_{sur} smouldering probability is the minimum $P_н$ in time.

The probability of transformation into flame combustion is determined via the components of the Canadian Forest Fire Behavior Prediction System [29] — Head Fire Intensity (HFI) and Rate of Spread (ROS). If the predicted values of HFI or ROS are more than some of their threshold values, then the probability of transformation to flame combustion equals one, otherwise – zero [26].

The moisture content is determined though FWI module components of the Canadian Forest Fire Weather Index System [26]:

$$mc = \frac{147,2(101 - \text{FFMC})}{59,5 + \text{FFMC}},$$

$$mc = \exp(244,72 - \text{DMC}/43,43) + 20.$$

The values of FFMC and DMC parameters are spatially interpolated according to the data from weather observation stations for each smouldering spot [26].

Fig. 2.12 illustrates the chart of information streams in a computer program that implements this model.

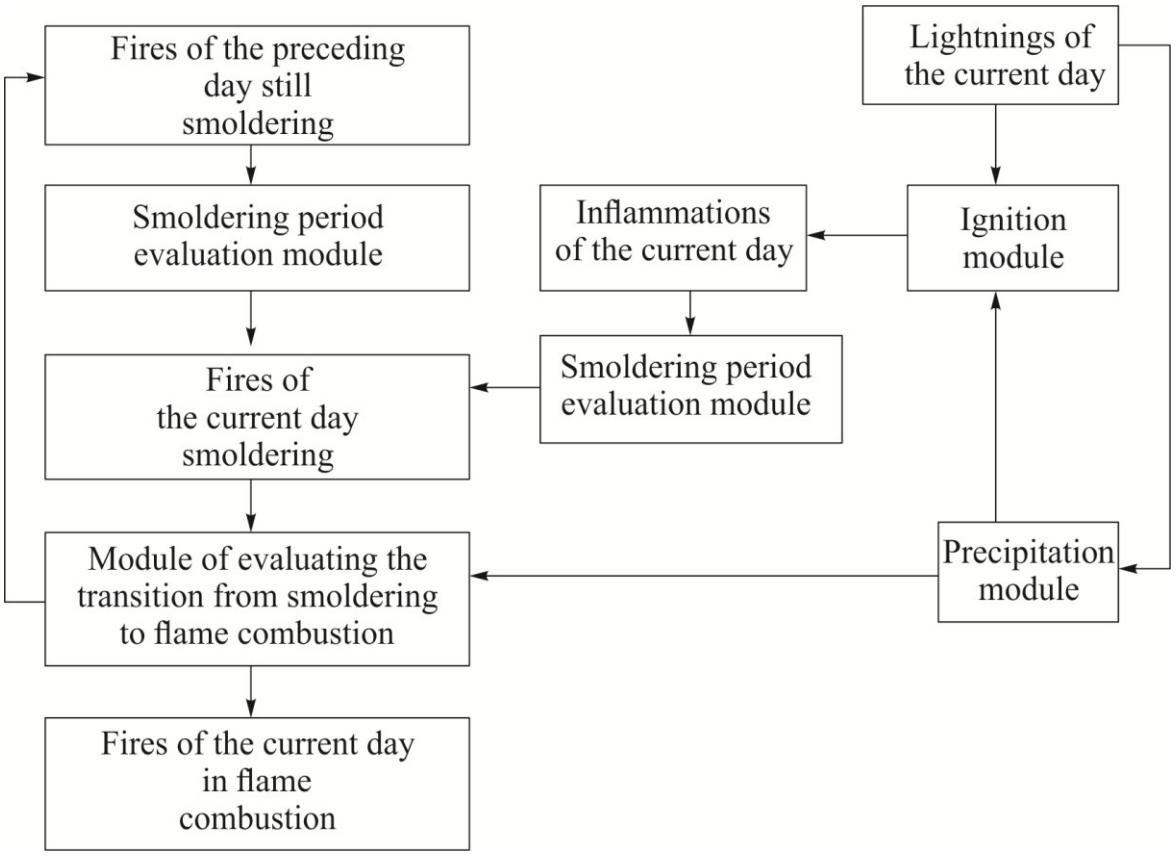

Fig. 2.12. The chart of information streams in the computer system of evaluating the probability of storm-induced forest fire occurrence [26]

Apart from that, the system gives the data on the expected number of storm-induced forest fires on a controlled forested area. The model's validation has been carried out on the area of the Saskatchewan primary zone. Data of six fire seasons (from May 1 to August 31) have been processed within 1994-1999; a retrospective analysis has been carried out on their basis (Fig. 2.13).

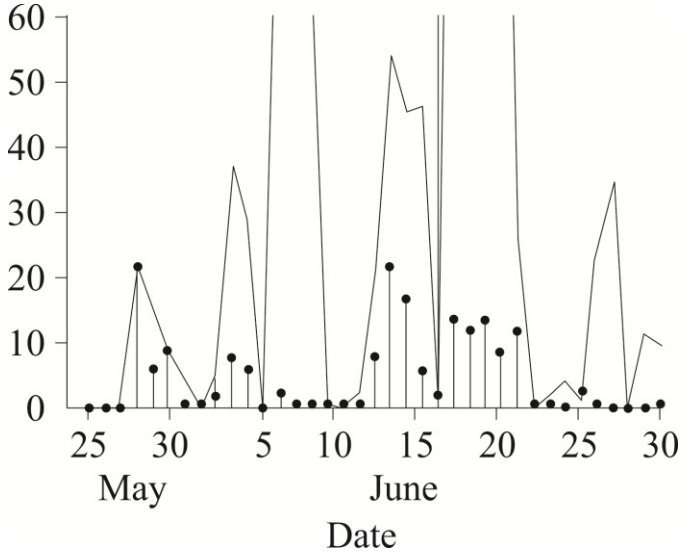

Fig. 2.13. The predicted (lines) and actual (dots) number of forest fires in the Saskatchewan primary zone in May-June 1995 [26]

The results of the model's testing [26] have shown that good coordination of retrospective and predictive data was acquired in 1994, 1996, and 1997. In 1995, 1998 an overestimated, and in 1999 an underestimated prediction of forest fire numbers was acquired [26]. The analysis of the results presented on Fig. 2.13 shows that the model predicts the general tendency in forest fire danger start rather well, however, it sometimes has an incorrect output of predicting the number of the expected forest fires.

The discovered deviations in the prediction results and retrospective data of forest fires demand a special attention. For example, in June 1995 Model [26] predicted hundreds of daily occurring forest fires, but in fact far fewer occurred. The lowest prediction quality was acquired on June 19: around 250 fires opposed to the 14 registered in the reality [26]. The analysis of daily records and cards [26] has shown that on June 17 the value of DMC ≈ 90 (fairly high to take the impact of any amount of precipitation accompanying the storm into account). A contrary situation was formed in the second half of July 1999 when 1.2 forest fires were predicted but in fact 124 incidents were recorded [26].

This implies that Model [26] is very sensitive to forest fuels moisture content. Errors in defining the spatial interpolation of forest fuels moisture content along with the conditions when a certain storm has a large amount of ground discharges may lead to incorrect prediction of the expected forest fire number. Moreover, poor accuracy in predicting the number of forest fires may be explained by the precipitation module functioning [26].

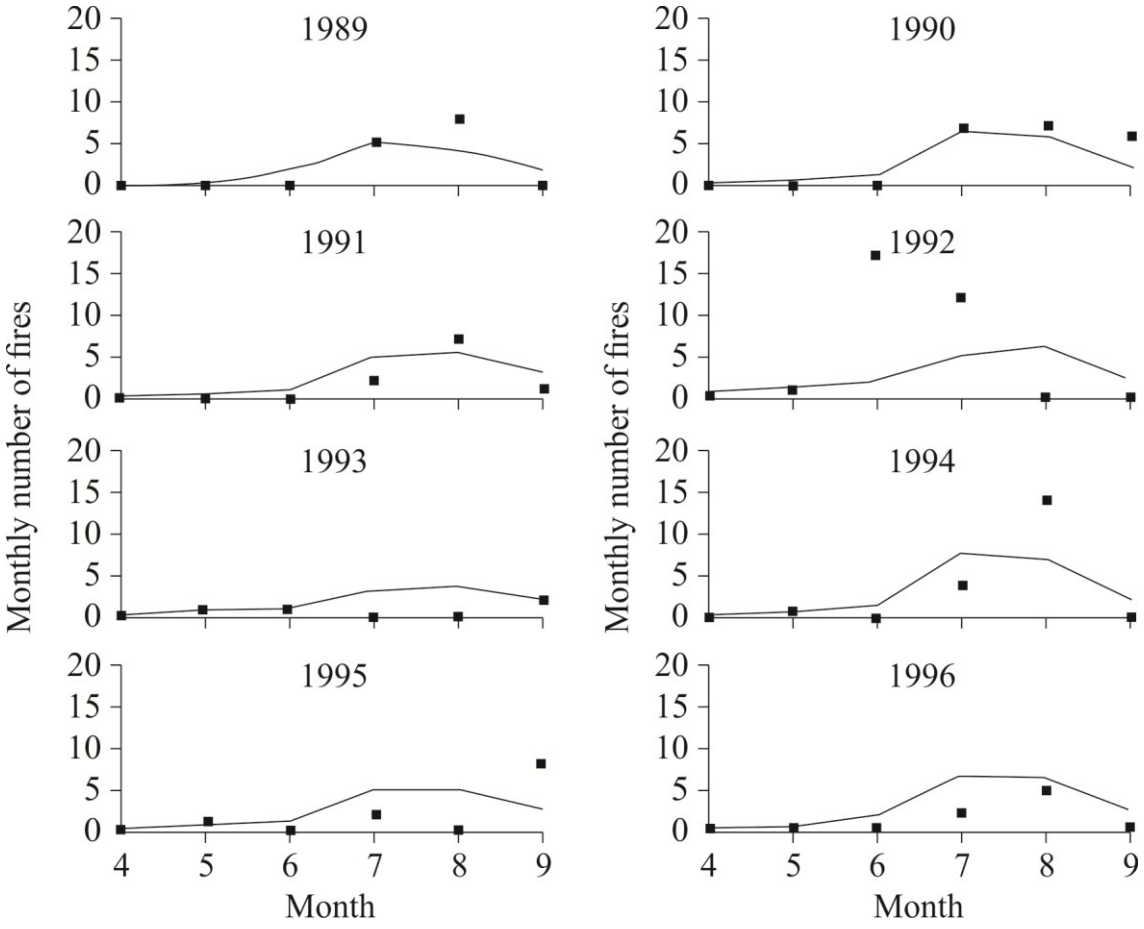

Fig. 2.14. Predicted and actual number of forest fires in Oregon [30]
Lines – prediction, points – observed data.

2.10. The probability model of forest fire danger evaluation (USA)

The probability model of evaluating forest fire danger has the following outline [30]

$$P(\mathrm{LFO}) = P(\mathrm{FO})P(\mathrm{LF}/\mathrm{FO}), \qquad (2.11)$$

where P(LFO) is the probability that conflagration will happen; P(FO) is the probability that a forest fire incident will happen; P(LF/FO) is the probability that the fire increases in its size conditioned that forest fire incident occurs. To evaluate the probable formula members (2.11) logistical and regression models are used. Counting that fire probabilities in a separate voxel are very small, the expected number of fires in the region is evaluated by the sum of fire probabilities in each voxel. A voxel is a volume picture element containing the value of the element on regular network in three-dimensional space, similar to the pixel in the two-dimensional space. The voxel is often used to visualize the medical and scientific information. The method application is demonstrated on forest fire incident statistics within an eight-year period in Oregon. Fig. 2.14 illustrates the predicted and actual fire number in a month for different fire danger seasons.

The goal [30] was to develop the space-time probability model and evaluating procedure, but not to investigate fire occurrence mechanisms, be it anthropogenic load or storm activity. Model [30] demonstrates fairly good coordination of prediction results and retrospective data on the forest fire number. In the region under survey no conflagration has been recorded during the investigation period (8 years) [30]. According to the prediction model's application [30], the occurrence probability of at least one conflagration was 4 % (95-percent confidential interval, from 0,4 to 30 %). It may be affirmed that Model [30] predicts forest conflagration occurrence probability correctly.

2.11. The model of fire frequency (based on the example of Catalonia, Spain)

For the work of forest fire services the evaluation of forest fire frequency is necessary. The forest fire frequency in Catalonia (Spain) was evaluated between 1975 and 1998 according to the map archives of the burnt area [31]. Satellite images allowed identifying the fire with an area over 30 ha and were used to characterize the spatial distribution of forest fires in Catalonia. For data processing within the given period different models of forest fire frequency were used: Natural Fire Rotation Period (NFR), Poisson Process Model (PPM), Mean Fire Interval (MFI). The most simple of them is NFR, it enables estimating the number of years necessary for an area similar to the area studied to burn down completely [31]:

$$\mathrm{NFR} = N/(A/S),$$

where N is the number of years in a period, A is the total burnt area, S is the size of the area under study.

Some forest areas were imposed to a repeated burning. A significant and positive interconnection between the fire number and the total burnt area was discovered. A large number of forest fires is concentrated simultaneously in one place in dry seasons.

2.12. Application of the Canadian method in other countries

The Canadian method is used in various scales in such countries as the USA, New Zealand, Fiji, Argentina, Mexico, Indonesia, and Malaysia [32]. In New Zealand and Fiji, FWI System was accepted for application in pine plantations in 1980 and 1988 correspondingly. The research carried out in 1994 has shown that this decision was correct. The system was successfully applied in both Finland and Sweden [32].

During 1981-1991 the Ontario Natural Resources Ministry finished a project in developing a modeling system of forest fire management that includes a sub-system of forest fire danger evaluation for the North-East China [32]. The project included work in installing a fire weather station network, manufactured in Canada; it also included creation of combustible material type maps and computer embedding of the FWI System and daily strategic plan preparation system.

The Canadian system is also accepted on the territory of Alaska since there is a similarity between forest fuels types in Alaska and Canada. Consequently, some US

States, like Minnesota and Michigan, have partially adopted the Canadian system on their territory. In 1990 a five-year project was started that is aimed at creating a fire danger evaluation system in the South-East Asia on the basis of the Canadian system. In 2000 a pilot project on using the FWI System in some parts of Argentina was started.

2.13. The Determinate-Probability Method of Predicting Forest Fires Probability and their Number

The determinate-probability model of forest fire danger prediction may be used for solving many tasks [33]. The probability of forest fire occurrence is evaluated with the formula

$$P_j = \left[P(A)P(A_j / A)P(FF / A, A_j) + P(L)P(L_j / L)P(FF / L, L_j)\right]P_j(D) \quad (2.12)$$

Here P_j is the probability of forest fire occurrence for a j interval at a controlled forest area; P(A) is the probability of anthropogenic load; $P(A_j/A)$ is the probability of fire source existence on the j day; $P_j(FF/A, A_j)$ is the probability of fire occurrence as a result of the anthropogenic load in the stratum; P(L) is the probability of dry storm occurrence on the stratum territory; $P(L_j/L)$ is the probability of ground storm discharge; P_j $(FF/L,L_j)$ is the probability of lightning-induced forest fire occurrence under the condition that dry storm may occur on the stratum territory; P_j(D) is the probability of fire occurrence in weather conditions of forest fire maturation (the probability of the forest fuels layer to be dry); j index corresponds the day of fire danger season. The following behavior scenario of a human in the forest is chosen: when the storm occurs, the human is trying to leave the forested area or to find shelter, i.e. there is no anthropogenic load when there is a storm (incompatible events). The probable members are estimated through the frequency of events [33]:

$$P(A_j/A) \approx \frac{N_{FDW}}{N_{FW}} \quad P(A) \approx \frac{N_A}{N_{FS}} \quad (2.13)$$

$$P_j(FF/A, A_j) \approx \frac{N_{FA}}{N_{FT}} \quad (2.14)$$

$$P(L_j/L) \approx \frac{N_{LH}}{N_{LD}} \quad P(L) \approx \frac{N_L}{N_{FS}} \quad (2.15)$$

$$P_j(FF/L, L_j) \approx \frac{N_{FL}}{N_{FT}} \quad (2.16)$$

where N_A is the number of days in a fire danger season when there is the anthropogenic load; N_{FA} is the number of fires caused by the anthropogenic load; N_{FT} is the total fire number; N_L is the number of days when lightnings have taken place (during dry storms); N_{FS} is the total number of fire danger season days; N_{FL} is the

number of lightning-induced fires during dry storms; N_{FDW} is the number of fires on a certain week day; N_{FW} is the total number of fires in a week; N_{LH} is the number of ground storm discharges that happened in a certain hour, starting from 00.00 o'clock; N_{LD} is the total number of ground discharges per day. It is obvious that the more cases are viewed for a particular forestry, the higher will be the accuracy of probability estimation with (2.13)—(2.16) formulae. Therefore all the listed parameters of the fire danger season must be annually registered in forestries in order for this method to be realized. Furthermore, such forest mensuration units as fullness and growth class are counted [34]. This model has been adapted for steppe fire danger prediction [35, 36].

A determinate-probability model that considers the mutual impact of the anthropogenic load and storm activity has been developed:

$$P_j = [P(A)P(A_j / A)P(FF / A_j, A) + P(L)P(L_j / L)P(FF / L_j, L) - \\ - P(A)P(A_j / A)P(L)P(L_j / L)P(FF / A_j, A, L_j, L)]P(D) \quad (2.17)$$

Here the additional probability coefficient $P(FF / A_j, A, L_j, L) = \frac{N_{FAL}}{N_{FT}}$ is used that describes the probability of forest fire occurrence as a result of the mutual impact of the anthropogenic load and storm activity (Table 2.6, Fig. 2.15, 2.16).

A mathematical model of integral estimation of forest fire danger on the controlled forested area has the following outline

$$P(\mathrm{A}) = 1 - \prod_{i=1}^{n} (1 - P(\mathrm{A}_i)),$$

where $P(A)$ is the probability of forest fire occurrence on the controlled forested area, $P(\mathrm{A}_i)$ is the probability of forest fire occurrence on a separate stratum area.

The scope of effect of meteorological conditions on the integral estimation of forest fire danger may be evaluated, for instance, by varying the amount of precipitation fallen on the forested area. For this reason a corresponding precipitation recording coefficient is introduced [38]:

Precipitation, mm	No	0.1—0.9	1.0—2.9	3.0—5.9	6.0—14.9	15.0—19.9	20 and more
k_h	1.0	0.8	0.6	0.4	0.2	0.1	0,0

Table 2.6. The probability of fire source existence $P(\mathrm{A}_j/\mathrm{A})$ in the Tomsk Region according to the week days [37]

Week day	Forestry	
	Timiryazevskoye	Moryakovskoye
Monday	0,777	0,135
Tuesday	0,694	0,054
Wednesday	0,822	0,108
Thursday	0,711	0,135
Friday	0,694	0,027
Saturday	1,000	0,189
Sunday	0,855	0,216

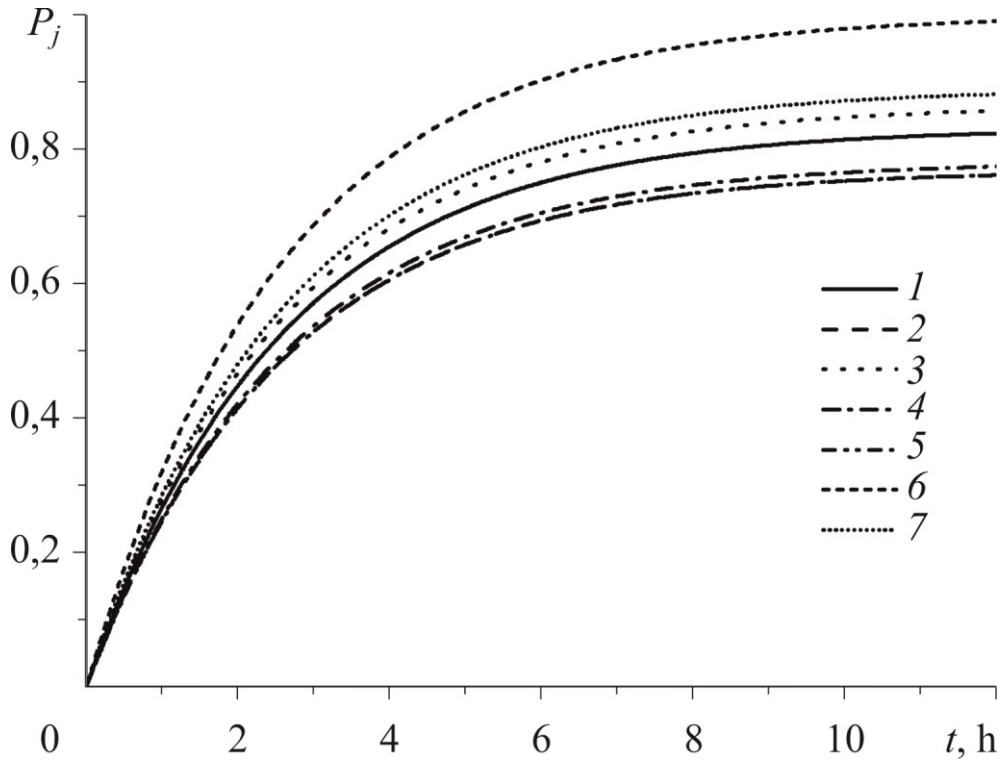

Fig. 2.15. The probability of forest fire occurrence depending on the time of the day for different week days (*1* — Monday., … , *7* — Sunday.). The Timiryazevskoye Forest District of the Timiryazevskoye Forestry

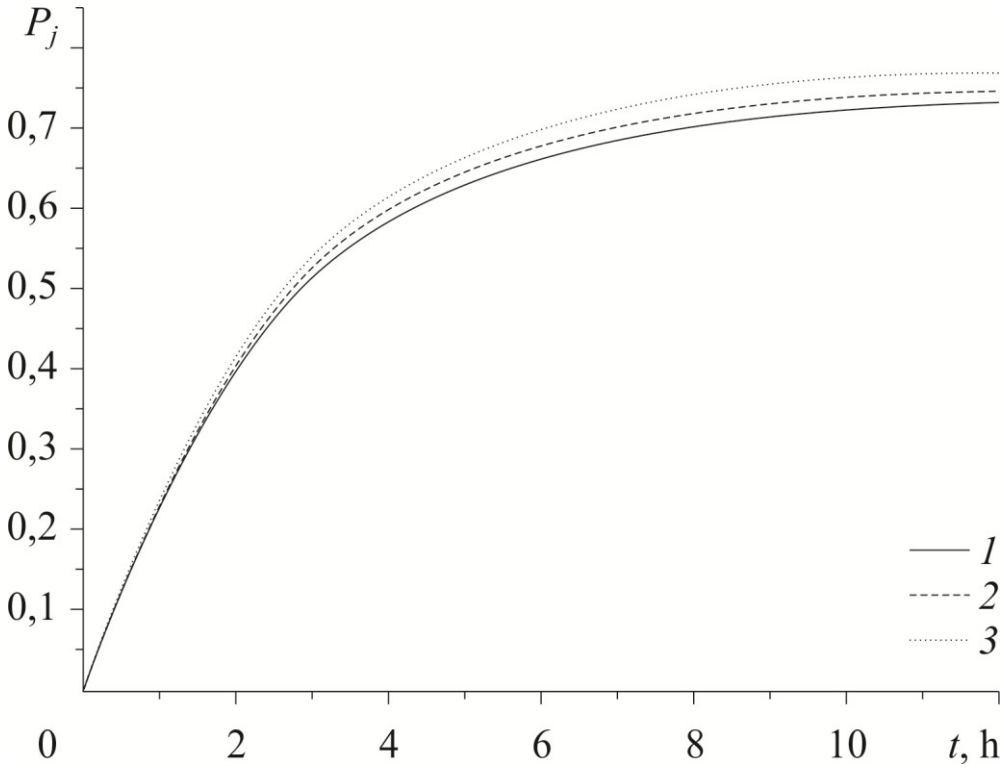

Fig. 2.16. The probability of forest fire occurrence depending on the number of stormy days (*1* — 20, *2* — 25, *3* — 30).

The anthropogenic load within 60 days of the fire danger season (Saturday)

For example, on the territories of the Timiryazevskoye, Moryakovskoye, Bogorodskoye, Kireyevskoye and Zhukovskoye forest districts of the Timiryazevskoye forestry, the Tomsk Region, the amount of precipitation was 0, 0.5, 1.5, 4.0, 15 mm correspondingly. Fig. 2.17 illustrates the probability of forest fires on each separate forest district or forestry area.

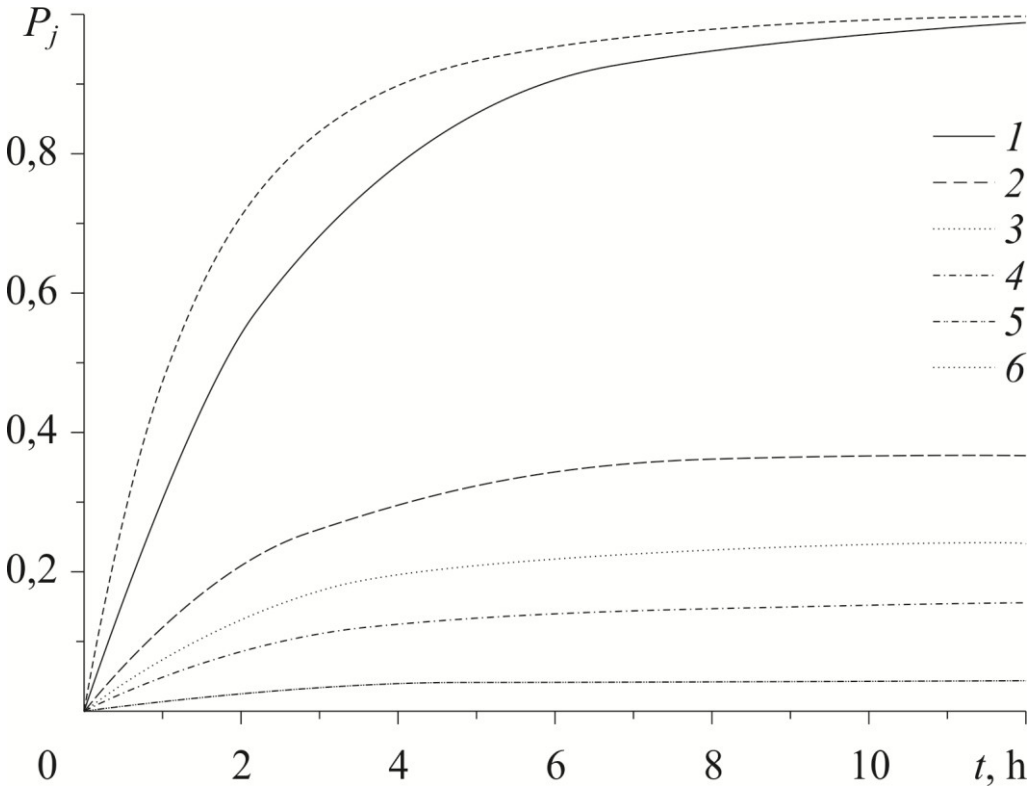

Fig. 2.17. The impact of precipitation on forest fire occurrence probability. *1* — Timiryazevskoye, *2* — Moryakovskoye, *3* — Bogorodskoye, *4* — Kireyevskoye, *5* — Zhukovskoye forestries, *6* — the probability of forest fire occurrence for a forestry in general

The Timiryazevskoye forestry is situated close to a large settlement and the probability of forest fire occurrence at other equal conditions in it is higher. The formula for estimating the probability of forest fire's transforming into a city one has the following outline [39]

$$P(\mathrm{UF}) = P(\mathrm{FF})P(\mathrm{UF}/\mathrm{FF}),$$

where P(UF) is the urban fire probability, P(FF) is the forest fire probability, P(UF/FF) is the city fire probability conditioned that a forest fire occurs. P(FF) may be calculated, according to the formula (2.12) or (2.17), and the conditional probability may be estimated from the statistical data, according to the following formula:

$$P(\mathrm{UF/FF}) \approx \frac{N_{UF}}{N_{FT}}$$

where N_{FT} is the total number of forest fires, N_{UF} is the number of forest fires transformed into the city ones. Fig. 2.18 illustrates the results of estimating the probability of forest fire's transitioning to a settlement.

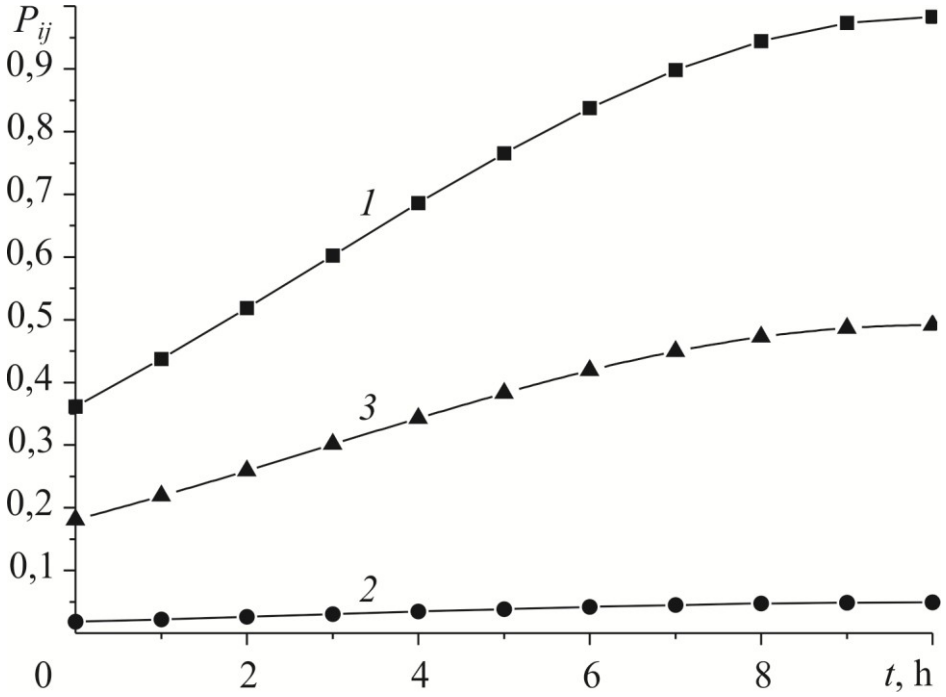

Fig. 2.18. The transition of the forest fire on a settlement

1 — Probability of forest fire occurrence in the territory, bordering with the settlement; *2* — the probability of transitioning onto a settlement if the stratum occurs but rarely in the inflammation statistics; *3* — the probability of fire's transition onto a settlement if the stratum often occurs in the inflammation statistics.

For a short-term prediction of forest fire number on the controlled forested area a sub-system [40, 41] may be used

$$\mathrm{PNF}(d) = \frac{\mathrm{RNF}(d-1)P_j^0(d)}{P_j^0(d-1)},$$

where PNF(d) is the predicted forest fire number; RNF($d-1$) is the recorded forest fire number; P_j^0 is the probability of forest fire occurrence; d и $d-1$ are the current and the preceding day correspondingly. Fig. 2.19 illustrates the results of a retrospective analysis of the forest fire number on the territory of the Timiryazevskoye Forest District, the Timiryazevskoye Forestry. The largest number of fires occurs on Saturdays. The average relative poor accuracy in the prediction was 10,4 % that proved to be a good result.

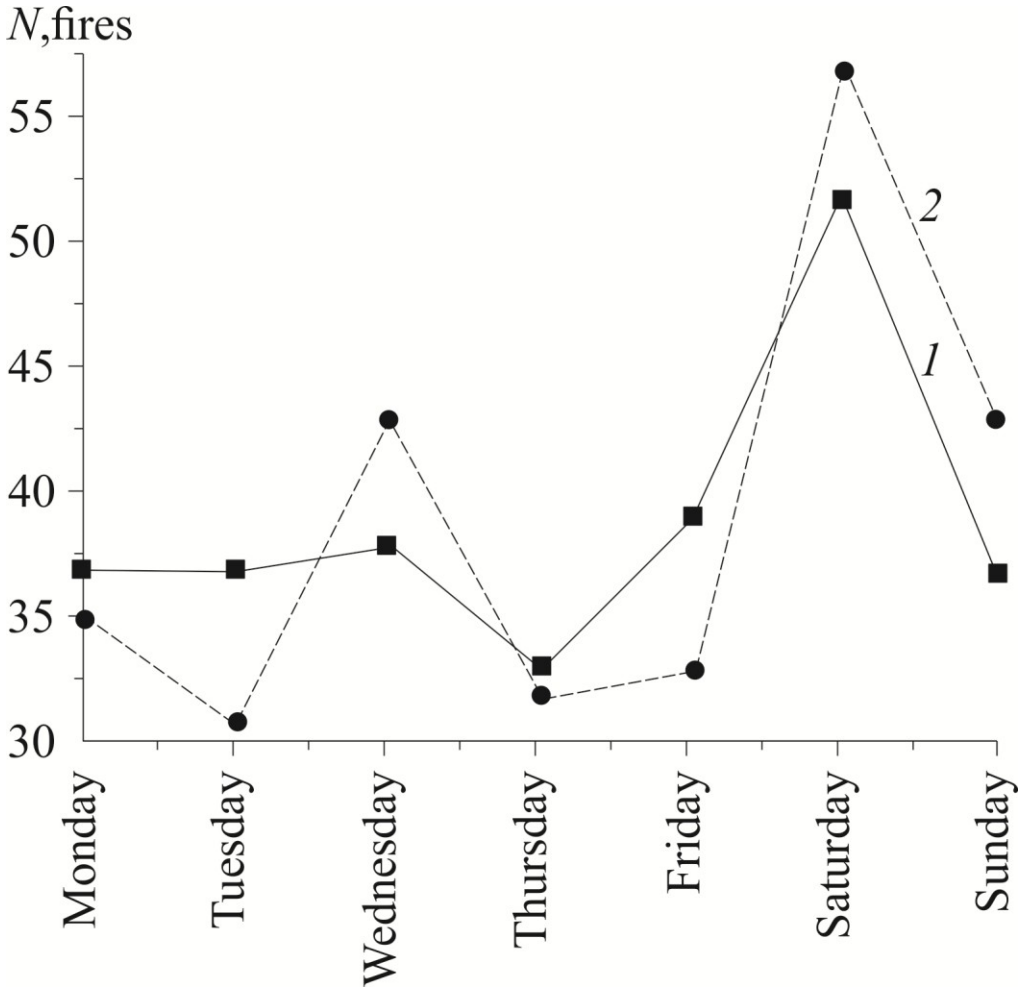

Fig. 2.19. A retrospective analysis of the forest fire number in the Timiryazevskoye forest district of the Timiryazevskoye forestry.

1 — statistical data according to the forest fire number within a week, *2* — the predicted number of forest fires within a week

Model [40] includes two methods for evaluating the probability of forest fire occurrence: according to the weather conditions [37] and according to the inflammation scenarios [42]. The probable members are generally evaluated through the frequency of the events by means of using the statistics on forest fires on a specific forested area [39]. However, the determinate models of drying and inflaming the forest fuels layer allow estimating such parameters that enter the probable members as the period for drying the forest fuels layer and the period of delaying the inflammation of forest fuels layer by a particle heated to high temperatures. Apart from that, the model enbles considering some forest mensuration characteristics to differentiate the impact of the solar radiation on the drying of the forest fuels layer under the stand's canopy.

The time of inflammation delay may be estimated as a result of the quantitative solution for the problem of forest fuels layer inflammation by a single particle heated to high temperatures [43]. The following physical model is analyzed. The underlying surface has a forest fuels layer onto which a particle heated to high temperatures falls. Heating of the forest fuels layer occurs and its thermal decomposition with an

emission of gaseous pyrolysis products (for example, CO) takes place. The pyrolysis products diffuse into the air that contains an oxidizer (i.e. oxygen) and the inert component (i.e. nitrogen). In the gas phase at certain temperatures and reacting gases concentrations a reaction of oxidizing the gaseous flammable pyrolysis products occurs and a gas-phase inflammation of the oxidizer and the flammable matter takes place. The main hypotheses accepted at the problem statement: 1) the particle heated to high temperatures is modeled by a final width plate (one-dimension statement); 2) carbon (this variant corresponds the scenario of mass forest fire occurrence due to the shift and throwing out of the charred burning twigs and forest fuels remains onto the forest fuels layer untouched by the fire) and steel (this variant corresponds the scenario of the anthropogenic fire source, like electric welding) particles are considered; 3) the gas mixture is accepted as of three components containing the oxidizer (oxygen), flammable components (gaseous pyrolysis products – carbon oxide) and inert components (nitrogen, carbon dioxide); 4) the moisture in the forest fuels layer is considered to be absent (the hypothesis corresponds a rather typical for many territories scenario of the catastrophic fire danger).

The system of unstable differential equations on thermal conductivity and diffusion for the gas mixture – particle – forest fuels system that corresponds the formed physical model has the following outline [43, 44]:

The equation on the energy for forest fuels layer:

$$\rho_3 c_3 \frac{\partial T_3}{\partial t} = \lambda_3 \frac{\partial^2 T_3}{\partial x^2} + q_p \cdot k_1 \cdot \rho_3 \cdot \varphi_1 \cdot \exp\left(-\frac{E_1}{RT_3}\right). \quad (2.18)$$

The equation on the energy for the carbon (or steel) particle:

$$\rho_2 c_2 \frac{\partial T_2}{\partial t} = \lambda_2 \frac{\partial^2 T_2}{\partial x^2}. \quad (2.19)$$

The equation on the energy for the gas mixture:

$$\rho_1 c_1 \frac{\partial T_1}{\partial t} = \lambda_1 \frac{\partial^2 T_1}{\partial x^2} + q_5 (1 - \nu_5) \cdot R_5. \quad (2.20)$$

The boundary conditions for Equations (2.18)—(2.20):

$$x = 0, \ \alpha_1 (T - T_e) = \lambda_1 \frac{\partial T_1}{\partial x};$$

$$x = \Gamma_2, \ \lambda_1 \frac{\partial T_1}{\partial x} = \lambda_2 \frac{\partial T_2}{\partial x}, \ T_1 = T_2,$$

$$x = \Gamma_1, \ \lambda_2 \frac{\partial T_2}{\partial x} = \lambda_3 \frac{\partial T_3}{\partial x}, \ T_2 = T_3;$$

$$x = L, \ \alpha_2 (T - T_e) = \lambda_3 \frac{\partial T_3}{\partial x}.$$

The initial conditions for Equations (2.18)—(2.20):

$$t = 0,\ T_3 = 300\ \text{K},\ T_1 = 300\ \text{K},\ T_2 = 700\ \text{K}.$$

The kinetic equation and the initial condition:

$$\rho_3 \frac{\partial \varphi}{\partial t} = -k_1 \rho_3 \varphi \exp\left(-\frac{E_1}{RT}\right),\ t = 0, \varphi = \varphi_0.$$

The equation on diffusion for the oxidizer:

$$\frac{\partial C_4}{\partial t} = D\frac{\partial^2 C_4}{\partial x^2} - \frac{M_4}{M_5} R_5. \qquad (2.21)$$

The boundary and initial conditions for Equation (2.21):

$$x = 0,\ \rho D \frac{\partial C_4}{\partial x} = 0;$$

$$x = \Gamma_2,\ \rho D \frac{\partial C_4}{\partial x} = 0;$$

$$t = 0,\ C_4 = 0,3.$$

The equation on diffusion for gaseous flammable products of pyrolysis:

$$\frac{\partial C_5}{\partial t} = D\frac{\partial^2 C_5}{\partial x^2} - R_5. \qquad (2.22)$$

The boundary and initial conditions for Equation (2.22):

$$x = 0,\ \rho D \frac{\partial C_5}{\partial x} = 0;$$

$$x = \Gamma_2,\ \rho D \frac{\partial C_5}{\partial x} = Y_5;$$

$$t = 0,\ C_5 = 0, 0.$$

The equation on mass balance:

$$C_6 = 1 - C_4 - C_5.$$

The expression for the mass reaction speed R_5 [45]:

$$R_5 = k_5 M_5 T^{-2,25} \exp\left(-\frac{E_5}{RT}\right) \cdot \begin{cases} x_1^{0,25} x_2,\ x_1 > 0,05, \\ x_1 x_2,\ x_1 < 0,05; \end{cases}$$

$$x_i = \frac{C_i}{\sum_{k=4}^{6} \frac{C_k}{M_k} M_i},$$

where T is the temperature (of: 1 — air, 2 — particle, 3 — forest fuels layer); C is the concentration (of: 4 — oxidizer, 5 — flammable gas, 6 — inert air components); ρ_i, c_i, λ_i are the density, heat capacity and thermal conductivity (of: 1 — air, 2 — plate, 3 — forest fuels layer); q_p is the thermal effect of the forest fuels pyrolysis reaction; k_1 is the pre-exponential factor of the forest fuels pyrolysis reaction; E_1 is the activating energy the forest fuels pyrolysis reaction; R is the universal gas constant; φ is the volume fraction of the dry organic matter of the forest fuels; q_5 is the thermal effect of the carbon oxide's oxidation reaction; ν_5 is the heat amount consumed by the forest fuels layer; R_5 is the mass speed of carbon oxide's oxidation reaction; α_1 is the heat exchange coefficient; α_2 is the heat exchange coefficient; M_i is the molecular mass of the gas-phase components (4 — oxygen, 5 — carbon oxide, 6 — nitrogen); k_5 is the pre-exponential factor of carbon oxide's oxidation reaction; E_5 is the activation energy of carbon oxide's oxidation reaction; D is the diffusion coefficient.

Table 2.7 illustrates the periods of delaying the inflammation for differet temperatures of the carbon particle. Table 2.8 illustrates the periods of delaying the inflammation for various temperatures of the steel particle.

*Table 2.7.*Time for delaying the inflammation of a carbon particle [43]

Particle's temperature, K	Time for inflammation delay, s
900	2,63
1000	0,46
1100	0,19
1200	0,099

Table 2.8 Time for delaying the inflammation for a steel particle [43]

Particle's temperature, K	Time for inflammation delay, s
900	0,3
1000	0,07
1100	0,05
1200	0,02

The lowest inflammation limit is the particle's temperature of 900 K. The distinguished temperature range in which the dry forest fuels are inflamed corresponds to real temperatures that can be reached in practically important fire danger situations like the wind inflating the unextinguished bonfires and separate particles of unburnt wood (coals) flying around up to 1—3 m from the open fire source. In the case under study, the presence of the temperature's limit value at which inflammation of forest fuels still occurs is not only determined by the processes of thermal decomposition and gas-phase inflammation of the flammable and oxidating matters. An important factor is also the fact that the particple, apart from the massive heated body, has a limited heat storage .

The analysis of temperature distribution in the gas mixture – particle – forest fuels system allows to reach a conclusion that inflammation takes place in the gas phase in close proximity from the particle' surface (Fig. 2.20). In this zone, where blowing of gaseous pyrolysis products occurs, the carbon oxide concentration is maximum and reaches 1 (Fig. 2.21). The concentration of the oxidizer (oxygen) decreases upon

approaching the particle surface due to blowing of gaseous pyrolysis products, and also the flow of the oxidizer on the carbon oxide's oxidation reaction (Fig. 2.22). The concentration of inert components may change adequately at the changes in concentration of the carbon oxide and oxidizer. A certain maximum of inert component concentration in the inflammation area within the gas phase may be distinguished due to the carbon dioxide's inflow after the oxidation reaction of gaseous pyrolysis products (Fig. 2.23). The distinguished regularities are analogical to both the carbon and the steel particles. The differences are that warming and all the other processes in the steel particle case happen quicker due to a larger thermal conductivity of the steel.

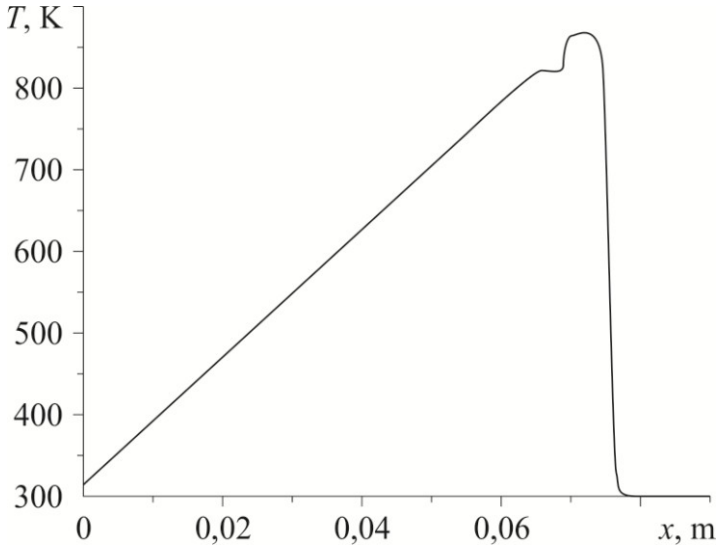

Fig. 2.20. The distribution of temperature in a system of gas mixture – particle – forest fuels layer [43]

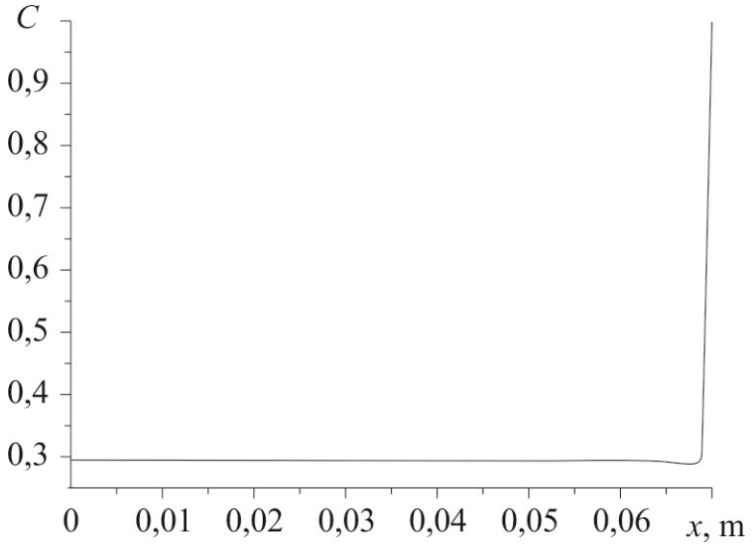

Fig. 2.21. The distribution of carbon oxide in the gas phase [43]

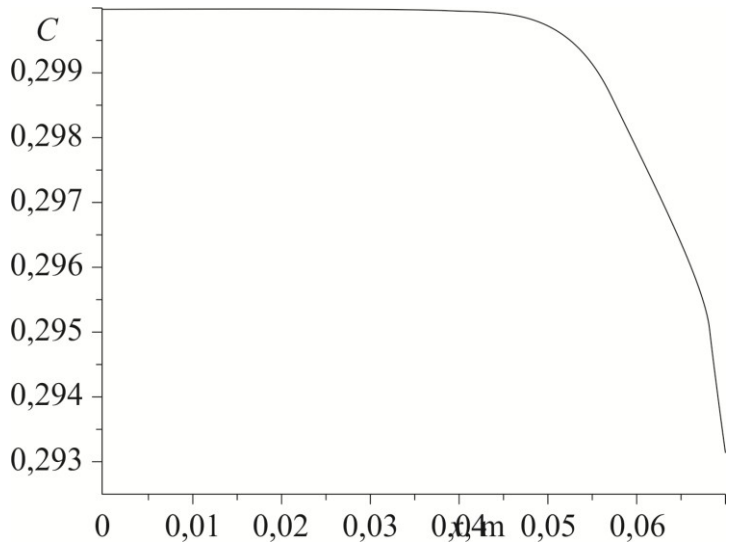

Fig. 2.22. The distribution of the oxidizer in the gas environment [43]

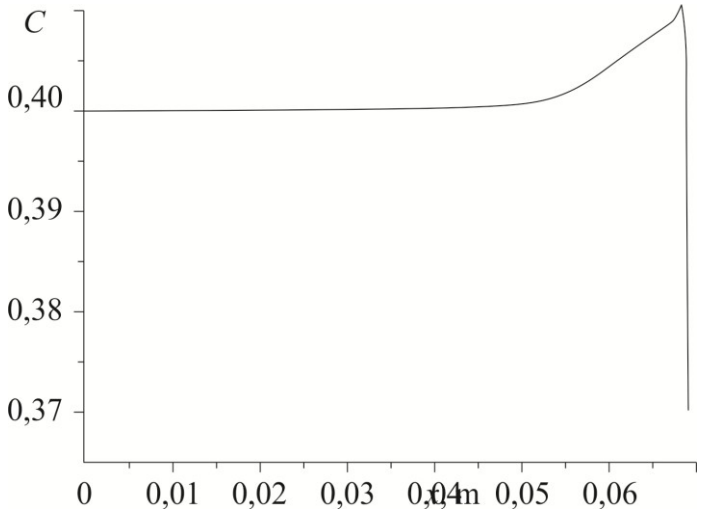

Fig. 2.23. The distribution of inert components in the gas mixture [43]

There is a version of the model [46] that connects the existing State Standard and the probability of forest fire occurrence with regard to the anthropogenic load and storm activity.

To evaluate the forest fire danger probability according to the weather conditions, we should normalize the complex meteorological characteristic by one:

$$P_j(D) = \frac{CMF_D}{CMF_{\max}}$$

where CMF_D is a value of the complex meteorological factor for the day of forecast; CMF_{max} is the maximum value of complex meteorological factor. Then the size of forest fire danger probability change, according to the weather conditions, will be within 0 and 1.

The complex meteorological characteristic may be calculated with the formula [11]

$$\mathrm{CMF} = \sum_{n} t(t - r),$$

where t is the air temperature; r is the dew point temperature; n is the number of days after the last rainfall.

2.14. Concept of forest fire danger prediction

A concept of predicting forest fire danger has been created [47, 48]. Its main principles are the following.

1. The existing methods of predicting forest fire danger may be improved by developing physical and mathematical models for drying, pyrolysis and inflammation of the forest fuels layer by various sources of both the anthropogenic (heated particles of different forms, massively heated body, etc.) and natural character (ground storm discharges of different polarity). The physical and chemical processes of drying and inflaming the forest fuels are the basic factors of forest fire danger.

2. An active interaction of forest fire danger prediction systems with program complexes that realize atmosphere or climate models may provide the presence of predicting information on weather parameters with a high spatial resolution. Furthermore, perspectives of short- and medium-term forest fire danger prediction are revealed.

3. To record the space-time changes in the human-induced forest fire danger level it is necessary to develop a system of data acquisition about the anthropogenic load on the controlled forested area [49, 50].

4. In the forest fire protection system it is necessary to create a computing center for a centralized initial information processing and prediction development.

The basis for this concept is illustrated on Fig. 2.24.

The input information on weather parameters is generated in programs that realize global or regional atmosphere models (the numerical weather forecast), and enters as the input one [51] into the sub-systems of evaluating the probability of forest fire occurrence according to the weather conditions and inflammation scenarios. The experience of an analogous forest fire danger monitoring organization according to the weather conditions is known [52]: the use of a mesoscale atmospheric MM5 model along with the American forest fire danger prediction system. The system of assimilating data on the level of anthropogenic impact generates information fields on the anthropogenic load level on the controlled forested area in order to count its space-time characteristic. Information from the direction finding systems of cloud-earth class comes into the model as input data. As the result, the determinate-probability model (criterion) allows estimating the forest fire occurrence probability on the controlled forested area.

It is possible to create a nationwide center for forest fire danger monitoring that will accumulate the initial information and eventually generate prediction information and send it to the interested consumers [53]. The model of forest fire monitoring center is presented on Fig. 2.25.

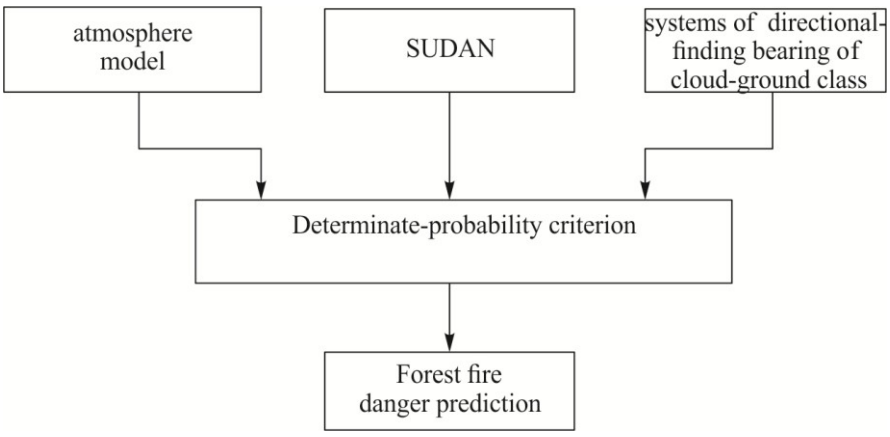

Fig. 2.24. The basis for forest fire danger prediction concept

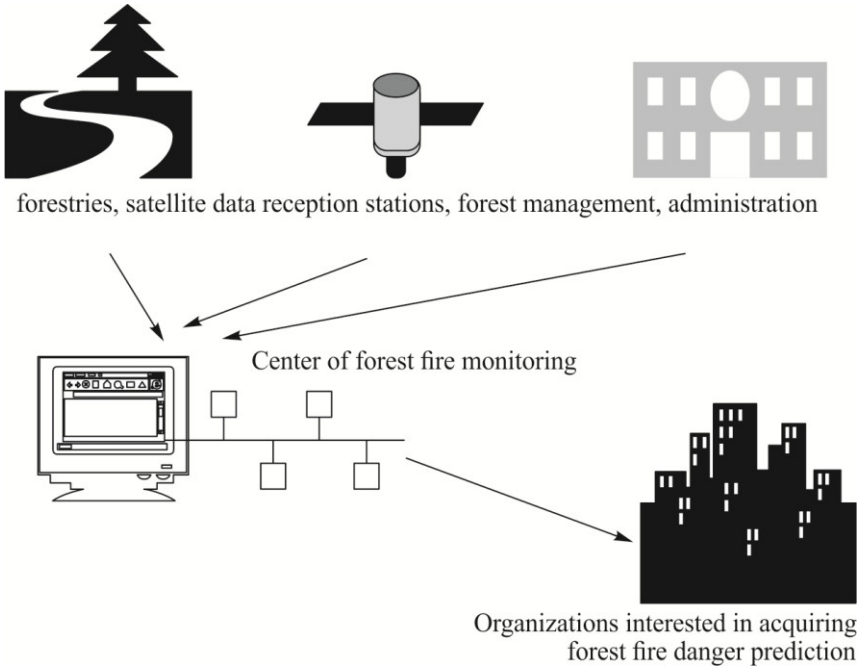

Fig. 2.25. A model of forest fire monitoring center [54]

A multiprocessor computer system functions in the center that is the core of all the information computation system [55]. The system may also be distributed; it is important, however, that rapid information transmission from different sub-systems for processing at a multiprocessor computer system be feasible.

REFERENCES

1. Lee B.S., Alexander M.E., Hawkes B.C. et al. (2002) Information systems in support of wildland fire management decidion making in Canada // Computers and Electronics in Agriculture, 37(1—2), 185—198.
2. Stocks B.J., Alexander M.E., McAlpine R.S. et al. (1987) Canadian Forest Fire Danger Rating System. Canadian Forestry service, 500 p.
3. Martell D.L. (1999) A Markov chain model of day to day changes in the Canadian Forest Fire Weather Index // Int. J. Wildland Fire, 9(4), 265—273.
4. Nazarov A.A., Terpugov A.F. (2006) Theory of probability and random processes: textbook. Tomsk: Izd-vo NTL, 204 p. (In Russian)
5. Kurbatskiy N.P., Kostyrina T.V. (1977) National system of fire danger calculation in the USA // Obnaruzhenie i analiz lesnykh pozharov / ILiD SB AS USSR. Krasnoyarsk, P. 38—90. (In Russian)
6. Deeming J.E., Burgan K.E., Cohen J.D. (1978) The National Fire-Danger Rating System. Ogden, Utah: USDA Forest Service, General Technical report. INT-39, 66 p.
7. Kurbatskiy N.P. (1970) Seasonal changes of needles, leaves and branches humidity of major wood species of taiga. // Voprosy lesnoy pirologii / ILiD SO AN, USSR. Krasnoyarsk, P. 155—185. (In Russian)
8. Nesterov V.G. (1949) Forest fireability and methods of detection. Moscow; Leningrad: Г Gosles-bumizdat, 76 p.
9. Nesterov V.G., Gritsenko M.V., Shatulina T.A. (1968) Use of dew point temperature for calculation of forest burning factor // Meteorologiya i gidrologiya, 9, 102—104. (In Russian)
10. Korovin G.N., Pokryvaylo V.D., Grishman Z.M. et al. (1986) Main trends of development and improvement of fire danger estimation and forecast // Lesnye pozhary i borba s nimi / LenNIILH. Leningrad, P. 18—31. (In Russian)
11. GOST R 22.1.09-99. Monitoring and prediction of forest fires. General requirements. Moscow: Gosstandart RF, 1999. 10 p. (In Russian)
12. Dorrer G.A. (1985) Model of daily dynamics of moisture content of burning conductors // Forest fires and their consequences / ILiD SO AN, USSR. Krasnoyarsk, P. 110—124. (In Russian)
13. Yakimov S.P. (1996) Algorithms of forest fire danger, according to remote sensing data: Dissertation … Phd.Eng. Krasnoyarsk: KGTA. 155 p. (In Russian)
14. Garcia Diez E. L., Rivas Soriano L., de Pablo F., Garcia Diez A. (1999) Prediction of the daily number of forest fires // Int. J. Wildland Fire. 9(3), 207—211.
15. Garcia Diez E.L., Labajo Salazar J.L., De Pablo F. (1993) Some meteorological conditions associated with forest fires in Galicia (Spain) // Int. J. of Biometeorology, 37, 194—199.
16. Garcia Diez E.L., Rivas Soriano L., De Pablo F. (1994) An objective forecasting model for the daily outbreak of forest fires based on meteorological considerations // J. Appl. Meteorology, 33(4), 519—526.
17. Garcia Diez A., Soriano L.R., Garcia Diez E.L. (1996) Medium-Range forecasting for the number of daily forest fires // J. Appl. Meteorology. 35(5), 725—732.
18. Viegas D.X., Bovio G., Ferreira A. et al. (1999) Comparative study of various methods of fire danger evaluation in Southern Europe // Int. J. Wildland Fire. 10(4), 235—246.
19. Camia A., Barbosa P., Amatulli G., San-Miguel-Ayanz J. (2006) Fire danger rating in the European Forest Fire Information System (EFFIS): Current developments // Forest Ecology and Management. 234, suppl. 1. P. S20.
20. Grishin A.M. Filkov A.I. (2005) Prediction of forest fires occurrence and distribution. Kemerovo: Praktika, 202 p. (In Russian)
21. Filkov A.I. (2005) Determintate-probability system of forest fire danger prediction. Dissertation… PhD.Phys.Math.Sci. Tomsk: TSU, 163 p. (In Russian)

22. Gorev G.V. (2004) Assessment of climate predisposition of the territory to forest fires (based on the example of Tomsk region): Autoref. thes. … Phd.Geogr.Sci. Tomsk: TSU. 24 p. (In Russian)
23. Draper N. R., Smith H. (2007) Applied regression analysis. 3-rd Ed. Moscow: Williams, 912 p. (In Russian)
24. Mukhin A.R. (1996) Upgrading of software in forest fire protection: Autoref. thes. … DSci. Moscow: MGUL, 24 p. (In Russian)
25. Marchenko N.A. (2005) Landscape framework for regional forest fire monitoring // Int. Forest Fire News (IFFN), 32, 55—61.
26. Anderson K. (2002) A model to predict lightning-caused fire occurrences // Int. J. Wildland Fire, 11(3—4), 163—172.
27. Latham D.J., Schlieter J.A. (1989) Ignition probabilities of wildland fuels based on simulated lightning discharges / USDA Forest Service Res. Pap. INT-411. 16 p.
28. Hartford R.A. (1990) Smoldering combustion limits in peat as influensed by moisture, mineral content and organic bulk density // 10th Conference on Fire and Forest Meteorology. Downsview, ON: Atmospheric Environment Service, P. 282—286.
29. Development and structure of the Canadian Forest Fire Behaviour Prediction System. Information Report ST-X-3. Ottawa: Forestry Canada, 1992. 66 p.
30. Preisler H.K., Brillinger D.R., Burgan R.E., Benoit J.W. (2004) Probability based models for estimation of wildfire risk // Int. J. Wildland Fire, 13(2), 133—142.
31. Diez-Delgado R., Lloret F., Pons X. (2004) Statistical analysis of fire frequency models for Catalonia (NE Spain, 1975—1998) based on fire scar maps from Landsat MSS data // Int. J. Wildland Fire. 13(1), 89—99.
32. Taylor S.W., Alexander M.E. (2006) Science, technology and human factors in fire danger rating: the Canadian experience // Int. J. Wildland Fire. 15(1), 121—135.
33. Baranovskiy N.V. (2007) Mathematical modeling of the most probable scenarios and conditions of forest fires occurrence. Dissertation… PhD.Phys.Math.Sci. Tomsk: TSU, 153 p. (In Russian)
34. Baranovskiy N.V., Grishin A.M. (2002) Mathematical modeling of forest fire fuels layer drying under pine wood canopy // Vychislitelnye tekhnologii, 7(1), 320—324. (In Russian)
35. Baranovskiy N.V. (2006) Prediction of steppe fire danger // Works of International conference “Computing and information technologies in science, engineering and education”. T. I. Pavlodar: TOO NPF “Eko”, P. 202—208. (In Russian)
36. Baranovskiy N.V. (2006) Prediction of steppe fire danger // Ekologicheskie sistemy i pribory, 11, 42—46. (In Russian)
37. Baranovskiy N.V. (2004) Effect of anthropogenic load and thunderstorm activity on forest fires probability // Sib. ekol. zhurn., 6, 835—842. (In Russian)
38. Zhdanko V.A., Gritsenko M.V. (1980) Analysis method for forest fire seasons. Practical recommendations. Leningrad: LenNIILH. (In Russian)
39. Baranovskiy N.V. (2007) Determinate-probability model of a forest fire transition onto a population settlement // Ekologicheskie sistemy i pribory, 3, 59—63. (In Russian)
40. Baranovskiy N.V. (2007) Prediction of forest fires number // Pozharnaya bezopasnost, 1, 123—127. (In Russian)
41. Baranovskiy N.V. (2006) Probability of forest fire danger and forest fires number prediction // Izv. vuzov. Physics, 49(3). Annex. P. 212—213. (In Russian)
42. Kuznetsov G.V., Baranovskiy N.V. (2006) Determinate-probability prediction of forest fire ignitions // Pozharovzryvobezopasnost, 15(5), 56—59. (In Russian)
43. Kuznetsov G.V., Baranovskiy N.V. (2006) Mathematical modeling of forest fire fuels layer ignition when heated by a particle up to high temperatures // Same. 15(4), 42—46. (In Russian)

44. Kuznetsov G.V., Baranovskiy N.V. (2006) Numerical modeling of forest fire fuels layer ignition when heated by a particle up to high temperatures // Works of International conference “Computing and information technologies in science, engineering and education”. T. I. Pavlodar: TOO NPF “Eko”, P. 673—680. (In Russian)
45. Grishin A.M., Shipulina O.V. (2002) Mathematical modeling of top forest fires propagation in homogeneous tracts of forest and along rides // Fizika Goreniya i Vzryva, 38(6), pp. 17-29.
46. Baranovskiy N.V. (2007) Method for prediction of forest fire danger as the basis for a new state standard // Pozharnaya bezopasnost, 4, 80—84. (In Russian)
47. Baranovskiy N.V. (2007) Forest fire danger prediction, based on a new concept // Materials of Intl. Conference “Rational Use and Reforestation in the Sustainable development System”. Gomel: In-t lesa NAN Belarusi, P. 129—132. (In Russian)
48. Baranovskiy N.V. (2007) New concept of forest fire danger prediction // Modern methods of mathematical modeling of natural and anthropogenic disasters: Thes. IX Rus. Conf (17—22 September 2007 г., Barnaul). Barnaul: Izd-vo Alt. Un-ta, P. 13. (In Russian)
49. Baranovskiy N.V. (2006) Mathematical basics of data assimilation system on anthropogenic load level in the controlled forest-covered territory // Nauka na rubezhe tysyacheletiy «Progressive technologies of development»: 3-rd Intl. Scientific Conf: 24—25 November 2006. Tambov: OAO «Tambovpoligrafizdat», P. 120. (In Russian)
50. Baranovskiy N.V. (2007) Testing of data assimilation system about anthropogenic load level for a linear source of anthropogenic load // Environmental safety management: collection of works of distant intl. conference. Yekaterinburg: UGTU; UPI. P. 319—322. (In Russian)
51. Baranovskiy N.V., Grishin A.M., Loskutnikova T.P. (2003) Inforemation-prognostic system of forest fire occurrence probability // Vychislitelnye tekhnologii, 8(2), 16—26. (In Russian)
52. Hoadley J.L., Rorig M.L., Bradshaw L. et al. (2006) Evaluation of MM5 model resolution when applied to prediction of National Fire Danger Rating indexes // Int. J. Wildland Fire, 15(2), 147—154.
53. Baranovskiy N.V. (2007) Global monitoring and forest fire danger prediction // Global research potential: Collection of materials. 3-rd Intl. Scientific Conf: 4—5 June 2007. Tambov: Tambovprint, P. 129—131. (In Russian)
54. Baranovskiy N.V., Grishin A.M. Loskutnikova T.P. (2002) Model of regional forest fire danger prediction system // Works of intl. conference ENVIROMIS-2002. Tomsk: Izd-vo CNTI, P. 347—352. (In Russian)
55. Baranovskiy N.V. (2007) New concept of forest fire danger prediction and landscape parallelization // High-performance parallel computations in cluster systems. Nizhniy Novgorod: Izd-vo Nizhegorodskogo gosuniversiteta, P. 33—40. (In Russian)

CHAPTER 3
PREDICTION OF FOREST FIRES' ENVIRONMENTAL EFFECTS

Abstract

The third paragraph deals with information on environmental pollution resulting of from forest fires. The project "Siberian Aerosols" and issues concerning transformation of air contaminants in the atmosphere and data assimilation are considered here. Also, impact of forest fires on weather, soil, phytocenosis, public health is discussed. The method to assess the probability of getting or aggravating a disease caused by forest fires is presented.

Keywords: forest fires, pollutants, greenhouse gases, soil, weather, health

3.1. Forest Fires as Sources of Pollutants and Greenhouse Gases

Forest fires pollute the atmosphere with forest fuels pyrolysis and combustion products [1]. Forest fires were considered as potential and significant sources of polychlorinated dibenzo-p-dioxins and polychlorinated dibenzofurans, PCDD/Fs emissions [2—4]. However, some researches were successul in measuring p-dioxins and furans concentration in the atmosphere during a forest fire [5, 6], and the data about forest fires as potential sources of these pollutants were not found. Study of soil and vegetation after fires in order to assess the environmental pollution with these substances and estimate a total mass of the substances prior and after a modeled forest fire [2, 7—12] have shown that experiment couldn't identify the increase of these substances concentration after burning process. In other words, forest fires, cannot probably be potential sources of the designated polluting agents.

Forest fires emission can seriously impact on the air quality on both local and regional scale. For instance, the fires of 1998 in Mexico City and Central America caused a pollutants emission, which resulted in a "smog in a dozen of cities", moving from Florida to North Dakota.

Open air fires, for example, forest fires and prescribed burnings, can emit particles and other pollutants in the atmosphere [13]. Assessment of pollutant emission from forest fires in Texas territory (the USA) based on observations and field survey data of fire-affected and forest-covered area with inclusion of literature data on forest fuels consumption and emission factors.

Individual fire cases were described properly in documents, but annual fire occurrence rate and spatial location have a poor description. As a result of spatial and time distribution analysis of various fire cases in Texas [13], the following conclusion was made that fires can significantly contribute to total particles concentration in the air of extensive agricultural and forestry regions, such as Texas. Annual data on particles, carbon monoxide (CO), methane (CH_4), non-methane hydrocarbons (NMHC), nitrogen oxide (NO_x) and ammonium hydrate (NH_3) emission is available.

Emission data from different fire cases were divided into the following types [13]:

a) Forest fires — undesirable or accidental, deliberate arsons (incendiary fire), and also naturally caused (thunderstorms);

b) Prescribed burning — nonagricultural controlled burns by forestry services, except for felling fires;

c) Felling fires выжигания на рубках — planned nonagricultural burning during lumbering and clearing activity;

d) Agricultural burnings — agricultural land burning for the purpose of territory clearing, burning of fallow fields with stubble remains, burning of harvest wastes, and burning sugarcane fields.

A comparative analysis has been conducted for emission particles from vegetation burning near Houston [13] with levoglucosan from cellulose burning [14].

Estimating of pollutant emission can be done according to the formula [13]

$$Q = K_{\alpha} CF,$$

where Q — emission, lbs.; K_{α} — emission factor, lb/t; C — fuel consumption, t/acre; F — burned land, acres.

Emission factor values are given in documents of the US Environmental Protection Agency (EPA) [15—17]. According to the data [13], emission from prescribed burnings is five times more than from any other category.

Smoke from agricultural wastes burning includes components [18], liable to reaction under sunlight effect, generating a “photochemical smog”, which typical feature is a higher ozone concentration in comparison to the natural background. Measurements of ozone concentration in forest fire plumes by aircraft [19] have proved the fact of ozone generation in forest fire smokes under the sunlight effect. Ozone concentration is zero near the flame, but when the smoke rises, ozone is registered in the upper plume layer. Ozone measurements were done as part of the general research on controlled forest waste burning aspects [20].

Vast information on substances, emitted from vegetation biomass fires in Africa in 2000, is available (table 3.1).

There was also emission factors found for these pollutants, but for grass vegetation fires [21].

Emission from flammable vegetation (FV) burning [22] is a basic source of pollutants in the air (Table 3.2).

Emission of organic air pollutants, including organic pollutants from forest fires, vegetation and prescribed burning, can be quite large-scale [23]. Organic aerosol from burning of deciduous and coniferous tree biomass of temperate climate zones [24, 25] was studied in detail. Pollutants emission was estimated in field surveys during the savanna prescribed fires [26]. Emission of non-volatile organic compounds during forest fuel burning was studied in the laboratory [27]. A considerable amount of methoxyphenol discharge was estimated.

Table 3.1. Emission factors of various pollutants for the forest territory during drought period [21], g/kg

Pollutant	Emission factor		June/September ratio
	June	September	
1	2	3	4
Carbon dioxide (CO_2)	1622 ± 67	1673 ± 51	0.97
Carbon monoxide (CO)	104.3 ± 30.4	81 ± 21.9	1.29
Methane (CH_4)	3.82 ± 1.59	2.61 ± 1.19	1.47
Non-methane hydrocarbons (NMHC)	2.72 ± 0.60	2.26 ± 0.45	1.20
Dimethyl sulfide (CH_3SCH_3)	0.0028 ± 0.0001	0.0024 ± 0.0004	1.17
Methyl bromide (CH_3Br)	0.0018 ± 0.0001	0.0014 ± 0.0004	1.30
Methyl chloride (CH_3Cl)	0.088 ± 0.014	0.077 ± 0.011	1.14
Methyl iodide (CH_3I)	0.0019±0.0003	0.0017±0.002	1.12
Methyl nitrate (CH_3ONO_2)	0.00055 ± 0.00016	0.00042 ± 0.0001	1.30
Ethane (C_2H_6)	0.265 ± 0.079	0.205 ± 0.060	1.30
Ethene (C_2H_4)	0.915 ± 0.273	0.706 ± 0.205	1.30
Propane (C_3H_8)	0.080 ± 0.024	0.061 ± 0.018	1.30
Propene (C_3H_6)	0.312 ± 0.126	0.218 ± 0.092	1.43
Acetylene (C_2H_2)	0.256 ± 0.076	0.198 ± 0.057	1.30
Isobutane (*i*-C_4H_{10})	0.0052 ± 0.0025	0.0034 ± 0.0018	1.56
n-butane (*n*-C_4H_{10})	0.026 ± 0.008	0.020 ± 0.006	1.30
Trans-butene-2 (C_4H_8)	0.026 ± 0.008	0.020 ± 0.006	1.30
Butene-1 (C_4H_8)	0.063 ± 0.022	0.047 ± 0.016	1.36
Cis-Butene-2 (C_4H_8)	0.018 ± 0.006	0.014 ± 0.004	1.30
Isopentane (*i*-C_5H_{12})	0.0027 ± 0.0008	0.0021 ± 0.0006	1.30
n-pentane (*n*-C_5H_{12})	0.011 ± 0.003	0.0089 ± 0.0020	1.23
Butadiene -1,3 (C_4H_6)	0.082 ± 0.027	0.061 ± 0.021	1.34
3-METHYL-butene-1 (C_5H_{10})	0.0092 ± 0.0027	0.0071 ± 0.0021	1.30
Trans-Pentene-2 (C_5H_{10})	0.0052 ± 0.0024	0.0034 ± 0.0018	1.56
2-Methyl-butene-2 (C_5H_{10})	0.0092 ± 0.0027	0.0071 ± 0.0021	1.30
2-Methyl-butene-1 (C_5H_{10})	0.010 ± 0.030	0.0078 ± 0.0023	1.30
Isoprene (C_5H_8)	0.062 ± 0.016	0.050 ± 0.012	1.24
n-Heptane (C_7H_{16})	0.019 ± 0.006	0.015 ± 0.0043	1.30
Benzene (C_6H_6)	0.265 ± 0.079	0.205 ± 0.060	1.30
Toluene (C_7H_8)	0.192 ± 0.057	0.148 ± 0.043	1.30
Formaldehyde (HCHO)	1.50 ± 0.38	1.21 ± 0.286	1.24
Methanol (CH_3OH)	1.84 ± 0.58	1.40 ± 0.44	1.32
Acetic acid (CH_3COOH)	3.85 ± 1.24	2.91 ± 0.93	1.33
Formic acid (HCOOH)	0.950 ± 0.205	0.793 ± 0.154	1.20
Ammonia (NH_3)	0.380 ± 0.101	0.302 ± 0.076	1.26
Hydrocyanic acid (HCN)	0.630 ± 0.084	0.566 ± 0.063	1.11
Particles <2.5 mcm	13.1 ± 5.9	8.57 ± 4.47	1.53
Partcles (all)	22.7 ± 8.0	16.6 ± 6.0	1.37
Organic carbon	4.39 ± 1.01	3.61 ± 0.80	1.21
Black carbon	0.531 ± 0.158	0.410 ± 0.12	1.30
Chlorides (Cl^-)	2.57 ± 1.06	1.75 ± 0.0	1.46
Nitrates (NO_3^-)	0.320 ± 0.065	0.270 ± 0.049	1.19
Sulfates (SO_4^{2-})	0.394 ± 0.147	0.281 ± 0.111	1.40
Potassium (K^+)	1.46 ± 0.44	1.13 ± 0.33	1.30

*Table 3.2.*Emission pollutants from flammable vegetation in different regions [22]

Region	Population (1995), mln.people	Emission, kg/year		
		CO_2	CO	NO
Africa	728	296	28	0.50
Asia	3386	886	84	1.51
Latin America	482	110	10	0.19
Oceania	29	3	0	0
North America	293	114	11	0.19
Europe	506	40	4	0.07
Former Soviet countries	292	46	4	0.08
Total worldwide	5716	1495	141	2.54
All anthropogenic sources		7100	925	34

In [27] emission of polychlorinated dibenzo-furan from from standardized forest fires of wood (Oregon and North Carolina) was discovered. Оценена Inorganic pollutants emission, such as sulfates, chlorides and metals, from vegetation fires was estimated in the Amazon's watershed [28]. Ashes after natural fires can contain different cyanides [29]. Consolidated information on basic organic contamination agents from natural fires is given in Table 3.3.

*Table 3.3.*Emission from prescribed burnings and forest fires (mg/kg of fuel) [23-29]

Class	Composition	Savanna and grassland vegetation	Tropical forests	Extratropical forests
VOCs	Butadiene	70		60
	Benzene	230	400	490
	Toluene	130	250	400
	Xylenes	45	60	200
	Ethylbenzene	13	24	48
	Styrene	24	30	130
	Methyl chloride	75	100	50
	Methyl bromide	2.1	7.8	3.2
	Methyl iodide	0.5	6.8	0.6
	Acetonitrile	110	180	190
SVOCs	Furan	95	480	425
	2-Methylfuran	46	170	470
	3- Methylfuran	8.5	29	50
	2- Ethylfuran	1	3	6
	2,4-Dimethylfuran	8	24	19
	2,5-Dimethylfuran	2	30	50
	Tetrahydrofuran	16	16	20
	2,3- Dihydrofuran	12	13	17
	Benzofuran	14	15	26
	Furfural	230	370	460
	Polycyclic aromatic compounds	2.4	25	25
	Phenol	3	6	5
Carbonyl compounds	Methanol	1300	2000	2000
	Formaldehyde	350	1400	2200
	Acetaldehyde	500	650	500
	Acrolein	80	180	240
	Propionic aldehyde	9	80	140
	Butanal	53	71	210
	Hexanal	13	31	20
	Heptanal	3	3	4
	Acetone	435	620	555
	Methyl-ethyl ketone	260	430	455
	2,3-Butanadion	570	920	925
	Pentanone	15	28	90
	Heptanon	6	2	5
	Octanon	15	19	20
	Benzaldehyde	29	27	36

Organic pollutants emissions from agricultural and landfill burnings are various [23].

Chemical processes of forest fires and subsequent fogging can be described on a regional scale [30]. Over 100 substances were identified in the forest fire smoke composition. Combustion products of vegetation biomass can have a different impact. For example, CO_2 and CH_4 contribute to global warming, NO_x and SO_2 have impact on atmospheric fallout acidity. If smoke includes particles and polynuclear aromatic hydrocarbons, they can influence the health of people [30]. Transformation of primary emitted substances into secondary, such as ozone, takes place as a result of photochemical reactions. Emission of acidifying compounds does not have a strong effect on acidity, because acid forming gases, dissolved in water, are neutralized under effect of alkaline substances (on the basis of Ca, Mg, K), which are also emitted during forest fires. As there is no complete data available on transformation of major pollutants, emitted during forest fires (for example, for tropical forest fires it is 80 % for the burned phytomass volume [31]).

Forest phytomass burns in accordance with the chemical reaction equation in ideal conditions [30]

$$CH_2O + O_2 \rightarrow CO_2 + H_2O.$$

Incomplete burning results in generation of CO and many other hydrocarbons. S and N; those, present in phytomass, oxidize to SO_2 and NO:

$$S + O_2 \rightarrow SO_2,$$

$$2N + O_2 \rightarrow 2NO.$$

Studying of polluting substances emission from tropical grassland vegetation during fires [32], the following pollutants were defined: particles of smoke and CO, HC, NO_2. Data on annual emission of these pollutants in the tropics are given in the Table 3.4.

Table 3.4.Annual emission of pollutants in the tropics [32]

Part of the tropics	Burned area, ha	Emission, 10^6 t			
		Smoke particles			Smoke particles
Africa	838	29.4	134	34	3.4
Central America	123	4.2	22	5	0.4
South America	249	8.4	40	10	1
Asia	341	11.6	54	13.6	1.4
Oceania	247	8.4	40	9.8	1
Total	1818	62	290	72.4	7.2

Experiments on determining the pollutants emission from peat burning [33] at different temperatures show that in this case nomenclature of emitted compounds is not wider than from other forest fuels burning.

Smoke composition from a real forest fire front [34] according to determined compounds nomenclature matches in many aspects with experiment data and field studies.

According to some evaluations [35, 36], boreal zone provides about 37 % of total earth's carbon and, consequently, this region has an extreme value for the earth's carbon cycle. Carbon preservation and yield in the boreal zone are controlled by six fac-

tors, such as: speed of vegetation growth, biomass decomposition, permafrost generation, and also size, frequency and severity of forest fires, which are a strong disturbing regional factor [37, 38].

Special attention is drawn to CO emission from forest fires in the north-western America [39] and other boreal regions [39—42]. Increase of carbon emissions from forest fires was registered after reforestation activities [43].

Methane emission is possible from phytomass burning in tropical forests [44]. So-called ratio of emissions can be used for comparing various greenhouse gas emissions, which is calculated by the formula [45]

$$ER = \frac{\Delta X}{\Delta CO_2},$$

where ΔX — concentration of a specific emitted compound, $\Delta X = X^* - X$, X^* — concentration, measured in the plume, X — a baseline concentration value; $\Delta CO_2 = CO_2^* - CO_2$, where CO_2 — a baseline concentration of carbon dioxide in the air.

Data on greenhouse gases emission from forest fires during 1997—2001 [46] are very informative; it was a highly active period for forest fires. Global content of carbon dioxide and methane in the Earth's atmosphere grows, but with a various speed in different years [47—51].

Carbon dioxide emission during forest fuels burning [52] — fall, cedar needles and *Cladonia* lichen, was researched in the laboratory. Quantitative analysis of carbon dioxide in the ЛГМ combustion products was done at the experimental unit, based on the gas analyzer unit GIAM-15. The RF Ministry of Ecology has approved the calculation method for pollutants emission from forest fires in 1997 [53, 54]. Carbon dioxide content is analyzed by an optical-acoustic method [55] to determine the numerical values of carbon dioxide emission factors. The obtained factors differ insignificantly from each other for various forest fuels (difference is commensurable with measurement accuracy).

Mercury is a very important element, which should have an ecological monitoring, as its harmful impact on human health is known. Gaseous mercury is not adsorbed by soil surface, water or vegetation during six months—two years [56], and therefore can be transported to vast distances [57, 58]. Gaseous mercury emission and transport from large-scale fires were established in boreal forests of Canada [59]. Field studies were done in Harvard Forest. It was found that a long-range transport of gaseous mercury in the smoke plume from forest fire series in the north Quebec boreal zone. studies were focused on a series of natural fires, which occurred approximately 500 km northward of Montreal, in early June of 2002. About 250 fires happened at that time. The dominating types in the region are *Picea mariana* and *Pinus lanskiana* [60]. Observations data analysis has shown a considerable and highly correlated increase of Hg and CO content during the plume observation. Data on Hg : CO ratio emission (8.61×10^{-8} mole/mole) were combined with earlier publications on CO emission and burned biomass to determine the Hg emission density in the territory of boreal forest fires (1.5 g Hg/ha), annual emission of Hg from forest fires in Canada (3.5 t), total worldwide and annual emission from boreal forests (22.5 t). Annual emission of Hg from boreal forest fires can be up to 30 % of annual anthropogenic

emission in Canada [59]. Specific ratio of Hg : CO [59] is much less than registered for fires in forests of temperate zone and Africa. It allows admitting that fire emission depends on type of vegetation and hypothetical total emission volume from fires only be estimated, by extrapolating an information on a single fire.

Forest fires are an important way of mercury exchange between biosphere and atmosphere [59]. As a result of their effect, reemission of previously accumulated anthropogenic mercury occurs together with some mercury fraction, contained in soil [61]. It can be assumed that in the last case an effect of soil fires is meant.

Research on spatial-temporal distribution of the emitted mercury from forest fires in the Mediterranean region and Russian Federation is quite representative [62]. In the Mediterranean region this problem was solved by ground-based observations, and satellite technologies for mercury distribution analysis in the Russian Federation territory. Among European countries mercury emission is maximal in Italy and Portugal.

The estimation formula for mercury emission from vegetation burning looks as follows [63, 64]

$$Q_{\mathrm{Hg}} = AM\mathrm{Hg}_c E_c E_{\mathrm{Hg}},$$

where Q_{Hg} — emission mercury from forest fire, kg/year; A — burned area, ha/year; M — phytomass amount, kg/ha; Hg_c — mercury concentration in phytomass , mg/kg; E_c — efficiency of phytomass burning; E_{Hg} — efficiency of mercury discharge in the air.

Efficiency of phytomass burning E_c depends on the ecosystem, climate and hydrological conditions to a great extent. Its value varies from 0.5 to 1 depending on the density of piling, forest fuels type, air content in the layer, moisture content, as well as on the surface of burning, and reasons for firing [65, 66]. Elements E_{Hg}, E_c, Hg_c can be combined in an integrated complex, called the emission factor, which value varies from 14 to 71 mg/kg of dry phytomass [64].

Mercury can be present in the underlayer as well [64]. The process of mercury emission from soil is defined by a mercury concentration in the soil substrate, lighting intensity, and temperature [67—69]. Mercury yield from the upper soil layer during a forest fire depends mainly on temperature increase that leads to a difficult transport of mercury from low soil levels in the upper layers [70], which results in a mercury flow within range from 1 to 5 $\mathrm{mg/m^2}$ [71]. Mercury emission from phytomass was evaluated for different European countries (fig. 3.1), Asia and Africa (kg/year), and also a specific contribution of these countries (g/ha) [62].

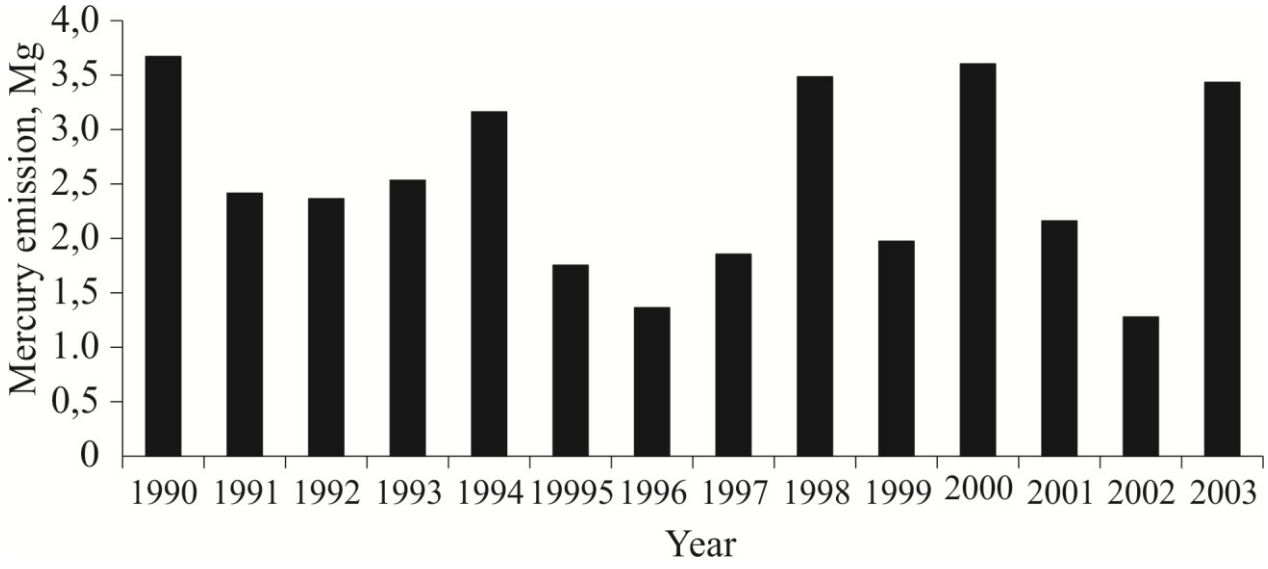

Fig. 3.1. Annual mercury emission from forest fires in countries of the EU, Norway and Switzerland during period of 1990—2003 [62]

Information on mercury emission in the Russian Federation, evaluated according to the data of ground and satellite observations, is given in Table 3.5.

Table 3.5. Emission mercury in the Russian Federation [62], Mg/year

Year	Ground observations	Satellite observations
1996	14.5	13.4
1997	6.2	3.4
1998	33.5	22.8
1999	6	14.6
2000	11.9	20.2
2001	7.7	13.3
2002		24.8

Mercury emission from forest fires in the Mediterranean and the Russian Federation has a secondary value in comparison to its emission from anthropogenic sources [62].

Recurring emission of radionuclides is of special interest during forest fires beginning in the contaminated forest-covered territories (for example, redistribution of radionuclides in the contaminated zone of Chernobyl accident [72, 73]). Contribution of radionuclides ^{90}Sr, ^{238}Pu, $^{239+240}$Pu in the radioactive contamination of the territory is found [72]. Empirical data arrays, required for development and verification of corresponding models were obtained as a result of controlled fires [74].

A large-scale contamination of soil and surface waters with ^{137}Cs is possible after forest fires. For example, in Las Alamos [75] concentration of ^{137}Cs on the soil surface is 40 times higher than the initial in ash deposit and three times higher than in the top 50 mm of soil in comparison with values prior the fire. Concentration of this polluting agent increases in the surface water flow after the fire.

When forest phytocenoses, damaged after Chernobyl AES accident, burned, radioactive products in the form of smoke, carbon black and aerosols are emitted in the air, which concentration can exceed the allowable standard many times [76]. Carryover of radionuclides from the fire zone and inclusion in atmosphere flows with transportation to vast distances facilitates their redistribution and contamination of clean zones [76]. Radionuclides, remaining in the ashes, can be spread by wind erosion in large areas and also further the secondary contamination [77] and emerging of additional radiation exposures [78]. Forest fires accelerate the process of radionuclides transition from vegetation layer in the mineral part of soils at the radioactive contaminated territories and deprive the forest of its accumulating capability that leads to losing its importance in stabilization of radioecological situation [79]. Comparison of various elements content (cesium-137 and heavy metals during forest fires in Yamal-Nenets Autonomous District [80]) in soils, lichens and cedar needles in the burned areas and beyond show a steady carryover of radiocesium, mercury and lead from the burned areas. During forest fires the losses of cesium-137 are 24 and 27 %, mercury — 16 and 16.3 %, lead — 3.6 and 11.5 % from their initial amount in the forest cenosis. Majority of heavy metals are accumulated in the burned soils.

3.2. The Earth's Atmosphere

There is a close interaction between forest and atmosphere. Phytocenosis —an elementary uniform community of plants, biocoenosis — and elementary community of all life forms. Together with environment conditions, biocenosis forms the biogeocenosis, which part is the atmosphere [81]. The main condition of all life forms existence is the interchange with the environment. Life forms adapted to the present air composition.

Atmosphere air is a mixture of gases, the main of them are nitrogen, oxygen, argon, carbon dioxide and water vapor. Description of the atmosphere gas composition up to the altitude of 100 km is given in Table 3.6 [82].

The actual atmosphere includes such impurities, as methane, carbon monoxide and other compounds and free radicals, disperse inclusions, called aerosols [83, 84].

All of the atmosphere's oxygen has a biogenic origin, coming to the atmosphere as a result of green plants photosynthesis. The planet's forests are of a great importance here.

Ozone is of great significance for the atmospheric and biospheric processes, as it protects life forms from the UV-radiation. Its content grows with the height increase. Stratospheric ozone is generated as a result of photochemical reactions, taking place under the effect of ultraviolet radiation. Major part of ozone comes in the troposphere from the stratosphere as a result of vertical air mixing. Some amount of ozone can be generated in the troposphere as well — during lightnings and photochemical smog. Ozone is the main toxic agent of photochemical smog (damages respiratory organs, conjunctiva, etc.). High concentration of ozone also harms plants (leaves, mainly).

There are several classifications of vertical structure of the atmosphere. Most common is the classification of atmosphere layers by air temperature change with increasing altitude [85]. Atmosphere is divided into five major layers — troposphere, stratosphere, mesosphere, thermosphere and exosphere. There are transition layers of

a short vertical height between major ones — tropopause, stratopause, mesopause and thermopause. Troposphere is the lowest atmosphere layer, which differs in temperature decrease with the altitude increase with the average gradient of 0.65 °C for every 100 m of altitude. About 80 % of atmosphere mass and almost all of water vapor are concentrated in the troposphere. Here processes of air mixing, thermal and moisture circulation take place, as well as interaction with the earth surface [85]. According to the nature of interaction with Earth's surface, boundary layer (up to the altitude of 1—1.5 km) and free atmosphere are specified. Friction force of earth surface influences the air movement in the boundary layer. The bottom part of the boundary layer up to 50 — 100 m is called the surface layer [85].

Table 3.6. Gas composition of atmospheric air [82]

Gas	Volume content, %	Relative molecular mass	Density in relation to dry air density
Nitrogen	78.084	28.0134	0.967
Oxygen	20.946	31.9988	1.105
Argon	0.934	39.948	1.375
Carbon dioxide	0.033	44.00995	1.529
Neon	$1.818 \cdot 10^{-3}$	20.183	0.695
Helium	$5.239 \cdot 10^{-4}$	4.0026	0.138
Krypton	$1.140 \cdot 10^{-4}$	83.800	2.868
Hydrogen	$5.0 \cdot 10^{-5}$	2.01594	0.070
Xenon	$1.818 \cdot 10^{-3}$	131.300	4.254
Ozone	10^{-5}—10^{-6}	47.9982	1.624
Dry air	100	28.9645	1.000

Atmospheric pressure varies with altitude, factoring in the temperature variation [86]:

$$p(z) = p_0 \exp\left[-\int_{z_0}^{z} \frac{g}{RT_{\text{v}}} dz \right],$$

where p — pressure, z — altitude, q — weight fraction of water vapor in the air, R — universal gas constant, T_{v} — virtual temperature.

Some particular cases are often considered in practice, when atmosphere density does not change with altitude (homogeneous atmosphere), temperature does not change with altitude (isothermal atmosphere), temperature varies according to linear law (polytrophic atmosphere).

Stable air is the air which does not move in the vertical plane. Rate of rising air cooling ~1 °C/100 m — is called dry adiabatic gradient. As it is known, the rising air, containing water vapors, widens and cools, but its relative humidity increases. If this process goes on, the relative humidity reaches 100 %, in this case we speak about air saturation. Dew point conditions arise at a certain temperature. If this air continues rising, condensation starts with a latent heat release. Its release results in slower air cooling than by dry adiabatic gradient, and continues rising. The process of latent heat release is called moist-adiabatic gradient.

3.3. Pollution of Various Media and The Maximum Permissible Concentrations

Atmospheric pollution is bringing of physical and chemical agents and substances in the atmosphere or their generation, conditioned both by natural and anthropogenic factors [87]. Forest fires are one of the main atmosphere pollution sources (Fig. 3.2)

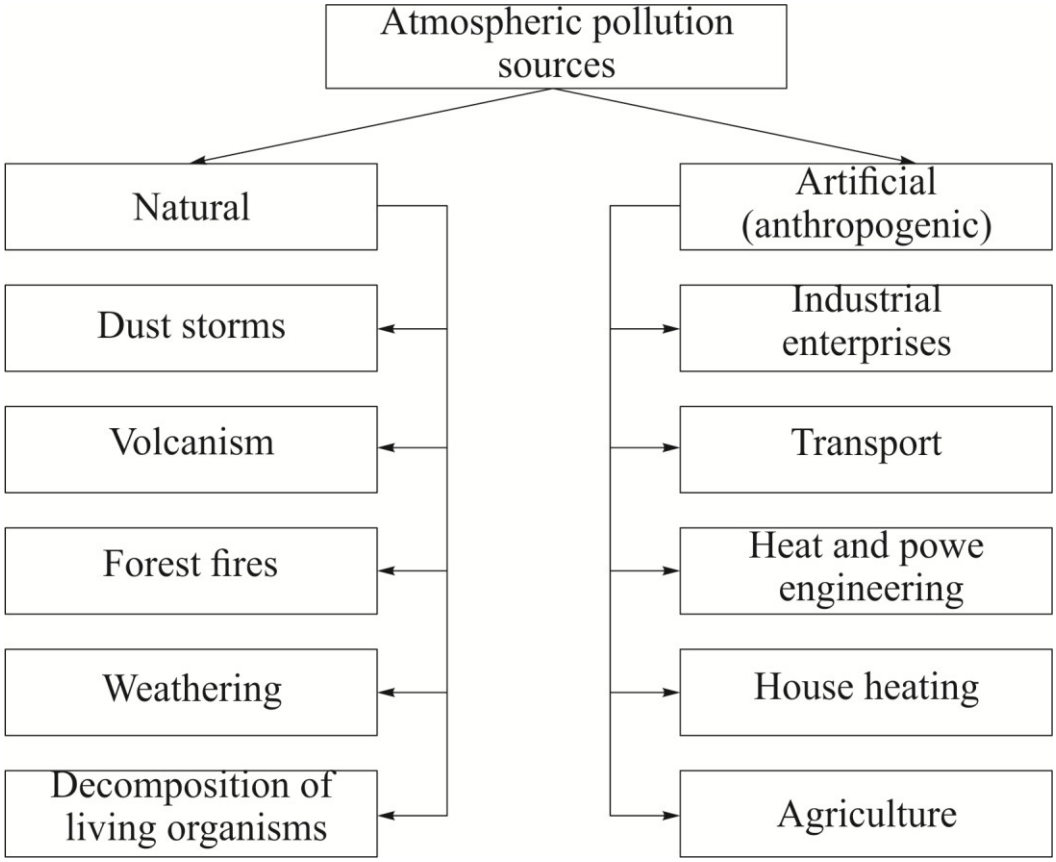

Fig. 3.2. Sources of atmospheric pollution [87]

Major environmental impacts of atmospheric pollution are greenhouse effect and acid rains [83], and ozone layer violation. Types of standards on the atmosphere air protection are given in Fig. 3.3 [87].

Content of hazardous substance in the atmosphere air of populated areas is limited by MPC values, average daily concentration of substance (MPC_{AD}) and the maximum single (MPC_{MS}) are rated [87].

A limiting (determinative) factor of harmfulness is described by direction of a substance's biological effect*: reflex (refl.) and resorptive effect (res.). Reflex effect means reaction of the upper air passages' receptors: sense of smell, irritation of mucous membranes, breath-holding and other. The stated effects appear under a short-term exposure to hazardous substances, therefore a reflex effect is the basis for the maximum single MPC_{MS} [87]. The resorptive effect means an opportunity of devel-

* Some of coloring agents (dyes), which provide neither reflex, nor resorptive effect in a low concentration, when deposited from the air, they can give an unusual color to environmental objects. For example, snow; thus, causing a sense of danger or sanitation and hygienic discomfort with humans. Due to this fact, a sanitation and hygienic factor is set as the limiting factor for dying agents, which allows avoiding an unusual color of objects when MPC is complied with [88].

opment of general toxic, gonadotoxic, embriotoxic, mutagenic, cancerogenic and other effects, arising of which does not only depend on substance concentration in the air, but also the period of inhalation. For the prevention of resorptive effect development, an average daily MPC_{AD} is established. An extract from hygienic standards GN 2.1.6.695-98B is given in Table 3.7.

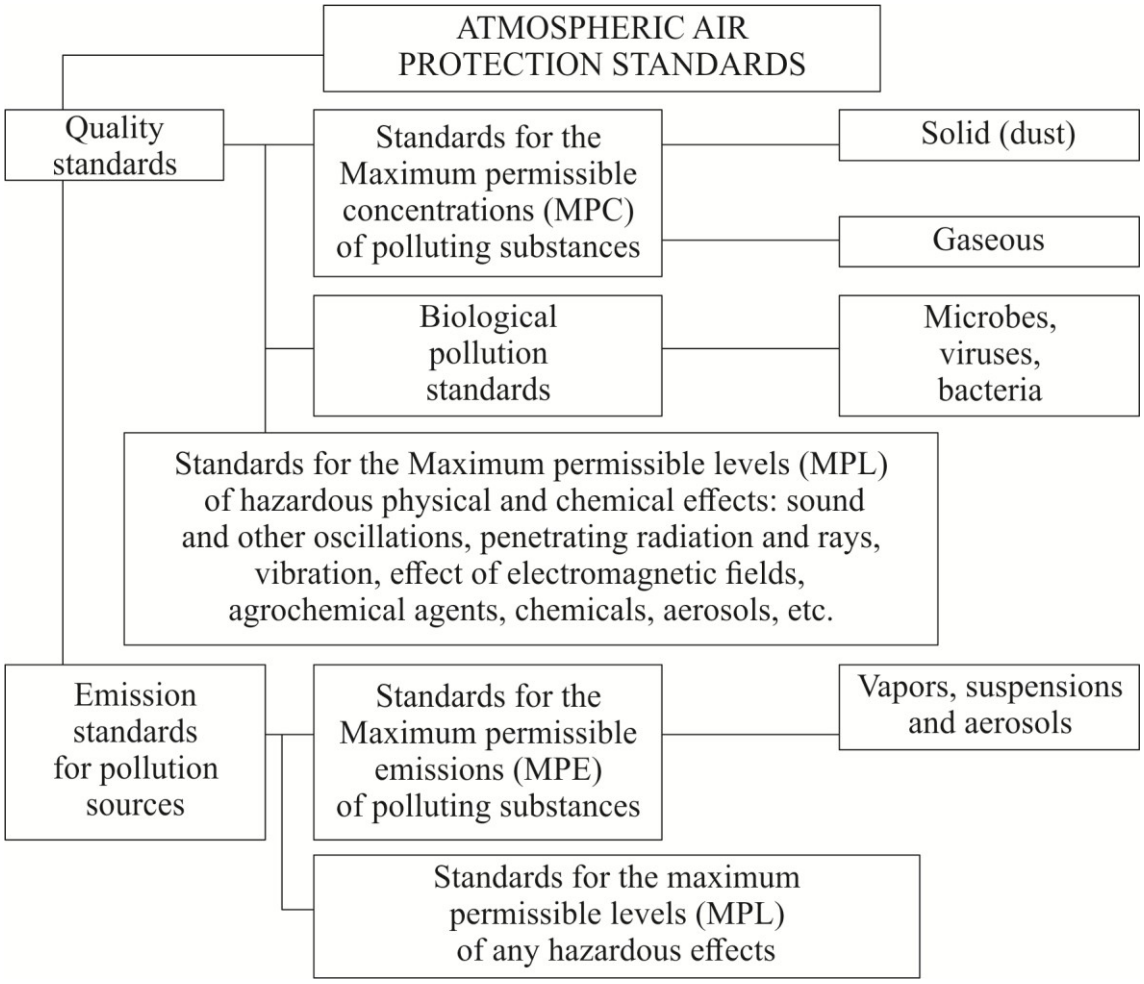

Fig. 3.3. Standards of atmospheric air protection [87]

Table 3.7. Maximum permissible concentration (MPC) of polluting substances (mg/m^3) in the atmospheric air of populated areas [88]

Substance	MPC_{MS}	MPC_{AD}	Limiting factor	Hazard class
Nitrogen oxide (II)	0.4	0.06	Refl.	3
Ammonia	0.2	0.04	Refl.-res.	4
Benzene	0.3	0.1	Res.	2
Formaldehyde	0.035	0.003	Refl.-res.	2
Acetic acid	0.2	0.06	Refl.-res.	3

When several substances, co-present in the air, possess the effect of summation; sum of their concentrations shall not exceed 1 (one unit) when calculated by the formula [88]

$$\frac{C_1}{\text{MPC}_1} + \frac{C_2}{\text{MPC}_2} + \ldots + \frac{C_n}{\text{MPC}_n} \le 1,$$

where C_1, C_2, …, C_n — are actual concentrations of substances in the air; MPC_1, MPC_2, …, MPC_n — are the maximum permissible concentrations of the same substances. For example, ammonia and formaldehyde, as well as nitrogen dioxide and formaldehyde have the summation of effect.

Water pollution shows in changing of physical and organic properties, increasing of different impurities content, including heavy metals, appearance of radioactive elements, pathogenic bacteria, and reduction of water-dissolved oxygen [87].

Standardization of water quality is done according to hygienic standard GN 2.1.5.1315-03 [89]. For a water medium the MPC of polluting substances means such concentration of these substances in water, above which it becomes inapplicable for one or several types of water use [87]. MPC for polluting substances are established separately for potable waters (Table 3.8) and fishery water basins.

Table 3.8. Maximum permissible concentration of hazardous substances in potable waters, mg/l [88]

Substance	MPC	Hazard class
Ammonia	1.5	4
Benzene	0.01	1
1,3- Butadiene	0.05	4
1-Butene	0.2	3
Formaldehyde	0.05	2

Soil is a natural formation, consisting of genetically related levels, formed as a result of lithosphere surface layers transformation under the impact of water, air and life forms [90]. For the plants to survive, soil as a habitat, shall satisfy their need in mineral elements, water and oxygen [87]. Pollutants are brought into the soil with atmospheric precipitation, deposit in a kind of dust and aerosols, get saturated directly by gaseous compounds, and get with plant litter. A possibility of soil pollution with heavy metals and radioactive substances should be mentioned, as well as recontamination and pollutants re-distrubution due to natural fires.

Standardization of soil chemical contamination is done using the maximum permissible concentrations MPC_S [91]. Values of MPC_S differ significantly for such water and air, as polluting substances from soil get into the human body in exceptional cases, mainly indirectly — through air, water and plants [87].

MPC_S — is a chemical substance concentration in a tilth-top soil (kg), which shall not cause direct or indirect impact on the media, in contact with soil, and human health, as well as on self-purification capacity of soil. MPC for soil are given in Table 3.9.

Table 3.9. Maximum permissible concentration of hazardous substances in soil (mg/kg) [91]

Substance	$MPC_П$
Acetaldehyde	10
Benzapyrene	0.02
Mercury	2.1
Styrene	0.1
Formaldehyde	7

3.4. Impurity Transfer and Transformation in The Atmosphere

Development of prediction methods for air pollution is based on the results of theoretical and experimental investigation of laws of impurities distribution from their sources. Two main areas can be specified: theory development of atmospheric diffusion and empirical and statistical analysis of pollutants distribution in the atmosphere. However, difficulty in obtaining a prompt information about emissions, as well as information on vertical distribution of meteorological values complicates improvement of forecast schemes. Limitation of statistical schemes is related mainly to insufficient degree of used models physicity. Application of the developed atmospheric models is possible for obtaining meteorological parameters.

Processes of migration, transfer and distribution of substances with account for physical and chemical interactions with the environment can be only simulated by a more detailed elaboration. However, it brings some technical problems. Paralleling of computing operations and differentiated development of particular implemented models of different sophistication levels, depending on the specific conditions, can be used as one of the solutions. Majority of the used models of air medium dynamics and impurities distribution includes Navier–Stokes equations and convection-diffusion equation, and also boundary and initial conditions. A special interest for air pollution prediction presents a definition of expected concentrations near the earth surface.

For example, physical and mathematical models are known of convection column formation and impurity rising, as a result of rocket propulsion operation, impurity distribution under windless conditions [86]:

$$\frac{\partial \rho}{\partial t}+\frac{\partial \rho u}{\partial z}+\frac{1}{r}\frac{\partial \rho uvr}{\partial r}=0,$$

$$\frac{\partial \rho u}{\partial t}+\frac{\partial \rho u^2}{\partial z}+\frac{1}{r}\frac{\partial \rho uvr}{\partial r}=-\frac{\partial (p-p_{\text{stat}})}{\partial z}+\frac{\partial}{\partial z}\left[\mu_{\text{e}}\left(2\frac{\partial u}{\partial z}-\frac{2}{3}\left(\frac{\partial u}{\partial z}+\frac{1}{r}\frac{\partial vr}{\partial r}\right)\right)\right]+$$
$$+\frac{1}{r}\frac{\partial}{\partial r}\left[\mu_{\text{e}} r\left(\frac{\partial u}{\partial r}+\frac{\partial v}{\partial z}\right)\right]+(\rho_{\text{env}}-\rho)g,$$

$$\frac{\partial \rho v}{\partial t}+\frac{\partial \rho uv}{\partial z}+\frac{1}{r}\frac{\partial \rho uv^2 r}{\partial r}=-\frac{\partial p}{\partial z}+\frac{\partial}{\partial z}\left[\mu_{\text{e}}\left(\frac{\partial v}{\partial z}+\frac{\partial u}{\partial r}\right)\right]+$$
$$+\frac{1}{r}\frac{\partial}{\partial r}\left[\mu_{\text{e}} r\left(2\frac{\partial v}{\partial r}-\frac{2}{3}\left(\frac{\partial u}{\partial z}+\frac{1}{r}\frac{\partial vr}{\partial r}\right)\right)\right]-\mu_{\text{e}}\frac{v}{r^2}.$$

Here r and z — axial and radial coordinates; ρ — density; ρ_{env} — air density in the в atmosphere undisturbed by impurity emission; $\mu_{\text{e}} = \mu_0 + \mu_{\text{t}}$ — viscosity effective value, equal to the sum of molecular and turbulent viscosity; u, v, w — axial, radial and tangential velocities; p — dynamic pressure.

Turbulence features are defined on the basis of two-parameter model, using the balance equations for turbulent kinetic energy *k* and its dissipation velocity ε, subject to buoyant force effect and the smallness of Re numbers [86]. Convection, as well as heat and mass exchange processes are described by equations of thermal conductivity and impurity diffusion.

Wind weakening in the surface layer is observed before windless weather more frequently in areas of continental climate during anticyclonic weather periods. This is especially characteristic of the Siberian regions [92], in which the vertical length of calm layers can reach several hundred meters. Impurity distribution under windless conditions is described by absence of convective transport. Here diffusion transfer, depending on the turbulent diffusion factor, is the determinant [86].

In conditions of weak atmospheric turbulence, overheated gases, generated during impurity emission, form a pilot flame. Leading edge of the flame has a dome-shape and is similar to thermals, which formed as a result of instant buoyant effect. The base of pilot flame is similar to the initial area of fixed spray (Fig. 3.4, *a*—*e*).

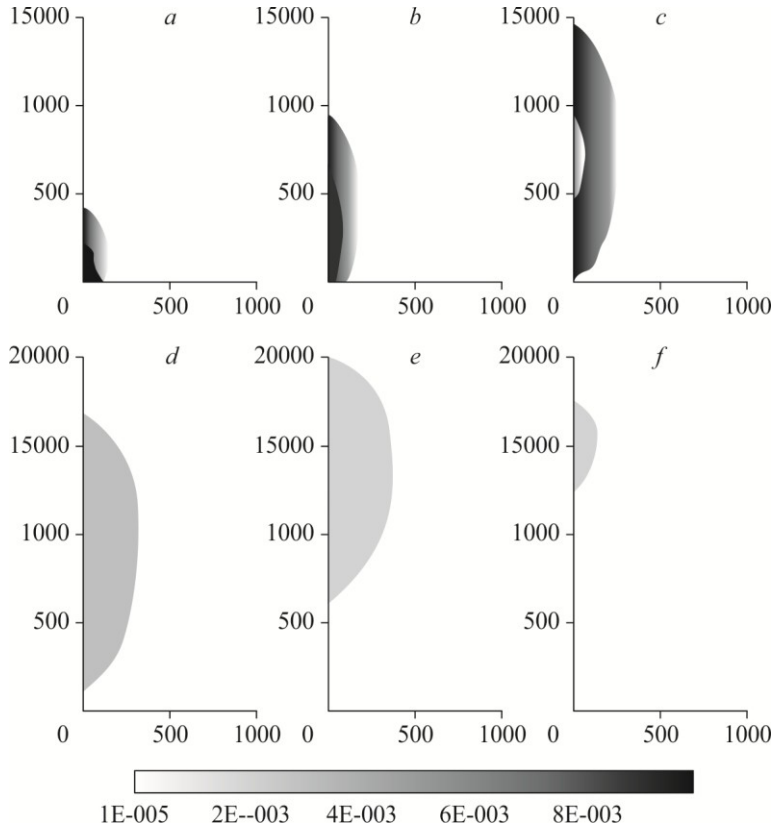

Fig. 3.4. Concentration variation in the initial flare [86], c: 30 (*a*), 60 (*b*), 120 (*c*), 180 (*d*), 420 (*e*), 600 (*f*)

Upon cease of source effect, the base degradation of pilot flame occurs. In this case, impurity emission can be classified as thermal (See Fig. 3.4). The generated thermal rises in the atmosphere, involving the surrounding air in the movement. Here the thermal mass increases in several times due to involvement process and impurities concentration falls. Buoyant force is the determinant at the initial stage of current, accelerating the rise of leading edge of the column.

A typical feature of a 24-hour temperature variation is its fall with the altitude increase during daytime. As a result of nocturnal cooling of underlying surface, a ground inversion layer is formed where temperature grows with the altitude increase. Above the inversion layer, temperature decreases with altitude. Analysis of altitude influence of the inversion layer's lower boundary shows that when altitude decreases, an impurity keeps closer to the ground surface what results in a sharp increase of pollution rate [86].

The main objectives of air quality forecast are identification of peculiarities of pollutants distribution over the controlled territory in various weather conditions and studying of a separate source contribution to a total balance of air medium pollution, especially in populated areas.

Different types of pollutants sources can be specified for forest fires. Point source is a particular source of a forest fire. Line source is a fire front, extended along one of the coordinates. In case of mass forest fires, which are described by multiple sources in the controlled forest-covered territory, area source of pollutants can be considered. It is rational to pool separate emissions and move to values, averaged for the area [93].

Products of forest fuels and flammable vegetation burning, which pollute the atmospheric air, can be divided into two categories. The first one includes those emitted directly from the fire source, the second — those generated from first category substances as a result of chemical reactions, including with air components. Gases and aerosols of the first and second category have a recognized name of primary and secondary pollutants, accordingly. Some of pollutants can be referred to both categories [94].

Pollution level is described statistically as monthly and annual average concentrations of hazardous impurities, the maximum single concentrations, number of cases when concentrations exceeded MPC in 10 times and over [94]. Degree of total atmospheric pollution by a range of substances is estimated, using a complex factor — an Air Pollution Index (API) [95]. A complex index of air pollution is calculated by the following formula:

$$I(m) = \sum_{i=1}^{m} I_i = \sum_{i=1}^{m} \frac{c_i k_i}{MPC_i}$$

where c_i — average annual concentration of the i-th substance ($i = 1, 2, \ldots, m$); MPC_i — its daily average MPC; k_i — dimensionless factor, which allows bringing a pollution degree by the i-th substance to an air pollution degree by sulfur dioxide. Values of k_i are equal to 0.85, 1.0, 1.3 and 1.5 for substances of 4, 3, 2 and 1 hazard class, accordingly.

Air pollution index shows an actual level of air pollution (in MPC units of sulfur dioxide), i. e. in how many times a total air pollution level exceeds the permissible value for the studied pool of impurities in general. Pollution level is assumed low if API is lower than 5, increased - at API от 5 to 6, high - at API from 7 to 13 and extremely high - at API, equal to or over 14.

Meteorological conditions influence the impurity distribution in the air [94]. Wind field determines an impurity distribution across the surface layer. Direction of impurity distribution will depend on wind direction, and impurity plume width – on wind

variability. Vertical impurity distribution is determined by atmosphere turbulence level and vertical distribution of air temperature. The most unfavorable conditions for impurity accumulation in the air are observed under weak wind conditions.

Air quality monitoring is usually done, using instruments at the stations, which register meteorological parameters and take air samples. Sometimes such stations pool in networks of the regional or national scale (Canada, Denmark and other). By means of fast channels the data is collected and processed in a centralized manner. Thus, information-measuring systems for air quality monitoring and forecast are established (access to the data is often possible via Internet). Shortcomings of such systems are a small coverage zone and large distance between monitoring stations. Computing and information systems, based on mathematical models of impurity transport, are more advanced [96, 97]. A higher accuracy of evaluation and air quality forecast is conditioned by solving the three-dimensional non-stationary transport equations of advection-diffusion. Here information on pollutants emission sources and meteorological parameters distribution with inclusion of atmospheric boundary layer models is used. Data from the stations are used for assigning the initial and boundary conditions. Computing systems of parallel architecture are usually applied.

Models of atmospheric boundary layer, which allow forecasting the meteorological parameters, are divided into macro- (global) [98], meso- (regional) [99, 100] and microscale (for example, consideration for urban building system) [101, 102]. This division is conventional to some degree.

As a rule, a core of mesoscale models is a complete non-hydrostatic Navier-Stokes equation [103, 104]. Differential turbulence models are used for turbulent closure [99, 105]. Computational grid is adjusted for orography inhomogeneity [106]. Direct numerical modeling is also used for turbulence simulation [107], which assumes that a particular implementation of a turbulent velocity field satisfies the non-stationary equations of hydrodynamics. A single calculation allows only obtaining of one implementation from the statistical assembly [107, 108]. In order to get a stable statistical average value, it is required to do over 100 of independent computations of target values. Considerable computing resources, especially for big Re numbers (for example, about 10^{14} of volume knots of difference grid is needed for Re of the 10^6 order) are required for every independent computation. Complexity of initial conditions selection is typical for this method [108]. Existence of computational errors limits researchers to quite unrealistic initial conditions for turbulence. Besides, the method requires economical numerical algorithms and has strict limitations on the steps for time and space [108]. This method is applicable mainly for homogenous turbulence modeling with moderate Re numbers, and possibility of its application to actual inhomogeneous turbulent flows is doubtful [107, 108].

One more approach in turbulence simulation was named the Large Eddy Simulation [109]. It allows modeling the subgrid. The simplest parameterization assumes application of turbulent viscosity for unresolved turbulent movements of subgrid scale. Mathematical division of major and minor eddies is done, using a space weighted operation of averaging of hydrodynamic equations [94]. As a result, a field of large-scale turbulent disturbances (eddies) is specified.

LES-simulation of penetrating convection processes, as well as cloud and precipitation formation allows describing of large-scale eddies (over 100 m), which are re-

produced on the basis of non-hydrostatic equations of thermohydrodynamics, and the smaller ones are parameterized [110].

Two approaches can be specified in the area of impurity transport mathematical simulation: the continual, or Eulerian, when total volume is considered; and Lagrangian, when impurity behavior is estimated by trajectory of tracer particles movement. So-called models of the Gaussian type, which allow computing impurity distribution from continuous point source slightly raised above the surface, are used in many applications [111]. Gaussian model has the following limitations [94]:

1) It is applicable to flat and open surface, as it is difficult to consider the effects from obstacles in it;

2) Weather and surface conditions are constant along the entire distance that a gas cloud passes;

3) It is only applicable for gases with density, close to air density;

4) Wind of speed over 1m/sec is obligatory.

An extremely important applied meaning has an Eulerian prediction model of impurity transport. Using the Reynolds approach, original equations are formulated, which describe impurity distribution in the air and its concentration changing in time. Using the known averaging methods, we can move from diffusion equations of instantaneous concentration values to equations of mean value [94].

Within the framework of Lagrangian stochastic dispersion model, pollutants distribution in the limited area, which includes an emission source, is evaluated by paths of numerous tracer particles, moving in the air under influence of wind and turbulent fluctuations. When a particle reaches the upper or lower boundary of computational domain, its ideal reflection is assumed. If a particle crosses a lateral boundary of solution region, then further computation of the path stops [94]. A particular effectiveness of Lagrangian models shows during simulation of pollutants distribution near a point source [112] and estimation of gaseous and dispersed impurity transfer with a wide range of sizes. When moved away from the source, simulation requires more computational resources [94]. Hybrid method of impurity transfer simulation suggests simulating an impurity by Lagrangian approach near the point source, and, starting from some distance, Eulerian model is to be applied [113].

Global model of chemical transport, called MOZART (Model for OZone And Related chemical Tracers) is used for studying of biomass fires impact on troposphere ozone distribution and its forerunners in Indonesia [114]. This is three-dimensional model of chemical transport for the global troposphere [115]. In the first generation models of MOZART temporal distribution of 56 chemical components was computed in a global scale from surface to mid-stratosphere. The model accounts for emission from the surface of such compounds as N_2O, CH_4, CO, NO_x, NMHCs, CH_2O and acetone, advective transfer (a semi-Lagrangian transport scheme is used), convective transport, diffusive exchange in the boundary layer (based on Holtslag and Boville parameterization), chemical and photochemical reactions, wet deposition of 11 soluble compound and dry deposition near the surface. Chemical scheme includes 140 chemical and photochemical reactions and studies photochemical oxidation schemes of methane (CH_4), ethane (C_2H_6), propane (C_3H_8), ethylene (C_2H_4), propylene (C_3H_6), isoprene (C_5H_8), terpenes (such as α-pinene, $C_{10}H_{16}$) and n- butane (C_4H_{10}) as a substitute of heavy hydrocarbons.

Natural fires in boreal forests may initiate so-called pyro-convection, which transports pollutants to the upper troposphere and lower part of stratosphere [116]. Three-dimensional model of substances blowing, emitted from forest fires, in the lower stratosphere by pyro-convection [116], is based on the Active Tracer High resolution Atmospheric Model (ATHAM) [117, 118]. The approach is used for plume simulation both from volcanoes and forest fires. The main objective is high energy plume simulation with large gradients of velocities and temperature. Concept of such approach is solving of a complete system of Navier-Stokes equations. The model works in 2*D* axisymmetric, 2*D* and 3*D* Cartesian (rectangular) geometry and includes a complex of dynamics, turbulence, microphysics of clouds, aggregation of ashes and cinder modules, as well as gas, chemistry, radiation, soil modules. A comparative analysis of numerical results with the data, obtained from observation Chisholm fire in Alberta (Canada, 2001), is conducted.

Since 1980, the study of atmosphere ozone and acidic deposition [119] was done, using complete 3D-models, such as Acid Deposition and Oxidant Model (ADOM), and Regional Acid Deposition Model (RADM). These models include chemical modules, which allow for a large number of chemical substances and reactions, what creates serious difficulty in verifying them and considerable computational costs. It is required for efficient prediction to develop models, which conform to observation data but do not need big computational resources. A simpler model was developed on the basis of ADOM technology, and does not need considerable computer resources and uses a chemical scheme by G.Johnson. The simplified scheme can be used for prediction of ozone level and acidic deposition mapping [119].

G. Johnson has simplified a description of photochemical process of ozone generation and used a Generic Reaction Set [120].

Radionuclides get in the atmosphere as gases and aerosols with a wide range of particle sizes [121]. Some models of atmospheric pollutants transfer do not allow for influence of radionuclide particle size and aerosol transformation. Physical and chemical properties of nuclide have impact on its behavior in the atmosphere and can change during transfer process. Dynamics of the atmospheric radioactive aerosol and various processes, including generation of condensation nuclei, condensation and coagulation of radionuclides, wet and dry deposition processes of various size particles, is studied in [121]. Processes of condensation nuclei generation and condensation can be described by the corresponding kinetic equations. However, it is difficult to do for the radionuclide I-131. At a first approximation, this process can be described using the following equation [121]:

$$\frac{dc}{dt} = \left(\frac{v_{\text{dg}}}{h} + \frac{1}{\tau} \right) c + \frac{c_{\text{g}}(0)}{\tau} \exp\left(-\frac{v_{\text{dp}}}{h} t \right),$$

where c and c_{g} — concentrations of gas phase and particles; v_{dg} and v_{dp} — velocity of gas and particles deposition; h — mixing height; τ — time scale.

Aerosol transport is always accompanied by the process of particles size increasing. Coagulation process is described by Smoluchowski equation [121]

$$\frac{\partial\varphi(g)}{\partial t} = \frac{1}{2}\int_0^g \tilde{K}(g, g_1)\varphi(g-g_1)\varphi(g_1)dg_1 - \varphi(g)\int_0^\infty \tilde{K}(g, g_1)\varphi(g_1)dg_1 + I(g,t),$$

where g_1 — an integration variable (mass); $\varphi(g)$ — concentration of particles of weight within range from g to $g+dg$; $\tilde{K}(x, y)$ — a share of particles collisions with masses x and y; $I(g,t)$ — a share of new particles generation with mass g.

Dry deposition velocity depends on many features of surface, surface layer and deposited particle, including its size. Wet deposition is possible [121]. Simulation, based on the example of Cesium-137 inflow in the air as a result of hypothetical accident in the Kola Peninsula, was done. 20 different particle fractions were considered. A spectrum of particles at altitudes of 150 m (on the left) and 400 m (on the right) is given in Fig. 3.5.

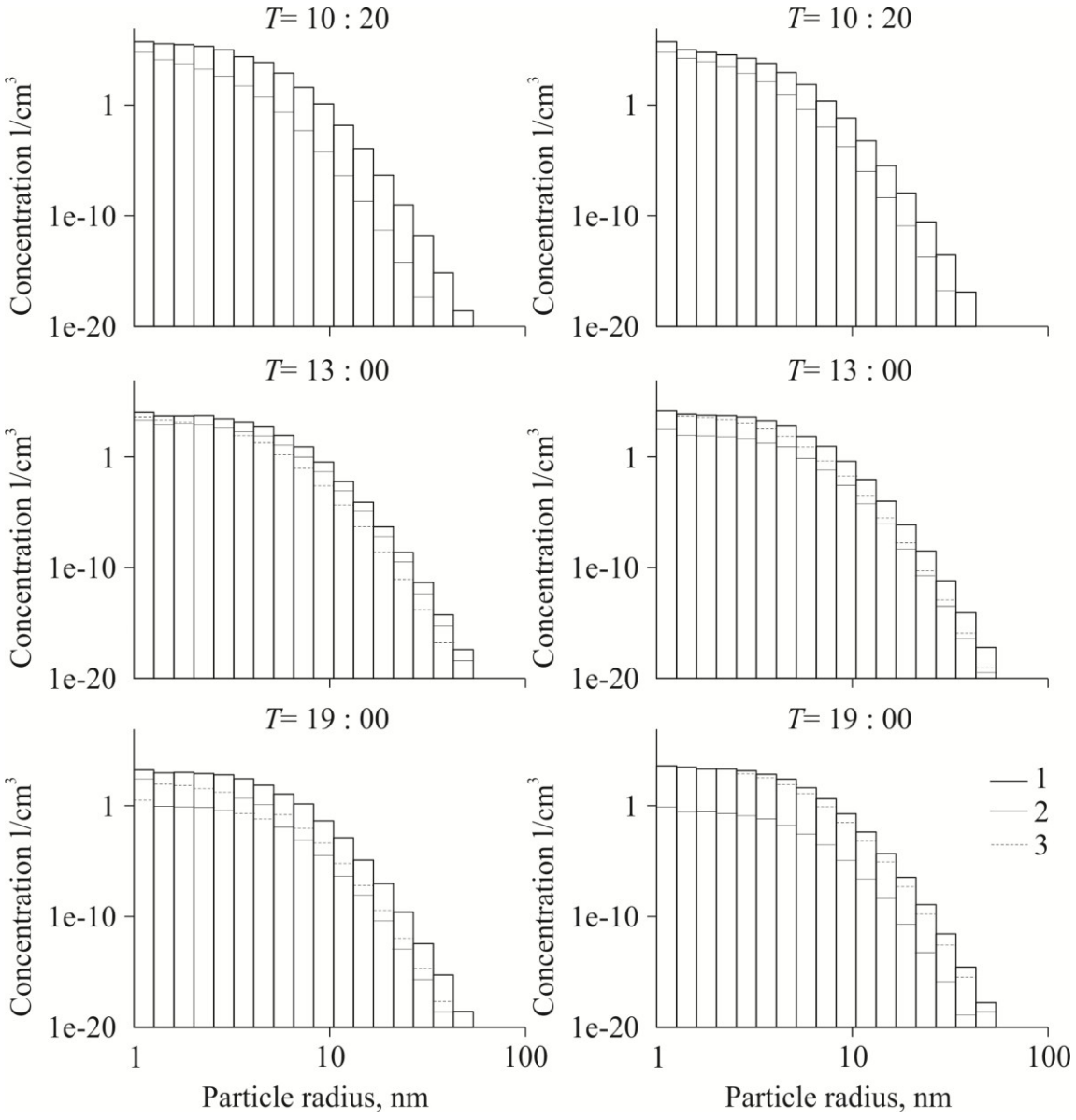

Fig. 3.5. Range of particle sizes at altitudes of 150 m (on the left) and 400 m (on the right) at time points 80, 240 and 600 minutes after egress [121]

1 — source, 2 — plume center, 3 — plume's peripheral zone.

Radioactive particles are concentrated mainly in a narrow zone near the emission source. Their size range is transformed significantly due to coagulation, especially near the source (as the coagulation process intensity is in square-law dependence on concentration) [121]. At the same time, a particle size range does not differ at altitudes of 150 and 400 m in the peripheral zone of radioactive cloud.

When emission process ceases, radioactive cloud moves slightly towards the background flow. Larger particles concentration in the “rear” (western) part of a cloud is more than in its “front” (eastern) part. Coagulation processes play a very important role in radioactive aerosol evolution only during first hours after emission [121].

Air pollution due to smoke dispersion from a forest fire plume is considered in [122]. Lidar measurements and a fluid mechanics model by Navier-Stokes, averaged according to the Reynolds method, were used for smoke dispersion process analysis. Comparison of numerical simulation and experiment results has shown that model [122] adequately describes smoke dispersion from hot plume of a forest fire, considering the wind speed and turbulence effect. Moreover, it became possible to determine a three-dimensional structure of plume and absolute value of smoke particles concentration by analyzing a lidar signal, using the Klett's inversion method. The following equation system was used:

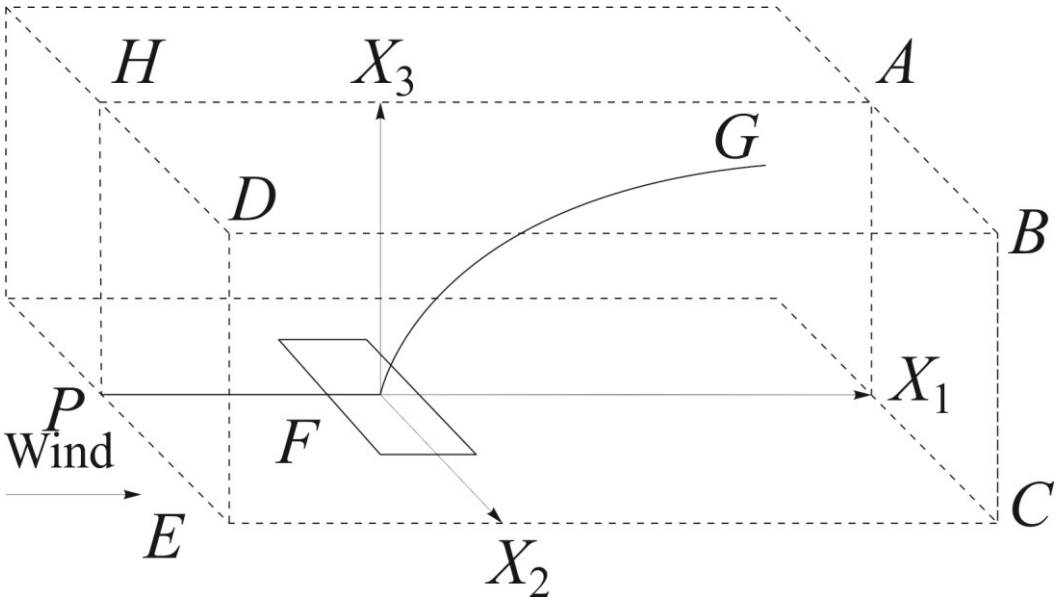

Fig. 3.6. Computational diagram [122]

$$\frac{\partial}{\partial x_j}(\rho u_j) = 0, \qquad (3.1)$$

$$\frac{\partial}{\partial x_j}(\rho u_j u_i) = \frac{\partial}{\partial x_j}\left(\mu_{\text{eff}}\frac{\partial u_i}{\partial x_j}\right) - \frac{\partial p}{\partial x_i} + S_i, \qquad (3.2)$$

$$\frac{\partial}{\partial x_j}(\rho u_j h) = \frac{\partial}{\partial x_j}\left(\frac{\mu_{\text{eff}}}{\text{Pr}}\frac{\partial h}{\partial x_j}\right), \qquad (3.3)$$

$$\frac{\partial}{\partial x_j}(\rho u_j k) = \frac{\partial}{\partial x_j}\left(\frac{\mu_{\text{eff}}}{\sigma_k}\frac{\partial k}{\partial x_j}\right) + P_t + G - \rho\varepsilon, \qquad (3.4)$$

$$\frac{\partial}{\partial x_j}(\rho u_j \varepsilon) = \frac{\partial}{\partial x_j}\left(\frac{\mu_{\text{eff}}}{\sigma_k}\frac{\partial \varepsilon}{\partial x_j}\right) + c_1\frac{\varepsilon}{k}(P_t + c_3 G) - c_2\rho\frac{\varepsilon^2}{k}, \qquad (3.5)$$

$$S_i = \frac{\partial}{\partial x_1}\left(\mu_{\text{eff}}\frac{\partial u_1}{\partial x_i}\right) + \frac{\partial}{\partial x_2}\left(\mu_{\text{eff}}\frac{\partial u_2}{\partial x_i}\right) + \frac{\partial}{\partial x_3}\left(\mu_{\text{eff}}\frac{\partial u_3}{\partial x_i}\right) - g_i(\rho - \rho_{\text{ref}}), \qquad (3.6)$$

where x_i — Cartesian coordinates; u_i — velocity vector components in the corresponding direction; g — free fall acceleration, ρ — density; μ_{eff} —viscosity; p — pressure; h — enthalpy; Pr —turbulent Prandtl number; k — kinetic energy of turbulence; ε —dissipation rate of kinetic energy. Generation of turbulence kinetic energy is described by the following equation

$$P_t = \mu_t \frac{\partial u_i}{\partial x_j}\left(\frac{\partial u_i}{\partial x_j} + \frac{\partial u_j}{\partial x_i}\right), \qquad (3.7)$$

where μ_t — turbulent viscosity.

Buoyant effect is described by the expression [122]:

$$G = g\frac{\mu_{\text{eff}}}{\text{Pr}}\frac{1}{\rho}\frac{\partial \rho}{\partial x_3}. \qquad (3.8)$$

Dependence of turbulent viscosity on other flow parameters is described by the following ratio

$$\mu_t = c_\mu \rho \frac{k^2}{\varepsilon}. \qquad (3.9)$$

The following set of constants [123]: Pr = 0.7, c_1 = 1.44, c_2 = 1.92, c_3 = 1.00, c_μ = 0.009, σ_k = 1.0, σ_ε = 1.3, was used for calculations of the equations (3.1)—(3.9) (Fig. 3.6).

Calculations area is presented by the parallelepiped $PHAx_1EDBC$. F is the fire center. FG is the central line of plume. Flow is symmetrical relative to $PHAx_1$ plane. The equation system (3.1)—(3.9) is closed up by corresponding boundary conditions.

The following conditions were used for the left boundary $PEDH$. Horizontal velocity (wind profile) is found from the equation [124]

$$u_1(x_3) = u_{\text{wind}} \left(\frac{x_3}{H} \right)^{\frac{1}{7}},$$

where u_{wind} — wind velocity at H height. Vertical and transversal velocities on this face are as follows:

$$u_2 = u_3 = 0.$$

Temperature profile:

$$T_{\text{left}} = T_{\text{air}}.$$

The left boundary

$$k_{\text{left}} \equiv k_{\text{air}} = 0.04 \frac{u_1^2}{2},$$

$$\varepsilon_{\text{left}} \equiv \varepsilon_{\text{air}} = 0.001 \ \text{m}^2/\text{s}^3.$$

Conditions of the lower boundary Px_1CE. Adiabatic conditions for temperature $\frac{\partial T}{\partial x_3} = 0$ and adhesion conditions for velocity are used outside the plume. Estimation of kinetic energy of turbulence and its dissipation rate is done, using the method suggested in [123]. Inside the plume:

$$u_3 = u_{\text{jet}}, \ u_1 = u_2 = 0, \ T = T_{\text{jet}},$$

jet — a flow.

Kinetic energy of turbulence inside the plume is determined by the expression

$$k_{\text{jet}} = 0,01 \frac{u_{\text{jet}}^2}{2}.$$

Dissipation rate is calculated by the following formula

$$\varepsilon_{\text{jet}} = \frac{k_{\text{jet}}^{3/2}}{(L_{\text{per}} / 4)},$$

where L_{per} — perimeter of rectangular area of burning.

The following boundary conditions were used on the border of $PHAx_1$ flow symmetry [122]:

$$u_2 = 0,$$

$$\frac{\partial u_1}{\partial x_2} = \frac{\partial u_3}{\partial x_2} = \frac{\partial T}{\partial x_2} = \frac{\partial k}{\partial x_2} = \frac{\partial \varepsilon}{\partial x_2} = 0.$$

Symmetrical conditions were used for the front and upper boundaries $EDBC$ and $HABD$ [122]:

$$u_2 = 0,$$

$$\frac{\partial u_1}{\partial x_2} = \frac{\partial u_3}{\partial x_2} = \frac{\partial T}{\partial x_2} = \frac{\partial k}{\partial x_2} = \frac{\partial \varepsilon}{\partial x_2} = 0,$$

$$u_3 = 0,$$

$$\frac{\partial u_1}{\partial x_3} = \frac{\partial u_2}{\partial x_3} = \frac{\partial T}{\partial x_3} = \frac{\partial k}{\partial x_3} = \frac{\partial \varepsilon}{\partial x_3} = 0.$$

Ambient pressure shall be specified on the right border x_1ABC. According to SIMPLE algorithm [125], there is no necessity to know the boundary conditions for velocity components, and for h, k and ε "soft" boundary conditions are used [122]:

$$\frac{\partial h}{\partial x_1} = \frac{\partial k}{\partial x_1} = \frac{\partial \varepsilon}{\partial x_1} = 0.$$

Chemical reactions are not considered. Acceleration is relatively low in the plume. Consequently, traditional approaches to smoke simulation can be applied. It is assumed that a hard phase (carbon black particles) is generated and transported in the same way as their temperature and velocity vary, which coincide with gas phase parameters [126]. As a result, a field of particles concentration $n(x_1, x_2, x_3)$ is similar to temperature field [122]:

$$\frac{n - n_{\text{air}}}{n_{\text{jet}} - n_{\text{air}}} = \frac{T - T_{\text{air}}}{T_{\text{jet}} - T_{\text{air}}}.$$

Experimental [126] and calculated profiles of dimensionless temperature are given in Fig. 3.7. Both qualitative and quantitative consistency of experimental and theoretical results is observed. Considering the complexity of the studied phenomenon, we can state that model [122] describes the emerging smoke flow in an adequate manner.

Contours of smoke particles concentration in the vertical cross-section along the plume symmetry axis, which are obtained, using models [122], are given in Fig. 3.8. The minimum and maximum concentrations are $5 \cdot 10^{10}$ м$^{-3}$ and $5 \cdot 10^{12}$ м$^{-3}$. Parameters of models [122]: $u_{\text{wind}} = 4$ m/s, $T_{\text{jet}} =$ $= 1170$ K, $k_{\text{air}} = 0.04u_{\text{l}}^2 / 2$ (a); $u_{\text{wind}} = 3$ m/s, $T_{\text{jet}} = 1170$ K, $k_{\text{air}} = 0.4u_{\text{l}}^2 / 2$ (*b*); $u_{\text{wind}} = 6$ m/s, $T_{\text{jet}} = 1170$ K, $k_{\text{air}} = 0.04u_{\text{l}}^2 / 2$ (*c*); $u_{\text{wind}} = 3$ m/s, $T_{\text{jet}} = 319$ K, $k_{\text{air}} = 0.04u_{\text{l}}^2 / 2$ (*d*); $u_{\text{wind}} = 3$ m/s, $T_{\text{jet}} = 1170$ K, $k_{\text{air}} = 0.02u_{\text{l}}^2 / 2$ (*e*).

Contour lines of smoke particles concentration in horizontal cross-section (altitude $x_3 = 72$, 78, 84 m for *a*—*c,* accordingly), calculated, using models [122] are given in Fig. 3.9. The minimum and maximum concentrations are $2 \cdot 10^{11}$ m^{-3} и $5 \cdot 10^{12}$ m^{-3}, accordingly. Contour lines of smoke particles concentration in sections towards the flow, obtained from models [122]: $x_1 = 104$, 302, 400 m for drawings *a*—*c,* accordingly, are given in Fig. 3.10. The minimum and maximum concentrations were $5 \cdot 10^{10}$ m^{-3} and $5 \cdot 10^{12}$ m^{-3}.

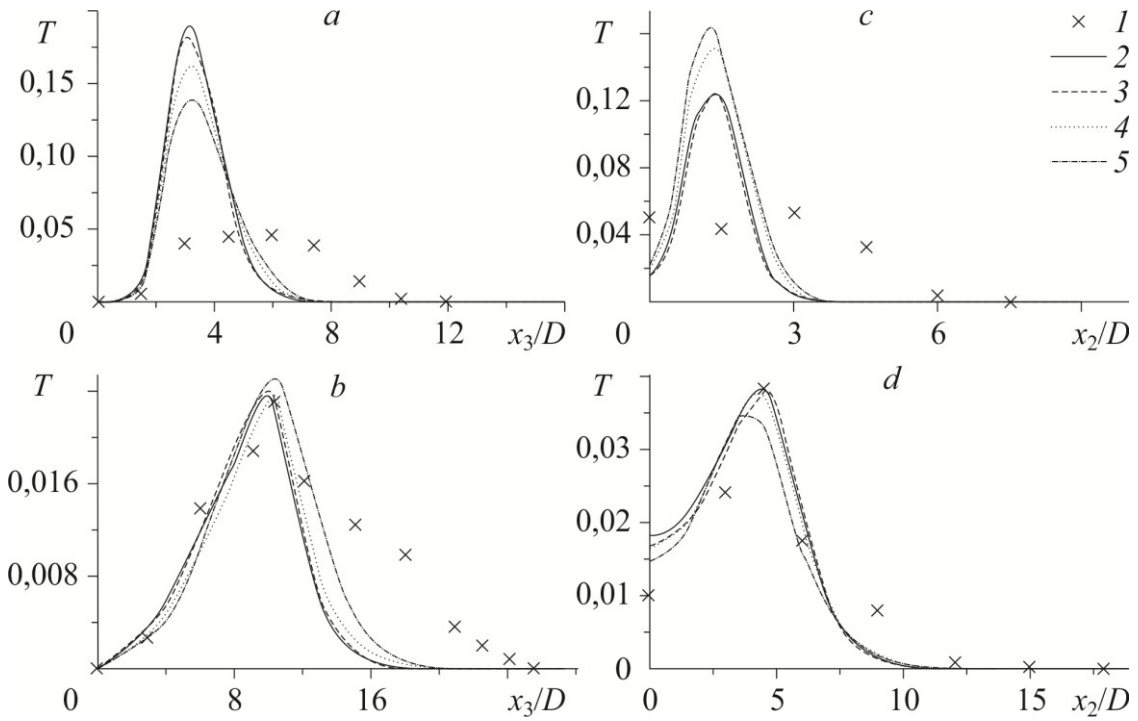

Fig. 3.7. Experimental [126] and theoretical [122] profiles of dimensionless temperature: $x_1 = 10D$, $x_2 = 0.05D$ (*a*); $x_1 = 40D$, $x_2 = 1.69D$ (*b*); $x_1 = 10D$, $x_3 = 6D$ (*c*); $x_1 = 40D$, $x_3 = 9.09D$ (*d*).

1 — experiment, *2*—*5* — grid calculations: 93 × 74 × 79 (*2*), 74 × 59 × 63 (*3*), 59 × 47 × 50 (*4*), 47 × 37 × 40 (*5*).

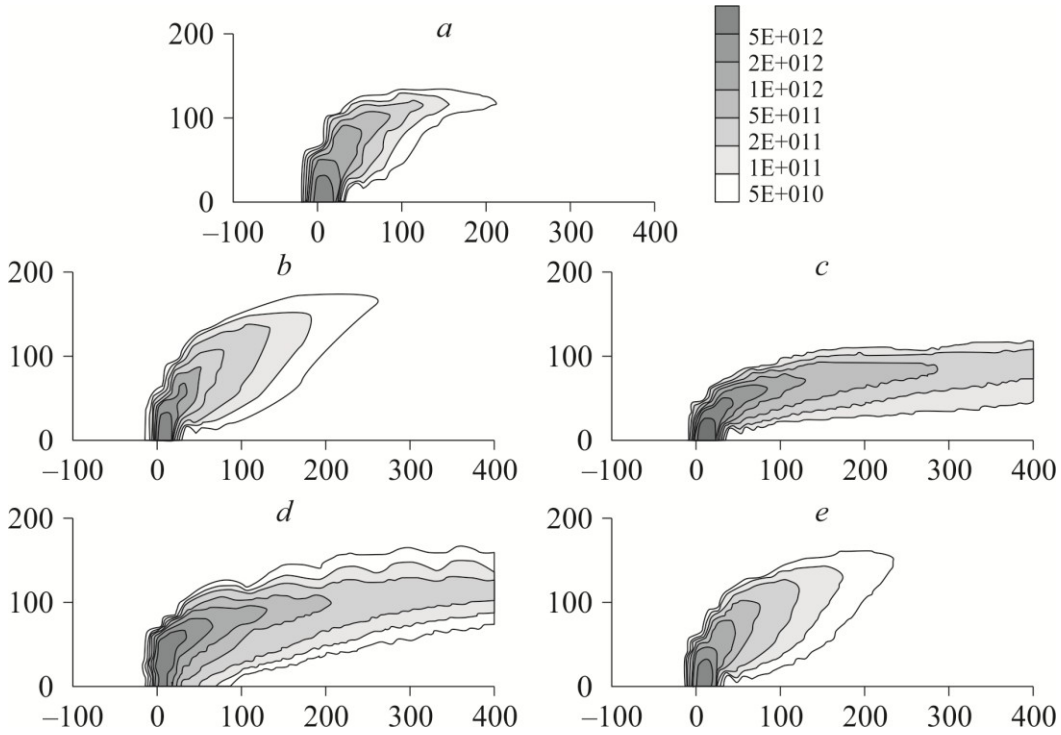

Fig. 3.8. Contours of smoke particles concentration in vertical cross-section along the plume symmetry axis, obtained using the models [122]

See explanation in the text.

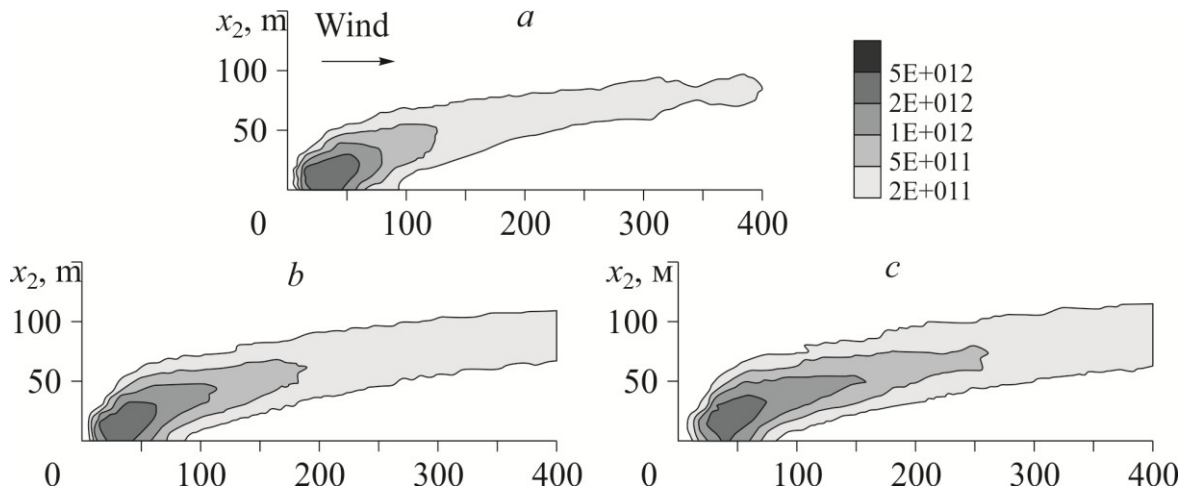

Fig. 3.9. Contours of smoke particles concentration in horizontal cross-section, computed, using the model [122]

See explanation in the text.

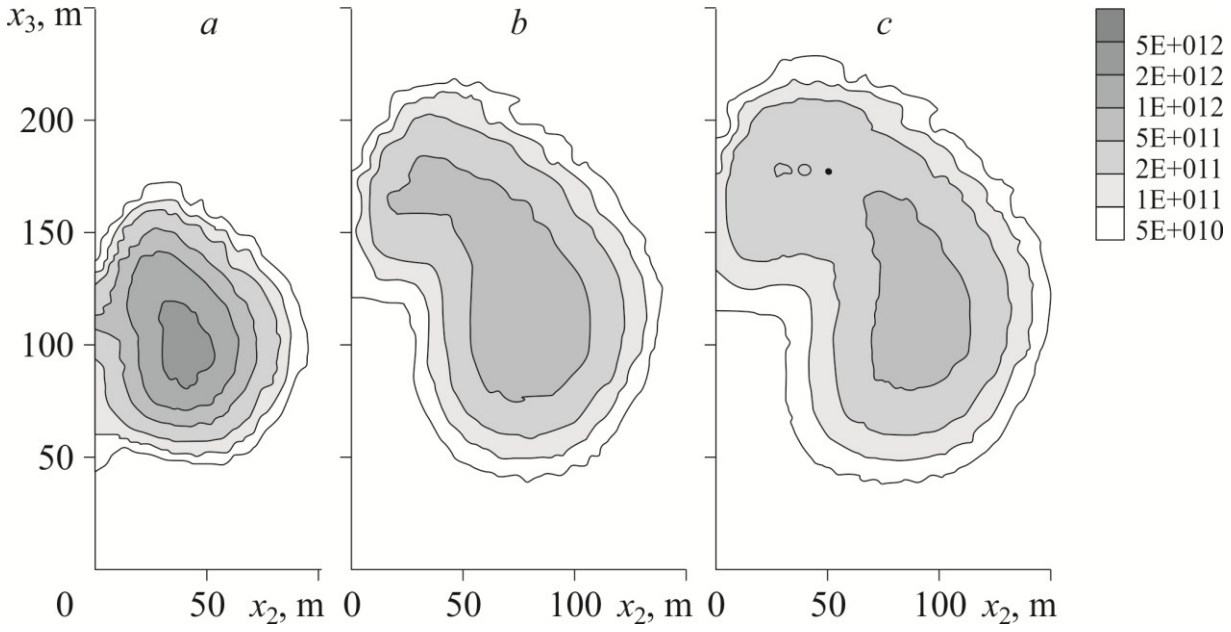

Fig. 3.10. Contours of smoke particles concentration in sections in the direction of flow, obtained using the model [122]

See explanation in the text.

For altitudes between 0 and 50 m the plume rises nearly vertically. Influence of transverse wind in this part of trajectory is insignificant, because smoke flow pulse prevails over wind force [122]. Wind force influence in the direction of wind dominates, the plume bends, and at the altitude of over 50 m its rising speed is lower. The plume has a significant asymmetry in the wind direction.

As a result, concentration gradient is much higher in the windward rather than downwind side of the plume [122]. The plume extends considerably toward the wind direction.

It was determined [122] that double decrease of k_{air} has a slight influence on the plume shift, and insignificant variation of wind parameters do not provide a sharp qualitative impact on plume behavior.

For description of lower atmosphere layers, a notion “air quality” is introduced [127]. Following cooperation of a number of Australian organization, the Australian Air Quality Forecasting System (AAQFS) was developed on the basis of high-resolution models. The model consists of five interrelated components, among them components including an information module on 53 chemical substances emission flows, the module of chemically active impurity transport (generates a forecast for 25 pollutants, including PM1, PM2.5, PM10, formaldehyde, butadiene, photo oxidants). Chemical model Generic Reaction Set [120] is used.

On January 11—12, 2001, there was a very poor visibility in Melbourne, which was conditioned by a thick smoke from natural fires at Kings Island (about 300 km southward of Melbourne) and in place called Winchelsea (100 km south-westward of Melbourne). Fire at Kings Island started on January 3, 2001, and in next 7 days approximately 2000—3000 ha of vegetation were burned in the fire. On the 10th of January the fire was taken under control, but on January, 11, a strong wind re-ignited the fire and an additional 4500-5000 ha was burned.

To study the AAQFS capabilities of forecasting in such situations, a simplified model for computation of hourly emission of PM10, carbon monoxide, butadiene, reactive organic carbon, nitrogen oxide was developed, assuming that flammable materials have a constant consumption.

AAQFS system has generated transport and distribution of smoke plume correctly and to a high quality in accordance with the satellite and monitoring stations observation data (Fig. 3.11, 3.12).

Predicted location of the plume is corresponds quite well to the observed one. Due to a cold front passage after 17-00, on January, 11, both plumes, forecasted and observed from King Island, spinned clockwise [127]. The plume covered Melbourne from the south-east at 2-00, January, 12. The eastern edge of the plume crossed the Port-Phillip Bay at 6-00, and the eastern urban agglomeration at 7-00. However, the region has been smouldered again between 10-00 and 11-00. Simulation has shown that re-pollution by PM10 is caused by rising air masses as a response to convection growth in the surface layer.

Three air quality monitoring stations in the east of Melbourne registered content of PM10 particles during plume effect [127]. Observation data proved the air pollution model patterns. Research of the impact scenarios on a smoke effective plume height have shown the dependence of the time it takes a plume to reach the Melbourne territory on a studied parameter. In conclusion, it can be stated that AAQFS system demonstrates a good qualitative agreement of simulation results with observation data.

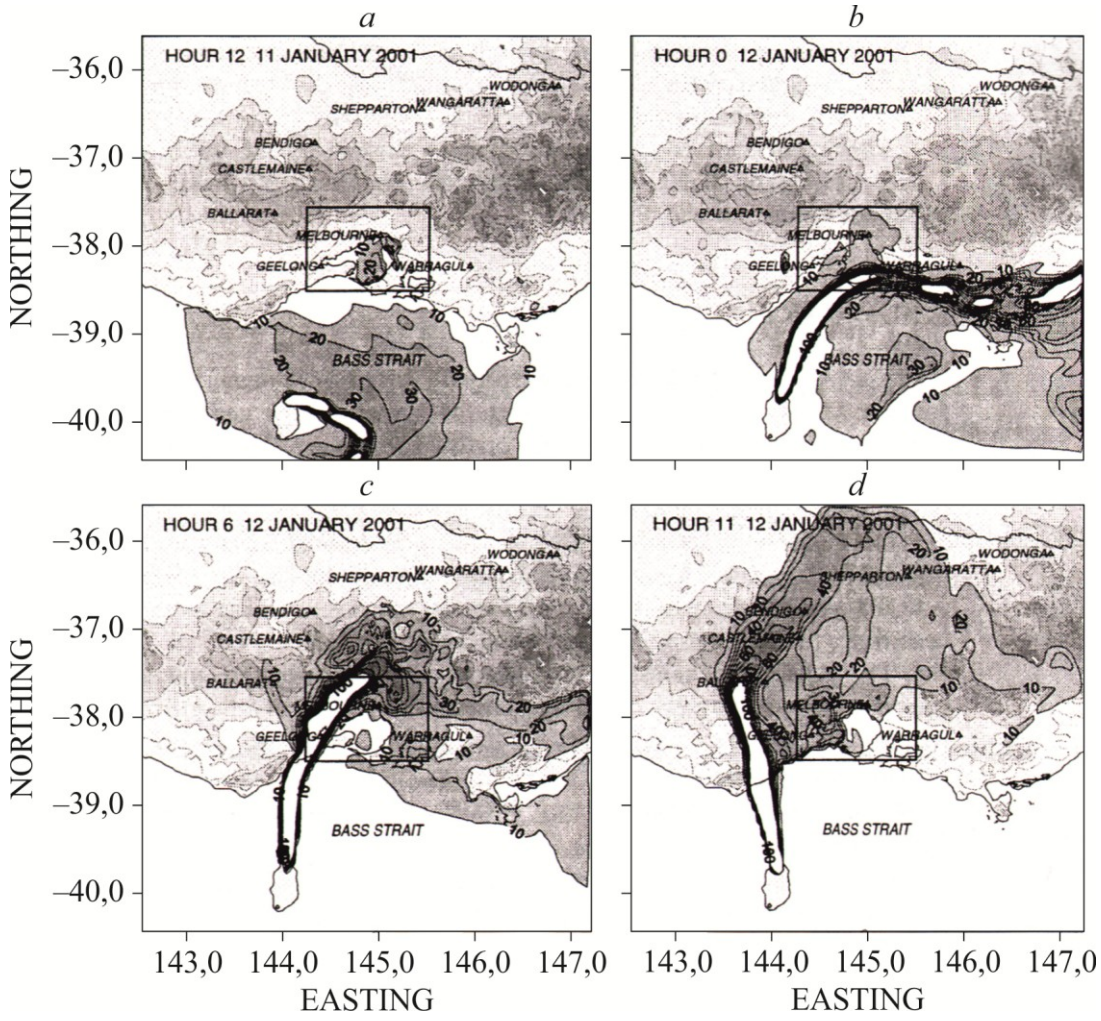

Fig. 3.11. The King Island's smoke plume (January 11—12, 2001) [127]

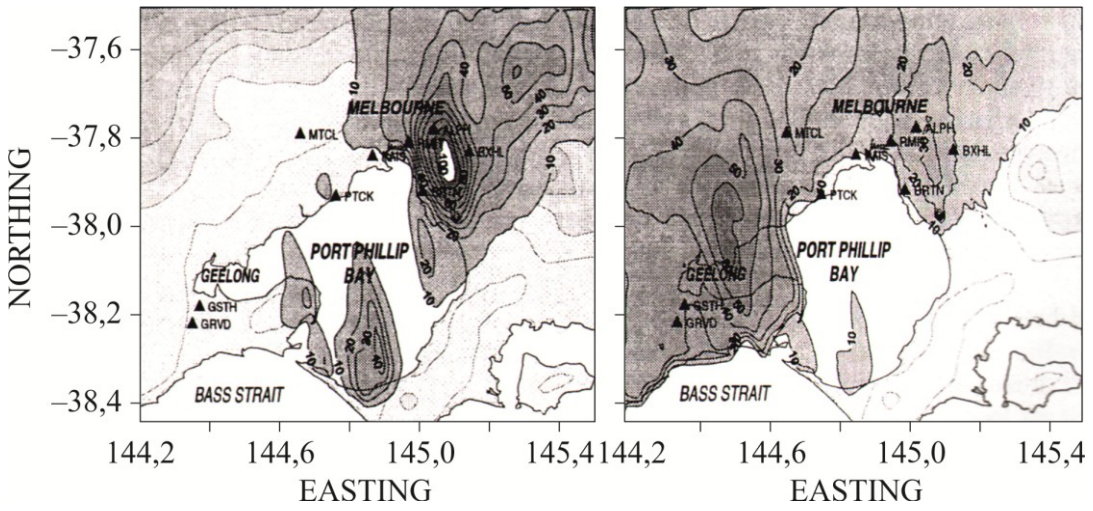

Fig. 3.12. Concentration particles of PM10, January, 12, 2001. [127]

Air pollution, generated in one country, may have impact on the other states. Estimation of transboundary air pollution in South-Eastern Europe is of interest [128]. Long-range transport of pollutants between Greece and neighboring states is considered. Simulation is conducted for every day of 1995 with spatial resolution of 50 km in the area of 1500 × 1500 km, which included Balkan Peninsula and part of Italy and Turkey. Transboundary pollution with sulfur and nitrogen oxides was studied, as they considerably contribute to increase of water and soil acidity, and photochemical smog generation [128]. Spatial distribution of pollutants correlates both with emission templates and meteorological conditions. Meteorological conditions determine the transfer distance and dry deposition of emitted substances by means of wind filed, aerodynamic resistance in the surface layer and mass exchange with free atmosphere, dependent on a vertical wind constituent.

Modeling was carried out using non-hydrostatic mesoscale MEMO models and Eulerian dispersion model TRAPPA. Different pollution scenarios were considered. MEMO is a prognostic model of local and regional scale, which allows describing air movement and dispersion of inert pollutants above a complex surface. Under the MEMO models equations, expressing laws of conservation, momentum, mass and other scalar values, such as temperature, turbulent kinetic energy and specific humidity are solved. To calculate a dispersion of inert pollutants, a specially adjusted Eulerian dispersion model, TRAPPA, was applied. A numerical method for final volumes in was used in models. Advection was processed by means of Flux Corrected Transport Adam-Bashford Scheme [129]. Vertical turbulent diffusion was solved, using a second-order Crank–Nicolson method, and a dry deposition process was described using "big-leaf" models.

General fluxes over the balance area, deposition and pollutants emission, calculated under TRAPPA models for the period from 1 January till 31 December 1995, are given in Table 3.10.

Table 3.10. General fluxes over the balance area, deposition and pollutants emission, calculated under TRAPPA models for the period from 1 January till 31 December 1995. [128], kt

Scenario		Lateral inflow	Lateral outflow	Deposition	Emission
1	SO_2	11656	11451	772	525
	NO_x	2096	2209	336	362
2	SO_2	57	306	202	409
	NO_x	55	235	106	261
3	SO_2	11599	11145	570	116
	NO_x	2041	1974	230	101

Pollutants fluxes over the balance area, calculated under TRAPPA models for the period from January till 31 December 1995, are given in Table 3.11.

Table 3.11. Pollutant fluxes over the balance area, calculated under TRAPPA models for the period from January till 31 December 1995 [128], kt

Scenario	Pollutant	North	West	South	East	Total
			Inflow			
1	SO_2	3017	3176	2030	3433	11656
	NO_x	863	608	130	495	2096
2	SO_2	24	20	1	12	57
	NO_x	26	16	1	12	55
3	SO_2	2993	3155	2029	3422	11599
	NO_x	837	591	129	484	2041
			Outflow			
1	SO_2	2475	4298	2356	2322	11451
	NO_x	477	803	497	432	2209
2	SO_2	108	115	41	42	306
	NO_x	85	83	31	36	235
3	SO_2	2367	4183	2315	2280	11145
	NO_x	392	720	465	397	1974

As a result of modeling, it was established that general outflow of pollutants from Greece territory was more than their inflow. About half of emitted pollutants have a local distribution. Modeling had also been carried out using the abovementioned models for selected days in 1995 that represent 14 various synoptic types.

In [130] photo-oxidation processes over the Eastern Mediterranean Basin were researched in summer period, using multi-scale analysis of atmosphere circulation. For evaluation of spatial and temporal scale of photochemical activity a numerical modeling (Regional Atmospheric Modeling System (RAMS), Comprehensive Air quality Model with extensions (CAMx), Mesoscale Dispersion Modeling System (MDMS))
was used in combination with experimental researches.

In [131], a mesoscale RAMS model has been used to simulate the wind flow in a real fire situation in the Spanish Mediterranean basin in July 1991. Number of forest fires has increased in this region.

RAMS is a numerical weather model [132], developed by researchers from Colorado State University. The model consolidates non-hydrostatic cloud-scale model [133] and two mesoscale weather models [134, 135]. Two-way grid nesting technology has been additionally introduced. It was done to resolve small-scale phenomena (such as wind flows) at the time when the model does a parallel large-scale computation under a larger grid. A complete system of simple dynamic equations is supplemented with optional parameterizations for turbulent diffusion, solar and terrestrial radiation, heat exchange between earth layers, vegetation bed, water surface, rain processes, kinematic effects of cumulus convection, etc.

RAMS has two initialization options for atmospheric variables [131]: HHI, or horizontally homogeneous initialization, when atmospheric fields were determined on the basis of a single atmospheric probing and were taken identical along the heights of Cartesian surfaces in all horizontal directions. In VI, or horizontal inhomogeneous initialization, horizontal gradients are allowed in the initial atmospheric fields.

The RAMS model was used for modeling of a wind field during a forest fire in Bunol. The situation was modeled for the period from 27 July 00:00 till 31 July 18:00, 1991. For VI-initialization the following data were acquired from the Europe-

an Centre for Medium-Range Weather Forecasts (ECMWF): 3D-fields, containing horizontal components of velocity, temperatures, geopotential height, and relative humidity at 00:00, 06:00, 12:00, and 18:00 for the period.

There were three nested grids applied. Grid 1 covered the Iberian Peninsula and western part of the Mediterranean Sea, Grid 2 - Valencia region, Grid 3, with the highest resolution, the region concerned. All grids were centralized in Bunol area.

32 levels were used at the following altitudes, m: 22.7, 82.9, 170.2, 296.8, 480.3, 746.5, 1132.4, 1692.0, 2503.4, 3707.6, 5198.5, 6703.9, starting from this point up to 35200 m, the height increase to the next level was 1500 m. Time interval — 60 s.

Fields, obtained from numerical modeling, agreed well with real data on the fire and weather conditions in the modeled period. It is important to mention that these results were acquired without consideration of interaction between fire and atmosphere.

General scheme of Lagrangian atmospheric modeling [136] is given in Fig. 3.13. Forecast simulation of impurity transfer and transformation can be used for risk management and assessment of forest fires impact on the environment and health of people. Chart of strategy development for mitigating the risk of air pollution [136] is given in Fig. 3.14.

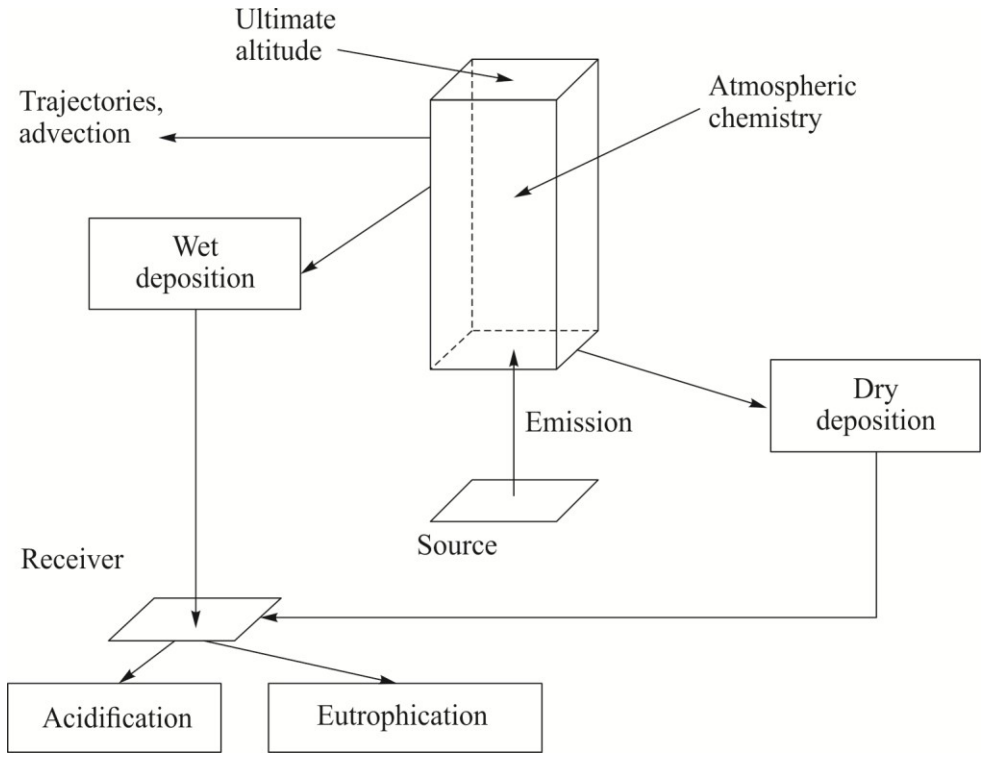

Fig. 3.13. Lagrangian atmospheric model. Source—receiver [136]

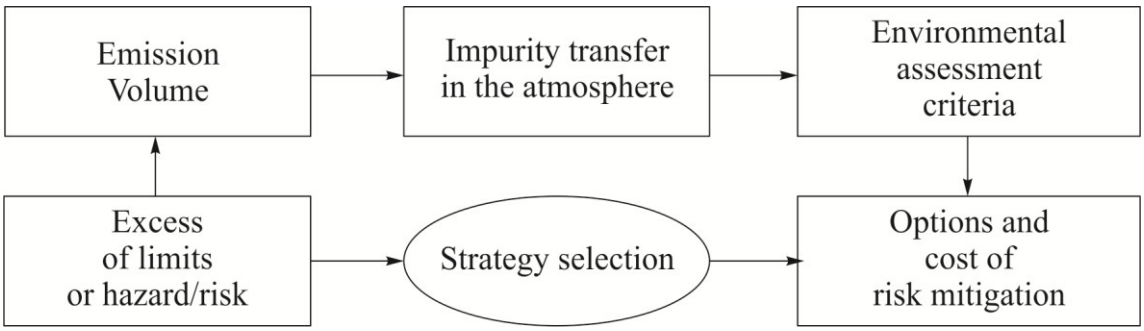

Fig. 3.14. Selection of air pollution risk mitigation strategy [136]

Estimation of ozone concentrations and its precursors within the city is possible, based on a mathematical model [137]. The Eulerian model of turbulent diffusion, which contains description of a transport equation, subject to advection, turbulent diffusion and chemical reactions, is applied for this [92]:

$$\frac{\partial C_i}{\partial t} + U\frac{\partial C_i}{\partial x} + V\frac{\partial C_i}{\partial y} + W\frac{\partial C_i}{\partial z} = -\frac{\partial}{\partial x}\langle c_i u\rangle - \frac{\partial}{\partial y}\langle c_i v\rangle - \frac{\partial}{\partial z}\langle c_i w\rangle + S_i + R_i,$$

$$i = 1, \ldots, n, \qquad (3.10)$$

where $C_i(t, x, y, z)$ — concentration of the i-th impurity component, S_i —source term, describing emission of impurity components in the air and their deposition on underlying surface. R_i describes a substance generation due to chemical reactions with impurity components involved. Averaged constituents are marked in capital letters, and lower-case — pulsating, angle brackets mean averaging in time.

A comparative analysis of three simplified kinetic schemes of air secondary pollutants generation was carried out. Selected models [138—140] are applied for identification of peculiarities of urban air pollution with ozone and its precursors, establishing of factors, influencing the pollutant generation and destruction, and for specifying the dynamics of ozone distribution above Tomsk city during 24-hour period in different seasons. Modeling and measuring results analysis allows speaking about applicability of the schemes, which main advantage is efficiency, what is of major importance for air quality forecast for the urban area.

During last decades mathematical modeling is widely used for scenario computations, which main purpose is to identify peculiarities of pollutant distribution above the concerned territory in different weather conditions [141]. Usually a scenario analysis is conducted to study a contribution of different sources in total air pollution balance or possible impact assessment from accidents in hazardous facilities [142]. Mathematical models are also included in air quality control and analysis systems, which operate in a real-time mode, use measuring data from fixed stations, and provide a fast acquiring of a detailed pollutant concentration distribution above urban areas, territory of which was not covered by observation points.

For computation of secondary pollutants concentrations, impurity transport mathematical models are used, which have integrated schemes of chemical reactions, described by chemical kinetics equations. For modeling of photochemical pollution in Tomsk and its suburbs [137] three models were used: semi-empirical schemes Azzi,

included in the Harley model [138], photochemical AIRCHEM module [430], a reduced kinetic mechanism RADM [140].

The area of research and fixed air pollution sources (marked in black) in Tomsk and its suburbs [143] are given in Fig. 3.15. During the computation 119 line, 12 area and 338 point sources were considered. It was assumed that rate of impurity inflow from cars varies during the 24-hour period, according to the dependence given in Fig. 3.16 [144].

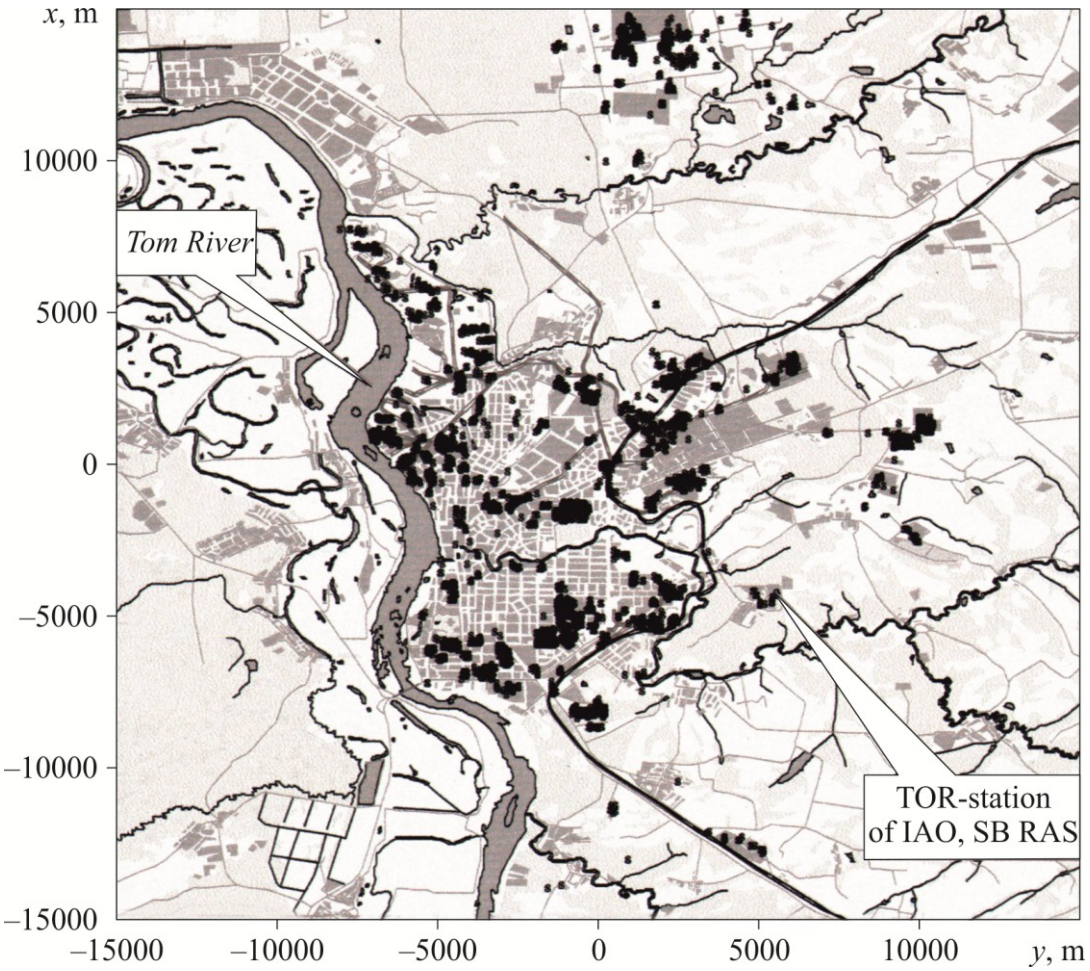

Fig. 3.15. Area of research and fixed air pollution sources (marked in black) in Tomsk and its suburbs [143]

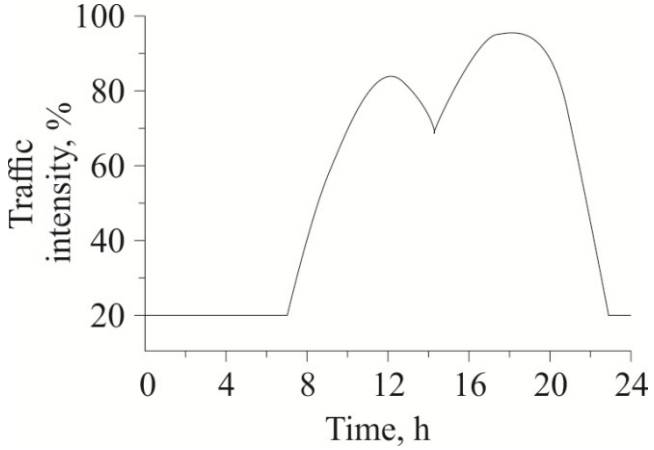

Fig. 3.16. Rate of impurity inflow from cars during 24-hour period [144]

Figure 3.17 demonstrates comparison of computed results for different models with observation data on ozone, nitrogen dioxide and oxide concentrations, total solar radiation, wind direction and velocity for conditions as of 19—20 February 2004. Negative segment of the time axis corresponds to the first 24-hours of modeling, positive — the second. Symbols show the measured values, curves— computation (solid line — a reduced RADM mechanism (See below about these mechanisms), dash-and-dot line — AIRCHEM mechanism, dashed line — GRS model). The following input background values were used for computations: O_3 — 29 mcg/m^3, NO_2 — 28 mcg/m^3, NO — 4.3 mcg/m^3, CO — 0.1 mg/m^3.

Comparison of computed results for different models with observation data on ozone, nitrogen dioxide and oxide concentrations, total solar radiation, wind direction and velocity for conditions as of 26—27 May 2004, is given in Fig. 3.18. The following input background values were used: O_3 — 49 mcg/m^3, NO_2 — 93.5 mcg/m^3, NO — 4.3 mcg/m^3, CO — 0.1 mg/m^3.

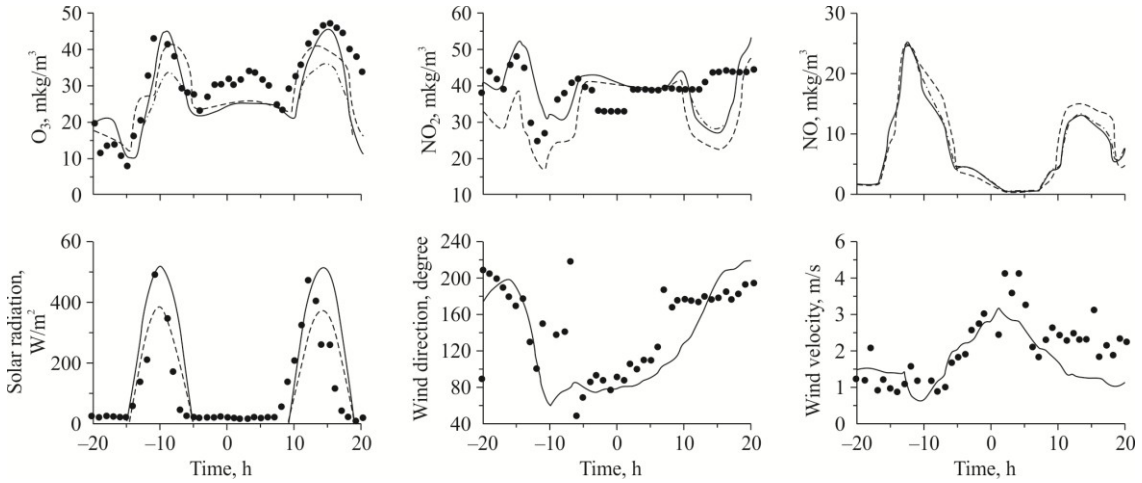

Fig. 3.17. Comparison of computed results for different models with observation data on ozone, nitrogen dioxide and oxide concentrations, total solar radiation, wind direction and velocity for conditions as of 19—20 February 2004 [143] See explanation in the text.

Main requirements, to which a modern model of urban air quality shall satisfy [94], are quite suitable for mathematical models development of переноса pollutants transfer from forest fire sources and their environmental impact assessment. The requirements are as follows:

1) To use spatial non-stationary equations for impurity components transfer;

2) To apply algebraic ratios for turbulent heat and mass flows, included in the transfer equation;

3) To account for deposition of impurity heavy fractions on surface;

4) To account for chemical and photochemical reactions, occurring in the atmosphere, by including state-of-the-art mechanisms of chemical kinetics;

5) To use non-stationary forecasting models of atmospheric boundary layer, which accounts for terrain inhomogeneity and a complex underlying surface nature;

6) To use a high spatial resolution;

7) To use effective numerical methods and capabilities of parallel computational systems.

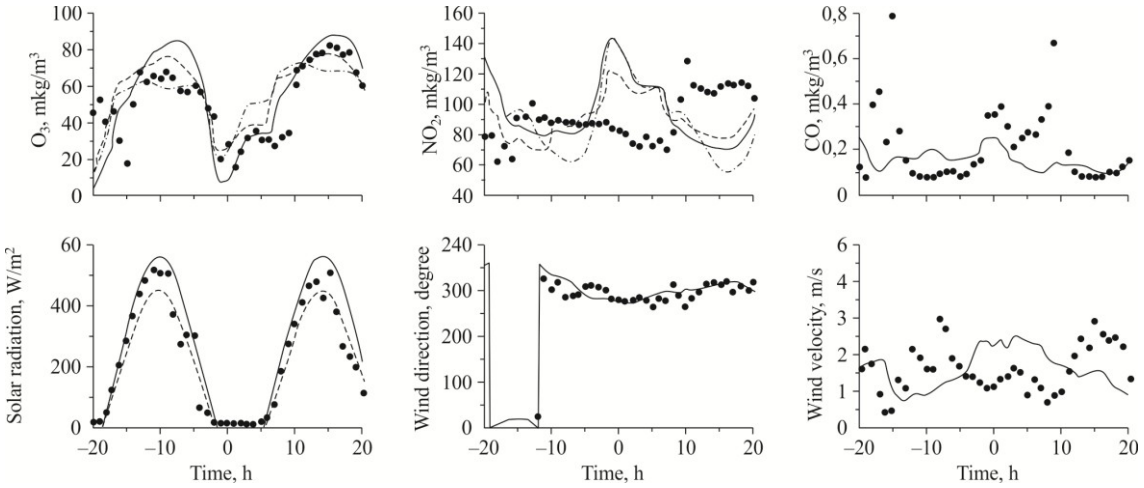

Fig. 3.18. Comparison of computed results for different models with observation data on ozone, nitrogen dioxide and oxide concentrations, total solar radiation, wind direction and velocity for conditions as of 26—27 May 2004 [143]
See explanation in Fig. 3.17.

AIRCHEM model is a block of chemical reactions of a double system HIRES—AIRCHEM, which is applied for research of the secondary pollutants generation problem both on a local and regional level. In the version concerned there are 10 components: ozone O_3, nitrogen oxide NO, nitrogen dioxide NO_2, aldehydes ALD, hydroxyl radical OH, hydrocarbon radicals RO_2, hydrocarbon compounds CH, peroxy radical HO_2, carbon oxide CO, atomic oxygen O, which participate in 10 reactions (Table 3.12).

Table 3.12. Reactions and reaction rates of photochemical module AIRCHEM [139]

Reaction	Reaction rate
$RH + OH \rightarrow 4RO_2 + 2ALD$	$R_1 = k_1 C_{HC} C_{OH}$
$ALD + h\nu \rightarrow 2HO_2 + CO$	$R_2 = k_2 C_{ALD}$
$RO_2 + NO \rightarrow NO_2 + ALD + HO_2$	$R_3 = k_3 C_{RO_2} C_{NO}$
$HO_2 + NO \rightarrow NO_2 + OH$	$R_4 = k_4 C_{HO_2} C_{NO}$
$NO_2 + h\nu \rightarrow NO + O_3$	$R_5 = k_5 C_{NO_2}$
$NO + E_3 \rightarrow NO_2 + O_2$	$R_6 = k_6 C_{NO} C_{O_3}$
$O_3 + h\nu \rightarrow O_2 + O(^1D)$	$R_7 = k_7 C_{O_3}$
$O(^1D) + H_2O \rightarrow 2OH$	$R_8 = k_8 C_{O(^1D)} C_{H_2O}$
$NO_2 + OH \rightarrow HNO_3$	$R_9 = k_9 C_{NO_2} C_{OH}$
$CO + OH \rightarrow CO_2 + HO_2$	$R_{10} = k_{10} C_{CO} C_{OH}$

Three different scale problems were researched by means of HIRES—AIRCHEM [139]. In the local level a problem of ozone pollution of the Sydney air was studied. The second problem was solved in combination of local and regional levels, namely, a smoke tail from a forest fire, at the distance of 100 km away, passing via Sydney,

was reviewed. And the third task solved a problem of far smoke transfer in South-East Asia from Indonesian forest fires.

An abridged mechanism of RADM [140] includes 11 components: ozone O_3, nitrogen oxide NO, nitrogen dioxide NO_2, atomic oxygen O, hydrocarbon compounds RH, peroxide radical HO_2, peracetylnitrate $RC(O)O_2NO_2$, interacting with each other in 12 reactions (Table 3.13).

Table 3.13. Photochemical reactions and reaction rates of scheme of abridged kinetic mechanism RADM [140]

Reaction	Reaction rate
$NO_2 + h\nu \rightarrow NO + O$	$R_1 = k_1 C_{NO_2}$
$O + O_2 \rightarrow O_3$	$R_2 = k_2 C_O$
$NO + O_3 \rightarrow NO_2$	$R_3 = k_3 C_{NO} C_{O_3}$
$RH + OH \rightarrow RO_2$	$R_4 = k_4 C_{RH} C_{OH}$
$RCHO + OH \rightarrow RC(O)O_2$	$R_5 = k_5 C_{RCHO} C_{OH}$
$RCHO + h\nu \rightarrow RO_2 + HO_2$	$R_6 = k_6 C_{RCHO}$
$NO + HO_2 \rightarrow NO_2 + OH$	$R_7 = k_7 C_{NO} C_{HO_2}$
$RO_2 + NO \rightarrow NO_2 + HO_2 + RCHO$	$R_8 = k_8 C_{RO_2} C_{NO}$
$RC(O)O_2 + NO \rightarrow NO_2 + RO_2$	$R_9 = k_9 C_{RCOO_2} C_{NO}$
$NO_2 + OH \rightarrow NO + H_2O$	$R_{10} = k_{10} C_{NO_2} C_{OH}$
$RC(O)O_2 + NO_2 \rightarrow RC(O)O_2NO_2$	$R_{11} = k_{11} C_{RCOO_2} C_{NO_2}$
$RC(O)O_2NO_2 \rightarrow RC(O)O_2 + NO_2$	$R_{12} = k_{12} C_{RCOO_2NO_2}$

Major part of pollutants comes to the atmosphere and reacts chemically in the gas phase; however, some important chemical transformations take place in liquid or solid phases [94]. Currently a range of chemical transformation schemes in the surface layer has been developed.

The CB4 (Carbon Bond 4) mechanism was developed in 1989 and at first included 36 components and 91 reactions (11 photochemical) [145]. Such organic compounds, as ethylene, isoprene, formaldehyde, are presented in the mechanism explicitly, and the rest are given as classes, specified by the link type of carbons in the molecule. Versions of the given mechanism have been developed with account for water-phase reactions or aerosol generation reactions.

RADM2 mechanism [146] is an updated version of RADM mechanism. The basic version includes 57 components and 158 reactions (21 are photochemical). Such compounds, as methane, ethylene, isoprene, formaldehyde, participate in the reactions explicitly, and the rest are given as classes, specified by their reaction ability with hydroxyl radical OH and/or their molecular weight. There are also versions which account for water-phase reactions or aerosol generation reactions.

Based on the RADM2, a more perfect RACM mechanism was developed [147]. The mechanism includes 77 components and 237 chemical reactions. Laboratory researches have helped to specify the reactions rates and add some components and reactions to the mechanism.

SAPRC family of atmospheric chemistry mechanisms should be mentioned. The first version SAPRC-90 was developed in 1990 and includes 59 components and 129

reactions [148]. The version SAPRC-97 includes 82 components and 184 reactions [149]. In 1999 a new version SAPRC-99 was presented, which includes 113 components and 318 reactions (25 are photochemical).

EMEP mechanism [150] describes tropospheric gas-phase chemistry by means of 137 (24 photochemistry reactions) chemical reactions and 61 compounds.

Mechanism of KOREM [151] includes 39 photochemical reactions and 20 reacting compounds. It is a combination of inorganic reactions of CERT mechanism [152] and organic reactions of Bottenheim and Strauss scheme [151]. Five groups of organic compounds were studied: alkanes, alkenes, aldehydes, saturated and aromatic hydrocarbons.

A chemical scheme SMOG [443] is used for a summer photochemical smog modeling. This model is developed under the "Air Pollution in Prague" Project at the Department of Meteorology and Environmental Protection, Faculty of Mathematics and Physics, Charles University (Prague). The model describes and increase of ozone concentration due to photochemical reactions of precursors — nitrogen oxides NO_x and volatile organic substances. The chemical mechanism is given in Fig. 3.19.

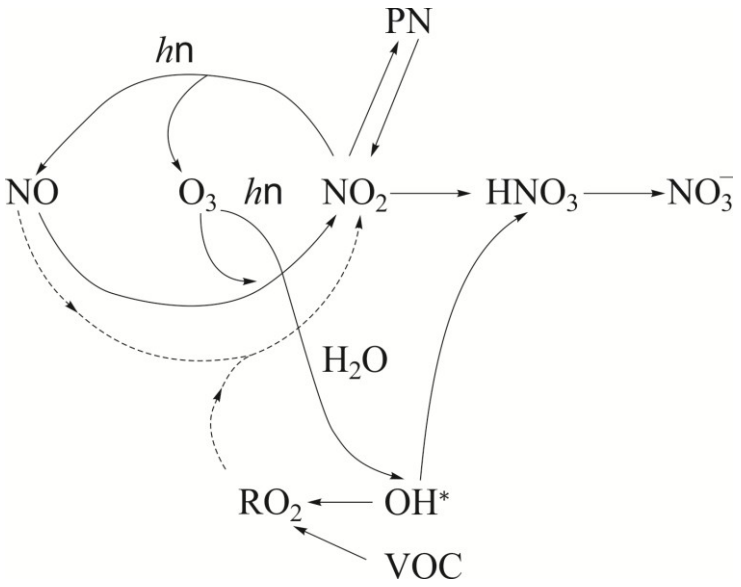

Fig. 3.19. Chemical mechanism SMOG [153]

3.5. Problems of Data Assimilation

Now it is accepted to conduct a space-time data processing with involvement of predicative models for description of meteorological fields' distribution in time and space [154]. A task of combined record of observations data and a predicative model for a more accurate description of space-time distribution of meteorological fields is called and objective of data assimilation (in foreign literature - data assimilation) [155]. Preparing of initial data fields for a numerical weather forecast, which would conform to laws of Physics and balance ratios, was the main reason of data assimilation systems development. There are two main types of assimilation: continuous and discrete. Assimilation of observations data (analysis step) is done at the moment, corresponding to the observation moment in continuous systems, and in discrete — at time moments, corresponding to synoptic observation dates [155].

Processing of actual observation data is an important task during studies of atmospheric processes. Uneven distribution in space and accidental errors of measurement is typical for all data types [155]. Observation data are not always accurate and include information not in all points of the studied area that compels to attract additional information about recoverable fields. Climatic data, analysis of a previous time moment or prediction by the results of previous moment analysis are usually used for these purposes. It is accepted to call such a priori information the first approximation. Currently existing methods can be conventionally divided into four groups [155]: 1) empirical methods, 2) spectral methods, 3) variational analysis (3DVAR), 4) statistical (optimal) interpolation.

The first methods of data analysis were empirical. For example, a method of successive corrections is known [156, 157] for carrying out an objective data analysis [158]. This term means development and implementation of methods, which enable an objective restoring of meteorological elements fields by the meteorological measurement results at the stations; or at least get their values in points of some regular grid [158]. These values can later be used as input information for numerical forecast of meteorological fields. Mathematical statement of analysis problem was suggested in [154, 155]. In the first case the optimal interpolation method is suggested [144], in the second — a variational approach [159]. The optimal interpolation method consists of minimization of the mean for the realizations set of an analysis error, considering statistical features of observation errors and some field, called “the first approximation”.

The data assimilation problem was solved for the Eulerian model of chemical transport REM3, using an optimal interpolation [160]. Main result of data assimilation for Eulerian-type models is analysis of concentration fields (combination of model and observation results). Information from both sources is consolidated in accordance with their statistics mistakes. This feature is inherent in all data assimilation technologies, based on statistics.

In the method of optimal interpolation the analyzed value x_{Ia} in point I of the grid is a sum of value of the first approximation x_{Ib} and weighted value of measurements increment in N of adjacent places of measurement ($i = 1, \ldots, N$) [160]:

$$x_{\text{Ia}} = x_{\text{Ib}} + \sum_{i=1}^{N} a_i (y_i - x_{i\text{b}}),$$

where a_i — weight of measurements value in point i, y_i — the measured parameter value in point i.

Optimal interpolation can be compared to other spatial interpolation procedures, for example, with splines. Methods differ in three criteria [160]: 1) what weights of measurement data are used for forming a value in the analyzed point, 2) whether (and how) the observation errors are accounted, 3) whether contribution of measurement grid inhomogeneity is compensated.

The problem of joint accounting of observation results and a predicative model is solved on the general optimization approach basis with inclusion of a variational statement or estimation theory. In the first case, an assimilation method 4DVAR is developed, in the second — assimilation algorithm, based on Kalman filter [161].

Systems of meteorological data assimilation, based on different versions of Kalman filter algorithm [161—165], are applied.

To implement a Kalman filter algorithm with a computer in full definition is yet impossible, because a covariance matrices order reaches 1 mln. for modern global models. One of the solutions to this problem is using of simplified models for calculation of forecast error covariance matrices. Such algorithm is called suboptimal algorithm of Kalman filter [163, 164, 166, and 167]. The second approach to organization of covariance matrices calculation is based on the assumption of ergodicity of considered random fields of errors. In this case, probabilistic averaging can be replaced with time averaging [168]. Problem statement of optimal filtering is given in detail in [154, 169].

An important applicative meaning the data assimilation problem has for environmental impact assessment; for example, for analysis of passive impurity concentration [165]. Preliminary estimate of impurity concentration fields is done, using the model of passive impurity transfer and diffusion:

$$\frac{\partial s}{\partial t}+\frac{u}{a\cos\varphi}\frac{\partial s}{\partial \lambda}+\frac{v}{a}\frac{\partial s}{\partial \varphi}+(w-w_{\mathrm{g}})\frac{\partial s}{\partial z}=$$

$$=\frac{1}{a^2\cos^2\varphi}\frac{\partial}{\partial\lambda}\left(k_1\frac{\partial s}{\partial\lambda}\right)+\frac{1}{a^2\cos\varphi}\frac{\partial}{\partial\varphi}\left(k_2\cos\varphi\frac{\partial s}{\partial\varphi}\right)+\frac{\partial}{\partial z}\left(k_3\frac{\partial s}{\partial z}\right)+f,$$

$$s(\lambda,\varphi,z,t)=s(\lambda+2\pi,\varphi,z,t),$$

$$s=s_G \text{ with } \varphi=0,$$

$$\nu\frac{\partial s}{\partial z}=\alpha(s-s_0) \text{ with } z=b+h,$$

$$\nu\frac{\partial s}{\partial z}=0 \text{ with } z=H.$$

Here λ — longitude, φ — latitude, z — altitude above the sea level; s — impurity concentration; $(u, v, w - w_{\mathrm{g}})$ — velocity vector components in the directions λ, φ, z accordingly, w_{g} — gravitational deposition velocity; a — the Earth's mean radius; k_1, k_2 — factors of turbulent exchange in horizontal and k_3 — vertical directions; f — a function, describing sources location and capacity; $b(\lambda, \varphi)$ — a function, describing the underlying terrain; h — height of atmospheric surface layer; H — the upper boundary of computational domain; α — a parameter, describing interaction of atmosphere and underlying terrain; s_G — value in the computational domain boundary G [170].

A transfer and diffusion model of discrete space-time type is recorded in the following way [165]:

$$x_k = A_{k-1}x_{k-1}. \qquad (3.11)$$

Here x_k — n-vector of forecasted impurity concentration values at point of time t_k. Its dimensionality is equal to the number of grid points $n = n_\lambda n_\varphi n_z$, where n_λ — number of points for longitude, n_φ — for latitude, n_z — for altitude.

True concentration value at time point t_k is described by a vector equation

$$x_k^t = A_{k-1}x_{k-1}^t + \varepsilon_{k-1}^t, \qquad (3.12)$$

where ε_k — a random vector of noise model, meeting the following conditions

$$E\varepsilon_k^t = 0, \;\; E(\varepsilon_k^t)(\varepsilon_l^t)^T = Q_k\delta_{kl}. \qquad (3.13)$$

Vector of observation data can be presented as

$$y_k^0 = M_k x_k^t + \xi_k^0, \qquad (3.14)$$

where y_k^0 — m-vector of observation at time point t_k, M_k — $(n \times m)$-matrix, ξ_k^0 — a random m-vector of observation errors, meeting the conditions

$$E\xi_k^0 = 0, \;\; E(\xi_k^0)(\xi_l^0)^T = R_k\delta_{kl}, \; E(\xi_k^0)(\varepsilon_l^t)^T = 0.$$

An optimum estimate of concentration x_k^a, according to observation data (3.14), impurity transfer and diffusion model (3.11) is found under condition of the minimum spur of estimation error covariance matrix. Solution to this problem is an algorithm of Kalman filter [169]:

$$x_k^f = A_{k-1}x_{k-1}^a,$$

$$P_k^f = A_{k-1}P_{k-1}^a A_{k-1}^T + Q_{k-1},$$

$$K_k = P_k^f M_k^T (M_k P_k^f M_k^T + R_k)^{-1},$$

$$P_k^a = (I - K_k M_k)P_k^f,$$

$$x_k^a = x_k^f + K_k(y_k^0 - M_k x_k^f),$$

$$P_k^f = E(x_k^f - x_k^t)(x_k^f - x_k^t)^T, \;\; P_k^a = E(x_k^a - x_k^t)(x_k^a - x_k^t)^T.$$

Here x_k^f — concentration prediction by the model, x_k^a — a vector of analyzed values in point of time t_{k-1}, i. e. the sought estimation, which is obtained at the $(k-1)$-th time step, estimate x_{k-1}^a is called an analysis estimation; P_k^f, P_k^a — forecast and analysis errors covariance matrices, accordingly, K_k — weight matrix.

Assimilation systems, based on the cycle forecast—analysis—initialization [171], have been updated lately, involving a general variational problem statement. A conjugated model, based on known results of the optimal control theory, is used for minimization of the corresponding functional [172, 173]. A range of developments in the area of data assimilation is done in terms of estimation theory, involving a Kalman filter algorithm [161]. There are joint estimation and process control algorithms [154]. Currently, variational (4DVAR) [174] and dynamic- stochastic (Kalman filter) [155] approaches are used mainly.

Developments in the area of meteorological parameters observation data assimilation can become the basis for creation of data assimilation system for anthropogenic load level on the controlled forest-covered territory.

3.6. Forest Fires and “Aerosols of Siberia” Project

Forest fires are a powerful source of aerosols in Siberia [175]. During period from 1991 till 2003 systematic complex theoretical and experimental researches of space-time variability of microphysical and chemical features of atmospheric aerosols are conducted in different regions of Siberia and the Arctic basin of Russia (“Aerosols of Siberia” Project). Goals of this project are as follows[84]: 1) studying the regularities of aerosols generation, transformation and transfer in the Siberian region on a local, regional and global levels for detection of their main sources and flows; 2) assessment of atmospheric aerosols impact on air quality, contamination levels of vegetation, soil and water, velocity of different substances and elements migration in environmental objects; 3) investigation of different atmospheric aerosols impact on atmospheric processes, health of people and animal world. At present, a ground system of atmospheric aerosols monitoring has been organized in Siberia, covering the territory of Western and Eastern Siberia with observation points' remoteness up to 1500 km. As a rule, fixed stations of different institutes of the Siberian Division of Russian Academy of Science (SD RAS) are used (Fig. 3.20).

Fig. 3.20. Network of observations after aerosols in Siberia [84]

The Space monitoring system is also developed, by means of which an important information on the scales of boreal forest fires in Siberia is acquired. These data make it possible to identify specific sources of forest fires and their smoke areas. Smoke plumes have impact in local and regional scales. Sources of aerosol emission have a complicated structure, which is determined by a spatial location of individual fires, type of forest, fire intensity and weather conditions [84]. Since year of 2000 space observations are accompanied by ground experiments on a special test site, where a value of gas-aerosol emissions, depending on forest fuels type and burning conditions, is determined, in particular. The first experimental data were obtained, which enabled determining of emission factors of radioactively active gas and aerosol emissions for the burned forest fuels weight, and chemically generated aerosols of submicron and coarse-fine fraction. These results are used for assessment of gaseous and aerosol emissions impact on climatic and environmental consequences of forest fires in the boreal Siberian forests [84].

Properties of atmospheric aerosol are determined by a range of sizes, concentrations, chemical composition and particles structure. Meteorological Potential of Atmosphere Self-purification (MPAS) is designed to identify the reasons, forming a high level of air pollution [176]. It is determined by the ratio of calmness and fog frequency sum, as factors of impurity accumulation, to the sum of atmospheric precipitation (over 0.5 mm) and strong wind (over 6 m/s) frequency, as factors of air purification from impurities:

$$\mathrm{MPAS} = \frac{P_{\mathrm{clm}} + P_{\mathrm{f}}}{P_p + P_{\mathrm{w}}},$$

where P — frequency, %: clm — calmness, f — fogs, p — atmospheric precipitation ≥0.5 mm, w — wind ≥6 m/s.

Smoke is a mixture of aerosol different size particles, from submicron aerosols to coarsely dispersed objects of dozens of microns size. Mechanisms of their generation are different, as well as their physical and chemical, optical properties. A significant part of fire aerosol emission consists of soil particles, which accumulated on trunks, stems and leaves for a long period before the fire. In fire these particles are subject to vigorous heating, the major part of their organic substance burns, and they become almost completely mineral. Some chemical elements are included in the composition of plant biological tissues, and due to a fire part of them gets in the air as aerosol [84]. Carbonaceous aerosol, which are a result of thermal destruction of biomaterial particles and incomplete burning of its organic and chemical substances, can have both submicron sizes (for example, generated from condensation and adsorption of low-volatile organic substances beyond the hot burning area), and sizes of several microns or even dozens of microns (for example, from incomplete burning of particles-chips during thermal cracking of wood) [84].

Fine-dispersed submicron aerosols, containing a large amount of element carbon (for example, in kind of soot particles), influence considerably on sunlight absorption and scattering in the atmosphere and, consequently, on local and regional climatic processes [177]. A more coarsely dispersed part of fire emission can cause impact on chemical processes in the atmosphere (for example, formation of smog and fogs, as well as directly influences on the inhaled air quality [178]).

Research of aerosol emission is a part of international project FIRE BEAR (Fire Effects in the Boreal Eurasian Region), aimed at research of forest fires breaking reasons, their behavior, burning conditions for forest biomass, natural carbon cycle, forest and forest biocenosis resistance towards forest fires impact of different intensity [84]. Researches were carried out in summer seasons of 2000—2003 in three forest polygons of the Forestry Institute of SD RAS (Yartsevo, Govorkovo, Khrebtovskiy), located 600—700 km northward and north-eastward of Krasnoyarsk (pine tree is a prevailing forest tree). Nature's imitation of real forest fires in boreal pine forests of Siberia was conducted at the polygons. Instrumentation, installed on the sites, includes devices for velocity and direction of fire front movement along the site, as well as thermocouple temperature meters on five height levels. A video camera, placed in a heat-protective case, and infrared recording instruments, installed in a helicopter, were also used.

Aerosol sampling in ground conditions was done near the side edge of burning area by pumping the smoke-filled air both via aerosol thin-fiber polymeric filters AFA-HA (20 cm^2, Russia), and via fiberglass filters Gelman (15 cm^2, USA). Experimental data on the content of microelements in samples from AFA-HA aerosol filters are given in Table 3.14.

Based on these results, we can state that typical aerosol emission concentrations near the burning surface during fires in Siberian boreal forests vary within the range of 30—70 mg/m^3 [84]. Taking into consideration that amount of burnt forest fuels usually is 15—25 t/ha during forest fires [84, 179], we can reckon that 1—4 % of burned material turns into an aerosol emission during a typical fire in Siberian boreal forests.

Using the information on concentration of some elements in standard soil media, we can assume that source of elements is the burnt biomass, or emission of mineral dust particles from soil and plants surface took place.

The measured concentration of elements should be standardized for iron concentration (Table 3.15) [84].

When a relative content of some element in the aerosol sample exceeds a natural soil value in ten times and over, a substantiated conclusion can be made on mainly vegetational origin of this element in aerosols. In case when emission-soil ratio does not differ much from the unit, it can be considered that these elements have a mineral-soil origin [84].

Data on content of carbonaceous substances in kind of organic compounds and element carbon (for example, carbon black) in aerosol emission are given in Table 3.16.

Comparison of mass concentration values, content of element and organic carbon in aerosol emission from different intensity fires has shown a considerable decrease of a full mass concentration of smoke emission during an intensive fire [84].

Table 3.14. Total mass concentration of aerosol emission C_0 and partial concentrations of chemical microelements [84], mkg/m^3

Sample number	Mass concentration C_0	K	Ca	Ti	Cr	Mn	Fe	Co	Zn	As	Se	Br	Rb	Sr	Mo	Pb
1	30800	445	72	5.9	0.0	6.0	27.9	0.52	11.1	0.00	0.23	4.3	2.2	0.14	0.00	2.5
4	14700	141	129	14.7	0.0	5.0	24.1	0.00	3.8	0.00	0.00	0.5	0.8	0.08	0.12	2.4
6	35700	439	54	0.0	5.0	0.4	22.5	1.04	6.1	0.00	0.12	2.6	1.8	0.06	0.25	3.1
7	38500	233	100	2.1	1.9	11.0	49.2	0.31	3.3	0.94	0.00	0.8	0.9	0.14	0.09	0.0
8	78100	144	53	0.0	5.6	3.8	33.1	0.00	0.0	0.00	0.00	0.4	0.0	0.13	0.38	1.0
12	43500	113	174	10.9	7.4	2.2	28.3	0.00	0.0	0.00	0.18	5.6	0.0	0.00	0.45	3.6
17	37700	455	38	0.0	0.0	2.3	10.0	0.0	14.5	0.23	0.26	2.3	1.8	0.00	0.00	1.3
20	22000	88	70	1.8	2.6	19.6	9.5	0.11	0.0	0.00	0.00	0.2	0.3	0.10	0.00	1.0
25	42100	185	61	3.0	0.0	4.6	11.4	0.00	1.7	0.27	0.13	0.9	0.8	0.03	0.12	0.7
28	29100	206	274	16.5	5.2	10.9	13.4	0.13	2.7	0.80	0.00	0.4	0.6	0.20	0.00	0.0
32	50000	205	65	0.0	8.5	0.0	5.0	0.23	1.5	0.35	0.25	1.1	0.8	0.00	0.27	0.9
58	29800	412	17	3.9	0.0	1.8	8.2	0.33	5.3	0.26	0.12	3.9	1.7	0.00	0.00	2.6
Average value	50300	266	86	4.6	2.4	5.9	18.3	0.18	3.3	0.16	0.06	2.3	1.1	0.13	0.09	1.1
Standard error	7800	45	13	1.3	0.6	1.1	2.5	0.07	0.8	0.06	0.02	0.8	0.2	0.03	0.03	0.2

Table 3.15. Relative concentrations (enrichment factors) of microelements, and iron concentration standardization [84]

Indicator	K	Ca	Ti	Cr	Mn	Fe	Co	Zn	As	Se	Br	Rb	Sr	Mo
Aerosol emission	14.6	4.6	0.25	0.13	0.32	1.0	0.01	0.18	0.0087	0.0033	0.13	0.06	0.007	0.005
Soil (Reference data)	0.58	0.55	0.12	0.0023	0.017	1.0	0.0005	0.002	0.00012	0.0002	0.0007	0.004	0.001	0.0001
Aerosol/soil ratio	25	8	2	56	19	1	20	90	73	165	186	15	7	50

Table 3.16. Content of carbonic substances in aerosol emission (ground sampling) [84]

Sample # (glass filter)	Full mass concentration, mg/m^3	Full sample weight, mg	Amount of organic substance		Amount of element carbon		Cumulative percentage of carbonic substances, %
			mg	%	mg	%	
Govorkovo. Site No. 1							
61	69.9	5.8	1.88	32	0.74	13	45
62	21.0	3.4	0.97	29	0.28	8	37
81	60.3	3.8	1.4	37	0.18	5	42
82	79.1	6.8	1.6	24	0.24	4	28
93	58.3	2.1	0.53	25	0.32	15	40
94	11.8	1.2	0.39	33	0.08	7	–
Average	50	–	–	30	–	9	39
Yartsevo. Site No. 20							
1	17.1	2.4	1.15	48	0.25	11	59
3	8.4	1.3	0.36	27	0.04	3	30
5	10.9	1.8	1.44	80	0.24	13	93
6	14.7	2.2	1.26	57	0.12	5	62
Average	12.8	–	–	53	–	8	61
Yartsevo. Site No. 4							
9	80.9	3.8	1.95	51	0.36	10	61
10	16.2	1.2	0.72	60	0.05	4	64
11	24.6	1.5	0.82	54	0.23	15	69
12	6.4	0.7	0.57	81	0.05	7	88
17	13.9	1.0	0.75	73	0.06	6	79
Average	28.4	–	–	64	–	8	72
Average for all samples	28.0	–	–	45	–	8	53

3.7. Effect of Forest Fires on Weather

Climate warming can cause and overall increase of fire incidents [180]. However, some researchers doubt that [181]. A particular forest fire is a result of a great number of complex interactions, including fire sources, condition of forest fuels, topography and weather conditions (temperature, relative air humidity, wind velocity, amount and frequency of precipitation). Temperature increase does not still guarantee an increase of fire disturbances. However, some known researches prove an increase of forest fires severity in the territory of Canada, Alaska and Russia [182]. A more credible scenario of climate development is when due to weather variations in central and northern parts of North America and Europe, there will be a significant increase of fire hazard in some regions, while severity of fire-hazardous weather changes will reduce owing to increased amount and frequency of precipitation in the other regions [183].

It is known that increase of greenhouse gases concentration in the atmosphere results in a global temperature increase on the planet, especially in Arctic and boreal regions [184]. Future increase of ambient temperature can extend duration of fire-hazardous season and increase probability of fires in boreal ecosystems that allows forming a hypothesis of a reaction between warming, fire activity, loss of carbon and future climatic changes [185, 186]. At the same time, effects of a forest fire can be

different. For example, aerosol emission from the forest fire front can bring to both warming and cooling on a regional level, depending on such factors as aerosol composition, Earth surface and clouds albedo [187].

In no-wind conditions, as a result of aerosol transfer, generated in the forest fires zone, a convection column is formed, which is a strong vertical jet [188]. It can be seen visually due to a large smoke concentration. Velocity of ascending flows is about 7 m/s. During a crown fire of moderate intensity, the jet top reaches two-kilometer height. The emitted combustion products are carried upwards. A mushroom-shaped structure of a concentration field is formed. If a fire stops, then cloud deposits and creates discomfort conditions on a site of about 100 km^2.

When there is a horizontal transfer, an impurity cloud does not spread higher than 500—600 m above the ground and is elongated along the wind direction at the distance of 10—20 km from the fire source. If fire stops, then an impurity deposition zone will have a shape of a flame, extended along the wind direction. If wind velocity is over 10 m/s, then a cloud of impurity spreads to the distances up to 200 km from the fire source [188].

Heat, moisture and aerosols are brought to the troposphere above burning zones during forest fires. Impact of these substances on could and precipitation formation process is studied [188—191] by means of numerical eddy-resolving model of the atmospheric boundary layer. Model of atmospheric boundary layer is based on the non-hydrostatic equations of thermohydrodynamics in approximation of deep convection with edge conditions, providing for conjugation with synoptic processes in the free atmosphere [192, 193]. Mathematical statement of problem [188, 192—196]:

$$\frac{du}{dt} = -\frac{\partial \pi}{\partial x} + l(v - v_g) + D_{xy}u + \frac{\partial}{\partial z}K\frac{\partial u}{\partial z}, \quad (3.15)$$

$$\frac{dv}{dt} = -\frac{\partial \pi}{\partial y} + l(u - u_g) + D_{xy}v + \frac{\partial}{\partial z}K\frac{\partial v}{\partial z}, \quad (3.16)$$

$$\frac{dw}{dt} = -\frac{\partial \pi}{\partial z} + g\left(\frac{\vartheta}{\Theta} + 0,61q - q_l\right) + D_{xy}w + \frac{\partial}{\partial z}K\frac{\partial w}{\partial z}, \quad (3.17)$$

$$\frac{\partial u}{\partial x} + \frac{\partial v}{\partial y} + \frac{\partial w}{\partial z} = 0, \quad (3.18)$$

$$\frac{d\vartheta}{dt} + w\frac{\partial \Theta}{\partial z} = D_{xy}\vartheta + \frac{\partial}{\partial z}\hat{K}\frac{\partial \vartheta}{\partial z} + \frac{L_v}{\rho c_p}(\Phi_1 + \Phi_2 + \Phi_4) +$$

$$+ \frac{L_s}{\rho c_p}(\Phi_3 + \Phi_5 + \Phi_6) + \frac{L_f}{\rho c_p}(\Phi_7 + \Phi_{10} + \Phi_{13}), \quad (3.19)$$

$$\frac{dq}{dt} = D_{xy}q + \frac{\partial}{\partial z}\hat{K}\frac{\partial q}{\partial z} - \Phi_1 - \Phi_2 - \Phi_3 - \Phi_4 - \Phi_5 - \Phi_6, \quad (3.20)$$

$$\frac{dq_c}{dt} = D_{xy}q_c + \frac{\partial}{\partial z}\hat{K}\frac{\partial q_c}{\partial z} + \Phi_1 + \Phi_7 - \Phi_8 - \Phi_9 - \Phi_{10}, \quad (3.21)$$

$$\frac{dq_i}{dt} = D_{xy} q_i + \frac{\partial}{\partial z} \hat{K} \frac{\partial q_i}{\partial z} + \Phi_1 + \Phi_5 - \Phi_7 + \Phi_{11} - \Phi_{12}, \quad (3.22)$$

$$\frac{dq_r}{dt} - W_r \frac{\partial q_r}{\partial z} = D_{xy} q_r + \frac{\partial}{\partial z} \hat{K} \frac{\partial q_r}{\partial z} + \Phi_2 + \Phi_8 + \Phi_9 + \Phi_{10} - \Phi_{13}, \quad (3.23)$$

$$\frac{dq_s}{dt} - W_r \frac{\partial q_s}{\partial z} = D_{xy} q_s + \frac{\partial}{\partial z} \hat{K} \frac{\partial q_s}{\partial z} + \Phi_2 + \Phi_8 + \Phi_9 + \Phi_{10} - \Phi_{13}, \quad (3.24)$$

$$\frac{dS}{dt} - w_0 \frac{\partial S}{\partial z} = F + D_{xy} S + \frac{\partial}{\partial z} \hat{K} \frac{\partial S}{\partial z}, \quad (3.25)$$

$$\frac{d}{dt} = \frac{\partial}{\partial t} + u \frac{\partial}{\partial x} + v \frac{\partial}{\partial y} + w \frac{\partial}{\partial z}, \quad D_{xy} = \frac{\partial}{\partial x} \hat{K} \frac{\partial}{\partial x} + \frac{\partial}{\partial y} \hat{K} \frac{\partial}{\partial y}. \quad (3.26)$$

Here t — time; u, v, w — velocity vector components along x, y, z axes; u_g, v_g — velocity vector components of geostrophic wind along x, y, z axes; π —analog pressure; ϑ — deviation of potential temperature from its value Θ in undisturbed atmosphere; q, q_c, q_i, q_r, q_s — concentration of vapor, cloud drops, ice crystals, rain drops and snow accordingly, $q_l = q_c + q_i + q_r + q_s$; S — concentration of smoke aerosol; F — operator, accounting for various types of aerosol interaction to each other and precipitation particles; g — free fall acceleration; l — Coriolis parameter; L_v, L_s, L_f —latent heat of condensation, sublimation and ice melting processes accordingly; c_p — specific heat capacity at constant pressure; K — coefficient of vertical turbulent exchange of subgrid scale (u, v), K_x, K_y — horizontal factors of turbulent exchange, calculated by the Smagorinsky method; Φ_i ($i = 1, \ldots, 13$) — rate of phase transformations [193]; W_r, W_s, w_0 —gravitational deposition rates for rain, snow and aerosol. Development of parameterization equations for the rates of phase transformations is based on the Kessler views, summarized with account for an ice phase [195].

Edge conditions for equations (3.15)—(3.26), subject to parameterization of heat and moisture exchange in the atmospheric surface layer, are of form [196]

$$\hat{K} \frac{\partial q}{\partial z} = C_\Theta |U| (q - q_0), \quad \hat{K} \frac{\partial \vartheta}{\partial z} = C_\Theta |U| (\Theta - \Theta_0),$$

$$K \frac{\partial u}{\partial z} = C_u |U| u, \quad K \frac{\partial v}{\partial z} = C_u |U| v,$$

$$w = 0, \quad \frac{\partial q_c}{\partial z} = 0, \quad \frac{\partial q_i}{\partial z} = 0, \quad \frac{\partial q_r}{\partial z} = 0, \quad \frac{\partial q_s}{\partial z} = 0, \quad \frac{\partial S}{\partial z} = 0, \quad \text{with } z = h.$$

Here h — an upper border of steady flow layer, $|U|$ — horizontal velocity module, C_u, C_Θ — resistance and heat exchange factors, calculated on the basis of surface layer model; q_0, Θ_0 — values of q, Θ at the roughness level.

Process of burning and aerosol emission are considered in the model [196] by means of edge conditions:

at $x, y \in R$, $z = h$, $S = S_0$, $\vartheta = T_п$,

at $x, y \notin R, z = h, S = 0, \vartheta = 0,$

where $T_{\text{п}}$ — temperature increase due to burning, $R(x, y)$ — a region of underlying surface, limited by a fire line, where heat, vapor and aerosol emission takes place. $T_{\text{п}}$ and S_0 are deemed as set values.

The following edge conditions are set the upper boundary of computational domain ($z = H$) [196]:

$$q = q_H,\ q_c = 0,\ q_i = 0,\ q_r = 0,\ q_s = 0,\ S = 0,\ u = u_{\text{g}},\ v = v_{\text{g}},\ w = 0,\ \frac{\partial \Theta}{\partial z} = \gamma,$$

where q_H — a set distribution of specific humidity at the upper border of atmospheric boundary layer, γ — determines a steady stratification in the troposphere. Normal derivatives of sought functions are equal to zero at the lateral boundaries of computational domain.

Distribution of temperature, humidity and also conditions of cloudiness and precipitation absence are assigned as initial conditions [196]:

$$\vartheta = 0, u = 0, v = 0, w = 0 \text{ at } t = 0.$$

In the mid-latitudes a significant decrease of precipitation sum above the territory of massive forest fires (forest fires of 2002 in Yakutia [197]) takes place in some cases. Such influence can be implemented through effect of smoke aerosols on cloud and precipitation formation [190, 191]. Scheme of interconversions in the vapor—water—ice system is given in Fig. 3.21. Fig. 3.22 shows aerosol influence on changing of fallen precipitation at different time moments at $T_h = 5$ °C. In Fig. 3.22 J — amount of fallen precipitation at the level $z = h$, t — time; *1* — aerosol is absent, *2* — aerosol concentration of 100 particles/m^3, *3* — aerosol concentration of 800 particles/m^3.

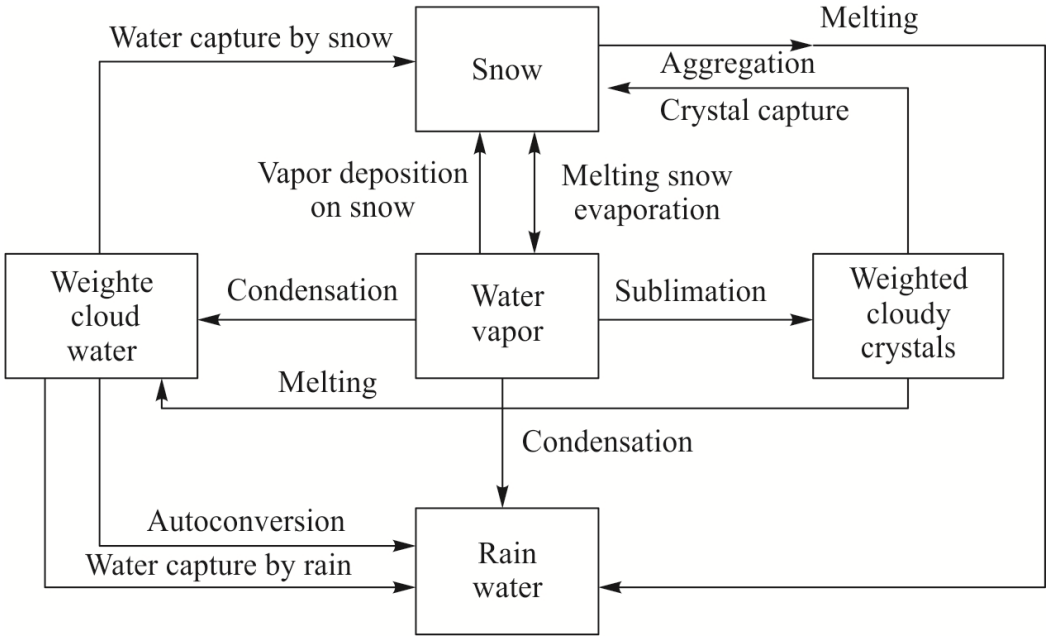

Fig. 3.21. Scheme of interconversions in the vapor—water—ice system [478]

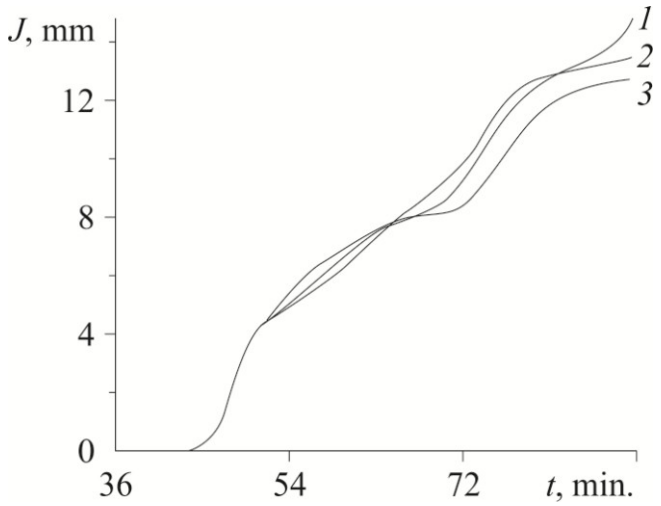

Fig. 3.22. Aerosol effect on the fallen precipitation changing at different time moments at T_h = 5 °C [188]. See explanation in the text

Heat and moisture, coming from the fire zone, intensify cloud formation processes, and aerosol, filling the atmosphere with nuclei of water vapor condensation, results in formation of weighted fine droplets in the areas below freezing level. If a cloud has a supercooled top, then a large amount of aerosol particles of 1 um size, reaching it, results in crystallization of supercooled drops [198]. Such clouds give much weaker precipitation, than clouds, which tops consist of superposition of ice crystals, snow and water drops [199—201]. Area of aerosol distribution during cloud formation at relative humidity of undisturbed atmosphere 30 (*a*) and 90 % (*b*) is given in Fig. 3.23.

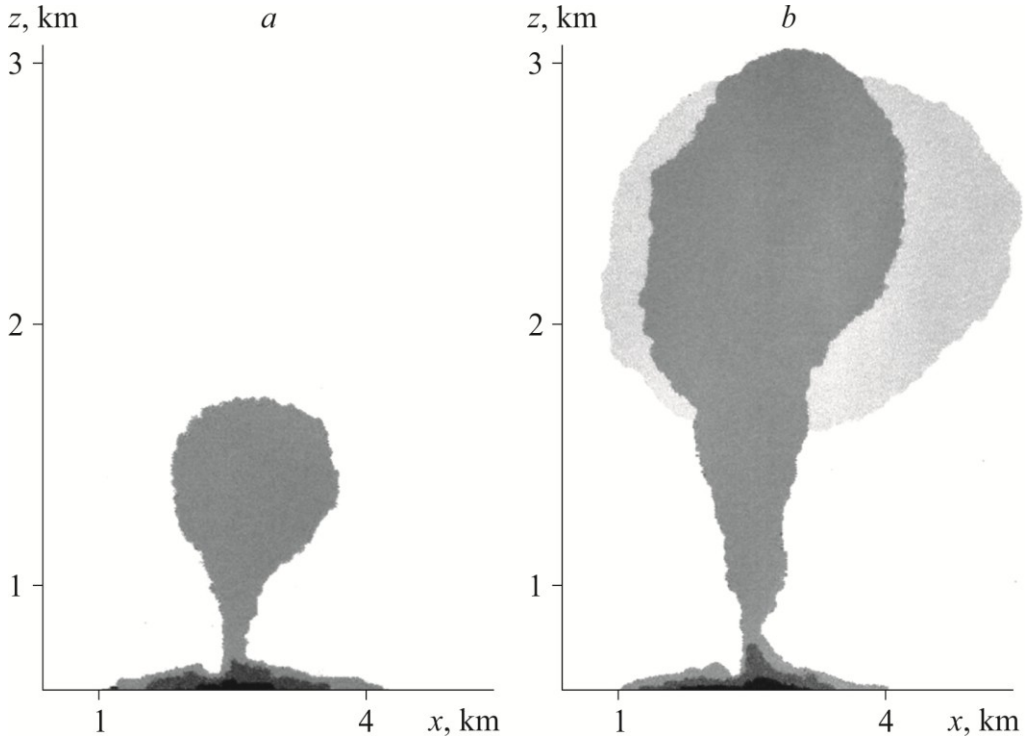

Fig. 3.23. Area of aerosol distribution during cloud formation [196] See explanation in the text.

Massive forest fires influence the cyclonic circulation [196]. Diagram of smoke aerosol spatial distribution in different synoptic conditions is given in Fig. 3.24.

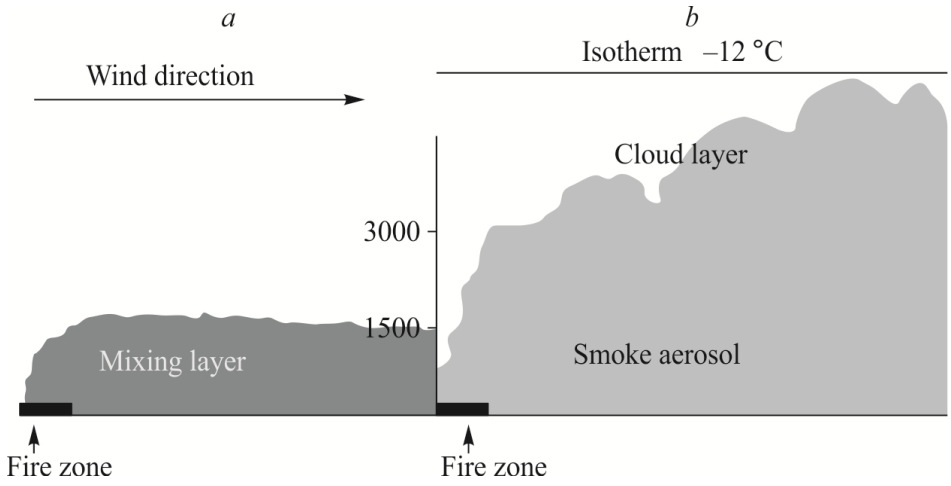

Fig. 3.24. Diagram of smoke aerosol spatial distribution in different synoptic conditions:
a — anticyclonic, *b* — cyclonic [196]

Reconstruction of air masses circulations above fire zone and its surroundings happens under the influence of insolation and heat from forest fire sources. Cyclone envelopes the territory of fires. Analysis of a large amount of satellite photographs of massive forest fires shows that this situation is quite characteristic of cyclonic conditions [196].

According to the hypothesis [196], under the influence of coarsely dispersed smoke aerosol a cloud depth on vast territories decreases, and precipitation formation process above the isotherm line –12 °C cease. Therefore, part of troposphere above this isotherm cools down and its temperature becomes lower than of a surrounding cloud space, which was not disturbed by the aerosol effect. Heavy cold air masses descend and suppress convection in lower layers. Intensity of precipitation formation decreases, what leads to further cooling of a cloud layer and intensification of downdraft. The process goes on, until a cloud layer disappears above the smoke zone. In clear weather conditions a mixed layer appears. Heat and smoke aerosol from forest fire sources do not penetrate above this layer [196]. There is a circulation arising during mass forest fires in major territories, with which cold air descends in the upper and lower parts of troposphere and spreads in the mixed layer.

Under the Coriolis effect a typical anticyclonic circulation, during which wind of this area changes its direction [196]. Ice particles, forming cirrus ice clouds, are generated as a result of crystallization. These clouds are located leeward of forest fires.

3.8. Effect of Forest Fires on Soils

A considerable part of properties, inherent in soil, belong to original rock. Lithogenous properties mainly include mineralogical, gross chemical and granulometric soil composition, composition density, water and thermal properties [202]. Soil is the steadiest component of landscape, able to reflect a natural potential of the territory fully. Namely soil cover determines stability of ecosystems, ability to recover its structure as if intact. When a soil component is disturbed, recovery of ecosystem to the initial state is almost impossible [202].

Forest soil properties are formed in a long period of time during multiple replacements of vegetation groups [202]. Evolutionary changes of soils occur against the background of dynamic rearrangement of forest vegetation. Soil changes in a natural, dynamic and syngenetic cycles of forest vegetation are related mainly to accumulation and transformation of forest litter on soil surface, reduction of evaporation and transpiration, changing of thermal conditions in old and overmature forests [202].

Forest fires provide both direct and indirect influence on forest zone soils. For example, over the last years forest fires in Altai region have led to vast areas of fire-damaged wood. Conditions, arising in fire-damaged wood soils, result in steppe formation [203]. A natural process of pine recovery occurs unevenly at different parts of mesorelief due to differences in hydrothermal soil conditions, solar insolation and other soil factors. Heat accumulation and transfer processes in soil profiles are determined by thermal and physical properties of soils. It is particularly topical for soils, exposed to fire effect.

Soil climate means multiyear conditions of soil temperature and humidity, soil air and other elements, depending on a complex of natural conditions and human operating activity and regulated by the latter in agricultural and other purposes [204]. It is complies with macroclimate conditions and features of meso- and microrelief.

Physics of soil moisture phase transitions (evaporation, condensation, freezing and thawing) is determined by soil temperature, thermal and physical features, its humidity and pressure, as well as their subsoil gradients and drops in the soil—plants—atmosphere system [203].

Temperature conditions of soil was researched under pinewood during experimental fires of low intensity (the maximum temperature didn't exceed 650 °C) [205]. It was established that due to low heat conductivity of soil and damper effect of litter is lethal for soil organisms, the temperature is only observed in several upper soil centimeters. It was also found that velocity of heat distribution is determined by moisture content in soil to a great extent.

Forest fires have effect on thermal and physical features of post-pyrogenic soils [203]. A section of forest-damaged wood and section of sod-podzolic soils from the territory, not affected by the fire [205].

Section 1/98

Horizon A_0 — 2 cm. Burned forest litter. In the form of black ashes.

Horizon A_1 — 2—8 cm. Light grey, weakly humus. In the lower part color is less intensive, weaved with roots, humid, sandy-loam.

Horizon A_1A_2 — 8—25 cm. It is colored by humus weakly, has a whitish shade, greatly penetrated by roots, humid, sandy. The transition is clear.

Horizon A_2 — 25—44 cm. Whitish color, weakly slab-shaped, characteristic of illuvial horizons, humid, sandy-loam. Transition is well-expressed.

Horizon B — 44—87 cm. It has a darker color, with yellowish shade from sesquioxides. Illuviation of iron and aluminum oxides, as well as organic-mineral compounds, is weak. Humid, sandy. Clear transition.

Horizon C — below 87 cm. Humid, light-color sand.

Soil — sod fine-podzolic, weakly soddy.

Section 5/98 [203]

It is planted among old broken forest under a cover of broken grass vegetation. Soil was not exposed to a forest fire. Underdeveloped grassy vegetation on the surface. Pine and aspen trees grow.

Horizon A_0 — 0—3 cm. Forest litter, mainly of needles. Fresh on the top, semi-decomposed in the lower part.

Horizon A_1 — 3—10 cm. Light grey with whitish shade, greatly penetrated by roots, humid, not less than in forest-damaged wood. Sandy. Transition is gradual.

Horizon A_1A_2 — 10—25 cm. Has a darker color, takes a slight slab shape, humid, sandy. Here an increased humus content and charcoal accumulation from previous fires were found.

Horizon A_2 — 25—45 cm. Light grey with whitish shade, a slab shape is observed, but structural partings fall easily into primary mechanical elements. It is weaved by roots. Humid, sandy. Transition is evident.

Horizon B_1 — 45—88 cm. Has a darker due to illuviated iron oxides and organic-mineral compounds; however, illuvial process is weakly shown. Humid, sandy, transition is gradual.

Horizon BC — 88—110 cm. Light grey, with traces of illuviation of iron oxides and organic-mineral compounds. Transition is weakly shown.

Horizon C — below 110 cm. Damp sand of light color.

Soil — sod fine-podzolic, weakly soddy.

Vegetation is pine and aspen trees.

Pyrogenic factor does not influence critically on granulometric composition of sod-podzolic soils, except for the upper ten-centimeter layer, where amount of silty particles in the fire-damaged wood is lower than in soils under the undisturbed forest [203]. Destruction of forest litter by a fire results in development of flow water erosion in the first spring after fire that can cause a wind erosion development. Forest fires have also effect on water conditions of sod-podzolic soils - in soils of the fire-damaged wood there is considerably more moisture (double increase in comparison to the undisturbed soils) [203]. The greatest impact a forest fire has on acidity of sod-podzolic soil. A significant acidity reduction of a fire-damaged wood is registered for all horizons down to 50 cm. As a result of fires, horizon A_0 (forest litter) is destroyed [203] in the first place that abruptly disturbs thermal (intensive heating of soil in a fire-damaged wood), water and microbiological conditions. Forest fires do not cause a direct effect on other horizons' morphology.

The maximum temperature conductivity is recorded in a less dense horizon A_1. In horizons A_2 and B of much higher density it decreases in 1.8 times in comparison to A_1. The control section shows a different distribution of temperature conductivity. Its maximum is recorded in the horizon A_2, and the minimum in the illuvial horizon B. In general, distribution of temperature conductivity and heat capacity per unit volume in these horizons is even. In fire-damaged wood the section is distinctly differentiated by heat capacity (Table 3.17) [203]. Moisture, contained in the soil, also has effect on soil's thermal and physical features.

Table 3.17. Thermal and physical features of sod-podzolic soils of ribbon pine forests of the Altai region [203]

Horizon	Depth, cm	Density, kg/m^3	Humus, %	Particles less than 0.01 mm, %	α, 10^{-6} m^2/s	C, 10^6 J/(m^3·K)	λ, W/(m^3·K)
A_1	3–10	1370	1.7	5.40	0.454	1.262	0.573
	(0–5)	1460	0.1	4.84	0.376	1.436	0.539
A_2	25–45	1640	0.4	4.72	0.256	2.101	0.538
	(30–35)	1490	0.4	3.75	0.447	1.574	0.704
B	44–88	1630	0.4	3.82	0.260	1.858	0.483
	(60–65)	1590	0.4	3.28	0.293	1.640	0.482
C	88–110	1500	–	4.32	0.408	1.594	0.650
BC	(95–100)	1580		2.72	0.395	1.578	0.624

In the upper humus layers, as well as in the horizons of less density and large volume of coarse-texture, the decaying effect of soil heat and temperature conductivity with moisture increase is less evident than in more dense and fine-pored horizons [203].

Carbon is present in many fragments of wood, litter, partially decomposed organic substance in forest ecosystems [206]. A large amount of carbon is reserved in the soil [207]. During decomposition 60—80 % of organic carbon returns to the atmosphere as CO_2. Further transformation processes of semi-decomposed organic matter are not only determined by biological activity process, but by abiotic factors as well, including fires [207].

Due to fires effect, new carbon forms are generated (i.e. it is contained in other compounds). Processes of volatile compounds distillation and organic carbon destruction start in soil within the range of 100—200 °C. Carbonization starts at temperatures above 200 °C. Temperature above 300 °C results in structural changes in soil macromolecules. Fires' influence on the amount of organic carbon in soil is also traced [207]. This effect is expressed in a wide range from complete destruction of organic substance by fire in soil up to 30 % of surface layer increase due to dry leaves (needles) and partially burnt vegetation particles from forest stand canopy. Sometimes a dramatic reduction of organic substance amount is observed due to changing of physical-chemical properties of soil after (for example, hydrophobicity). After-fire erosion processes cause destruction of the upper soil layer and erosion-controlled process of underground root system functioning. Increase of organic substance amount is observed during controlled fires [207]. C/N ratio in the after-fire soil is usually less than in the initial soil. A changed organic substance of soil is called pyromorphic humus [207]. Pyrograms of soil samples from different formations of pine forest are given in Fig. 3.25: not exposed to fire (I) and burnt due to fires (II).

Pyrolysis products are marked by corresponding numbers in Fig. 3.25. Explanation of names is given in Table 3.18.

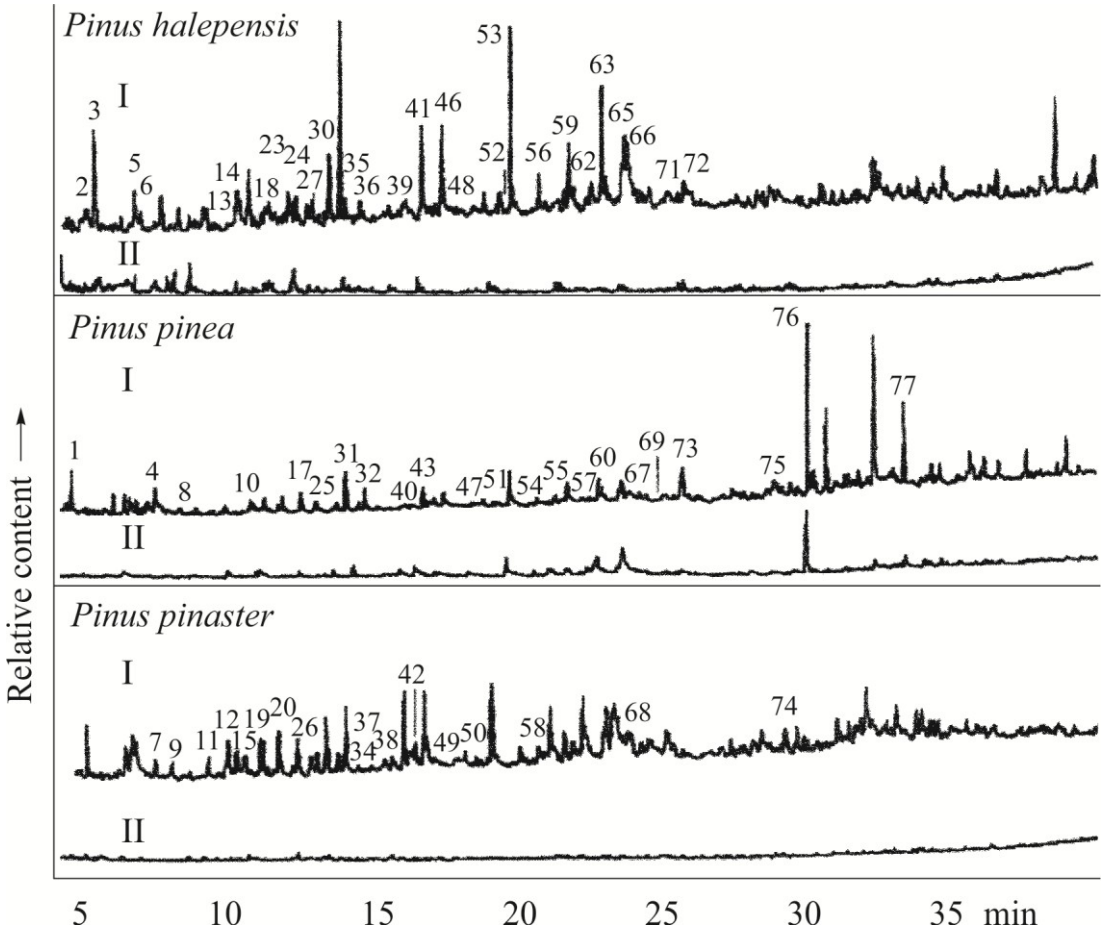

Fig. 3.25. Pyrograms of soil samples from different formations of pine forest [207]

Table 3.18. Pyrolysis products, found in soil samples [207]

1. Benzene	11. 2,3-Dihydro-5-methylfuran-2-one
2. 2-Methyl-2- Cyclopentene-1-one	12. 5-Methyl-2-Furfuraldehyde
3. Toluene	13. Benzyl alcohol
4. Furfural	14. Benzaldehyde
5. 3-Methyl-1H- Pyrrole	15. Phenol
6. 2-Hydroxymethylfuran	16. 5-Methyl-2- Furfuraldehyde
7. Styrene	17. 4-Hydroxy-5,6-dihydro-(2H)- pyran-2-ones
8. Cyclopent-1-ene-3,4-dione	18. 5,6- Dihydropyran- 2,5-dione
9. 2-Methyl-2-cyclopent-1-ene	19. 3-Hydroxy-2-Methyl-2-cyclopentene-1one
10. 2-Acetylfuran	20. 2,4- Dihydropyran -3

Continuation of Table 3.18

21. 2-Methoxytoluene
22. 2-Hydroxy-3-Methyl-2-cyclopentene-1-one
23. 4-Isopropyltoluene
24. Dimethylcyclopentene
25. Hydroxymethyldihydropyranone
26. 5-Ethyl-2-Furfural
27. *Ortho*-Cresol
28. 2-Furancarbonic acid methylester
29. *Para*-Cresol
30. 2,6-Dimethylphenol
31. Guaiacol
32. Levoglucosan
33. 3-Hydroxy-2-Methyl-(4H)-pyran-4-one
34. Dimethyldihydropyran
35. Phenylacetonitrile
36. 3-Hydroxy-di-methyl-(4H)-pyran-4-one
37. 2,4-Dimethylphenol
38. Benzoic acid
39. 4-Ethylphenol
40. Catechol
41. 2-Acetoxy-5-ethylfuran
42. 3,5-Dihydroxy-2-methyl-(4H)-pyran-4-one
43. Methylguaiacol
44. 5-Hydroxy-2-furfuraldehyde
45. Metoxymethylbenzene
46. 4-Vinylphenol
47. 4-Methylcatechol
48. 4-Ethyl-2-Methylphenol
49. 4-Ethylguaiacol
50. 4- Hydroxybenzyl alcohol
51. Indole
52. 1,4-Dideoxy-D-glicerohex-1-enopyranos-3-ulose
53. Vinylguaiacol
54. *Trans*- Propenylphenol
55. 2,6-Dimethoxyphenol
56. Eugenol
57. 4-Propylguaiacol
58. 3-Methylindole
59. Vanillin
60. *Cis*-Isoeugenol
61. 4- Hydroxyacetophenone
62. Homovanillin
63. *Tran*- Isoeugenol
64. 1-(4-Hydroxy-3-methoxyphenyl) propene
65. Acetovanillone
66. Vanillic acid methyl ester
67. 4-Ethyl-2,6-dimethoxyphenol
68. Guaiacyl acetone
69. 2,6-Dimethoxy-4-vinylphenol
70. 1,6-Anhydro-b-Glucofuranose
71. Guaiacol propane-2-one
72. Propiovanillone
73. Guaiacylvinyl-2-one
74. *Trans*-Coniferyl aldehyde
75. Retene
76. Myristic acid
77. Palmitic acid

Forest fire accidents influence the microbiological communities and soil organic substance and the entire soil dynamics. After fires a content of nutrient substances increases in soil, mainly in the form of water-soluble ashes components, which become available for living organisms. Increase of nitrogen-fixing bacteria presence is also observed after forest fires [208], growth of mineralization process rate in soils under pine forest stand (*Pinus Silvestris*) [209]. Changes in humus chemical properties under the fire effect serve the reason for changes in microbiological communities [210]. Chart of hypothetical process, taking place in organic substance of the Mediterranean forests soils (oak), exposed to forest fires, is given in Fig. 3.26.

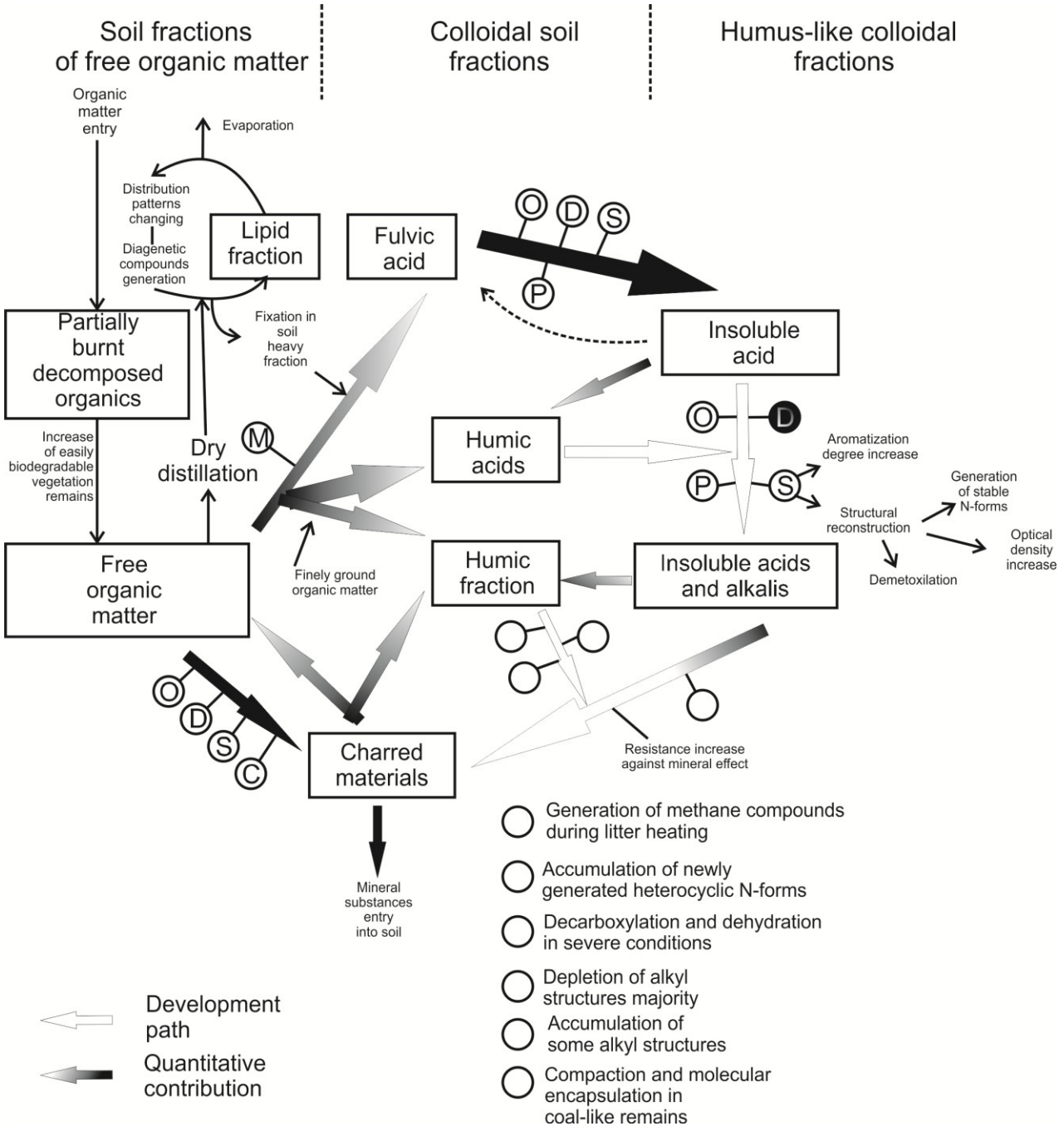

Fig. 3.26. Hypothetical chart of processes, taking place in the organic substance of the Mediterranean forest soils, subject to forest fires [207]

Free soil lipids are present in a wide range of hydrophobic substances from fatty acids to such complex substances as styrenes, terpenes, etc. After a forest fire the lipid fraction (after extraction) was six times higher than in the undisturbed territory [211, 212]. The given difference is explained by translocation of organic substances into the soil as a result of litter or biomass burning [213, 214]. After natural fires and laboratory experiments a relative increase of humic fraction excess in the tested soil is observed [209].

3.9. Effect of Forest Fires on Phytocenoses

Forest fires also have effect on forest phytocenoses [215]. In ancient times it would be practically impossible that a fire occurred in the same area more than twice in a millennium [216, 217]. Today fires can start in one and the same area twice in a decade, and their majority is associated with man-caused reasons [218]. This process, inter alia, leads to forest territory fragmentation into separate landscapes and death of trees [219—221]. The main hypotheses of trees' death due to fire activity include [222]:

1. Death of trees — a direct function of forest fires severity [223].

2. Increase of the period, during which trees fall after a forest fire, up to 1—2 years.

These hypotheses were tested in the region of the central Brazilian Amazonia, containing a whole mosaic of burnt and unburnt forest areas [222]. Forest fires seriously change the forest structure, its composition and dynamics in the absence of other disturbing factors, such as selective forest logging or forest fragmentation. Information on what vegetation parts respond to forest fire effect is given in Table 3.19 [224].

Table 3.19. Vegetation response to the forest fire effect [224]

Vegetation structures	Definition	Potential factors, associated to a fire response	Examples
Foliage	Leaves and needles	Moisture content, thickness, shape, leaf's area	Chamise
Crowns	Sum of Leaves and needles	Density and height of a crown	Pine tree
Tree bark	Dead, protection layer around the trunk	Bark thickness and its density, volatile substances	Pine tree
Roots	Underground structures, absorbing water and nutrient substances, strengthening the tree	Heat value and duration for depth below the surface	Mountainous misera

Different conceptual models of a particular vegetation type response to a forest fire for the purpose of fire effect prediction for a specific type or an entire vegetation community [225]. Microorganisms [226], animals, living in the trees, ad some bird kinds [227] die because of forest fires.

A special interest is given to global changes of ecological functions of boreal forests due to their disturbance by fires [228]. Ecological functions of forests include protection natural waters from chemical substance pollution, oxygen generation and carbon-dioxide absorption, protection of river and lake slopes from washout and their reinforcement, soil protection against erosion and deflation, even distribution of seasonal and increase of annual river годового river run-off, improvement of water conditions, landscape micro- and mesoclimate, reclamation of hydrological and chemical properties of washed out soils [228].

In ordinary years about 10 thous. fires arise in the area of 2—3 mln.ha in the Eurasian boreal forests. In the extreme years their number increases up to 30 thous., and area up to 10 mln.ha [229]. Scales of after-fire species shift are given in Table 3.20.

Shift of coniferous forests, described by a high environmental effect, to the derivative small-leaved ones, which ecological role is much lower happened in many landscapes of the Siberian boreal zone due to fires in a vast (prevailing in some landscapes) forest area [230].

Table 3.20. Scales of after-fire species shift in plain landscapes of the Pre-Yenisei part of West-Siberian Plain [228]

Landscape	Area, mln.ha			Disturbance of forests by fires, %
	landscapes	Primary forests	Derivative of after-fire forests	
Kas-Yenisei	0.61	0.42	0.19	32
Ket	1.11	0.39	0.72	65
Ulu-Yul-Chulym	1.89	0.83	1.06	56
Lower-Chulym	0.18	0.06	0.12	66
Kemchug-Chulym	1.14	0.88	0.26	23
Chet	0.29	0.09	0.20	67
Chulym-Ket-Ob	0.04	0.01	0.03	67
Total area of derivative forests 2.58				
Average disturbance by fires 54				

3.10. Effect of Forest Fires on People's Health

Forest fires also have effect on people's health. A population research was done regarding the smoke impact of forest fires on people's health in Indonesia [231]. Moreover, a research of aerosol content in the air was done by means of satellite technologies (Fig. 3.27, 3.28). Year of 1997 was the worst regarding the forest fire situation.

Large areas were destroyed on the Kalimantan and Sumatra islands. Some parts of the islands were covered with a smoke fog during several months. In Brunei, Singapore, Malaysia, Thailand and Vietnam the damage caused by forest fires was at least 4.5 billion dollars. A serious damage was caused to people's health, and population of Indonesia is deemed to suffer most of all [232].

Atmospheric air quality, containing smoke particles and gaseous compounds from forest fires, is the factor which increases a risk of death and influences the respiratory diseases occurrence [233—236]. Here the size of particle and gaseous compounds presence are important. Risk assessment of forest fires' smoke impact on human health was carried out [237]. One of the established facts is increase of particles content in the air causes increase of asthma episodes (Fig. 3.29).

Majority of researches were meant to study how forest fires effect on people's health during a short period after a forest fire incident [238]. According to these data, different bronchitis forms and bronchial asthma prevail (Table 3.21).

Combination of domestic survey results, which was done in 1993, when there were no serious forest fires, and data of 1997 [231], enabled to estimate the scale of fires' negative effect on population health in Indonesia. Besides, ground and satellite surveys of air quality were done. Joint analysis of medical data and air quality survey results speaks of coincidence of peaks of asthmatic attack cases in emergency centers.

Researchers of many countries are concerned of effect of forest fires on air quality [240—243].

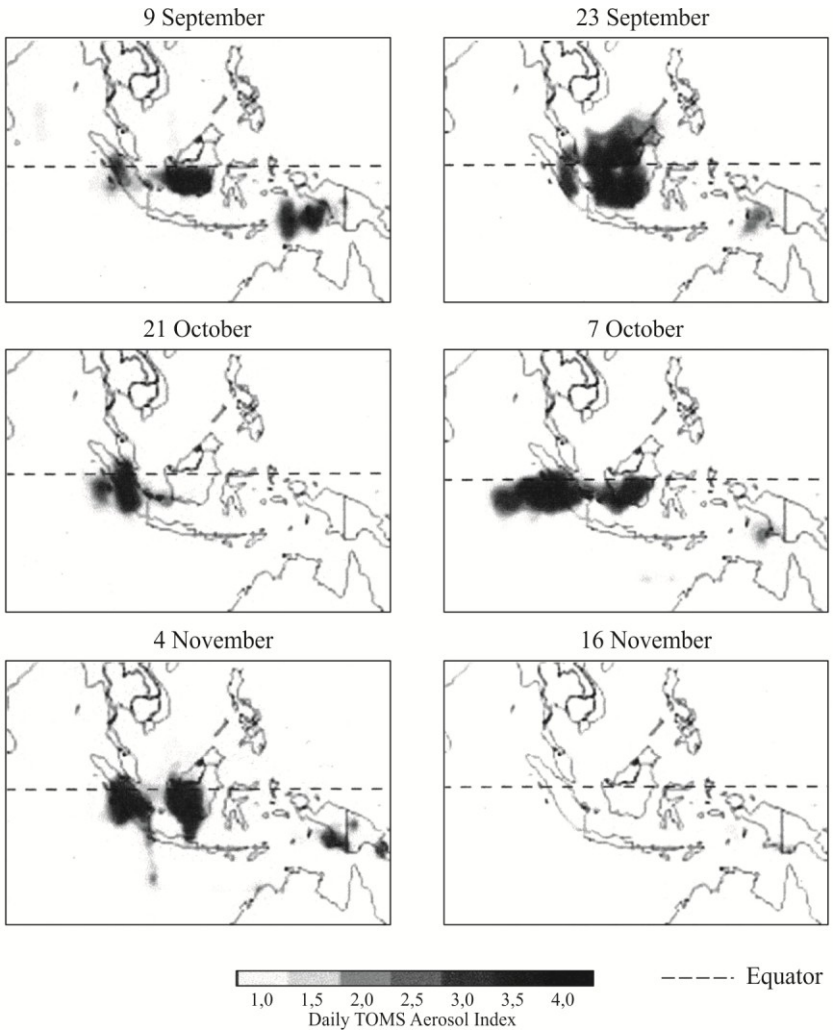

Fig. 3.27. Daily TOMS Aerosol Index for the period from 9 September till 16 November 1997 [231]

Table 3.21. Smog's effect on people's health (Indonesia, September—November 1997) [239]

Province	Number of population, subject to risk	Number of cases		
		Death	Asthma	Bronchitis
Riau	1701000	75	41028	7995
West Sumatra	2411000	106	58164	11332
Jambi	1478000	65	35650	6947
South Sumatra	2355000	104	56803	11069
West Kalimantan	1478000	74	44574	8686
Central Kalimantan	716000	29	17574	3366
South Kalimantan	1733000	69	41800	8145
East Kalimantan	118000	5	2846	555
Total	12360000	527	298125	58095

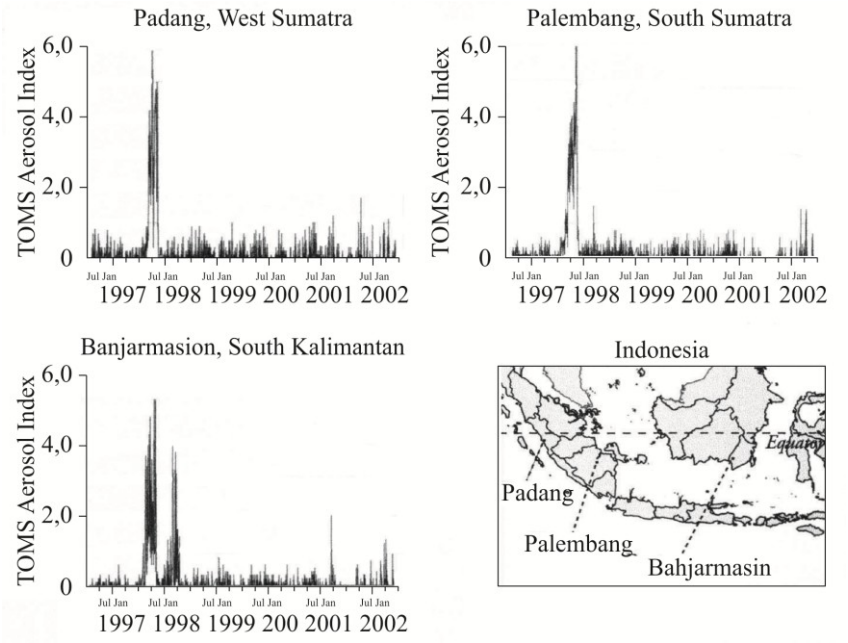

Fig. 3.28. Daily TOMS Aerosol Index for the period from July 1996 till July 2002 for major cities of the provinces [231]

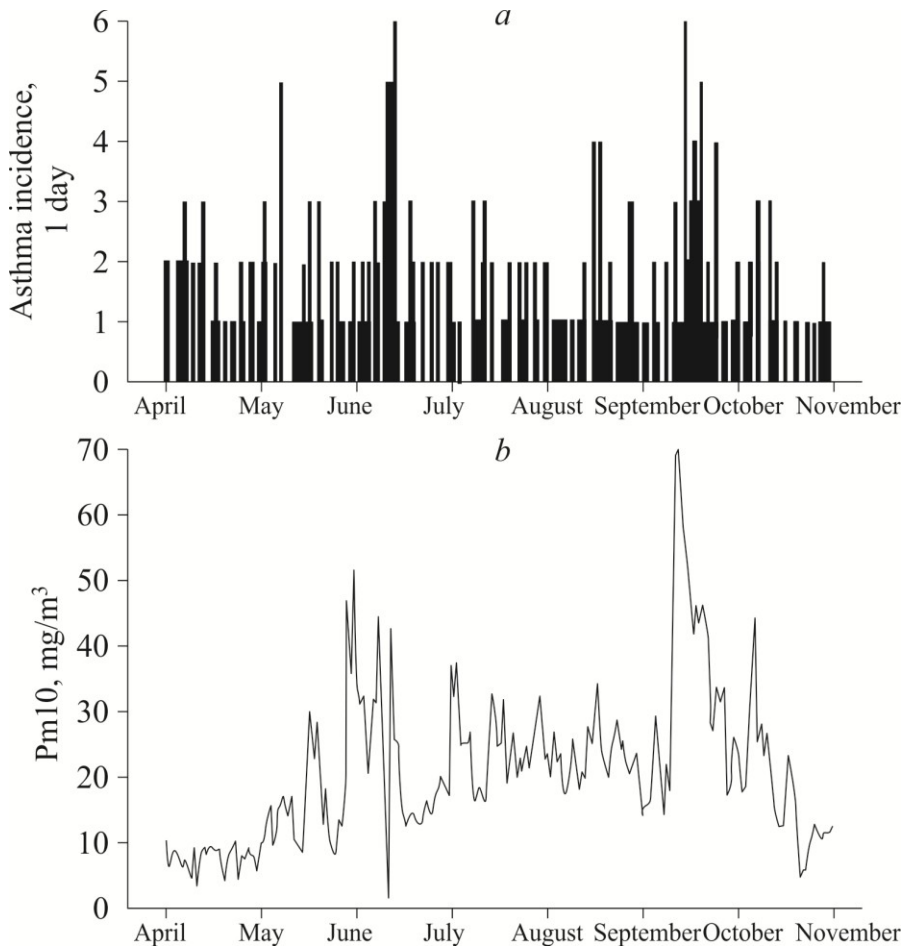

Fig. 3.29. Cases of asthma episodes in the emergency center of Royal Darwin Hospital (*а*) and average daily concentration of PM_{10} particles (*б*) [237]

3.11. Method for Estimation of Health Hazard Probability from Forest Fires

To solve medical and environmental problems, prediction of forest fires consequences in particular, it is suggested that area of questionnaire application should be wider. There are criteria required for determining of treatment effectiveness and clinical surveys, i.e. methods of the life quality assessment [244—254] (See. Annex), based on the questionnaires. Purpose of the method is to determine a probability of health hazard for population from forest fires. To solve the stated problems, integrated mathematical modeling and sociological survey methods were applied [253—256].

Basic provisions of probability theory were used during method development [257]. Mathematical modeling methods were widely applied in different fields of science and technology [258], including for social processes survey [259]. Data of sociological surveys of population can serve as input statistical information for model development [260].

Major harmful factors of a forest fire include [261]: physical and chemical (increased ambient air temperature, light and heat radiation, presence of carbon monoxide and dioxide in the smoke, burning particles of forest fuels); psychophysical (neuropsychological and physical loads), illnesses and damage to different systems and organs of human body — stress, burns, traumatism, carbon monoxide poisoning, death, allergy, asphyxia, provoking of chronic disease aggravation and attacks. A probability model of a number of diseases (traumas), as a result of forest fire's harmful factors effect (Fig. 3.30) [255].

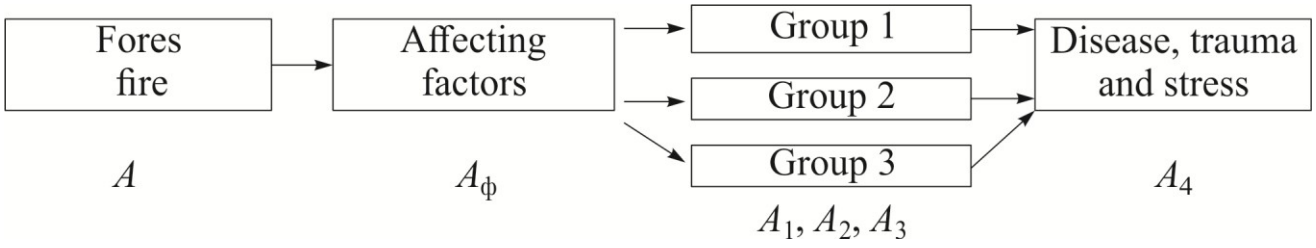

Fig. 3.30. Sequence of forest fire's effect on the population [255]
See explanation in the text.

The following events are considered: A — active forest fire, $A_ф$ — effect of forest fire's harmful factors on people, A_1 — person's belonging to group 1, A_2 — person's belonging to group 2, A_3 — person's belonging to group 3 (Group 1 — citizens, which are constantly on the territory of a locality, 2 — engaged in work activities at the adjacent territory to locality, 3 — engaged in work activities in the forest-covered territory), A_4 — occurrence of disease, physical or psychological trauma.

As a result of analysis of forest fire's harmful factors, geography of location, features of population and mechanism of disaster development can be recthe following formula for determining the probability of causing harm to people's health by forest fires [255]:

$$P(A, A_ф, A_1, A_2, A_3, A_4) = P(A, A_ф, A_1, A_2, A_3)\cdot P(A_4/A, A_ф, A_1, A_2, A_3) =$$
$$= P(A, A_ф)\, P(A_1, A_2, A_3/A, A_ф)\, P(A_4/A, A_ф, A_1, A_2, A_3,) =$$
$$= P(A)\, P(A_ф/A)\, P(A_1, A_2, A_3/A, A_ф)\, P(A_4/A, A_ф, A_1, A_2, A_3,);$$

$$P\,(A_1, A_2, A_3/A, A_ф) = P\,(A_1/A, A_ф) + P(A_2/A, A_ф) + P(A_3/A, A_ф),$$

where $P(A)$ — probability of a forest fire; $P(A_ф/A)$ — probability of a forest fire's harmful effect; $P(A_1/A,\ A_ф)$ — probability of that a person belongs to group 1; $P(A_2/A,\ A_ф)$ — probability of that a person belongs to group 2; $P(A_3/A,\ A_ф)$ — probability of that a person belongs to group 3; $P(A_4/A, A_ф, A_1, A_2, A_3,)$ — probability of the damage to health provided that forest fires exist. For calculation of probabilities numerical values, statistical data of forestries, population employment services and results of opinion polls can be used.

Numerical calculations of probability of asthma-like symptoms occurrence and asthma attacks of one locality residents in the Kemerovo region. Bronchial asthma is one of the common chronic diseases, to which people of any age are subject. According to epidemiological survey data, a considerable growth of this disease incidence has taken place lately both among children and adults [262]. Prevailing of severe forms of bronchial asthma is also registered and confirmed by death rate growth and increase of patient hospitalization cases. One of auxiliary tools for this pathology diagnostics are screening questionnaires. They help to estimate prevalence of asthma-like symptoms and asthma attacks among large population groups [262].

The method has a practical value and can be applied in organizations, monitoring the state of public health. The suggested method can be included as a component of the system of forest fire danger prediction that will allow estimating consequences of forest fires in terms of their impact on people's health that live in the locality [255].

REFERENCES

1. Grishin A.M. (1992) Mathematical modeling of forest fires and new methods of fighting them ними. Novosibirsk: Nauka, Sib.branch, 408 p. (In Russian)
2. Prange J.A., Gaus C., Weber R. et al. (2003) Assessing Forest Fire as a Potential PCDD/F Source in Queensland, Australia // Environmental Science & Technology, 37(19), 4325—4329.
3. Dioxin and furan inventories. National and regional emissions of PCDD/PCDF. Switzerland, Geneva: UNEP Chemicals, 1999. 116 p.
4. Czuczwa J.M., Hites R.A. (1984) Environmental fate of combustion-generated polychlorinated dioxins and furans // Environmental Science & Technology, 18, 444—450.
5. Tashiro C., Clement R.E., Stocks B.J. et al. (1990) Preliminary report: dioxins and furans in prescribed burns // Chemosphere, 20, 1533—1536.
6. Prange J.A., Cook M., Papke O. et al. (2002) PCDD/Fs in the atmosphere and combusted material during a forest fire in Queensland, Australia // Organohalogen Compounds, 59, 207—210.
7. Kim E.-J., Oh J.-E., Chang Y.-S. (2001) Does forest fire increase the PCDD/Fs level in soil? // Organohalogen Compounds, 50, 386—389.
8. Buckland S.J., Dye E.A., Leatham S.V., Taucher J.A. (1994) The levels of PCDDs and PCDFs in soil samples collected from conservation areas following bush fires // Organohalogen Compounds, 20, 85—89.
9. Martinez M., Diaz-Ferrero J., Marti R. et al. (2000) Analysis of dioxin-like compounds in vegetation and soil samples burned in Catalan forest fire. Comparison with the corresponding unburned material // Chemosphere, 41, 1927—1935.
10. Walsh P.J.J., Brimblecombe P., Creaser C.S., Olphert R. (1994) Biomass burning and polychlorinated dibenzo-p-dioxins and furans in the soil // Organohalogen Compounds, 20, 283—287.
11. Wunderli S., Zennegg M., Dolezal I. S. et al. (2000) Determination of polychlorinated dibenzo-p-dioxins and dibenzo-furans in solid residues from wood combustion by HRGC/HRMS // Chemosphere, 40(6), 641—649.
12. Nestrick T.J., Lamparski L.L. (1982) Isomer-specific determination of chlorinated dioxins for assessment of formation and potential environmental emission from wood combustion // Analytical Chemistry, 54, 2292—2299.
13. Dennis A., Fraser M., Anderson S., Allen D. (2002) Air pollutant emissions associated with forest, grassland, and agricultural burning in Texas // Atmospheric Environment, 36(23), 3779—3792.
14. Simoneit B.R.T., Schauer J.J., Nolte C.G. et al. (1999) Levoglucosan, a tracer for cellulose in biomass burning and atmospheric particles // Ibid., 33, 173—182.
15. Compilation of Air Pollution Emission Factors. V. I: Stationary Point and Area Sources. Fifth Edition, Ap-42, North Carolina: Research Triangle Park: US Environmental Protection Agency (EPA), 1995. 2038 p.
16. Evaluation of emissions from the open burning of land-clearing debris. EPA-600/R-96-128. US, North Carolina: Research Triangle Park, US Environmental Protection Agency (EPA), 1996. 115 p.
17. Compilation of Air Pollution Emission Factors. V. I. Stationary Point and Area Sources. Fourth Edition. AP-42. North Carolina: Research Triangle Park: US Environmental Protection Agency (EPA), 1985. 827 p.
18. Darley E.F., Burleson F.R., Mateer E.H. et al. (1966) Contribution of burning agricultural wastes to photochemical air pollution // J. Air Pollution Control Association, 11, 685—690.
19. Evans L.F., King N.K., Packham D.R., Stephens E. T. (1974) Ozone measurements in smoke from forest fires // Environmental Science & Technology, 8(1), 75—76.
20. Vines R.G., Gibson L., Hatch A.B. et al. (1971) On the nature, properties and behavior of bushfire smoke. Technical Paper 1. CSIRO Aust. Dip. Appl. Chem. Tech. Paper. N 1. 5 p.
21. Korontzi S. (2005) Seasonal patterns in biomass burning emissions from Southern African vegetation fires for the year 2000 // Global Change Biology, 11(10), 1680—1700.
22. Ludwig J., Marufu L.T., Huber B. et al. (2003) Domestic combustion of biomass fuels in developing countries: A major source of atmospheric pollutants // J. Atmos. Chem., 44(1), 23—37.

23. Lemieux P.M., Lutes C.C., Santoianni D.A. (2004) Emissions of organic air toxics from open burning: a comprehensive review // Progress in Energy and Combustion Science, 30(1), 1—32.
24. Oros D.R., Simoneit B.R.T. (2001) Identification and emission factors of molecular tracers in organic aerosols from biomass burning. P. 1. Temperature climate conifers // Appl. Geochem., 16(13), 1513—1544.
25. Oros D.R., Simoneit B.R.T. (2001) Identification and emission factors of molecular tracers in organic aerosols from biomass burning. P. 2. Deciduous trees // Ibid., 16(13), 1545—1565.
26. Masclet P., Cachier H., Liousse C., Wortham H. (1995) Emissions of polycyclic aromatic hydrocarbons by savanna fires // J. Atmos. Chem., 22(1—2), 41—54.
27. Gullett B., Touati A. (2003) PCDD/F emissions from forest fires // Atmospheric Environment, 37, 803—813.
28. Yamasoe M.A., Artaxo P., Miguel A.L.H., Allen A.G. (2000) Chemical composition of aerosol particulates from direct emissions of vegetation fires in the Amazon Basin: watersoluble species and trace elements // Atmospheric Environment, 34(10), 1641—1653.
29. Barber T.R., Lutes C.C., Doorn M.R.J. et al. (2003) Aquatic ecological risks due to cyanide releases from biomass burning // Chemosphere, 50, 343—348.
30. Radojevic M. (2003) Chemistry of forest fires and regional haze with emphasis on Southeast Asia // Pure and Applied Geophysics, 160(1—2), 157—187.
31. Crutzen P.J., Andrea M.O. (1990) Biomass burning in the tropics: impact on atmospheric chemistry and biogeochemical cycles // Science, 250, 1669—1678.
32. Root B.R. (1976) An estimate of annual global atmospheric pollutant emissions from grassland fires and agricultural burning in the tropics // The Professional Geographer, 28(4), 349—352.
33. Muraleedharan T.R., Radojevic M., Waugh A., Caruana A. (2000) Emissions from the combustion of peat: an experimental study // Atmospheric Environment, 34(18), 3033—3035.
34. Statheropoulos M., Karma S. (2007) Complexity and origin of the smoke components as measured near the flame-front of a real forest fire incident: A case study // J. Analytical and Applied Pyrolysis, 78(2), 430—437.
35. Zhang Y.-H., Wooster M. J., Tutubalina O., Perry G.L.W. (2003) Monthly burned area and forest fire carbon emission estimates for the Russian Federation from SPOT VGT // Remote Sensing and Environment, 87(1), 1—15.
36. Goldammer J.G., Furyaev V.V. (1996) Fire in ecosystems of Boreal Eurasia: Ecological impacts and links to the global system // Fire in Ecosystems of Boreal Eurasia. / Eds. J. G. Goldammer, V. V. Furyaev. Dordrecht: Kluwer, P. 1—20.
37. Fraser R.H., Li Z. (2002) Estimating fire-related parameters in boreal forest using SPOT VEGETATION // Remote Sensing of Environment, 82, 95—110.
38. Price C., Rind D. (1994) The impact of a $2 \times CO_2$ climate on lightning caused-fires // J. Climate, 7(10), 1484—1494.
39. Andreae M.O., Merlet P. (2001) Emission of trace gases and aerosols from biomass burning // Global Biogeochemical Cycles, 15, 955—966.
40. Wotawa G., Trainer M. (2000) The influence of Canadian forest fires on pollutant concentrations in the United States // Science, 288, 324—328.
41. Amiro B.D., Todd J.B., Wotton B.M. et al. (2001) Direct carbon emissions from Canadian forest fires, 1959 to 1999 // Canadian J. Forest Res., 31, 512—525.
42. Duncan B.N., Martin R.V., Staudt A.C., Yevich R., Logan J.A. (2003) Interannual and seasonal variability of biomass burning emissions constrained by satellite observations // J. Geophys. Res., 108, 4100—4110.
43. Choi C.-D., Chang Y.-S., Park B.-K. (2006) Increase in carbon emissions from forest fires after intensive reforestation and forest management programs // Science the Total Environment, 372(1), 225—235.
44. Gupta P.K., Prasad V.K., Sharma C. et al. (2001) CH_4 emissions from biomass burning of shifting cultivation areas of tropical deciduous forests — experimental results from ground-based measurements // Chemosphere — Global Ghange Science, 3(2), 133—143.
45. Global biomass burning: atmospheric, climate and biospheric implications / Ed. J. S. Levine. Cambridge, MA: MIT Press. 1991. 569 p.

46. Werf G.R. van der, Randerson J.T., Collatz C.J. et al. Continental-scale Partitioning of fire emissions during the 1997 to 2001 El Nino/La Nina period // Science. 303(1), 73— 76.
47. Keeling C.D., Bacastow R.B., Carter A.F. et al. (1989) A three dimensional analysis of atmospheric CO_2 transport based on observed winds. P. I.: Analysis of observational data // Aspects of Climate Variability in the Pacific and the Western Americas/ Ed. D. H. Peterson/ Geophys. Monogr. 55 / American Geophysical Union, Washington, DC, P. 165—236.
48. Conway T.J., Tans P.P., Waterman L.S. et al. (1994) Evidence for interannual variability of the carbon cycle from the National Oceanic and Atmospheric Administration. Climate monitoring and diagnostics laboratory Global Air Sampling Network // J. Geophys. Res. 99, 22831—22855.
49. Battle M., Bender M., Tans P.P. et al. (2000) Global carbon sinks and their variability inferred from atmospheric O_2 and $\delta^{13}C$ // Science, 287, 2467—2470.
50. Dlugokencky E.J., Steele L.P., Lang P.M., Masarie K.A. (1994) The growth rate and distribution of atmospheric methane // J. Geophys. Res., 99, 17021—17043.
51. Dlugokencky E.J., Walter B.P., Masarie K.A. et al. (2001) Measurements of an anomalous global methane increase during 1998 // Geophys. Res. Letters, 28(3), 499—502.
52. Dolgov A.A., Safonov V.R. (2000) Laboratory studies of carbon dioxide emission at burning of forest fuel // Sopryazhennie zadachi mekhaniki i ekologii: Selected reports of International conference. Tomsk: Izd-vo Tom. un-ta, P. 137-148. (In Russian)
53. Kuznetsov V.I., Kozlov N.I., Khomyakov P.M. (2005) Mathematical modeling of forest evolution for forestry management. Moscow: LENAND, 232 p. (In Russian)
54. Grishin A.M. Dolgov A.A., Tsymbalyuk A.F. (2006) Calculation of radionuclides emission from forest fires in radioactive phytocenoses // Ekologicheskie pribory i sistemy, 1, 40—44. (In Russian)
55. Chistyakov R.F., Radun D.V. (1972) Heat engineering measurements and instruments. Moscow: Vyssh. shkola, 392 p. (In Russian)
56. Munthe J., McElroy W.J. (1992) Some aqueous reactions of potential importance in the atmospheric chemistry of mercury // Atmospheric Environment, 26A, 553—557.
57. Lindquist O., Rodhe H. (1985) Atmospheric mercury — a review // Tellus, 37B, 136—159.
58. Bullock O.R. (2000) Current methods and research strategies for modeling atmospheric mercury // Fuel Processing Technology, 65—66, 459—471.
59. Sigler J.M., Lee X., Munger W. (2003) Emission and long-range transport of gaseous mercury from a large-scale canadian boreal forest fire // Environmental Science & Technology, 37(19), 4343—4347.
60. Lavoie L., Sirois L.J. (1998) Vegetation changes caused by recent fires in the Northern boreal forest of Eastern Canada // J. Vegetation Science, 9(4), 483—492.
61. Lindberg S.E., Hanson P.J., Meyers T.P., Kim K.-H. (1998) Air/surface exchange of mercury vapor over forests — the need for a reassessment of continental biogenic emissions // Atmospheric Environment, 32(5), 895—908.
62. Cinnirella S., Pirrone N. (2006) Spatial and temporal distributions of mercury emissions from forest fires in Mediterranean region and Russian Federation // Ibid., 40, 7346—7361.
63. Roulet M., Lucotte M., Farella N. et al. (1999) Effects of recent human colonization on the presence of mercury in Amazonian ecosystems // Water, Air and Soil Pollution, 112, 297—313.
64. Friedli H.R., Radke L.F., Lu J.Y. et al. (2003) Mercury emissions from burning of biomass from temperate North American forests: laboratory and airborne measurements // Atmospheric Environment, 37, 253—267.
65. Ward D.E., Susott R.A., Kauffman J.B. et al. (1992) Smoke and fire characteristics for Cerrado and deforestation burns in Brazil BASE-B experiment // J. Geophys. Res., 97(D13), 14601—14619.
66. Ward D.E., Hao W.M., Susott R.A. et al. (1996) Effect of fuel composition on combustion efficiency and emission factors for African savanna ecosystems // J. Geophys. Res., 101(D19), 23569—23576.
67. Ferrara R., Maserti B.E., Andersson M. et al. (1997) Mercury degassing rate from mineralized areas in the Mediterranean basin // Water, Air and Soil Pollution, 93, 59—66.

68. Engle M.A., Gustin M.S., Zhang H. (2001) Quantifying natural source mercury emissions from the Ivanhoe Mining District, north-central Nevada, USA // Atmospheric Environment, 35, 3987—3997.
69. Zehner R.E., Gustin M.S. (2002) Estimation of mercury vapor flux from natural substrate in Nevada // Environmental Science & Technology, 36, 4039—4045.
70. Iglesias T., Cala V., Gonzalez J. (1997) Mineralogical and chemical modifications in soils affected by a forest fire in the Mediterranean area // Sci. Total Environment, 204(1), 89—96.
71. Woodruff L.G., Harden J.W., Cannon W.F., Gough L.P. (2001) Mercury loss from the forest floor during wildland fire // Eos Transactions AGU, 82(47), Fall Meeting Suppl., Abstract B32B-0117. P. 199.
72. Yoschenko V.I., Kashparov V.A., Levchuk S.E. et al. (2006) Resuspension and redistribution of radionuclides during grassland and forest fires in the Chernobyl exclusion zone: P. II. Modeling the transport process // J. Environmental Radioactivity, 86(2), 260—278.
73. Kashparov V.A., Lundin S.M., Kadygrib A.M. et al. (2000) Forest fires in the territory contaminated as a result of the Chernobyl accident: radioactive aerosol resuspension and exposure of firefighters // J. Environmental Radioactivity, 51, 281—298.
74. Yoschenko V.I., Kashparov V.A., Protsak V.P. et al. (2006) Resuspension and redistribution of radionuclides during grassland and forest fires in the Chernobyl exclusion zone. P. I. Fire experiments // J. Environmental Radioactivity, 86, 143—163.
75. Johansen M.P., Hakonson T.E., Whicker F.W., Breshears D.D. (2003) Pulsed redistribution of a contaminant following forest fire: Cesium-137 in runoff // J. Environmental Quality, 32(11), 2150—2157.
76. Azarov R.I., Odnolko A.A. (1996) Assessment of fire danger territories, polluted by radionuclides // Lesnoye khozyaystvo, 3, 15—16.
77. Paliouris G., Taylor H.W., Wein R.W. et al. (1995) Fire as agent in redistributing fallout ^{137}Cs in Canadian forest // Sci. Total Environment, 1—3, 153—166.
78. Azarov R.I. (1996) Air pollution with ^{137}Cs from forest fires in the Chernobyl zone // Radiation Biology. Radioecology, 36(4), 506—515.
79. Kuchma N.D., Bednaya R.M., Usar L.R., Tereschenko O.N. (1994) Effect of fires on radionuclides distribution and migration in forest cenoses // Reports of Intl. sci-tech. conference «Summary of 8-year work on accident consequences elimination on ChNPS». Zelenyi myr. P. 166—167. (In Russian)
80. Scherbov B.L., Strakhovenko V.D. (2002) Behavior of ^{137}Cs and heavy metals in forest fires in the Extreme North // Works of Intl. Conf. Enviromis-2002. Tomsk: Izd-vo Tom. CNTI, P. 261—264. (In Russian)
81. Shilov I.A. (2003) Ecology: Textbook for biol. and med. schools. 4-th edition. Moscow: Vysshaya shkola, 512 p. (In Russian)
82. Semenchenko B.A. (2002) Physical meteorology. M.: Aspekt Press, 415 p. (In Russian)
83. Semenov M.Yu. (2002) Acid fallout in the territory of Siberia: Calculation and mapping of permissible loads. Novosibirsk: Nauka, SIF RAS, 143 p. (In Russian)
84. Aerosols of Siberia / Rev. K. P. Kutsenogiy. Novosibirsk: Izd-vo SB RAS, 2006. 548 p. (Integration projects of SB RAS, Issue 9). (In Russian)
85. Kosarev V.P., Andryuschenko T.T. (2007) Forest meteorology with basics of climatology: Uchebnoe posobie. 2-e izd., ispr. i dop. / Pod red. B. V. Babikova. SPb.: Lan, 288 p. (In Russian)
86. Mathematical modeling of burning and explosion of high-energy systems / Rev. I. M. Vasenina. Tomsk: Izd-vo Tom. un-ta, 2006. 322 p. (In Russian)
87. Trushina T.P. (2003) Ecological basics of nature management. 2nd edition. Rostov n/D: Feniks, 384 p. (In Russian)
88. Hygienic standards GN 2.1.6.1338-03. Maximum permissible concentrations (MPC) of pollutants in the air of populated places. Moscow: Minzdrav RF, 2003. 43 p. (In Russian)
89. Hygienic standards GN 2.1.5.1315-03. Maximum permissible concentrations (MPC) of chemical substances in water of water bodies for household and utility water use. Moscow: Minzdrav RF, 2003. 152 p. (In Russian)

90. Soviet Encyclopedia / Chief editor. A. M. Prokhorov. 3-rd editions. M.: Sov. Entsiklopediya, 1985. 1600 p. (In Russian)
91. GN 2.1.7.2042-06. Approximate permissible concentrations. Moscow: Minzdrav RF, 2006. 12 p. (In Russian)
92. Berlyand M.E. (1975) Modern problems of atmospheric diffusion and air pollution. Leningrad: Gidrometeoizdat, 448 p.
93. Oке T.P. (1982) Climate of the boundary layer. Leningrad: Gidrometeoizdat, 358 p. (In Russian)
94. Belikov D.A. (2006) Parallel realization of mathematical model of atmospheric diffusion for research of distribution of primary and secondary air pollutants above urban territory: Avtoref. diss.. … Phd. Phys.-Mat. Sci. Tomsk: TSU, 20 p. (In Russian)
95. RD 52.04.186-89 Guidelines for air pollution control. Moscow: Goskomgidromet, 1989. 327 p. (In Russian)
96. Carruthers D.J., McKcown A.M., Hall D.J., Porter S. (1999) Validation of ADMS against wind tunnel data of dispersion from chemical warehouse fires // Atmospheric Environment, 33, 1937—1953.
97. Elbern H., Schmidt H. (2001) Ozone episode analysis for four-dimension variation chemistry data assimilation // J. Geophys. Res., 106, 3569—3590.
98. Tolstykh M.A. (2001) Semi-Lagrangian atmospheric model with high resolution for a numerical weather forecast // Meteorologiya i gidrologiya, 4, 5—15. (In Russian)
99. Ilyushin B.B., Kurbatskiy A.F. (1996) Modelling of impurity distribution in convective boundary layer // Izv. RAS. Physics of atmosphere and ocean, 32(3), 307—321. (In Russian)
100. Starchenko A.V. (2004) Numerical modelling of urban and regional atmosphere and its effect estimation on impurity transfer // Vychislitelnye tekhnologii, 9, special issue, p. 2., 98—108. (In Russian)
101. Nuterman R.B., Starchenko A.V. (2003) Modelling of air movement in a street canyon // Atmospheric and Oceanic Optics, 16(5—6), 523—526. (In Russian)
102. Walton A., Cheng A.Y.S., Yeung W.C. (2002) Large-Eddy Simulation of pollution dispersion in a urban street canyon. P. I: Comparison with field data // Atmospheric Environment, 36, 3601—3613.
103. Atnospheric turbulence and modelling of impurity distribution / Rev. F. T. M. Niestadt and H. Van Don. Leningrad: Gidrometeoizdat, 1985. 350 p. (In Russian)
104. Skurin L.I. (2004) Marching and parallel algorithms of Navier-Stokes equations integrationfor gas and fluid. SPb.: Izd-vo SPb. Un-ta, 165 p. (In Russian)
105. Andren A. (1990) Evolution of a turbulence closure scheme suitable for air pollution application // J. Applied Meteorology, 29, 224—239.
106. Klemp J., Skamarock W., Fuhrer O. (2002) Numerical consistency of metric terms in terrain-following coordinates // Monthly Weather Rev., 122, 2260—2272.
107. Scardovelli R., Zaleski S. (1999) Direct numerical simulation of free-surface and intefacial flow // Annual Review of Fluid Mechanics, 31, 567—603.
108. Kurbatskiy A.F. (2000) Lectures on turbulence. In 2 parts. P. 2. Novosibirsk: Izd-vo Novosibirskogo un-ta, 135 p. (In Russian)
109. Sagaut P. (2006) Large Eddy Simulation for Incompressible Flows. Third Edition. Berlin; Heidelberg, New York: Springer, 573 p.
110. Volkov K.N., Yemelyanov V.N. (2008) Modelling ща major eddies in turbulent streams computing. Moscow: Fizmatlit, 368 p. (In Russian)
111. Berlyand M.E. (1985) Forecast and management of atmospheric pollution. L.: Gidrometeoizdat, 168 p. (In Russian)
112. Boybei Z., Zanetti P. (1995) Numerical investigation of possible role of local meteorology in Bhopal Gas Accident // Atmospheric Environment, 29(4), 479—496.
113. Uliasz M. (1992) The atmospheric mesoscale dispersion modelling system // J. Applied Meteorology, 32, 139—149.

114. Hauglustaine D.A., Brasseur G.P., Levine J.S. (2000) Impact of the 1997 Indonesian fires on tropospheric ozone and its precursors // Biomass burning and its interrelationships with the climate system. V. 3. Netherlands: Springer. P. 87—99.
115. Brasseur G.P., Hauglustaine D.A., Walters S. et al. (1998) MOZART: a global chemical transport model for ozone and related chemical tracers. P. 1. Model description // J. Geophys. Res., 103, 265—289.
116. Trentmann J., Luderer G., Winterrath T. et al. (2006) Modelling of biomass smoke injection into the lower stratosphere by a large forest fire (Part I): reference simulation // Atmospheric Chemistry and Physics, 6(12), 5247—5260.
117. Herzog M., Oberhurber J.M., Graf H.-F. (2003) A prognostic turbulence scheme for the nonhydrostatic plume model ATHAM // J. Atmospheric Sciences, 60, 2783—2796.
118. Oberhuber J.M., Herzog M., Graf H.-F., Schwanke K. (1998) Volcanic plume simulation on large scales // J. Volcanol. Geotherm. Research, 87, 29—53.
119. Tang A., Reid N., Misra P.K. (2001) Development of a regional model for ozone forecasting and acidic deposition mapping // Preprints of 25th NATO/CCMS International Technical Meeting on Air Pollution Modelling and its Application. Belgium, Louvain-la-Neuve: Catholic University of Louvain, P. 27—32.
120. Azzi M., Johnson G.J., Cope M. (1992) An introduction to the Generic Reaction Set photochemica smog mechanism // Proceedings of 11th International Clean Air Environment Conference (5—9 July 1992). Brisbane: Clean Air Society of Australia and New Zeland, P. 451—462.
121. Baklanov A., Aloyan A. (2001) Modelling of atmospheric radioactive aerosol dynamics and deposition // Preprints of 25th NATO/CCMS International Technical Meeting on Air Pollution Modelling and its Application. Belgium, Louvain-la-Neuve: Catholic University of Louvain, P. 33—44.
122. Lavrov A., Utkin A.B., Vilar R., Fernandes A. (2006) Evaluation of smoke dispersion from forest fire plumes using lidar experiments and modelling // Int. J. Thermal Sciences, 45(9), 848—859.
123. Launder B.E., Spalding D.B. (1974) The numerical computations of turbulent flows // Comput. Methods Appl. Mech. Engrg., 3, 269—289.
124. Schlichting H. (1968) Boundary layer theory. N. Y.: McGraw-Hill, 120 p.
125. Patankar S.P., Spalding D.B. (1972) A calculation procedure for heat, mass and momentum transfer in three-dimensional parabolic flows // Int. J. Heat and Mass Transfer, 15, 1787—1806.
126. Bornoff R.B., Mokhtarzadeh-Dehghan M.R. (2001) A numerical study of interacting buoyant cooling-tower plumes // Atmospheric Environment, 35, 589—598.
127. Lee S., Cope M., Tory K. et al. (2001) The Australian air quality forecasting system: Modelling of a severe smoke event in Melbourne, Australia // Preprints of 25th NATO/CCMS International Technical Meeting on Air Pollution Modelling and its Application. Belgium, Louvain-la-Neuve: Catholic University of Louvain, P. 75—82.
128. Sahm P., Flocas H.A., Naneris Ch. et al. (2001) Estimating transboundary air pollution in South-Eastern Europe: A modelling strategy // Ibid. P. 83—90.
129. Wortmann-Vierthaler M., Moussiopoulos N. (1995) Numerical tests of a refined flux corrected transport advection scheme // Environmental Software, 10, 157—175.
130. Varinou M., Gofa F., Kallos G. et al. (2001) Photo-oxidation processes over the Eastern Mediterranean basin in summer // Preprints of 25th NATO/CCMS International Technical Meeting on Air Pollution Modelling and its Application. Belgium, Louvain-la-Neuve: Catholic University of Louvain. P. 99—106.
131. Gomez Tejedor J.A., Estrela M.J., Millan M.M. (2000) A Mesoscale Model Application to Fire Weather Winds // Int. J. Wildland Fire, 9(4), 255—264.
132. Pielke R.A., Cotton W.R., Walko R.L. et al. (1992) A comprehensive meteorological modelling system—RAMS // Meteorology and Atmospheric Physics, 49, 69—91.
133. Tripoli C.J., Cotton W.R. (1982) The Colorado State University 3D cloud/mesoscale model. Part I: General theoretical framework and sensitivity experiments // J. Recherches Atmospheriques, 16, 185—219.

134. Mahrer Y., Pielke R.A. (1977) A numerical study of the airflow over irregular terrain // Contrib. Phys. Atmos., 50, 98—113.
135. Tremback C.J., Tripoli G.J., Cotton W.R. (1985) A regional scale atmospheric numerical model including explicit moist physics and a hydrostatic time-split scheme // Proceedings of the 7th Conference on Numerical Weather Precipitation, P. 433—434.
136. ApSimon H.M., Warren R.F., Mediavilla-Sahagum A. (2001) Applying risk assessement techniques to air pollution modelling&abatement strategies // Preprints of 25th NATO/CCMS International Technical Meeting on Air Pollution Modelling and its Application. Belgium, Louvain-la-Neuve: Catholic University of Louvain, P. 131—139.
137. Belikov D.A. (2006) Parallel realization of atmospheric diffusion mathematical mode of for study of primary and secondary pollutants over urban territory. Dissertation … PhD.Phys.Math.Sci. Tomsk: TSU, 177 p. (In Russian)
138. Hurley P.J. (1999) The air pollution model (TAPM) Version 1: Technical description and examples. CSIRO Atmospheric Research Technical Paper N 43. Aspendale: CSIRO, 39 p.
139. Morison R.P., Leslie L.M., Speer M.S. (2002) Atmospheric modelling of air pollution as a tool for environmental prediction management // Meteorological and Atmospheric Physics, 80(1—4), 141—151.
140. Korolenok E.V., Nagornov O.V. (2002) Modelling of surface concentrations of ozone of urban region // Mathematical modeling, 14(4), 80—94. (In Russian)
141. Moussiopoulos N., Sahm P., Kessler C. (1995) Numerical simulation of photochemical smog formation in Athens, Greece—A case study // Atmospheric Environment, 29(24), 3619—3632.
142. Penenko V.V., Korotkov M.G. (1988) Application of numerical models for emergency and ecological situations prediction in the atmosphere // Atmospheric and Oceanic Optics, 11(6), 567—572. (In Russian)
143. Belikov D.A., Starchenko A.V. (2005) Study secondary pollutants (ozone) generation in Tomsk air // Optika atmosfery i okeana, 18(5—6), 435—443. (In Russian)
144. Tulet P., Maaley A., Crassier V., Rosset R. (1999) An episode of photooxidant plume pollution over the Paris region // Atmospheric Environment, 33(11), 1651—1662.
145. Gery M.W., Whitten G.Z., Killus J.P., Dodge M.C. (1989) A photochemical mechanism for urban and regional scale computer modelling // J. Geophys. Res., 94, 12925—12956.
146. Stockwell W.R., Middleton P., Chang J.S., Tang X. (1990) The second generation regional acid deposition model chemical mechanism for regional air quality modelling // J. Geophys. Res., 95(22), 16343—16367.
147. Stockwell W.R., Kirchner F., Kuhn M., Seefeld S. (1997) A new mechanism for atmospheric chemistry modelling // Ibid., 102(22), 25847—25879.
148. Carter W.P.L. (1990) A detailed mechanism for the gas-phase atmospheric reactions of organic compaunds // Atmospheric Environment, 24A, 481—518.
149. Carter W.P.L., Wang L., Milford J.B. (2000) Uncertainty in Reactiving Estimates for N-Butyl Acetate and 2-Butoxy Etanoe. Final Report. (Contract N 95-331). Sacramento (CA): California Air Resources Board, 82 p.
150. Simpson D. (1993) Photochemical model calculations over Europe for two extended summer periods: 1985 and 1989. Model results and comparisons with observations // Atmospheric Environment, 27A, 921—943.
151. Bottenheim J.W., Strausz O.P. (1982) Modelling study of reactive power plant plume // Atmospheric Environment, 16, 85—106.
152. Aktinson R., Lloyd A.C., Wiges L. (1982) An updated chemical mechanism for hydrocarbon/NO_x/SO_2 photo-oxidation s suitable for inclusion in atmospheric simulation models // Ibid., 16, 1341—1355.
153. Bednar J., Brechler J., Halenka T., Kopacek J. (2001) Modelling of summer photochemical smog in the Prague region // Phys. Chem. Earth (B), 26, 129—136.
154. Ghil M., Malanotte-Rizzolli P. (1991) Data assimilation in meteorology and oceanography // Advances in Geophysics, 33, 141—266.

155. Klimova E.G. (2005) Reconstruction of meteorological fields, according to observation data: Dissertation … Dr.Phys-Math. Novosibirsk: ИВТ SB RAS, 233 p. (In Russian)
156. Bergtosson P., Doos B.R. (1955) Numerical weather map analysis // Tellus, 7, 329—340.
157. Cressman G.P. (1959) An operational objective analysis system // Monthly Weather Rev., 87, 367—374.
158. Gandin L.R. (1963) Independent analysis of meteorological fields. Leningrad: Gidrometeoizdat, 287 p. (In Russian)
159. Sasaki Y. (1958) An objective analysis based on the variational method // J. Meteorology Society Japan, 36, 77—88.
160. Flemming J., Reimer E., Stern R. (2001) Data assimilation for CT-Modelling based on optimum interpolation // Preprints of 25th NATO/CCMS International Technical Meeting on Air Pollution Modelling and its Application. Belgium, Louvain-la-Neuve: Catholic University of Louvain, P. 1173—1180.
161. Klimova E.G., Kilanova N.V. (2006) Numerical experiments of methane emission estimation, based on data assimilation system about passive impurity in the atmosphere of the Northern hemisphere // Atmospheric and Oceanic Optics. 19(11), 961—964. (In Russian)
162. Klimova E.G. (2001) Model for covariance calculation of forecast errors in the Kalman filter algorithm, based on complete equations // Meteorology and hydrology, 11, 11—21. (In Russian)
163. Klimova E.G. (1997) Method for meteorological observation data assimilation, based on summarized suboptimal Kalman filter // Meteorology and hydrology, 11, 55—65. (In Russian)
164. Klimova E.G. (1999) Asymptotic behavior of meteorological data assimilation scheme, based on Kalman filter algorithm // Meteorology and hydrology, 8, 55—65. (In Russian)
165. Kilanova N.V., Klimova E.G. (2006) Numerical experiments on model systematic error evaluation during task of data assimilation about passive impurity concentration // Vychislitelnye tekhnologii, 11(5), 32—40. (In Russian)
166. Klimova E.G. (2003) Numerical experiments on meteorological data assimilation using the suboptimal Kalman // Meteorology and hydrology, 10, 54—67. (In Russian)
167. Todling R., Cohn S. (1996) Suboptimal shemes for atmospheric data assimilation based on the Kalman filter // Monthly Weather Rev., 124, 2530—2557.
168. Sonechkin D.M. (1976) Dynamically-stochastic approach to task of independent analysis of diverse meteorological observation data // Tr. Gidrometcentr, USSR, 181, 54—76. (In Russian)
169. Jazwinski A.H. (1970) Stochastic processes and filtering theory. N. Y.: Academic Press, 377 p. (In Russian)
170. Marchuk G.I., Aloyan A.E. (1995) Global impurity transfer in the atmosphere // Izv. RAS. Physiscs of atmosphere and ocean, 31(5), 597—606. (In Russian)
171. McPherson R.D., Bergman K.H., Kistler R.E. et al. (1979) The NMC operational global data assimilation system // Monthly Weather Rev., 107(11), 1445—1461.
172. Penenko V.V. (1981) Methods for numerical modelling of atmospheric processes. Leningrad: Gidrometeoizdat, 351 p. (In Russian)
173. Lorenc A.C. (1981) A global three-dimensional multivariate statistical interpolation scheme // Monthly Weather Rev., 109(4), 701—721.
174. Shutyaev V. (1995) Some properties of the control operator in the problem of data assimilation and iterative algorithms // Rus. J. Numerical and Analitical Mathematical Modelling, 10, 357—371.
175. Koutsenogii K.P., Makarov V.I., Kovalskaya G.A. et al. (2000) The chemical composition of the aerosol particle produced by the forest fires in Siberia // Prop. of the Joint Fire Science Conference and Workshop Crossing the Millennium: Integrating Spatial Technologies and Ecological Principles for a New Age in Fire Management. V. II. Idaho, Boise, P. 219—222.
176. Selegey T.R., Yurchenko I.P. (1990) Potential of the atmosphere's dispersing capacity // Geogr. i prir. Resursy, 2, 132—138. (In Russian)
177. Reid J.S., Eck T.F., Christopher S.A. et al. (1999) Use of the Angstom exponent to estimate the variability of optical and physical properties of aging smoke particles in Brazil // J. Geophys. Res., 104, 27473—27489.

178. Kondratyev K.Ya., Isidorov V.A. (2001) Effect of biomass burning on chemical composition of the atmosphere // Atmospheric and Oceanic Optics, 14, 93—101. (In Russian)
179. Levine J.S., Cofer III W.R. (2000) Boreal forest fire emission and the chemistry of the atmosphere // Fire, Climate change, and Carbon Cycling in the Boreal Forest. Ecol. Studies. V. 138. P. 31—48.
180. Overpeck J.T., Rind D., Goldberg R. (1990) Climate-induced changes in forest disturbance and vegetation // Nature, 343, 51—53.
181. Flannigan M.D., Stocks B.J., Wotton B.M. (2000) Climate change and forest fires // Science of the Total Environment, 262(3), 221—229.
182. Stocks B.J., Fosberg M.A., Lynham T.J. et al. (1998) Climate change and forest fire potential in Russian and Canadian boreal forests // Climatic Change. 38, 1—13.
183. Flannigan M.D., Bergeron Y., Engelmark O., Wotton B.M. (1998) Future wildfire in circumboreal forests in relation to global warming // J. Vegetation Science, 9, 469—476.
184. Arctic Climate Impact Assessment (ACIA). UK, Cambridge: Cambridge Univ. Press, 2005. 1042 p.
185. Kurz W.A., Apps M.J., Stocks B.J., Volney W.J.A. (1995) Global climate change: Disturbance regimes and biospheric feedbacks of temperate and boreal forests// Biotic Feedbacks in the Global Climate System: Will the Warming Speed the Warming? / Eds. G. M. Woodwell, F. Mackenzie. UK, Oxford: Oxford Univ. Press, P. 119—133.
186. Kasischke E.S., Stocks B.J. (2000) Fire, Climate Change, and Carbon Cycling in the Boreal Forest. Ecological Studies / Eds. M. M. Cadwell et al. N. Y.: Springer.
187. Ramanathan V., Crutzen P.J., Kiehl J.T., Rosenfeld D. (2001) Aerosols, climate and hydrological cycles // Science, 294(5349), 2119—2124.
188. Lezhenin A.A., Malbakhov V.M., Shlychkov V.A. (2003) Numerica model of aerosol migration, generated in the forest fires zone // Atmospheric and Oceanic Optics, 16(5—6), 485—488. (In Russian)
189. Dubrovskaya O.A., Lezhenin A.A., Malbakhov V.M. et al. (2004) About fires effect on cloud and precipitation generation // Geogr. i prir. resursy. Special issues: Works of International conference on measurement, modelling and information systems for environemental research: ENVIROMIS-2004. P. 158—162. (In Russian)
190. Malbakhov V.M., Lezhenin A.A., Dubrovskaya O.A., Klimova E.G. (2006) Assessment of forest fires impact on cloud and precipitation generation // Vychislitelnye tekhnologii, 11, p. 3. Special issue, 135—142. (In Russian)
191. Dubrovskaya O.A., Kozlov B.P., Malbakhov V.M. (2005) Assessment of coarse smoke particles impact on precipitation generation processes // Atmospheric and Oceanic Optics, 18(5—6), 430—434. (In Russian)
192. Moeng C.-H. (1984) A large-eddy-simulation model for the study of planetary boundary layer turbulence // J. Atmospheric Science, 41(13), 2052—2062.
193. Malbakhov V.M., Shlychkov V.A., Lezhenin A.A., Dubrovskaya O.A. (2004) Numerical model of smoke plume distribution from forest fires with parametric aacount for burning proceses // Geografiya i prirodnye resursy. Special issue: Works of International conference on measurement, modelling and information systems for environemental research: ENVIROMIS-2004. P. 170—174. (In Russian)
194. Shlychkov V.A., Pushistov P.Yu., Malbakhov V.M. (2001) Effect of atmospheric convection on vertical transport of arid aerosols // Atmospheric and Oceanic Optics, 14(6—7), 578—582. (In Russian)
195. Rutledge S.A., Hobbs P.V. (1983) The mesoscale and microscale structure and organization of clouds and precipitation in midlatitude cyclones. VIII: A model for «Seeder-Feeder» process in warm-frontal rainbands // J. Atmospheric Science, 40(5), 1185—1206.
196. Dubrovskaya O.A., Malbakhov V.M., Shlychkov V.A. (2007) Mass forest fires' effect on cyclonic proceses in Siberia // Vychislitelnye tekhnologii, 12(2), 58—66. (In Russian)
197. Sukhinin A.I. (2003) Fires of Yakutia in 2002 as preimages of global ecological пdisasters // Materials of the 5-th International conference «Natural fires: outbreak, distribution, fighting and environmental consequences ». Tomsk: Izd-vo Tom. un-ta, P. 181—182. (In Russian)

198. Mason B.J. (1961) The Physics of Clouds. Leningrad: Gidrometeoizdat, 541 p. (In Russian)
199. Sulakvelidze G.K. (1963) Storm precipitation and hail. Leningrad: Gidrometeoizdat, 412 p. (In Russian)
200. Sutton R.T., O'Neill A., Taylor F.M. (1994) High-resolution stratospheric tracer fields estimated from satellite observations using lagrangian trajectory calculations // J. Atmospheric Science, 51, 2995—3005.
201. Belousov R.L., Yusupov Yu.I. (1991) Computing of three-dimensional paths of air particles // Meteorology and hydrology, 12, 41—48. (In Russian)
202. Dyukarev A.G. (2005) Landscape-dynamic aspects of taiga soil generation in Western Siberia. Tomsk: Izd-vo NTL, 284 p. (In Russian)
203. Bekhovykh Yu.V. (2003) Forest fireseffect on thermal physical properties and hydrothermal conditions of sod-podzolic soils of the south-western part of belt pine forests of Altai region: Dissertation … DSci. Barnaul: Altai State Agrarian University, 135 p. (In Russian)
204. Shulgin A.M. (1967) Soil climate and its management. Leningrad: Gidrometeoizdat, 298 p. (In Russian)
205. Valette J.-C., Gomendy V., Houssard C., Gillon D. (1994) Heat transfer in the soil during very low-intensity experimantal fires — the role of duff and soil-moisture content // Int. J. Wildland Fire, 4(4), 225—237.
206. Balesdent J., Mariotti A. (1996) Measurement of soil organic matter turnover using ^{13}C natural abundance // Mass Spectrometry of Soils / Eds. T. W. Boutton, S. I. Yamasaki. N. Y.: Marcel Dekker, P. 83—111.
207. Gonzalez-Perez J. A., Gonzalez-Vila F.J., Almendros G., Knicker H. (2004) The effect of fire on soil organic matter — a review // Environment International. 30(6), 855—870.
208. Johnson D.W. (1992) Effect of forest management on soil carbon storage // Water, Air, Soil Pollution, 64, 83—120.
209. Fernandez I., Cabaneiro A., Carballas T. (1997) Organic matter changes inmediately after a wildfire in an Atlantic forest soil and comparison with laboratory soil heating // Soil Biology and Biochemistry, 29, 1—11.
210. Pieticakainen J., Hiukka R., Fritze H. (2000) Does short-term heating of forest humus change its properties as a substrate for microbes? // Ibid., 32, 277—288.
211. Savage S.M. (1974) Mechanism of fire-induced water repellency in soil // Soil Science Society of America, 38, 652—657.
212. Almendros G., Martin F., Gonzalez-Vila F.J. (1988) Effects of fire on humic and lipid fractions in a Dystrict Xerochrept in Spain // Geoderma, 42, 115—127.
213. DeBano L.F., Savage S.M., Hamilton D.A. (1976) The transfer of heat and hydrophobic substances during burning // Soil Science Society of America Journal, 40, 779—782.
214. DeBano L.F., Mann L.D., Hamilton D.A. (1970) Translocation of Hydrophobic substances into soil by burning organic litter // Ibid., 34, 130—133.
215. Charles-Dominique P., Blanc P., Larpin D. et al. (1998) Forest perturbations and biodiversity during the last ten thousand years in French Guiana // Acta Oecologica, 19(3), 295—302.
216. Sanford R.L., Saldarriaga J., Clark K.E. et al. (1985) Amazon rain-forest fires // Science, 227, 53—55.
217. Turcq B., Sifeddine A., Martin L. et al. (1998) Amazonia rainforest fires: a lacustrine record of 7000 years // Ambio, 27, 139—142.
218. Cochrane M.A., Laurance W.F. (2002) Fire as a large-scale edge effect in Amazonian forests // J. Tropical Ecology, 18, 311—325.
219. Laurance W.F., Laurance S.G., Ferreira L.V. et al. (1997) Biomass collapse in Amazonian forest fragments // Science, 278, 1117.
220. Laurance W.F., Delamonica P., Laurance S.G. et al. (2000) Rainforest fragmentation kills big trees // Nature, 404, 836.
221. Mesquita R.C.G., Delamonica P., Laurance W.F. (1999) Effect of surrounding vegetation on edge-related tree mortality in Amazonian forest fragments // Biological Conservation, 91, 129—134.

222. Barlow J., Peres C. (2004) A. Ecological responses to El Nino-induced surface fires in central Brazilian Amazonia: management implications for flammable tropical forests // Philosophical Transactions of the Royal Society. B. Biological Sci., 359(1443), 367—380.
223. Uhl C., Kauffman J.B. (1990) Deforestation, fire susceptibility, and potential tree responses to fire in the eastern Amazon // Ecology, 71, 437—449.
224. Fites-Kaufman J., Bradley A.F., Merrill A.G. (2006) Fire and plant interactions // Fire in California Ecosystem / Eds. N. G. Sugihara, J. W. van Wagtendonk, K. E. Shaffer et al. Berkeley, Los Angeles; London: University of California Press, P. 94—117.
225. Nobble I.R., Slayter R.O. (1980) The use of vital attributes to predict successional changes in plant communities subject to recurrent disturbances // Vegetatio, 43, 5—21.
226. Neary D.G., Klopatek C.C., DeBano L.F., Ffolliott P.F. (1999) Fire effects on belowground sustainability: a review and synthesis // Forest Ecology and Management, 122, 51—71.
227. Peres C.A. (1999) Ground fires as agents of mortality in a central Amazonian forest // J. Tropical Ecology, 15, 535—541.
228. Furyaev V.V., Zlobina L.P. (2001) Global changes of ecological functions of Eurasian boreasl forests due to fire dsturbance // Sib. ekol. Zhurn, 6, 661—665. (In Russian)
229. Furyaev V.V., Goldammer J.G. (1996) Environmental problems of fires in boreal forests: experience and ways of international cooperation // Lesnoye khozyaystvo, 3, 7—8. (In Russian)
230. Furyaev V.V. (1996) Role of fires in forest generation process. Novosibirsk: Nauka, SIF RAN, 252 p. (In Russian)
231. Frankenberg E., Mckee D., Thomas D. (2005) Health consequences of forest fires in Indonesia // Demography, 42(1), 109—129.
232. Ruitenbeck J. (1999) Indonesia // in Indonesia's Fires and Haze: The Cost of Catastrophe / Ed. by D. Glover, T. Jessup. Singapore: Institute of Southeast Asian Studies, P. 86—112.
233. Sastry N. (2002) Forest Fires, Air Pollution, and mortality in Southeast Asia // Demography, 39(1), 1—23.
234. Churg A., Brauer M. (2000) Ambient atmospheric particles in the airways of human lungs // Ultrastructural Pathology, 24, 353—361.
235. Harrison R.M., Yin J. (2000) Particulate matter in the atmosphere: which particle properties are important for its effects on health? // Science of the Total Environment, 249(1—3), 85—101.
236. Dockery D.W., Pope C.A., Xu X. et al. (1993) An association between air pollution and mortality in six U.S. cities // New England J. Medicine, 329(24), 1753—1759.
237. Bowman D.M.J.S., Johnston J.H. (2005) Wildfire smoke, fire management and human health // Ecohealth, 2(1), 76—80.
238. Chretien J., Nebut M. (1996) Environmental Injuries of the airways // Environmental Impact on the Airways: From Injury to Repair / Ed. J. Chretien, D. Dusser. N. Y.: Marcel Dekker, P. 3—18.
239. Aditama T.Y. (2000) Impact of haze from forest fire to respiratory health: indonesian experience // Respirology, 5, 169—174.
240. Sapkota A., Symons J.M., Kleissl J. et al. (2005) Impact of the 2002 Canadian forest fires on particulate matter air quality in Baltimore City // Environmental Science and Technology, 39(1), 24—32.
241. Kislitsin V., Novikov S., Skvortsova N. (2005) Moscow smog of summer 2002. Evaluation of adverse health effects // Extreme Weather Events and Public Health Responses. P. 5. Berlin: Springer, P. 255—262.
242. Mott J. A., Mannino D.M., Alverson C.J. et al. (2005) Cardiorespiratory hospitalizations associated with smoke exposure during the 1997 Southeast Asian forest fires // Int. J. Hygiene and Environmental Health, 208(1—2), 75—85.
243. Emmanuel S.C. (2000) Impact to lung health of haze from forest fires: the Singapore experience // Respirology, 5, 175—182.
244. Guidelines for life quality survey in medicine. 2-nd edition / Rev. acad. RAMN Yu. L. Shevchenko. M.: ZAO «OLMA Media Group», 2007. 320 p. (In Russian)

245. Bowling A. (1996) Measuring Disease: A Review of Disease-specific Quality of Life Measurement Scales. Philadelphia: Open University Press, 374 p.
246. Quality of life and pharmacoeconomics in clinical trials. 2nd Ed./ Eds. B. Spilker. Philadelphia: New York Lippincott-Raven, 1996. 1259 p.
247. Quality of life assessment in clinical trials / Eds. M. J. Staquet. Oxford: Oxford University Press, 1998. 360 p.
248. Novik A.A., Ionova T.I., Kaynd P. (1999) Concept of life quality survey in medicine. SPb.: Elbi, 140 p. (In Russian)
249. Shevchenko Yu.A. (2000) Life qulity in cardiology // Vestnik RVMA, 9, 5—15. (In Russian)
250. Bone M.R. (1992) International efforts to measure health expectancy // J. Epidemiol. and Community Health, 46, 555—558.
251. Andrews F.M., Withey S.B. (1976) Social Indicators of Well-being: Americans Perceptions of Life Quality. New York: Plenum Press, 220 p.
252. Gandek B., Ware J. (1998) Methods for validating and norming translations of health status questionnaires: The IQOLA Project approach // J. Clinical Epidemiology, 51(11), 953—959.
253. Baranovskiy N.V., Baranovskaya S.V. (2006) Probability of asthma-like symptoms due to forest fires // Izv. vuzov. Fizika, 49(3). Annex. 214—215. (In Russian)
254. Baranovskiy N.V., Baranovskaya S.V., Isakova A.V. (2007) Asthma-like symptoms among population due to forest fires in the settlement surroundings // Health —the basis of human potential: problems and ways to solutions. Works of 2nd Rus. sci.-pract. conference with international participants. SPb.: Izd-vo Polytech. University, P. 24—30. (In Russian)
255. Baranovskiy N.V., Baranovskaya S.V., Isakova A.V. (2007) Method for forest fires impact assessment in population health // Pozharnaya bezopasnost, 3, 71—74. (In Russian)
256. Baranovskaya S.V., Baranovskiy N.V., Isakova A.V. (2007) Sociological survey of population health during forest fires in the settlement surroundings // Social ecology in changing Russi: problems and prospects: materials of regional conference (with intl.participation) (Belgorod, 5—7 October 2007.). Ch. I. Belgorod: Izd-vo BelGU, P. 267—272. (In Russian)
257. Nazarov A.A., Terpugov A.F. (2006) Theory of probability and random processes: textbook. Tomsk: Izd-vo NTL. 204 p. (In Russian)
258. Samarskiy A.A., Mikhaylov A.P. (2005) Mathematical modelling: Ideas. Methods. Examples. 2-nd edit., rev. Moscow: Fizmatlit, 320 p. (In Russian)
259. Weidlich W. (2005) Sociodynamics: a Systematic Approach to Mathematical Modelling in the Social Sciences: transl. from Eng. / Rev. Yu. R. Popkova, A. E. Semechkina. 2nd edition, stereot. Moscow: Editorial URSS, 480 p. (In Russian)
260. Agabekyan R.L., Kirichenko M.M., Usatinov R.V. (2005) Mathematical methods in sociology. Data analysis and logic of conclusion in empirical study. Textbook. R-na/D: Feniks, 187 p. (In Russian)
261. Tsai Yu.T., Lipina L.A. (2001) Protection of people against hazardous forest fires impact during forest fire works // Forest and steppe fires: outbreak, distribution, fighting and environmental consequences: Mater. of the 4-th internat. conference. Tomsk: Izd-vo Tom. un-ta, P. 157—159. (In Russian)
262. Bronchial asthma / Edited by the RAMN Academy member A. G. Chuchalin. V. I. M.: Agar, 1997. 432 p. (In Russian)

CHAPTER 4
SOFTWARE AND HARDWARE FOR FOREST FIRE PROTECTION

Abstract

The forth paragraph considers various tools used for prediction of forest fires and their impact on environment, namely, geographical information systems and their applications. Also, possibility of satellite-based monitoring of forest fires is shown, as well as information on parallel computing with use of supercomputers.

Keywords: geoinformation systems, parallel computing, satellite monitoring

4.1. Geoinformation systems (GIS)

4.1.1. General Provisions

In 2006 the Government of the Russian Federation approved "Concept for Establishment and Development of Spatial Data Infrastructure in the Russian Federation" [1]. The Spatial Data Infrastructure of the Russian Federation – is a geographically distributed system of spatial data collection, processing, storage and delivery to a customer. The following notions are used within the Concept:

1. Spatial Object – any specific object defined by individual content and boundaries which can be described in digital data.

2. Spatial Data – digital data on spatial objects including information about location, shape and properties presented in time (and space) coordinate system.

3. Basic Spatial Data – open digital data about most widespread spatial objects which are stable in space and time and used as a reference for positioning of other spatial objects.

4. Meta-data – data which describe the content, volume, location in space, quality and other characteristics of spatial data and objects.

The Concept analyzes current condition and challenges in establishing spatial data infrastructure, purposes and tasks, key principles of the Concept implementation, main stages and directions of its development [1].

Main purpose of the Concept – is to provide conditions ensuring a free access of governmental and local authorities, institutions and people to spatial data as well as their efficient use [1].

Efficient implementation of the Concept is impossible without technologies of spatial data analysis and display i.e. geographic information systems.

First geoinformation systems appeared in 60-s in Canada, the USA and Sweden (see [2]) but they had certain program and technical limitations. During next 20 years geoinformatics was evolving as a science, GIS techniques were being improved, mathematical tools were defined, data models and processing algorithms were being formed. It should be noted that the term GIS used to mean geographical information system. However, now geoinformation systems are able to solve various tasks in various branches. Thus, it is necessary to give a modern definition of GIS.

Geoinformation system – is a system used for collecting, storing, processing, displaying and distributing spatial data as well as for acquiring new information on spatial objects and phenomena [2].

4.1.2. GIS Software Functions

General view of the GIS software functional scheme is presented in the Fig. 4.1.

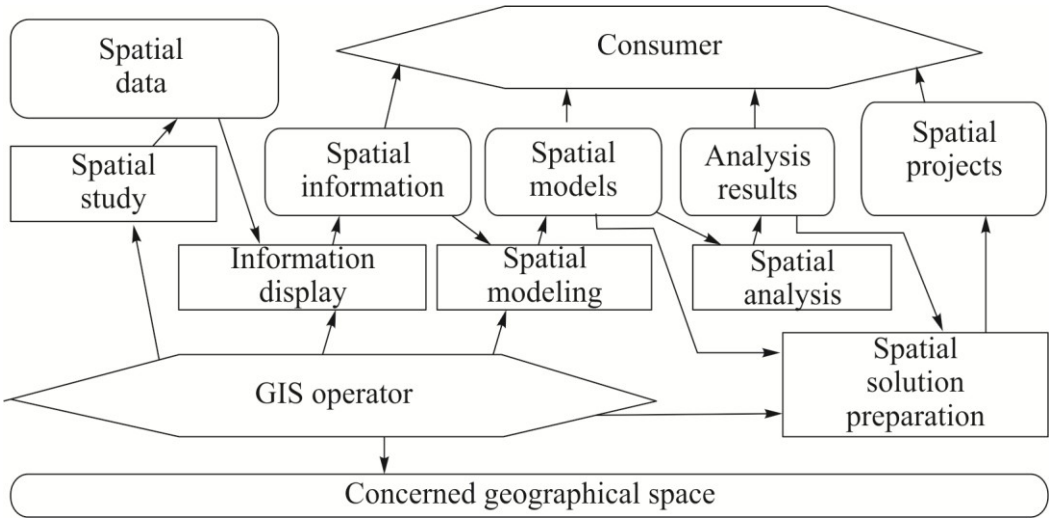

Fig. 4.1. Functional scheme of GIS software [3]

Direct survey methods of geographical space include observation, measurement and characterization (Fig. 4.2).

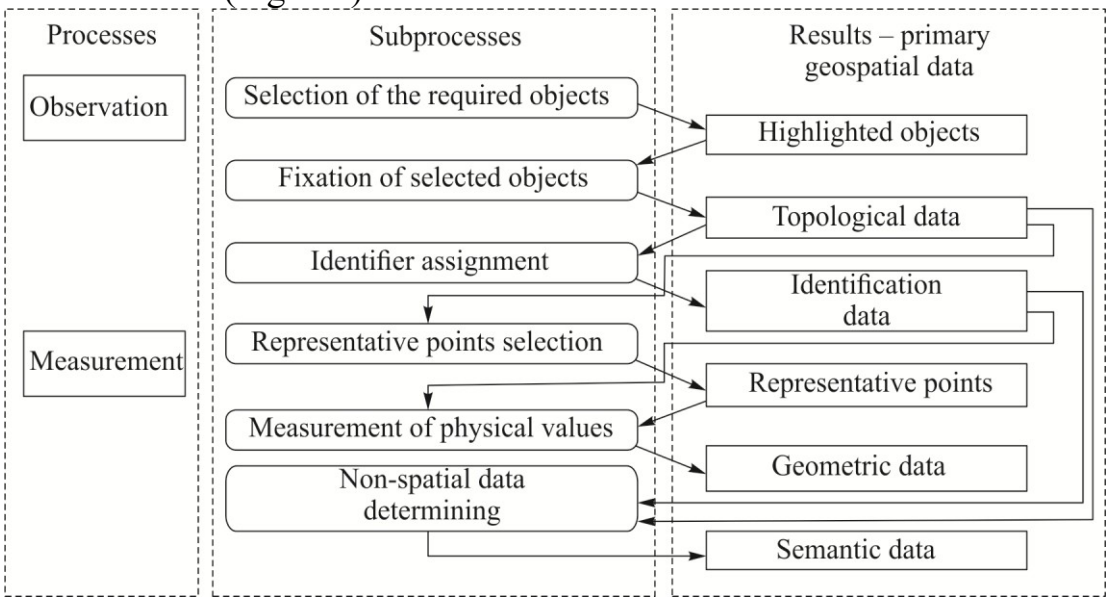

Fig. 4.2. Functional scheme of geographical space direct survey [3]

Spatial solution means designing spatial transformation of space itself or processes going in this space i.e. space management [3]. Management design involves organization changes in the functioning of life-support systems. Most highly important models include modeling of catastrophic and ecological natural and anthropogenic processes, operation and development of utilities and mains, transport engineering, exploration and production of fossil fuel deposits, administering of territories on federal and regional levels. Generally the development of these models requires spatial analysis functions and software i.e. traditional GIS tool [3].

GIS systems are based on the concept of spatial data layers when data of the same type are arranged on the Earth's surface into the layers (sometimes called themes) [2]. Array of all geospatial data forms a map.

Objects are divided into layers according to the type. Thus, each map layer displays objects which have either the same origin (roads, rivers, buildings) or the same topological arrangement and scale (i.e. then they can be described by points, lines or polygons).

Division into layers allows only using those GIS data which are required for solving the task. Thus user can simply exclude unnecessary layers.

The basis of GIS systems is made up from various data models which reflect real objects confined to the certain area, their interrelations and other additional information related to this space. Each GIS data model comprises different separate spatial objects united topologically.

Figure 4.3 shows main types of spatial objects, Figure 4.4 – spatial data models.

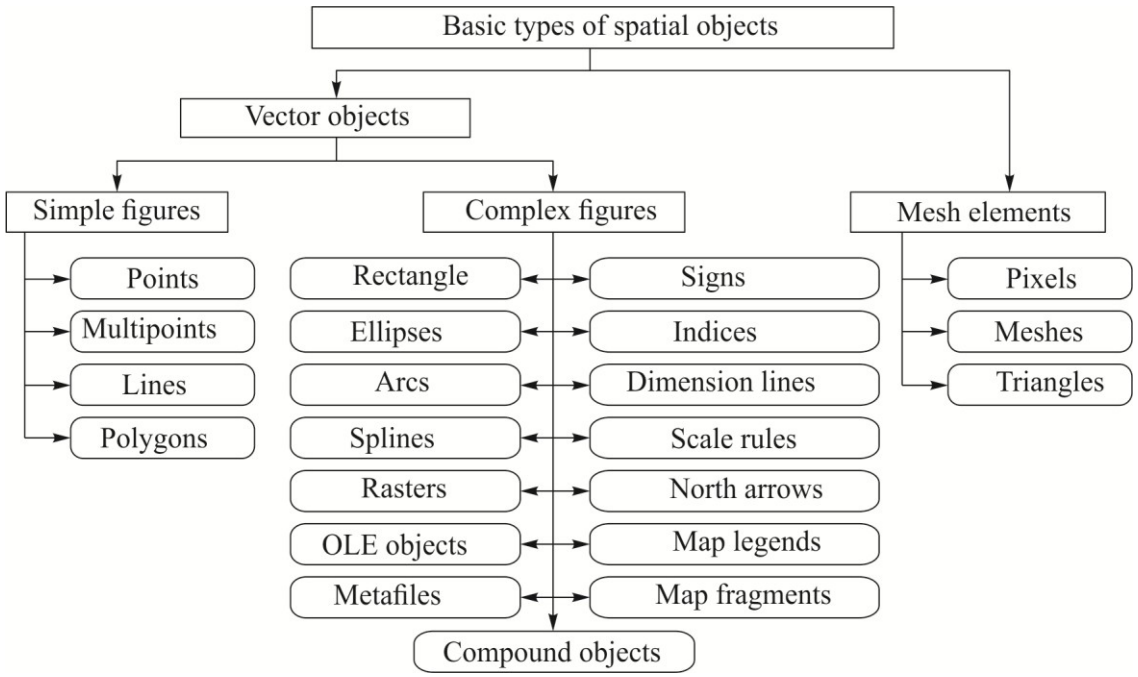

Fig. 4.3. Main types of spatial objects [2]

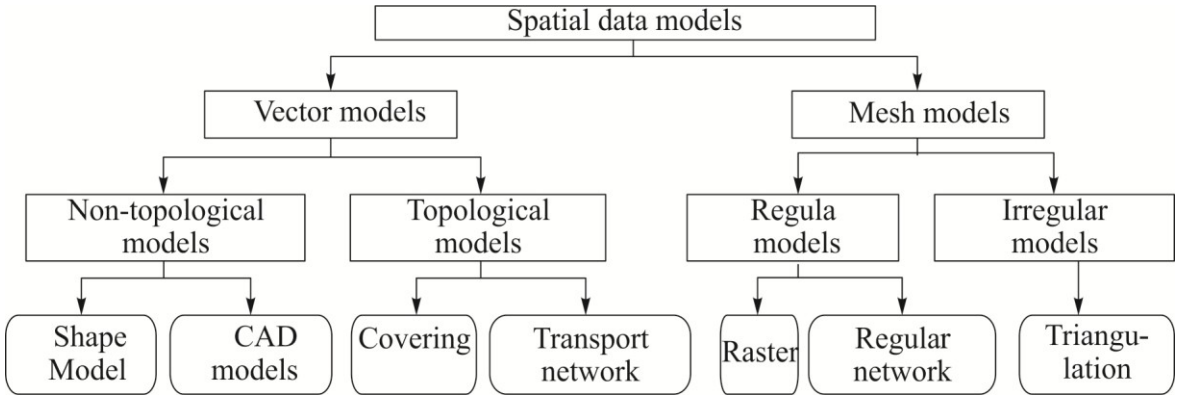

Fig. 4.4. Spatial Data Models [2]

4.1.3. Spatial Data Packet Processing

Most modern GIS systems are compatible with personal computers under MS Windows. Previous numerous GIS versions were developed for Unix workstations, however nowadays majority of manufacturers stopped producing this operational system [2].

Currently there are a lot of GIS which can be referred to as full-featured. Most powerful are American GIS: ArcGIS, MapInfo, Autodesk Map, GeoMedia, ERDAS Imagine. Russian manufacturers include IndorGIS, Geograf, Karta-2000, Ingeo etc. Despite foreign products being better than Russian ones in terms of function package, many Russian products have certain advantages which allow them to compete successfully in the domestic market. Table 4.1 presents key functional capabilities of main foreign and Russian GIS popular in Russia.

Geoinformation system ArcGIS 9.0 (ESRI, Inc.) is currently most powerful and dynamically developing vector GIS in the world. The system supports various data types, has spatial data servers and multifunctional applications. This system can be the basis either for a simple GIS or for full-featured corporate GIS system capable of processing huge data arrays which are accessible both from the local network and on the Internet [2].

Geoinformation system MapInfo (MapInfo Corp.) is the second most popular system in the world and in Russia. It possesses wide range of functions and additional modules which allow solving various GIS tasks but in general this system is much simpler than ArcGIS [2].

GIS IndorGIS (IndorSoft Ltd, Tomsk) is being applied in many fields of economics. It served as a basis for many applied solutions for roads and networks, land and real estate management. This system helps to do all kinds of works – from inserting, editing spatial data and mapping to data spatial analysis and decision-making.

4.1.4. GIS Application

Nowadays geoinformation systems are widely applied in various fields of human life.

For example, there are information, navigation and dispatching GIS. GIS are widely applied for demographic analysis, location selection and analysis, street advertising, direct mailing, real property purchase, authorities management, development planning of cities and regions, road management, agriculture, forest management, etc. [2]. It should be noted that almost every forestry has electronic maps of forests with forest survey plots (rarely – compartments) as minimal units. As a rule these maps contain forest estimation data and fire safety plan.

Forest fire danger [4] can be predicted by both remote sensing [5 - 8] and geoinformation systems [8]. The algorithm of fire danger strategic mapping includes 3 interrelated stages [4]:

1) Satellite signal detection and recording, data verification, navigation reference and sectorization;

2) Program computing of fire danger index;

3) Results processing by geoinformation technologies

Figure 4.5 shows a flowchart of the technique to create a map chart for short-term fire danger prediction basing on weather conditions. Currently this system is deployed for forests of Eastern Siberia.

*Table 4.1.*GIS Functional Capabilities [2]

Functional Capabilities	Foreign GISC					Russian GIS				
	ArcGIS	MapInfo	Autodesk Map	GeoMedia	ERDAS Imagune	IndorGIS	GeoGraf	Karta-2000	zinGeo	Object Land
1	2	3	4	5	6	7	8	9	10	11
Supported Data Models										
Non-topological vector	+	+	+	+	+	+	+	+	+	+
Topological vector	+	–	+	+	+	+	–	–	+	–
Vector with *Z*-axis	+	–	+	+	+	+	–	+	–	–
Transport network	+	–	–	–	–	+	–	–	–	–
Raster model	+	+	+	+	+	+	+	+	+	+
Regular surface model	+	+	–	+	+	+	–	+	+	–
Triangulated surface model	+	+	+	+	+	+	–	–	+	–
Object model	+	–	+	+	–	–	–	–	+	–
CAD-model	+	–	+	+	–	+	–	–	+	–
Geo-database	+	+	–	+	–	–	–	+	+	+
Geodetic Data Processing										
Data capture from geodetic instruments	–	+	+	–	–	–	–	–	–	–
Tachometric data diaries processing	+	+	+	+	–	+	–	+	–	–
Field books processing	+	+	+	–	–	+	–	+	–	–
Separate steps alignment	+	+	+	+	–	+	–	+	–	–
Steps' networks alignment	+	+	+	–	–	–	–	–	–	–
Geodetic survey (crossings)	+	+	+	–	–	+	–	+	–	–
Remote Sensing Data Processing										
Geometrical correction	+	+	–	+	+	–	–	–	–	–
Optical correction	+	+	–	–	+	–	–	–	–	–
Orthotransformation	+	–	–	–	+	–	–	–	–	–
Relief modeling	+	+	+	+	+	–	–	–	–	–
Photographic triangulation	+	–	+	–	+	–	–	–	–	–
Interpretation	+	–	–	–	+	–	–	–	–	–
Scanning and Vectorization										
Scanning	+	–	–	–	–	–	–	–	+	–
Raster editing	+	–	–	–	+	+	–	+	+	–
Raster geometry correction	+	+	+	+	+	+	+	+	+	+
Raster projection transformation	+	–	+	+	+	+	–	–	–	–
Semi-automatic vectorization	+	–	+	+	+	+	–	+	–	–
Automatic vectorization	+	–	+	+	+	+	–	–	–	–
Data Capture and Visualization										
Object selection by area	+	+	+	+	+	+	+	+	+	+
Object selection by other objects	+	+	+	+	+	+	+	+	+	+
SQL-like requests	+	+	+	+	+	+	+	+	+	+
Cartometry (lengths, areas, angles)	+	+	+	+	+	+	+	+	+	+
Conventions	+	–	+	–	–	+	–	–	+	+
Three-dimensional visualization	+	+	+	+	+	+	–	+	–	–
Spatial Analysis of Vector Objects										
Relational analysis	+	–	+	+	–	+	–	–	–	–
Cut-off	+	+	+	+	+	+	–	–	+	+
Overlay	+	+	+	+	+	+	+	+	–	–
Buffer zones	+	+	+	+	+	+	+	+	+	+
Convex cover	–	–	–	–	–	+	–	–	–	–
Zones of proximity (Voronoi diagram)	+	+	+	–	–	+	–	–	–	–
Proximity zone balancing	–	–	–	–	–	+	–	–	–	–
Generalization	+	–	–	–	+	+	–	–	–	–

End of Table 4.1

1	2	3	4	5	6	7	8	9	10	11
Network Analysis										
Shortest path finding	+	+	–	+	–	+	+	–	+	–
Optimal winding order search	+	+	–	+	–	+	+	–	+	–
Service area calculation	+	+	–	+	–	+	–	–	–	–
Transport availability calculation	–	–	–	–	–	+	–	–	–	–
Transport junctions calculation	–	–	–	–	–	+	–	–	–	–
Traffic flow calculation	–	–	–	–	–	+	–	–	–	–
Raster Analysis										
Mathematical operations with rasters	+	+	–	+	+	+	–	–	–	–
Logical operations with rasters	+	+	–	+	+	+	–	–	–	–
Buffer zones	+	+	–	+	+	+	–	–	–	–
Factor analysis	+	–	–	+	+	–	–	–	–	–
Surface Analysis										
Interpolation of heights	+	+	–	+	–	+	–	–	–	–
Profiling	+	+	–	+	–	+	–	–	–	–
Isometric lines plotting	+	+	+	+	+	+	–	+	–	–
Isometric contouring	+	+	–	+	–	+	–	–	–	–
Isometric slope designing	+	+	+	+	–	+	–	–	–	–
Calculating exposure of slopes	+	–	+	+	–	+	–	–	–	–
Ground works volume calculation	+	+	–	–	–	+	–	–	–	–
Surface difference calculation	–	+	+	–	–	+	–	–	–	–
Visibility analysis	+	+	–	+	+	+	–	–	–	–
Talwegs and water parting lines design	+	+	+	–	–	+	–	–	–	–
Water course analysis	–	–	+	–	–	+	–	–	–	–
Other Analytical Functions										
Geostatistics	+	+	–	–	+	–	–	–	–	+
Temporal data	+	–	–	–	–	–	–	–	–	–
Hydraulic calculations	–	–	+	–	–	+	–	–	+	–
Electric computation	–	–	+	–	–	+	–	–	+	–

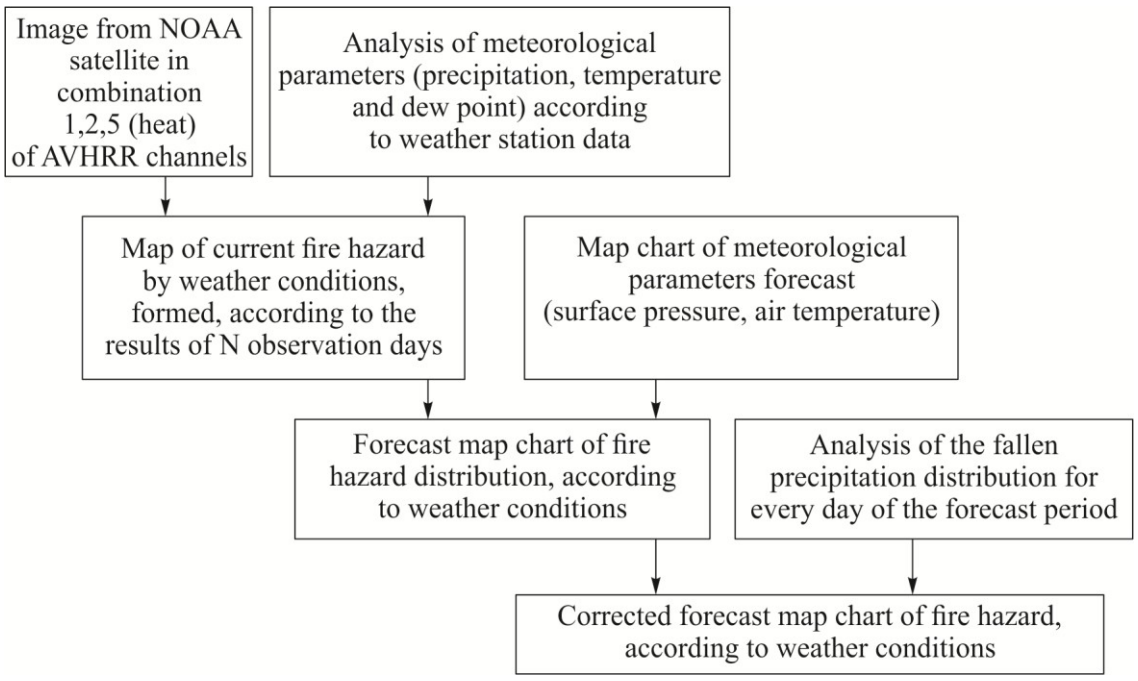

Fig. 4.5. Flowchart of the technique to create map chart of the short-term fire danger prediction based on weather conditions [4]

GIS system used for forest fire danger prediction in Timiryazevskiy forestry of Tomsk region [9] is based on deterministic-probabilistic technique of forest fire prediction [10]. Comprehensive individual pyrological characteristics of vegetation areas are ensured by large-scale maps of flammable vegetation [11] presented as a set comprising: 1) map, 2) full pyrological description of plots on the map, 3) tables with characteristics of flammable vegetation types. Technique and technology of large-scale flammable vegetation mapping using forest estimation information presented also in electronic version were tested in various regions.

GIS-based management system was created to decide on emergency situations with forest fires [12, 13]. ArcGIS system is used as an underlying geoinformation platform. The system includes a subsystem to assess forest fire spread based on such technologies as fuzzy logics [14, 15] and neural networks [16, 17].

One of the most promising directions for enhancing efficiency of forest fire safety management are geoinformation systems and remote sensing which can be used for immediate environmental and economic assessment of forest fire consequences [18]. The problem of fire spots detection is currently one of the most elaborated ones [19]. However it is impossible to define contours of fire-sites due to low resolution of IR images. Sizes of phytocenotic and soil contours with corresponding elementary landscapes constitute tens of meters [20, 21]. This fact stipulates using of high-resolution images which can be provided by spacecraft "Meteor-3M" (resolution 32^{o} m), "LandSat" (resolution 30^{o} m), SPOT (resolution 5^{o} m), "QuickBird" (resolution 2.4^{o} m) and others. Fire-site contour in space images is defined either by interpretation or by automatic classification of elementary landscapes with GIS tools. Figure 4.6 provides sequential chart of forest fire consequences assessment.

To deploy the presented technique of forest fires consequences, a special comprehensive set of information and prediction technologies based on ArcGIS 8.2 and ERDAS Imagine 8.5 GIS systems was created in the Centre for Remote Sensing of the Earth in Ugra Research Institute of Information Technologies (Khanty-Mansiysk). A digital map of species composition in Khanty-Mansy Autonomous Area forests is one of the key elements of this set.

Canadian Forest Service has developed spatial Fire Management System (sFMS) to provide certain range of functions for wildland fire management decision-making [22]. The sFMS can operate as a stand-alone system or be integrated in existing information systems. Enabling technologies include a GIS and relational database management systems. Fire management functions are supported by an integrated set of system modules which can be selected as required, depending on the task. The system is primarily used with current weather data and short-term forecasts to provide daily or hourly maps of fire weather, fire behavior, ignition probability and attack time [22]. The system can be used both at local and regional scales. In most cases, the maps are distributed via the Internet.

Natural resources Canada currently operates two national forest fire management information systems [22]: the Canadian wildland fire information system (CWFIS) and the fire monitoring, mapping and modeling system (Fire M3). Both of these systems incorporate components of CFFDRS and use the sFMS for data capture, management, modeling, analysis and presentation. Figure 4.7 gives examples of Fire Weather Index (FWI) maps a) and head fire intensity (b) for October 5, 1999.

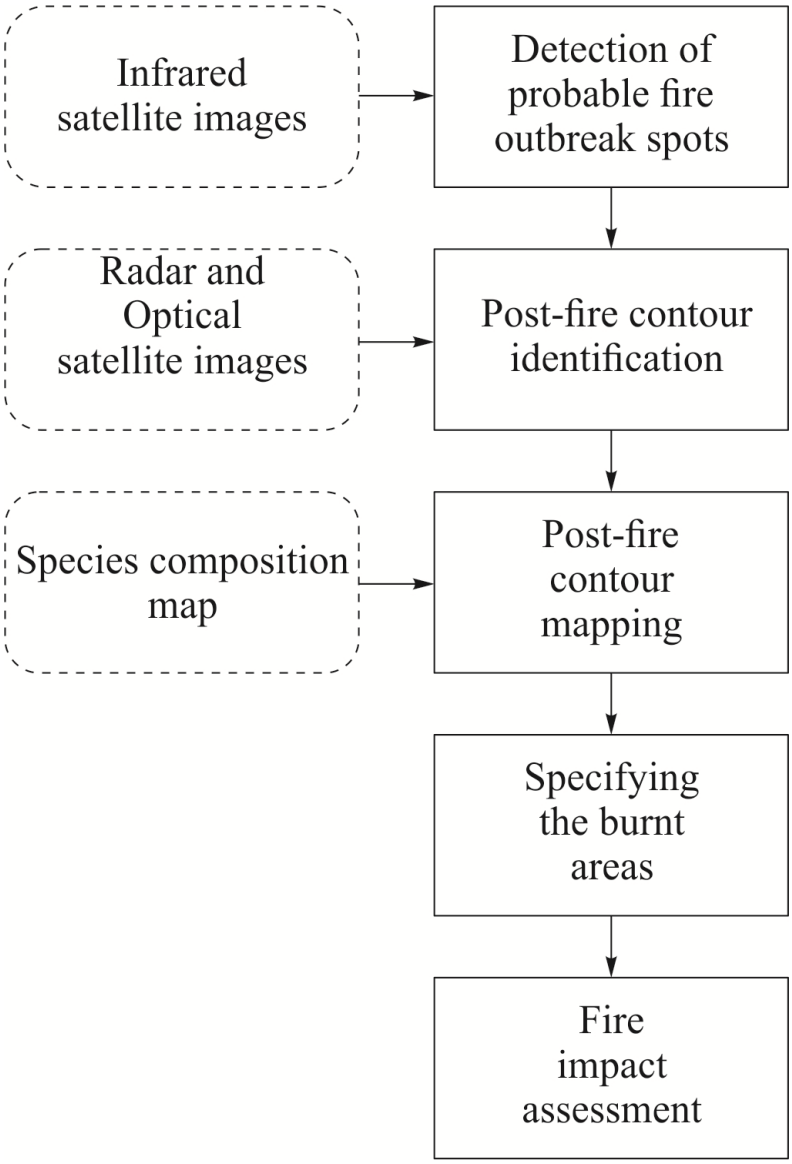

Fig. 4.6. Sequential chart of forest fire consequences assessment [18]

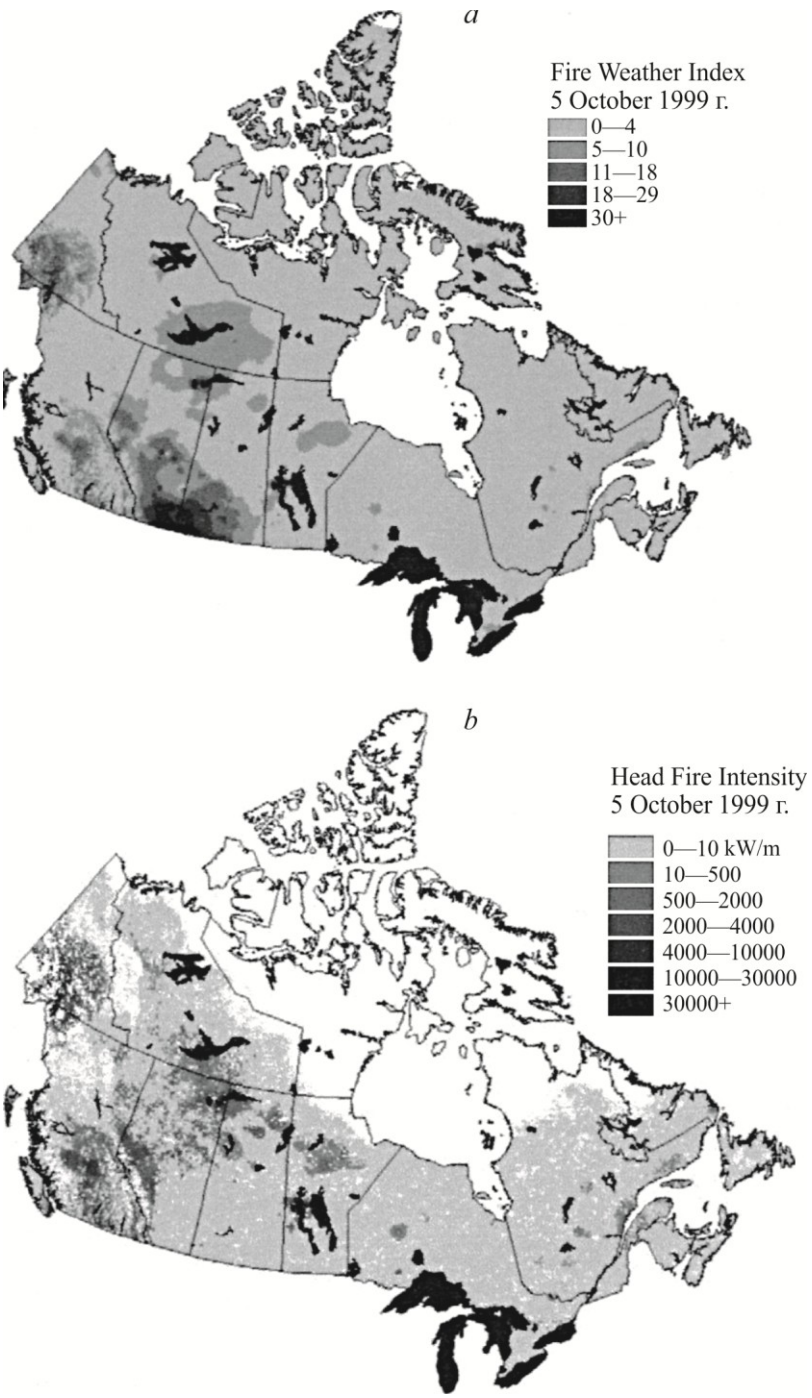

Fig. 4.7. Examples of Fire Weather Index (FWI) and fire intensity maps [22]
See explanation in the text.

Figure 4.8 shows example of the Fire M3 modeling component (screenshot). Hotspot attributes can be displayed by clicking on the hotspot locations. The attributes include fire weather conditions (TEMP – temperature, ^{o}C, RH – relative humidity, %, Wind Dir – wind direction, degrees; Wind Sp – wind speed, km/h); the six FWI System components, and selected FBP System outputs (CFB – crown fraction burnt, %; TFC – total fuel consumption, kg/m^2, HFI – head fire intensity, kW/m; ROS – head fire rate of spread m/min). Hotspots location is predicted by CWFIS.

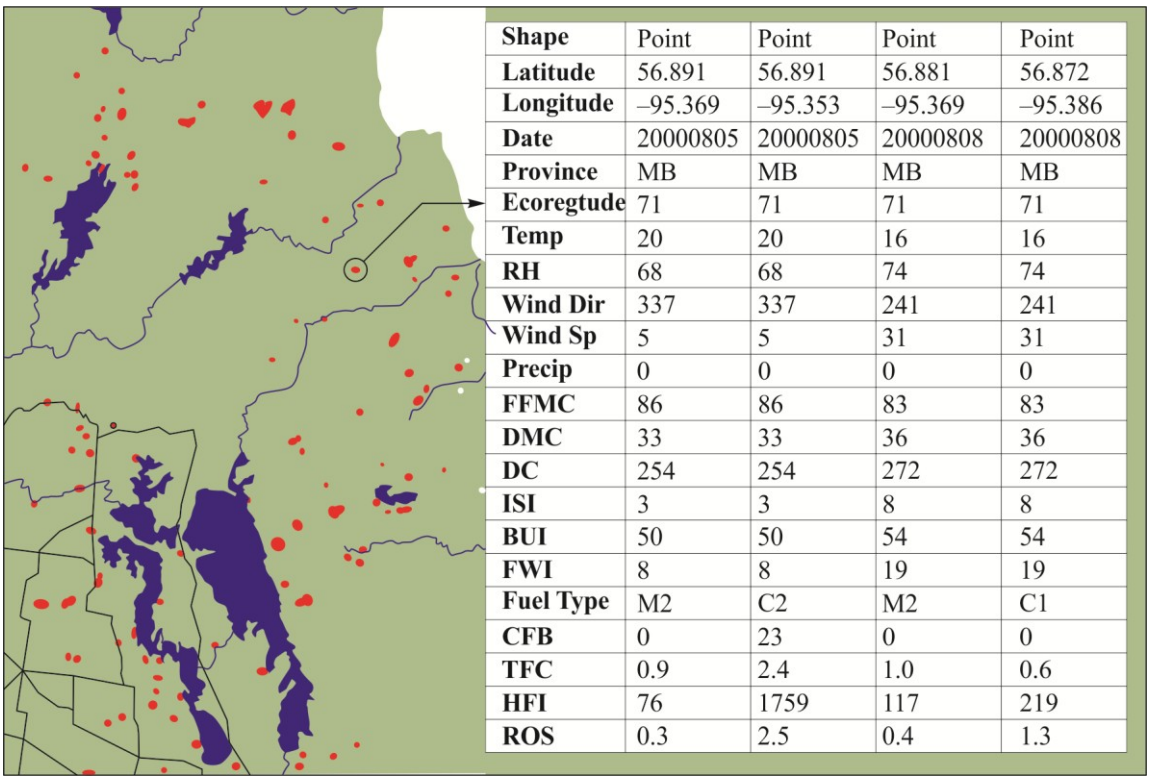

Shape	Point	Point	Point	Point
Latitude	56.891	56.891	56.881	56.872
Longitude	–95.369	–95.353	–95.369	–95.386
Date	20000805	20000805	20000808	20000808
Province	MB	MB	MB	MB
Ecoregtude	71	71	71	71
Temp	20	20	16	16
RH	68	68	74	74
Wind Dir	337	337	241	241
Wind Sp	5	5	31	31
Precip	0	0	0	0
FFMC	86	86	83	83
DMC	33	33	36	36
DC	254	254	272	272
ISI	3	3	8	8
BUI	50	50	54	54
FWI	8	8	19	19
Fuel Type	M2	C2	M2	C1
CFB	0	23	0	0
TFC	0.9	2.4	1.0	0.6
HFI	76	1759	117	219
ROS	0.3	2.5	0.4	1.3

Fig. 4.8. An example of the Fire M3 modeling component. A fragment of web-page with attributes of forest fire hotspots in northeastern Manitoba is displayed for August 5–8, 2000 [22]

Figure 4.9 gives examples of Fire M3 maps, published on the Internet.

Ecological monitoring is one of the most efficient methods of atmospheric data capture [23, 24]. GIS technologies allow to process primary data arrays and map them with high speed and accuracy. To make a digital model of concentrations distribution the method of radial basis functions with multiquadric basis function [23] was applied as an interpolation method.

GIS technologies are deployed for air quality assessment in Bangkok (Thailand) [25]. The input data are received from air analyzers manufactured by nano-technologies and integrated in PDA-like minicomputers with Bluetooth and GPS. Internet GIS technologies are also applied. User can get information from usual Internet browser without installing separate GIS system.

GIS technologies are widely used for the distribution analysis of man-induced forest fires in space and time [26]. Thus, GIS system was applied to make spatial identification of fires from 1950 to 1992 on the territory of temperate forests in Vancouver Island (Canada). The territory of the island is separated in 1x1 km size cells to define climatic conditions and distance to the nearest center of anthropogenic activity for each cell. Regression model was used to estimate probability of forest fire occurrence induced by a human for each cell. The model incorporated weather conditions and the distance to the nearest center of anthropogenic activity as main variables. More than 6000 ignitions were considered and it was stated that cells with high probability of fire occurrence tend to decrease the number of fires, and vice versa.

However, a more general problem, i.e. geoinformation mapping of ecological risks, is of high interest nowadays. Developed comprehensive technique models and

displays localized values of ecological risks [27] conditioned by the impact of polluted atmosphere on the people's health. The technique can be used to assist decision-making in the area of environmental quality management by specialists in ecology, life safety and medicine.

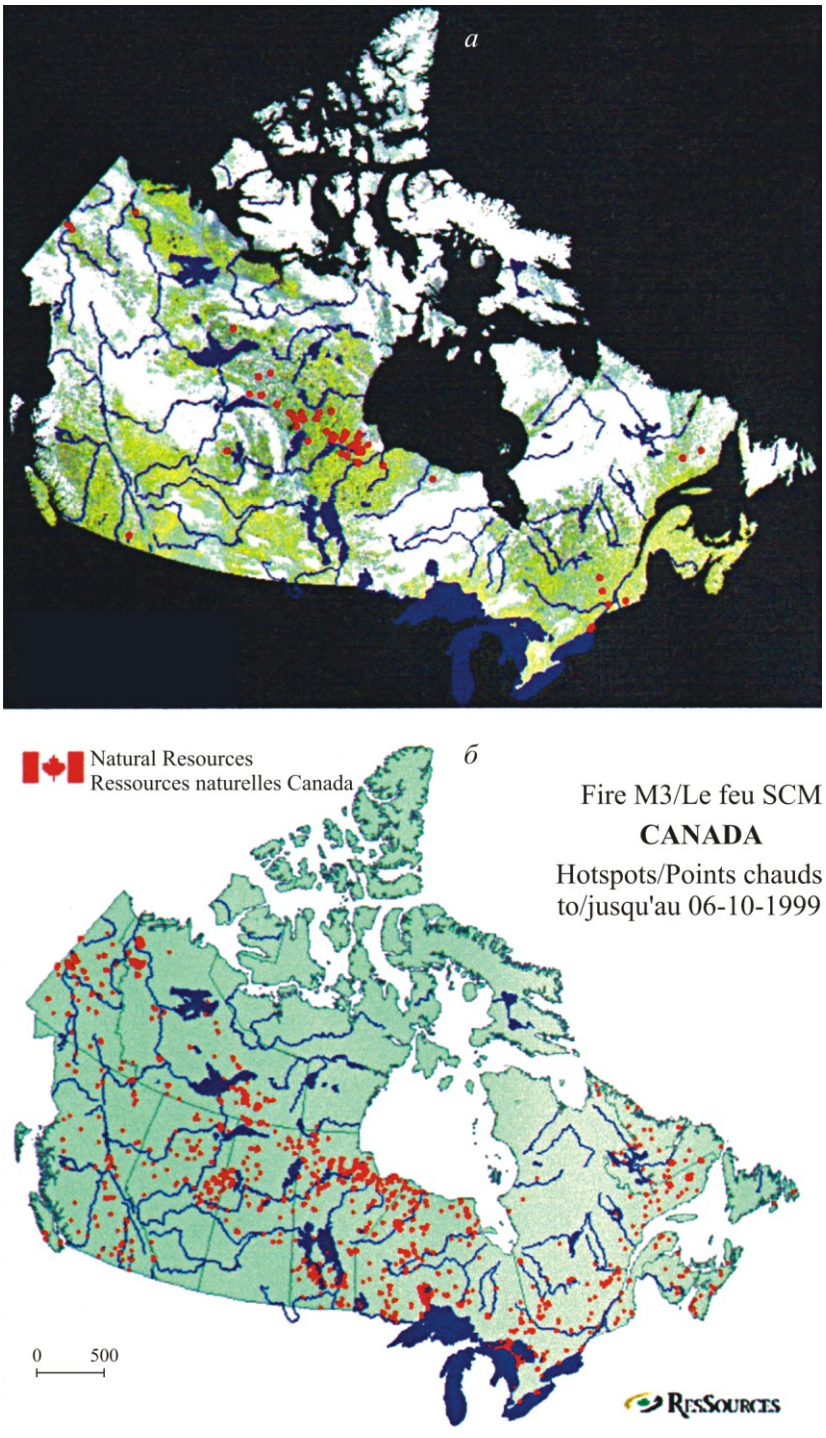

Fig. 4.9. Fire M3 products: (a) AVHRR satellite image (b) and a map of all hotspots detected during the 1999 fire season as of October 6, 1999. [22]

4.2. Satellite Monitoring of Forest Fires

To predict and monitor forest fires and their impact on global ecosystems, risk indexes obtained from satellite measurements are being widely used. In [28] on the basis of AVHRR data and normalized index NDVI a new index was defined. This index combines static fire probability maps and NDVI. It is suggested to use satellites for estimation of vegetation water content and surface temperature [28]. AVHRR – NOAA data allow receiving global information twice a day [29]. During this decade different indexes were presented with different underlying technologies [30], data on surface temperature and corresponding values of NDVI [31]. Also this decade featured the development of Fire Risk Dynamic Index (FRDI) (Fig. 4.10). Before that, Fire Risk Static Index (FRSI) was defined which considered such static factors as, for example, proximity of highways, type of vegetation cover, solar radiation impact, height above the sea level. Fusion of static index with vegetation water content index (obtained from NDVI data) allowed representing the dynamic index as static function of probability from NDVI.

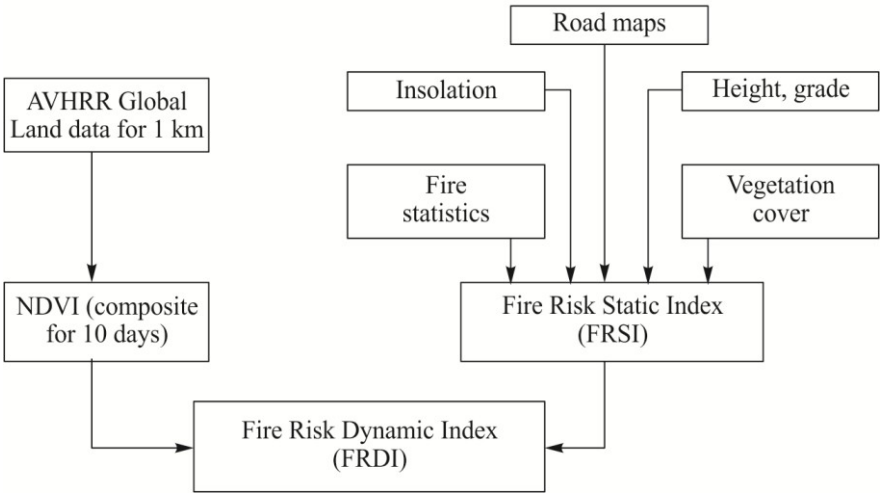

Fig. 4.10. FRDI dynamic index scheme [28]

There are surveys of water content in crown fuels [32] based on MODIS data [33], NDVI [34 - 36], SPOT VEGETATION [37].

In 1998 – 2000 specialists of the Optic Signals Distribution Laboratory, Institute for Atmospheric Optics SB RAS, conducted space monitoring of Tomsk regional forests fires by the order of the Tomsk Forest Management and the Tomsk Aviation Forest Air Protection. Satellites NOAA-12, 14 and 15 were located on the polar orbits of the Earth and received information of AVHRR radiometer which was measuring the upward radiation within five spectral channels— 0.58—0.68 (1), 0.725—1.1 (2), 3.55—3.93 (3), 10.3—11.3 (4) and 11.5—12.5 (5) [38]. Each satellite could have captured two images a day (before and after 12.00 noon time) with maximal spatial resolution. However in 1999 – 2000 low quality satellite information made authors [38] reject morning images and screen thoroughly faulty data for evening images.

A special center in the Institute of Forest SB RAS captures and processes information, transmitted from NOAA satellite [39]. The center has accumulated vast experience in forest fire danger assessment, basing on space information processing; moreover, it has developed fundamentals of fire aerospace monitoring [40]. Most prominent outputs of the center for the moment are as follows.

1. High Spatial Resolution Method which allows to identify emerging forest fires in space images from NOAA satellites. The method considers capacities of data-acquisition equipment, spatial and power characteristics of fires, condition of atmosphere and vegetation. Small-sized fires are detected through the difference in their emittance reflected on the channels of receivers 2, 3 and 5. Hence, the efficiency of forest firefighting is enhanced due to early detection.

2. Algorithm and program for fire destructive force detection basing on aerospace data and considering possible multiple spot fires to provide quick assessment of firefighting capacities and fire consequences.

Forest fire danger is predicted [4] by the method of V.G. Nesterov. Correlation analysis proved tight links between temperatures measured at meteorological station and radiant temperature received from AVHRR. To define the temperature of a subcloud layer (invisible for thermal channels of AVHRR) microwave sounding data can be used. These data are provided by aboard system TOVS which is able to retrieve vertical profiles of 15 parameters (including air temperature and dew point temperature) during one observation period in 600 points distributed in the visible area of coverage.

Interpretation of satellite images is closely connected with the issue of increasing the data reliability on potential spot fires. Thus, the comparative analysis of the latest images becomes most evident and simple method of reliability enhancement. Besides, there exist such problems of space monitoring as cloud blanketing of the Earth's surface and shielding of surface layer by the canopy.

Satellite technologies are very efficient in spot fire detection [38], head fire spread reconstructions [41], evaluation of area consumed by the fire [42, 43] and in emission assessment of spot fire pollutants [43, 44].

4.3. Parallel and Distributed Computing

The necessity of parallel computing and highly efficient computing systems in the area of forest protection is conditioned by several reasons:

1. To prevent destruction of the state forest fund and atmospheric pollution by products of thermal decomposition and fuel combustion, the spot fire probability assessment and fire condition development prediction should consider such a crucial parameter as the period of catastrophe induction (unfavorable situation inducing forest fire). Longer period means more time for forest protecting services to take preventive measures and actions to reduce expected ecological damage, death rate and injuries of people

2. Probability assessment of forest fire attacking the territory of a settlement or production facilities situated in forested is also dependent on time resource allowance necessary for taking measures aimed at damage reduction. In this case the period of catastrophe induction means the time of head fire spread from the spot fire to a strategic site.

Parallel computing allows working quickly with big volumes of information and significantly reducing of time for a forest fire situation analysis.

This section contains minimal necessary information on hardware and software of high-performance computing on parallel structured systems. Except for printed sources, materials of Information analytical center of parallel computing (www.parallel.ru) were used to prepare this section.

4.3.1. General Information

Application of multi-processor computing systems allows solving large-scale tasks which haven't been solved before, launch mathematical modeling of complex physical phenomenon, chemical processes and technical devices. Today supercomputers are universal and indispensable tool for both research and practical purposes.

Currently there are a big number of high-performance multi-processor computing systems and, hence, the specialist in parallel computing should have at least minimal knowledge of parallel computing systems architecture. It must be mentioned that non-standard means used for programming lead to problems in parallel programs transfer.

Main features of parallel computing are high efficiency of programs, application of special programming patterns and means which result in high complexity of programming and problems with program transferability [45]. Parallel program efficiency depends mainly on correlation of computing time with communication time between computers. The less is the share of time for communication in total time of computing the higher is the efficiency.

Cheap processors allow assembling relatively inexpensive supercomputer however the absence of parallel programs which use their capacities significantly inhibits distribution of such computers. It turned out that the development costs of such programs is extremely high which can be explained by several reasons.

First of all, developers have to learn to think with parallel categories. Secondly, almost all debugging systems of the program influence on its behavior. Thus, a single-step debugging which is very efficient for scalar machines is absolutely inefficient for parallel systems. Thirdly, programs created in majority of parallel systems require processing when transferring to machines different from the one they were created for. Typical approaches suggest that the number of processors and their interrelations are set at the stage of programming. During program transfer from one machine to another not only parameters but quite often the algorithm itself has to be changed.

The desire to get maximal performance from a computer makes developers create libraries of message transfer which consider peculiarities of a machine. This facilitates development of efficient but tailored for one machine programs. Meanwhile software developers offer various environments for data transfer independent of a specific platform. Every environment has its own interface presented as a set of procedures and functions (as a rule they are coded in two variants – for C and Fortran languages).

4.3.2. Architectures of Multiprocessor Computing Systems

Main parameter of parallel computers classification is having shared (symmetrical multiprocessor systems SMP) or distributed memory (massive parallel processing MPP) [46, 47]. NUMA architectures are placed somewhere in the middle between SMP and MPP: memory is physically distributed but logically shared. Cluster systems are a cheaper variant of MPP. If vector instructions are supported then we talk about vector pipeline processors which can be, in their turn, grouped into PVP systems with shared or distributed memory. Moreover, combination of various architectures under one system and creation of heterogeneous systems gain popularity nowadays. Distributed computing in global networks (Internet) deploys meta-computers which technically are not parallel architectures.

Massive parallel processing architectures (MPP) consist of homogenous computational nodes which include: one or several CPU's, local memory (random access to memory of other nodes is impossible), communication processor or network adapter, sometimes – hard disk (as in SP) and/or other input-output devices. Special input-output devices and control nodes can be added to the system. Nodes are connected via some communication environment (high-speed network, commutator, etc.). Figure 4.11 gives schematic overview of distributed memory architecture (MPP). Examples: IBM RS/6000 SP2, Intel PARAGON/ASCI Red, SGI/CRAY T3E, Hitachi SR8000, transputer system Parsytec. Total number of processors in real systems reaches several thousands (ASCI Red, Blue Mountain).

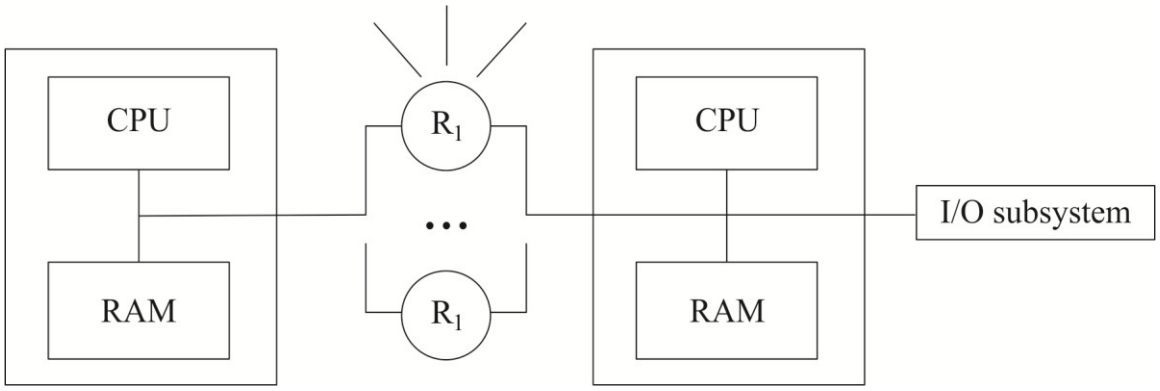

Fig. 4.11. Scheme of Shared Memory Architecture [48]

As for operating system (OS), there are two main variants.

1. Full-featured OS works only with controlling computer (front-end), nodes have limited OS version which provides functioning of parallel application branch installed in this machine. Example: Cray T3E.

2. Each node has full-featured UNIX-like OS (variant close to cluster approach). Example: IBM RS/6000 SP + OS AIX installed individually for each node.

Programming is going on within the message-passing model (MPI, PVM, BSPlib).

Symmetrical multiprocessor systems consist of several uniform processors shared memory array (several independent units). All processors have access to any part of memory with the same speed. Processors are connected to the memory either with the same bus (base two-four processor SMP servers) or with crossbar-commutators (HP

9000). Cache coherency is supported by equipment. Figure 4.12 shows the scheme of SMP architecture. Examples: HP 9000 V-class, N-class; SMP-servers and work stations based on Intel (IBM, HP, Compaq, Dell, ALR, Unisys, DG, Fujitsu and others). Shared memory simplifies interaction of processors but restricts their number – not more than 32 in real systems. Cluster or NUMA-architectures are used for SMP-based scalable systems creation.

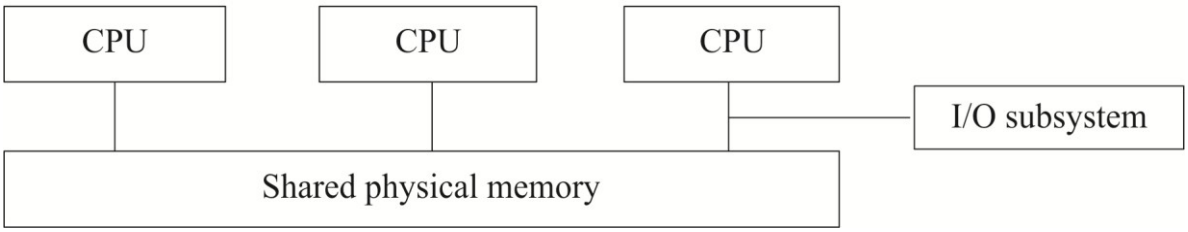

Fig. 4.12. SMP Architecture Scheme [48]

The whole system works under one OS (usually UNIX-like one, but for Intel-platforms Windows NT is provided). OS automatically distributes processes/threads among processors but sometimes direct binding is possible. Programming within shared memory model (POSIX threads, OpenMP). Sufficiently efficient means of automatic paralleling exist for SMP systems.

Systems with non-uniform memory access (NUMA) consist of homogenous base modules (boards) with several processors and memory unit. Modules are joined by high-speed commutators. Interconnect address space is supported as well as access to remote memory i.e. memory of other modules. However the access to local memory is faster than access to the remote one. If cache coherency is provided in the system (it is done usually) then we can talk about cc-NUMA (cache-coherent NUMA). Examples: HP 9000 V-class in SCA-configurations, SGI Origin2000, Sun HPC 10000, IBM/Sequent NUMA-Q 2000, SNI RM600. Scalability of NUMA-systems is limited by the volume of the address space, equipment capacities in terms of cache coherency support and capacities of operating system for multiprocessor system controlling. Figure 4.13 gives the scheme of NUMA architecture.

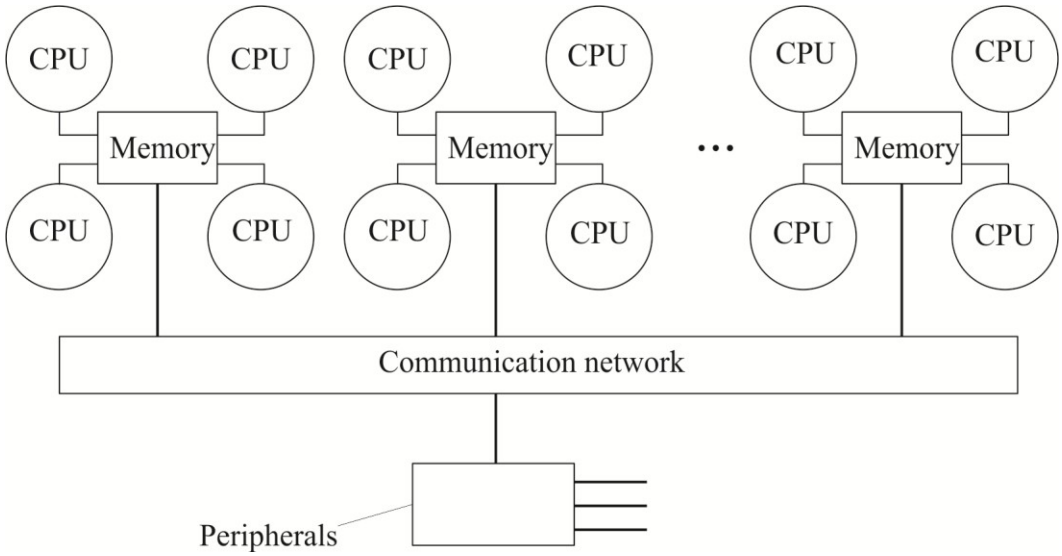

Fig. 4.13. NUMA Architecture Scheme [48]

As in the case with SMP, this system also functions under one OS. However some variants are possible like dynamic “subdivision” of the system, when separate “subdivisions” function under different OS (Windows NT and UNIX in NUMA-Q 2000). Programming model is analogical to SMP’s one.

Main feature of Parallel Vector systems (PVP) is a presence of vector-pipeline processors which provide typical processing of independent data vectors. This instruction is efficiently performed by pipeline devices. Usually several processors (1 - 16) work together with shared memory (as in SMP) within multiprocessor configurations. Several nodes can be united by a commutator (as in MPP). Examples: NEC SX-4/SX-5, the line of vector pipelined computers CRAY (CRAY-1, CRAY J90/T90, CRAY SV1), Fujitsu VPP series. Efficient programming means vectorization of cycles to reach rational performance of one processor and their paralleling for simultaneous loading of several processors by one application.

Cluster systems consist of the several work stations (or even PCs) which are used as a cheap variant of massively-parallel computer. To connect the nodes, one of standard network technologies (Fast/Gigabit Ethernet, Myrinet) based on bus architecture or commutator is used. Uniting into the cluster several computers with different capacities or different architectures means creating heterogeneous (non-uniform) clusters. Cluster nodes can be simultaneously used as user’s work stations. Architecture of a cluster computing system (method of processors interconnection) defines its performance to a greater extent rather than the type of processers deployed. Figure 4.14 shows the type of processor connection presented as a plane grating.

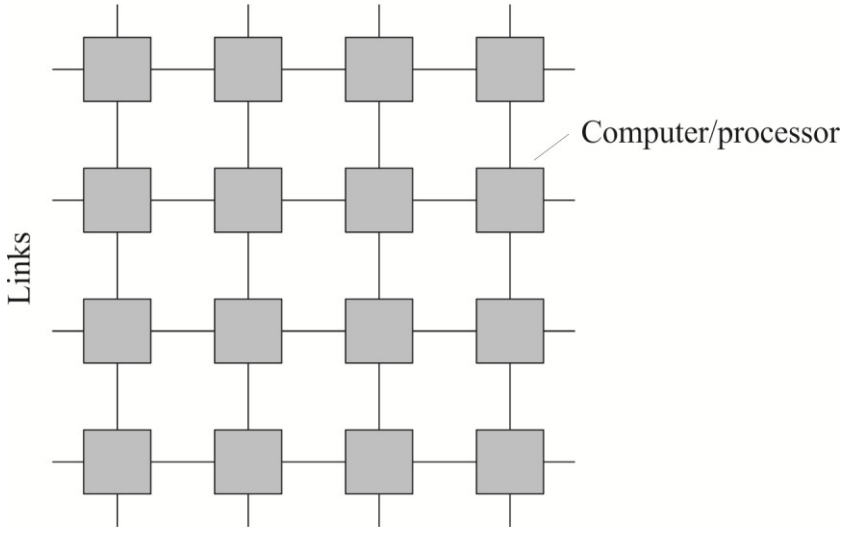

Fig. 4.14. Processors connected in a plane grating [48]

Figures 4.15 – 4.17. gives schemes of processors connections in the shape of three-dimensional cube, four-dimensional hyper-cube and rings with full connection by chords.

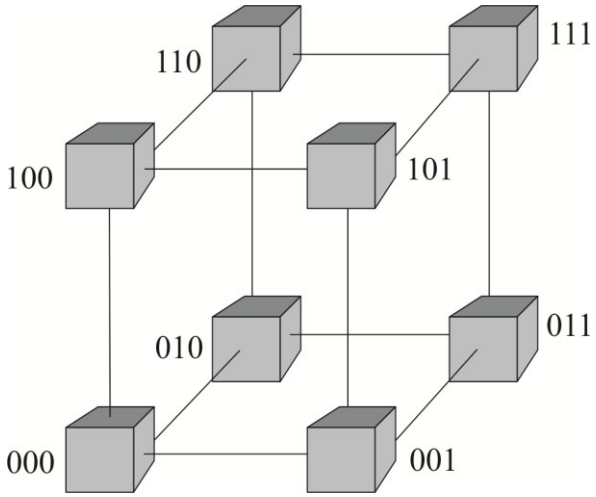

Fig. 4.15. Processors connected in three-dimensional hyper-cube [48]

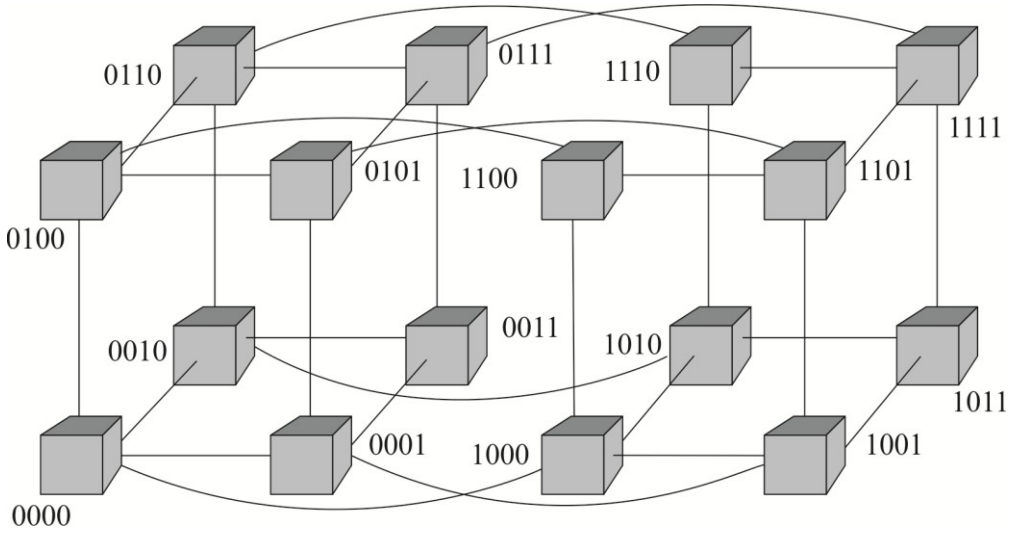

Fig. 4.16. Processors connected in four-dimensional hyper-cube [48]

Nodes of the cluster can be significantly simplified and/or set in the stand. Examples: NT-cluster in NCSA, Beowulf-clusters. Standard operating systems are used for work stations. Usually these are OS which are distributed freely – Linux/ FreeBSD. They are used together with special means for parallel computing and load distribution. Programming usually corresponds to the model of message passing (usually - MPI). Low cost of such systems brings about high indirect expenses for interaction of parallel processes thus narrowing the sphere of tasks to be solved.

Beowulf project [49] first appeared in NASA research space center – Goddard Space Flight Center (GSFC) and if, being more precise, in CESDIS (Center of Excellence in Space Data and Information Sciences) center created on its basis. Beowulf project was launched in summer 1994 with assembling 16-processor cluster (486DX4/100MHz processors, 16 Mbyte memory and three network adapters for each node, three "parallel" Ethernet-cables for 10 Mbit each). This cluster was named "Beowulf" and it was created as a computing resource for Earth and Space Science Project (ESS). Official web-site of Beowulf project – www.beowulf.org.

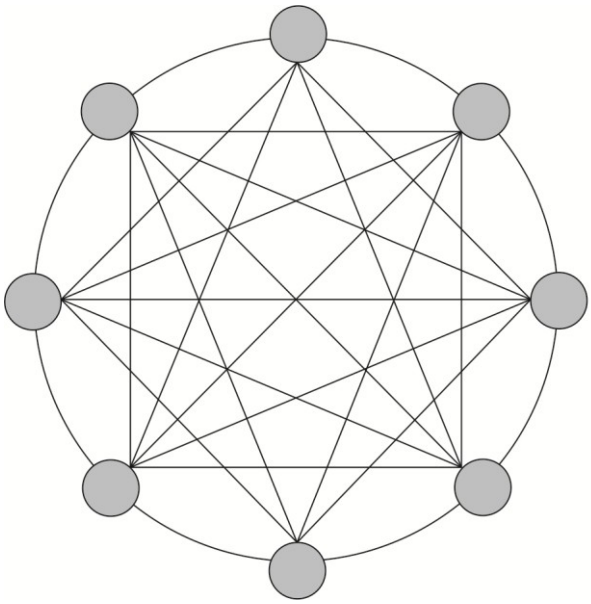

Fig. 4.17. Processors connected in a ring with full connection by chords [48]

In 1998 astrophysicist Michael Warren and other scientist in Theoretical Astrophysics Group from Los-Alamos National Laboratory built supercomputer Avalon which is a Linux-cluster on the basis of DEC Alpha/533MHz processors. Avalon consists of 150 processors. Each node has 256 Mbyte of RAM memory, EIDE hard disk drive for 3.2 Gbyte, Kingston network adapter. Nodes are connected by 36-port fast Ethernet commutators and "central" 12-port gigabit Ethernet commutator. Performance according to LINPACK (47.7 Gflops). Until recently Avalon has been used for astrophysical, molecular and other scientific computations. At the SuperComputing'98 conference creators of Avalon made a report called "Avalon: An Alpha/Linux Cluster Achieves 10 Gflops for $150k" and won the award for price/performance indicator («1998 Gordon Bell Price/Performance Prize») [50].

In October, 2000, Tomsk State University launched the computing cluster (Fig. 4.18) within the "Integration" project. Cluster consists of nine two-processor computers based on Intel Pentium III 650 MHz. One computer is a server with 512 Mb of RAM memory and two hard disk drives, 18 GB each. All other computers are nodes and used for parallel computing. RAM memory is 254 MB for each of them. The server and nodes are joined in the local area network 100 Mb Ethernet by means of Cisco Catalyst 2924 switch. General performance characteristics: 18 Pentium III 650 processors, 2.5 GB RAM, 36 GB disk space, software: OS Free BSD 4.2, cluster package LAM MPI v 6.3.2.

Fig. 4.18. Computing cluster of Tomsk State University
(Materials are taken from http://skif.tsu.ru)

Inter-regional computer center (ICC) of TSU was established in 2007 and belongs to the Tomsk state university. Supercomputer installed – SKIF-Cyberia (Table 4.2).

Main goals of the ICC:

1. Technical and technological support of high-performance computing by TSU resources to aid the solution of scientific and technical tasks.

2. Development and integration of means and methods for information protection.

3. Regional high-performance computing development basing on information and telecommunication systems.

4. Training of engineers and technical specialist for high-performance computing branch.

Systems can be divided into independent computing computational sections, isolated from each. The system comprises protective means against unauthorized intrusions, equipment for monitoring and system management. Computing system is supplied with auxiliary equipment:

1) system network InfiniBand to provide simultaneous work of all computing nodes;

Table 4.2. Configuration of SKIF Cyberia supercomputer (based on the materials from http://skif.tsu.ru)

System type	Cluster
Processor Architecture	x86 with support of 64-bit extensions
Number of Computing Nodes/Processors	283/566 (one node — controlling) (1132 cores)
Processor Type	Dual-core Intel®Xeon® 5150, 2.66 GHz (Woodcrest)
Message Transmission Rate between Nodes	950 MB/s with delay no longer than 2.5 us
Peak Performance	12 Tflops
Actual Performance from Linpack test	9.013 Tflops (75 % from the peak)
Total RAM Capacity	1136 GB
Total Disk Capacity	22.56 TB
External Disk Storage Systems	10 T6
Parallel File System	Total Network capacity 700 Mb/s
Power Intake	90 kW

2) auxiliary network Gigabit Ethernet to connect controlling and computing nodes;

3) service network to enable remote power supply on/off, console access to each computing node;

4) UPS which provides the work of the computing cluster during 7 min in case of a power-off;

5) data storage system;

6) climate control system to provide optimal conditions for the equipment within the temperature range – 40 C°÷ +40 °C.

System support and software installed [51]:

1) Operating System Linux SUSE Enterprise Server 10.0;

2) Operating System Microsoft Windows Compute Cluster Server 2003;

3) Support of MPI and OpenMP parallel programming standards;

4) Application building means – high-performance optimizing compilers from C/C++/Fortran (Intel 9.1) languages;

5) Total View Enterprise 8.2 which allows parallel debugging and tracking of applications;

6) task control systems, management and monitoring means for Ganglia supercomputer;

7) specialized software – Fluent and Ansys which provide capabilities to solve scientific and engineering tasks, MM5 and WRF simulators for weather and climate survey, CAMx and CMAQ systems to solve environmental tasks;

8) ScaLapack, PETs, FFTW, MKL, SPRNG libraries for parallel computing.

4.3.3. Computing Models and Parallel Computing

For parallel systems with message transfer the optimal ratio between computing and communications is provided by the so-called coarse-grain parallelization, when parallel algorithms are built of major and rarely interacting blocks.

MPMD-model. Parallel program is a combination of autonomous processes, functioning under control of their own programs and interacting by means of a stand-

ard set of library structures for message transfer and receipt. In a very general case a parallel program implements and MPMD programming model (Multiple Program — Multiple Data) [52].

SPMD-model. All processes fulfill different branches of one and the same program in general. Such approach is conditioned by the fact that a task can be quite naturally divided in sub-tasks, solved by one algorithm. In practice this very programming model is the most often encountered (Single Program — Multiple Data) [52].

SPMD-model in other words can be called a model of data parallelization. Essence of this method is as follows. Initial task conditions are distributed by processes (parallel algorithm branches), and algorithm is the same for all processes, but its actions are distributed according to the data available in the processes. For example, algorithm actions distribution is assigning of different values to the same cycle variables in different branches or execution of a different number of turns in the same cycles of different branches, etc. In other words, process of each branch follows different ways of the same program execution.

Basically, any set of MPMD-programs, designed for each of m processors, can be replaced with one merged program, here only memory requirements increase. Thus, a popular SPMD model does not put any considerable limitations in comparison to a pure MPMD model.

A simple testing, without formal validation of program correctness, is not able to provide the program correctness. Application of the formal methods only does not provide good results, as it is the same difficult to apply a formal method as develop it. In practice testing and formal proof of correctness should be combined [45].

The attention should be given to a dangerous seeming correctness of partially correct, but not totally correct programs, as quite often such program can work for a long period and error is found at the most inappropriate moment [53].

4.3.4. MPI Library

A standard message transfer interface MPI (Message Passing Interface Standard) was developed and adopted in 1994 [52]. It was prepared during period from 1992 till 1994 by the Message Passing Interface Forum group, which included representatives of over 40 organizations from Europe and America. MPI is a procedural interface for C and Fortran languages. It includes functions required for point-to-point message transfer and for collective exchanges.

The standard explicitly introduces the following notions: groups of processes, which can be operated both with finite sets, and communicators, realizing the context for message transfer. Owing to the notion of context it becomes possible to develop standard libraries of programs. MPI provides for message transfer in the heterogeneous medium and provides for data translation from the form, required for one processor, into the form, suitable for the other. The standard admits both programming in SPMD style, and programs, consisting of several textually different parts, each of them downloaded in a different processor. Currently several MPI realizations have been developed, part of them, being distributed for free. The standard combines the most successful aspects of predecessors majority: support of different-type processors (automatic conversion of transferred data is served), synchronous and asynchronous message transfer, their passing without blocking, broadcast mode “one-to-many”,

barrier synchronization, dispatch of array elements to a group of processors (scatter) and array collection from the data, distributed in several computational nodes (gather); reduction functions, which are determined by data, distributed to a processors group. The most important innovation, making the MPI a viable standard, is a communicator notion, which sets the one-to-many message transfer context. It made possible to design and encode standard libraries of parallel algorithms. It should be mentioned that in spite of a deep consideration of the standard, many issues remained ignored. First of all, this is a problem of dynamic balancing: it is still difficult to program an algorithm so that computations were passed automatically from the loaded processor to a temporarily idle one.

Now different groups of developers wrote several program packages, meeting the MPI specification, in particular: MPICH [54], LAM MPI [55, 56]. They serve as the basis for MPI transfer to new computer architectures.

Parallel application consists of several branches, or processes, or tasks, fulfilled simultaneously. Different processes can be carried out both by different processors, and by the only one — it is not important for the program as in both cases the data exchange mechanism is the same.

Many of MPI functions have a communicator among input arguments, which limits their scope by the region of communication, to which it is bound. Several communicators can operate for one region in such way that application would work with it as with several different regions. Identifier MPI_COMM_WORLD is often used in the initial texts of MPI examples [54]. This is the communicator name, developed by the library automatically. It describes a starting region of communication, integrating all of the application processes.

4.3.5. OpenMP — a standard for parallelization in the shared memory model

OpenMP interface [57] was designed as a standard for programming on the scalable SMP-systems (SSMP, ccNUMA and other) in the shared memory model. OpenMP standard includes specifications for a directives set of a compiler, procedure and medium's variables.

Supercomputers Cray Origin2000 (up to 128 processors), HP 9000 V-class (up to 32 processors in one node, and up to four nodes in the configuration—up to 128 processors), Sun Starfire (up to 64 processors) can serve as the examples of shared memory systems, scalable up to a big number of processors.

The standard is developed by OpenMP ARB (ARchitecture Board), which includes representatives of major companies — SMP architecture and software developers. Specifications for Fortran and C/C++ languages appeared in October 1997 and October 1998, accordingly.

OpenMP advantages:

1. Owing to the idea of incremental parallelization, OpenMP perfectly suits for developers, who want to parallelize their computational programs with large parallel cycles. A developer simply adds OpenMP-directives in the text of the sequential program, and does not to develop a new parallel program.

2. Moreover, OpenMP is a quite flexible mechanism, providing a developer great opportunities of control over parallel application performance.

3. It is assumed that OpenMP-program can be used as a sequential program based on a single-processor platform, i.e. no necessity to support sequential and parallel versions. OpenMP directives are simply ignored by a sequential compiler.

4. One of the OpenMP benefits its developers think support of so-called orphan directives, i.e. directives of synchronization and load distribution may not be included directly in the lexical extent of parallel regions.

For the purpose of generation of portable medium for parallel programs launch in OpenMP, a range of medium variables was determined, controlling the application performance. A set of library procedures is also provided for in OpenMP, which allow: control and inquire for various parameters during execution, defining application performance (such as number of threads and processors, feature of nested parallelism); for procedures of parameter setting to have the priority over respective variables of the medium; use synchronization, based on locks.

4.3.6. Parallel Virtual Machine (PVM) Library

PVM [58] software package allows connecting heterogeneous computers set in the network to be used as a parallel computer. PVM library realization supports:

Heterogeneity of computers, networks and applications;

An elaborate model of message passing;

Data processing, based on process execution;

Multiprocessor data processing (MPP, SMP);

Semi-transparent access to equipment (applications can ether ignore, or use the benefits of hardware differences);

Dynamically adjustable pool (processors can be added or removed dynamically).

It is possible to access the PVM functional capabilities from C++-programs using a set of library procedures. These PVM functions and procedures are usually divided into seven categories:

Processes management;

Message packing and their sending;

Message unpacking and their receipt;

Problems exchange by signals;

Communication buffer management;

Information processing functions and utility routines;

Group operations.

For execution of parallel PVM-programs it is first required to install PVM-medium. The program can be executed by one of three main ways: to launch an offline executable file, use PVM-console or XPVM medium.

Executable files of any programs, participating in the PVM medium, shall be placed on all computers, included in the PVM. In addition, each program shall be compiled for operation, subject to a specific architecture.

Each PVM-program is an autonomous C++-program, which has its own address space. Global variables of one PVM-task are invisible for the other PVM-tasks. A message transfer mechanism is used for separate tasks interaction. If the PVM-program is executed on one computer with several processors, then programs can additionally use a file system, FIFO-queues, and shared memory.

PVM is the simplest (in terms of usage) and the most flexible medium, available for parallel programming problems solving, which require use of different-type computers, working under different operation systems. PVM-library is especially useful for integration of several single-processor systems in the network to generate a virtual parallel machine. PVM can be used as both SPMD- and MPMD-models of programming. It was recommended in [58] to use a PVM-library for small and medium-volume tasks of parallel programming, and for more complex and volumetric — MPI-library.

4.3.7. High Performance Fortran

High Performance Fortran (HPF) is an extension of a programming language Fortran-90 and is quite commonly applied for parallel programs development [59]. HPF was designed by HPF Forum group, the leading role in which belonged to representatives of Cray Research, DEC, Hewlett Packard, IBM, Intel and other companies. If LAM MPI, PVM are free programs, then majority of HPF compilers are commercial.

HPF commands come to a small number of directives, realizing the SPMD-model parallel programming, i.e. all processors execute one and the same program. Each process handles an assigned part of total data array. HPF developers tried to save an application programmer from explicit message transfer. Some programs, written in HPF, cannot reach their realization effectiveness by means of message transfer. Besides, a program in Fortran-90, processed by an HPF compiler without any changes, will be parallelized by the system tools, and even such primitive way of parallelization can give a performance growth.

Syntax of HPF instructions makes them invisible for the basic language, as they look like remarks of Fortran-90. HPF does not interfere with the program actions practically, it only distributes the data. A program with HPF directives can be compiled by a Fortran-90 compiler and no changes will be required for the compilation process to progress successfully. PROCESSORS Directive is conceptual in the HPF. It introduces the description of pseudo-arrays of processors — virtual structures that do not have any relation to an actual set of physical processors. One program can describe several processors sets. Data in the arrays can be distributed only by a set of processors of the same rank as distributed arrays. DISTRIBUTE directive deals with data distribution. If a distribution method is omitted in this directive, then block distribution is engaged. If ONTO structure is omitted, then distribution is carried out, according to a processors set, by default, when a number of processors equals to a number of physical processors, a pseudo-array form corresponds to the form of distributed array. Maldistribution can result in a disastrous growth of exchange and critical performance decrease [59].

There are two types of distribution: block and cyclic. In a block distribution the array elements are distributed in parts, where elements follow in succession. The array is divided into large fragments. Cyclic distribution reminds dealing the cards during a game, when cards are given to everyone in turns. When all payers got the cards, and some cards are left, the dealing is repeated until a dealer runs out of cards. If there is no explicit instruction of iteration step in a cyclic distribution directive, elements are distributed by one. In case when an array size is unknown at the compiling

stage, memory for such array is allocated dynamically. Dynamic arrays can also be distributed, but their elements binding to the processors is done during execution. Scalar variables are copied for each processor and compiler is responsible for their values consistency. It means that initialization of a variable, bound to one processor, will cause a broadcast messages sending to synchronize an updated value in all processors.

4.3.8. Increase of Parallel Programming Level

An application expert would like to know as little as possible about specific computer devices during solving a particular applied task and not have any problems moving from one computer to the other. He would like to use routine means for programming and not investigate the features of compilers, programming languages, system library arrangement, issues of their effective use, etc.

During application programs development for a parallel computer, such comfortable model is usually difficult to realize. Main reasons are requirement to know and use notional from a new subject field — domain of parallel computations.

DVM-system [60], developed in the Keldysh Institute of Applied Mathematics of the RAS (Russian Academy of Science), allows developing parallel programs for computers of various architecture and computer networks in C-DVM and Fortran-DVM languages.

When using C-DVM and Fortran-DVM languages a programmer only has one program option both for sequential and parallel execution. This program, beside the algorithm description by common means of C or Fortran-77 languages, contains rules of parallel execution of this algorithm. The rules are formulated syntactically so they are “invisible” for standard compilers from C or Fortran-77 languages for sequential computing devices and do not hamper in execution and debugging of DVM-program in working stations as for a common sequential program.

Compiler translates a program in the C-DVM (Fortran-DVM) language into a program in a standard C (Fortran) language, extended by functions of DVM-programs support system, which uses standard communication libraries (MPI, PVM, Router) for interprocessor interaction.

However, nowadays it is difficult to name a universal technology, supporting a comfortable development of parallel application programs for solving grid computational tasks. In [61, 62] an approach to parallel programs development is investigated, based on application of the declarative Norma language.

Translator versions were realized from the Norma language, which make it possible to get output routines for distributed parallel computing systems (Norma memory model, parallel computations with message passing), parallel computing systems with a shared memory (NUMA memory model, parallel computations over the shared memory) and sequential computing devices. Выходные programs can be done in Fortran-77, Fortran PVM, Fortran MPI, Fortran GNS [63], and Fortran Convex [64] languages.

Experiment of solving a practical three-dimensional task in astrophysics field on different parallel computing systems with distributed memory is known [65]. When developing different program options for computations, Norma system was used [61, 62], which allowed getting output routines in the Fortran language, using the MPI

(Message Passing Interface) library in a message passing model. Primary attention was given to issues of a parallel program development, analysis of execution period, the given task parallelization efficiency and program portability, made with the help of the Norma system.

Manual translation of a sequential program into Norma language is a labor-intensive process. These difficulties can be avoided, if a program development in Norma language to carry out by computational formulae, and not by a ready sequential program. It is necessary to mention that Norma system allows obtaining both parallel and sequential realizations for one and the same Norma program.

4.3.9. Performance Analysis and Monitoring of Parallel Programs

Currently there are numerous different software, hardware-software systems, aimed at parallel program dynamic analysis. Two classes can be specified [66]:

Tracing + Visualization. It is a traditional approach to dynamic analysis, assuming two stages. During program execution a "trace" is assembled, which reflects the history of program operation. The obtained trace is viewed and analyzed.

Online analysis. This class of analyzing tools studies a program behavior directly during its execution, and long with that there is often an opportunity to influence the progress.

General shortcomings of tracing tools [66]:

1. The format of traces is not unified and is usually oriented to a specific library of message passing.

2. Information acquisition — poor capabilities of event filters setting (what events and what information to be included in the traces). Capability to vary the trace space.

3. Measurement effect is not taken into account – a tracing tool changes the program performance quite significantly.

Considering a general scheme of the dynamic analysis system for parallel programs, three stages can be specified [67]. The first stage is tracing of the analyzed program, the second — launch of changed program on a target computer and the third stage — analysis of the acquired information.

The system can support two basic operation modes: offline and online. In the offline mode all of three stages are executed sequentially, during online operation the second and third stages are overlapped, i.e. information acquisition and analysis occur simultaneously. Practical experience has shown that these tow modes add each other very well functionally.

Some of existing systems have a wide range of capabilities, but do not depend on a specific class of software-hardware platforms [66], thus Vampir system, developed by a German company Pallas, has a vast range of tools, but only oriented to the MPI library, and HP Pak complex, supplied by Hewlett-Packard company, can only work on this company's platforms. An interface of Vampir program is given in Fig. 4.19.

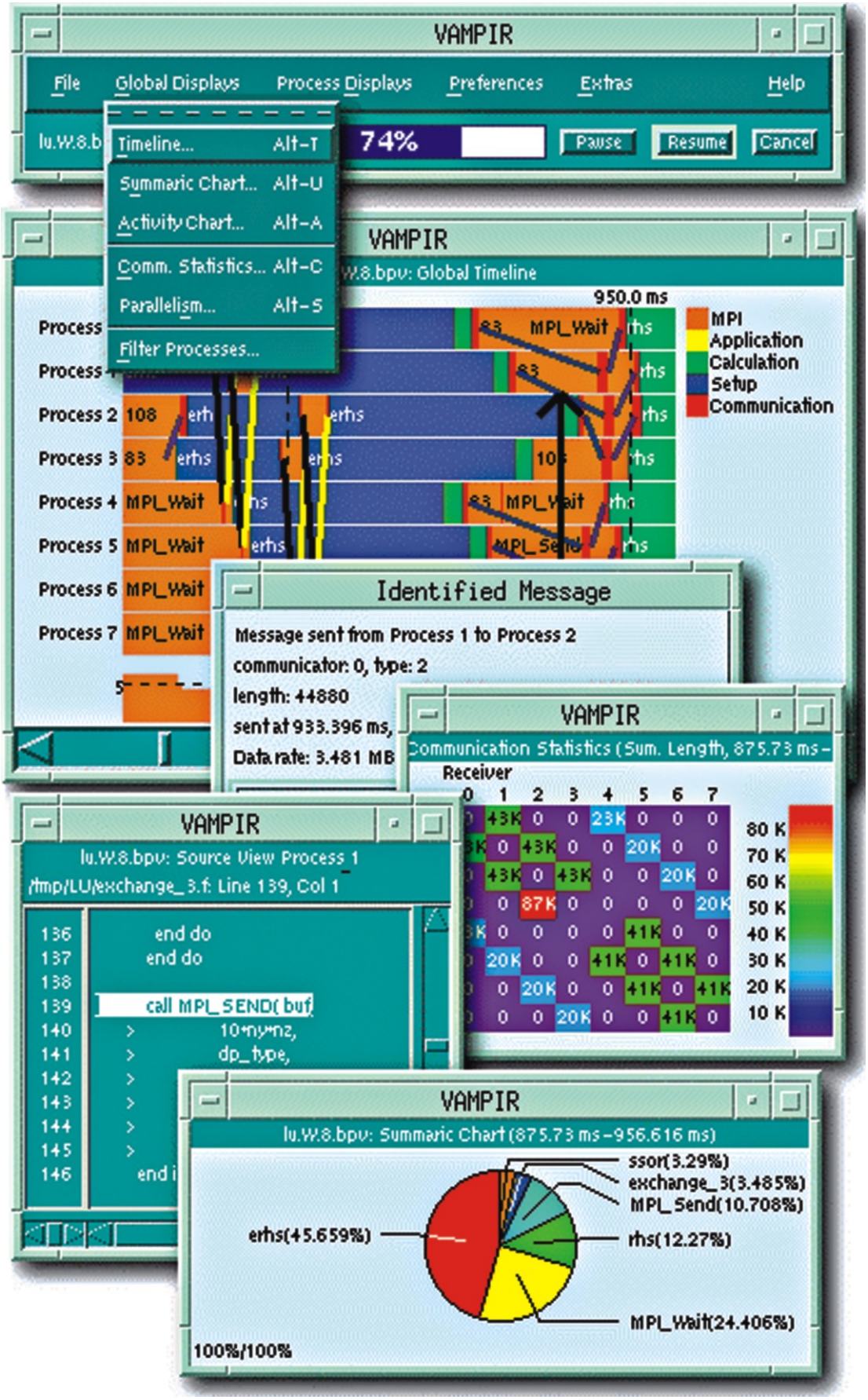

Fig. 4.19. Analysis and monitoring software interface for Vampir parallel applications

Other systems claim the versatility, but only solve some dynamic analysis tasks. A software complex Pablo Performance Analysis Toolkit Software, developed in the Illinois State University [68], can serve as an example. This complex has expanded visual analysis tools of different program characteristics, however, does not possess automated tools of statistics acquisition.

System of parallel programs dynamic analysis and visualization is known, which is included in V-Ray System complex [66], developed in the Research Computing Center of MSU together with the Institute of Computational Mathematics of RAS. Besides the tools, realizing both standard methods of dynamic analysis and new capabilities, this system allows working via Internet, when a supercomputer and user can be located on different continents, along with that a researcher has a fully functional and convenient interface for its program analysis. LAM/MPI package includes a graphical environment of MPI-programs XMPI launch and debugging.

Nowadays technologies of parallel computations have found application in different fields of science and technology. Urban air quality is evaluated using mathematical models of impurity transfer and transformation [69], for a numerical realization of which parallelization of computational operations is used [70, 71]. Spatial non-stationary equations (3.10) were solved numerically for a parallelepiped with multiple surface and altitude sources of an impurity. Approximation of differential operators in (3.10) is done with the second-order accuracy for coordinates and the first for time, using explicit difference schemes for all equation terms except for vertical diffusion [69]. Advective equation terms (3.10) are approximated using the Van Leer's monotonic upwind scheme. Parallelization of a numerical solution method for the considered equation is made using a geometric decomposition. The entire area of research was divided into sub-areas: the parallelepiped was cross-sectioned y = const with data distribution of each sub-area to a corresponding node MCS.

Inside each of sub-areas the finite-difference equations were solved simultaneously by the sweep method. However, a selection of differential template during calculation of concentration values along the boundary grid line leads to necessity to use two grid values from adjacent sub-area. Interprocessor exchanges of the boundary grid values are arranged for a correct operation of a parallel program [69].

If a small number of processors is engaged, then performance growth is observed, practically proportional to a number of engaged processors (10 processors — nine fold acceleration) (Fig. 4.20). Increasing the number of processors, a parallel program performance decreases (20 processors — 15-fold acceleration). A cluster of the Institute of Atmospheric Optics, the Siberian Branch of the Russian Academy of Science, was used for.

Parallel computations are applied for numerical weather forecast tasks. Mesoscale models MM5 and WRF are used for solving the environmental protection problems and for regional weather surveys [72]. Execution of a parallel program code in MCS provides a moderate acceleration of a numerical forecast (20 processors — almost 7-fold acceleration).

Parallelization of computational operations is also applied for a forest fire distribution modeling [73]. Simulation of forest fire distribution is done using computational hydrodynamics models. Dependence of parallel program acceleration on a number of engaged processors is given in Fig. 4.21.

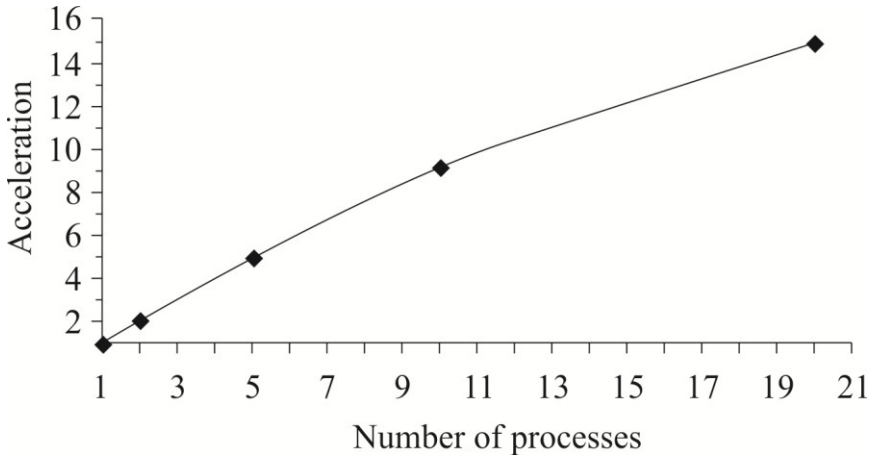

Fig. 4.20. Parallel program acceleration, depending on a number of processors [69]

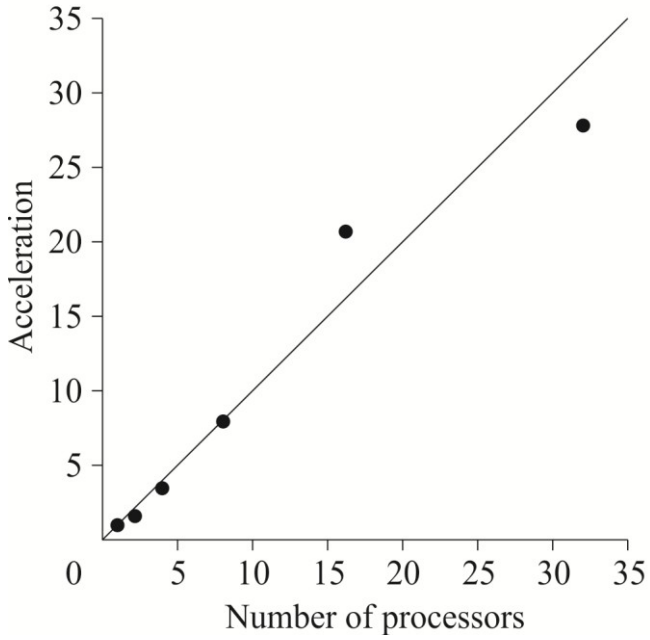

Fig. 4.21. Parallel program acceleration during forest fire modeling, depending on a number of processors [73]

As a result of computational experiments on the HP Integrity SuperDome system, it was established that a parallel program demonstrates a good scalability up to 16 processors. When 32 processors are used, the performance decreases and about 28-fold acceleration is reached.

It should be mentioned that test on 16 processors rises many questions, when almost 20-fold acceleration of computations takes place (Fig. 4.22). It should be assumed that some inaccuracy was admitted during results processing in their graphical presentation.

Technologies of PVM and MPI parallel computations arrangement were used for development of a parallel simulator of a forest fire distribution [74]. As a computer were used the following: clusters of working stations SUN and PC, and Parsytec CC. A forest fire distribution was researched using a global model [75], local model [76],

identification of a fire contour [77]. Approaches to data parallelization were used (an independent calculation of several fire front sections movement) and subprocesses of a forest fire distribution phenomenon (a simultaneous computation of several parts of one algorithm with interprocessor exchange organization). Dependence of parallel program acceleration on a number of engaged processors is given in Fig. 4.22.

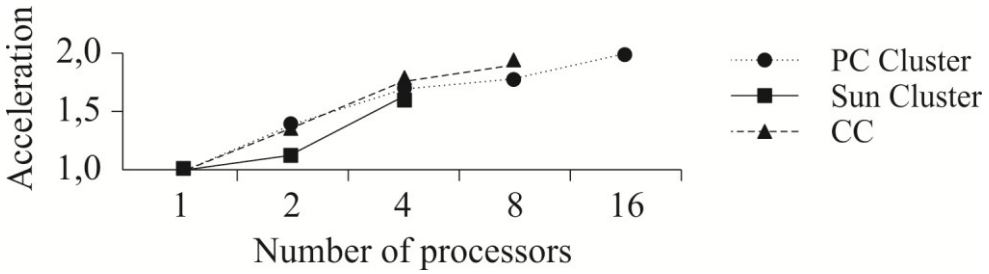

Fig. 4.22. Acceleration of parallel program in dependence from number of processors. Test using 16 processors [74]

Results analysis shows that different MCS have presented approximately equal results: computations acceleration takes place, but it is not significant (eight processors — almost double acceleration). Probably, it is explained by the use of low performance communication media (in comparison to 2009).

All of the above surveys have a similar characteristic: solution of the stated problems requires parallel programs development, during execution of which the information packages are exchanged among different program branches. As results analysis of computational experiment on a parallel program performance evaluation has shown, in some cases it causes a significant decrease of acceleration with the engaged processors number increase. As a consequence, some limitations and problems, regarding the scalability of MCS subprograms, arise with a larger number of processors. That means that advantages of parallel computations are somewhat balanced by limitations for a number of engaged processors in MCS. Their number increase leads to an unjustified growth of overhead costs for interprocessor exchanges.

In terms of performance increase, a parallel program will look more attractive, which does not exchange messages among different MCS nodes during computations. However, not all of problems have such properties of “natural” parallelism. Problems of forest fire danger prediction, level of which depends on meteorological conditions, anthropogenic load and thunderstorm activity can be specified in a special way. Assumption of fire hazard degree independence for specific controlled forest areas will be quite competent. As a result of high-performance parallel technologies use, solving the problems of forest fire danger prediction and monitoring will give the maximum efficiency and parallel programs acceleration.

4.3.10. Landscape Parallelization

Main provisions of landscape parallelization are as follows [78]:

1. Mathematical statement shall be such that computations for each specific homogenous forest site would not depend on other forest sites. In other words, it is nec-

essary to develop the mathematical statement that would let carry out computation for every allotment.

2. A homogenous forest site shall match with the homogenous forest sites, accepted in the forest mensuration descriptions [79]. The term landscape paralleling originates here.

3. It is required to use a data parallelization model to provide more or less even computational load for MCS processor nodes. For example, SPMD-computation model can be used for computations in MPI. Although an even data load does not always provide the evenness of computational load.

4. Capacity to provide a high performance rate (computer speed) of a parallel program on as high number of MCS as possible, of a different architecture, and at the same time having a good price/performance ratio, availability and mass distribution.

5. Provision of a less number of information packages exchanges among parallel program branches during its execution, as the main bottleneck of MCS is a communication medium, applied for communication among processor nodes. Thus, the most optimal option for price/performance criteria can be deemed cluster computing systems; however, having very low indices of processor nodes exchange speed. It conditions a necessity to have as few exchanges as possible and provide for a capability of computations and exchanges overlapping.

6. Provision of single-valued display of administrative, forest mensuration allotment of the state's forest resources (of the Russian Federation, at least) on MCS architecture. Breakdown of the forest resources into allotments and distribution of a computational load by MCS processor nodes.

Computations were done on a training computational cluster of the Tomsk State University [80—82]. Technical specifications are as follows: 18 processors Pentium III 650 MHz, 2.5 GB RAM, 36 GB of disk space, and Fast Ethernet. Program software: FreeBSD 4.2 operating system, cluster package LAM MPI v 6.3.2. Beside that a computational cluster based on computers of local computing network of the Department of Physical and Computer Mechanics of Tomsk State University was made and commissioned. Computers were connected by a network technology Ethernet. A cluster package LAM MPI 6.5.1 was installed for arrangement of parallel computations on the cluster. Cluster nodes can be simultaneously used both as a user station, and directly for computations. In 2002 the cluster was used in the training and research process.

Realization of a parallel MPI-program is done in the programming C language with application of MPI library. Algorithm of the parallel program [83]: input data are cut and dispatched by a root processor of parallel program. Then parallel program processes its part of data in each node. There are no interprocessor exchanges; parallelization is organized in coarse-grained blocks. Upon computations completion, a root process collects the results from all nodes and saves them in results file. Scalable parallel programs were developed (number of engaged processors is a program parameter). Results of a parallel program operation are given in Fig. 4.23, 4.24: efficiency E and acceleration S.

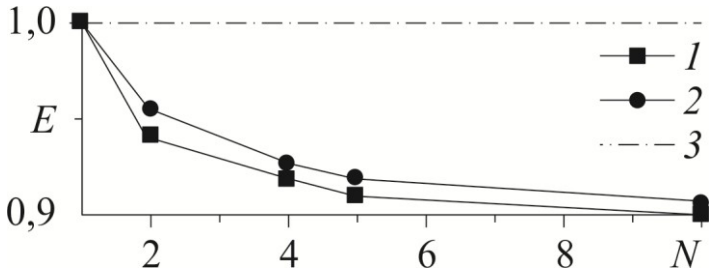

Fig. 4.23. Efficiency (E) of parallel program performance of forest fire fuels layer maturing estimation and forest fire probability [78]: *1* — 100000 allotments; *2* — 60000 allotments; *3* — E_0

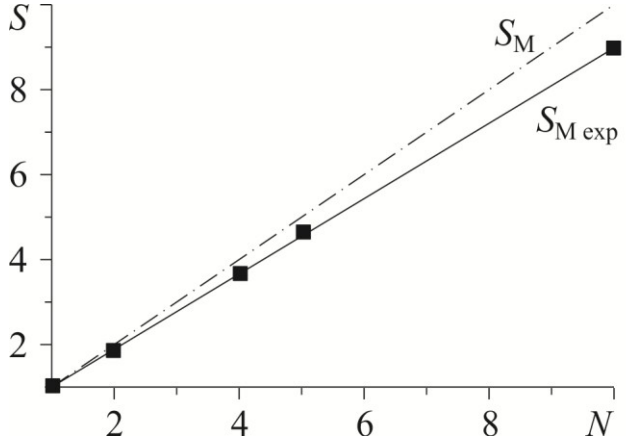

Fig. 4.24. Acceleration of parallel program operation for estimation of forest fuels layer maturing and forest fires probability [78]

Parallel program, which realizes a computation of forest fuels drying time on the underlying surface and probability of forest fire occurrence in vast territories, consists of one-dimensional cycle with index i and iteration amount NV over data structure D.

Algorithm of parallel program is a homogenous one-dimensional cycle on a virtual computation system W, which can be given as a complete graph with unlimited vertices, $w_i \in W$ ($i = 1, 2, ...$) [84]. During a parallel execution of cycle, the structure D components, which are processed in different cycle iterations, are placed in different vertices of virtual computing system W. Let cycle compute the value $F(D)$. In this case the i-th iteration of the considered cycle will be executed on vertex $w_i \in W$: is computed $F(d_i) = f_i(D_i)$, where $D_i \in D$, d_i — a component of structure D, distributed on vertex w_i, and function f_i provides operations, executed on the i-th iteration. As all f_i are equal for a homogenous cycle, then we will designate them by f. Sets D_i depend on D data structure and on the computations algorithm $F(D)$. D_i coincide with c d_i, because data are independent. There will be no exchanges among vertices.

In real life a parallel cycle is executed not on a virtual, but on a particular MCS. This system can be presented as a graph G with M nodes, where M —amount of computing system processors. Real function c ($c(g_k) = c_k$) is stated on G graph nodes, and on its arcs (couples of nodes) — a real function e ($e(g_k, g_j) = e_{kj}$). Values of these functions in every node or arc are determined according to the processor performance, presented by this node (number of operations per time unit), and data transfer

rate of the communication channel between computing system processors (data transfer rate of communication channel is determined by its capacity, i.e. amount of bytes, transferred per unit of time, and latency).

In case when a computing system consists of one node ($M = 1$), cycle execution time— $T_0 = pNV/c$, where p — number of operations, required for computations of one cycle iteration, NV — number of cycle iterations, c — node throughput. As computing system is homogenous, then at any k $c_k = c$, and for any k and j e_{kj} = e. Then, if $NV > M$ and NV is divided entirely by M, each processor executes NV/M cycle iterations, and time of cycle execution equals to $T_M = pNV/(Mc)$. We find acceleration S_M through ration of T_0 to T_M and as a result we obtain $S_M = M$. This formula for acceleration is fare with a complete absence of losses. Efficiency means ratio $E = \frac{T_0}{MT_M}$, which in this case will equal to one, as losses are not accounted.

If NV is not divided entirely by M, then task of optimal distribution of cycle iterations over the system's processor nodes is a task of integer programming and does not always have an exact solution [84]. Here we consider the following heuristics: first $[NV/M]$ of iterations is evenly distributed over nodes, then amount of remaining iterations is distributed to $NV - [NV/M]M$ processor nodes. It will lead to that there will be more iterations in some nodes than in the other.

Besides, before cycle execution, it is usually necessary to send input data to computing system nodes, and after a cycle execution it is necessary to gather results from processor nodes. Time, required for the stated actions execution, we designate by T'_M. If NV is not divided entirely by M, and during data distribution over nodes some heuristics was used, then extra data will go to a part of nodes [84], which processing time we also add to T'. In the end, time of parallel cycle execution is equal to $T_M = T_M^0 + T'_M = T_M^0 + \alpha_M T_M^0$, where T_M^0 — time of parallel cycle execution with absence of losses, and $\alpha_M = T'_M / T_M^0$. Thus, with account for acceleration losses it equals to $S_M = M/(1 + \alpha_M)$. When losses are required to be accounted, efficiency is calculated by the formula $E = \frac{T_0}{MT_M} = \quad = \frac{T_0}{M(T_M^0 + \alpha_M T_M^0)}$ and will equal to $1/(1 + \alpha_M)$.

Application of landscape parallelization allows solving many problems, which arise during solving the tasks of forest fire danger prediction: major volumes of computational load and required RAM, necessity to compute in a mode, in advance of real time of the process progress. Approach is a problem-oriented, but it is quite flexible and versatile within limits of its application. Approach can be applied not only to a forest fire danger prediction, but its environmental impact assessment and forest fires development.

As it is known, temporal characteristics influence the functionality of software tools [85] and problem of their prediction is urgent and economically important [86]. Temporal characteristics features can be determined in different ways. In the simplest case it is required to carry out an experiment with program algorithm realization and extrapolate the acquired results [86]. The other approach is application of method based on labor-intensity [86], determining amount of elementary operations in a formal record system, assigned by the algorithm, depending on input parameters [87].

However, due to different frequency occurrence of operations the results of comparative analysis for time of algorithm program realizations in a number of cases do not agree with analysis results for labor-intensity function [86]. Approach, based on time function of algorithm program realization, should be considered more adequate, but more difficult [86]. For example, approaches to temporal evaluation predictions, based on labor-intensity functions, can be also applied both to tasks of a rational algorithm selection for set forth for the criterion evaluation system [86, 87]. A more effective solution of this problem is possible, using the algorithm classification [87], reflecting both complexity and characteristic features of algorithms. The following algorithms classifications are known [87]: 1) by asymptotic complexity of labor-intensity function and 2) by characteristic features of input data sets. Researches on algorithm program realization make it possible to acquire information about effective capacity (required algorithm memory volume) and temporal efficiency (time, required for algorithms to solve a task) as functions of input length [88]. Input length is a certain measure of information amount at the algorithm input [88].

4.3.11. Distributed Systems and Computations

Owing to computer technologies development, it became quite easy to assemble a computer network, which is called a distributed system. Distributed system is a set of independent computers, seen by users as a single unified system [89]. Arrangement of distributed systems often includes an additional level of software, which is between the upper layer of users and applications and a lower layer of operating systems (middleware) for support of different computers and networks as a unified system.

Distributed systems can easily connect users with computing resources and successfully conceal the fact that resources are scattered around the network and can be open and scalable. Main task of distributed systems is facilitation for users' access to remote resources and provision of their joint use. One of the reasons of joint resources utilization is efficiency.

An important objective of distributed systems is to conceal the fact that processes and resources are physically distributed over set of computers. The distributed systems, which are a single computer system for users and applications, are called transparent [89]. The other important feature of distributed systems is openness. An open distributed system is a system, offering services, which activation requires standard syntax and semantics [89]. Scalability is one of the most important tasks during distributed systems design development.

The system can be scalable by three parameters:

1) Attitude to its size, what means ease of additional users and resources connection;

2) Geographically, i.e. users and resources can be spread spatially;

3) Administratively, i.e. it can be simple in management during operation in a set of administratively independent organizations.

However, the system, scalable by one or several of these parameters, often has performance loss during scaling [89].

In the basic model client—server all processes in distributed systems are divide into two, probably overlapping, groups [90]. Processes, realizing some service, for

example, a file system service or database, are called servers. Processes, requesting the services from servers by sending an inquiry and subsequent waiting for a reply from server, are called clients.

4.3.12. Metacomputing

The term metacomputing [91] appeared together with the development of a high-speed network infrastructure in the beginning of 1990s and referred to a coalition of several heterogeneous computing resources in a local organization for one task solving. When the main goal of a metacomputer was in the optimal distribution of load parts over the computing systems of different architecture and different capacities. For example, preliminary data processing and grid generation for computation could be done on a user's workstation, basic modeling— on a pipeline and vector supercomputer, solving of major systems of linear equations — on a massively parallel system, and results visualization— on a special graphic station.

In further research the metacomputing technologies were developed towards a homogeneous access to numerous computing resources (up to several thousand) computer in a local and global system. Metacomputer components can be both simple PC, and powerful massively-parallel systems. It should be noted that metacomputer may not have a constant configuration—particular components can be included in its configuration or be excluded from it; here the metacomputing technologies provide for a continuous functioning of the system in general.

Modern research projects in this area are aimed at provision of a transparent access for users via Internet to required distributed computing resources, as well as of a transparent connection of idle computing systems to metacomputers.

Globus Project [92]. An official site on the Internet — http://www.globus.org. Software development for distributed computations organization on the Internet. The project is implemented in Argonne National Lab. Purpose of the Globus Project is making so-called computational grids, containing computing systems, visualization systems and experimental units. Researched on distributed algorithms build, provision of metacomputers security and fault-tolerance are carried out under the project. Within the Globus project framework a range of software tools was developed: Globus Resource Allocation Manager —a uniform interface for different local systems of load distribution (LSF, NQE, LoadLeveler); a special language RSL — for description of application requirements to resources (Resource Specification Language); Globus Security Infrastructure — an authentication system, based on a public key and X.09-certificates; Metacomputing Directory Service (MDS) — an information repository about computing resources, included in a metacomputer; Nexus — a communication library; Heartbeat Monitor (HBM) — a monitoring tool that helps to detect a failure of some machines and processes, included in a metacomputer; Globus Access to Secondary Storage (GASS) — a tool providing access to remote data via URL. Software Globus 1.0.0 is free. MPI (MPICH-G) realization is also available above Globus.

The first real metacomputer GUSTO (testbed environment) [93], which includes about 40 components with a total peak capacity of 2.5 TFlops, was made for Globus testing.

4.3.13. Neural Systems

One of the most promising fields of principally new architectures development for computing systems is closely related to creation of new generation computers, based on principles of data information processing in artificial neural networks [48, 94]. Neural network usually means a combination of elementary information converters, called neurons, which are connected to each other in a certain way by information exchange channels — synaptic connections [48]. Neuron is actually a primitive processor, described by input and output states, transfer function and local memory. The state of neurons varies during functioning and generate a short-term memory of neuronet. Each neuron calculates a weighted sum of incoming signals over synapses and carries out a nonlinear transformation. When signals are sent over synapses, they are multiplied by some weight factor. The basic element of network design development is its learning. During neural network learning and re-learning its weight factors vary. Number of neurons in one network layer determines its resolution.

Artificial neural networks do not require a detailed software development and allow solving tasks, for which theoretical models and heuristic rules, determining the solution algorithm, are not available. Such networks have a capability to adapt to functioning conditions change, including the unforeseen factors [48]. Neural networks are the systems with a very high parallelism level.

4.4. Decision-Making Support Systems

There are situations when decision has to be made very fast during a short period (from several dozen minutes to several days). This is a time interval when it is difficult or impossible to invite consultants, gather experts and carry out a meeting. In this case we have to rely on a computer's opinion. In such situations the computer decision-making systems are not a desirable target, but a forced option of decision making under conditions of limited resources, first of all, time limitations [95]. System approach to this problem means analysis of all aspects of the investigated task, elaboration and modeling of a complete data processing cycle, starting from input and information acquisition prior to decision making [95]. Main idea of this method is accumulation of knowledge in a computer form of databases, with their subsequent use for decision making.

The following tasks shall be solved for generation of up-to-date intellectual information systems [95]:

1) Development of a problem-oriented user interface; information flows structure development, starting from an external data source and finishing by alternative projects of suggested solutions;

2) Generation of input, analysis and filtering subsystems for incoming information;

3) Development of a conceptual, logical and physical databases;

4) Generation of a subsystem for information database inquiries formation, analysis and presentation;

5) Building of a suggested solutions generator.

Especially important is generation of systems, which would support the entire cycle of information computer processing form input [96] to decision making [97]. In

case of decision selection task formalization, it is required to apply various well-developed approaches and methods [98].

When developing decision-making support systems, a promising field is development of multi-databases, enabling integration of traditional data types (numbers, lines, and dates) with video and audio data [95].

Decision making can be done algorithmically or heuristically, and final decision usually rests with DM (decision maker) [99]. Decision should be sustained and optimal. Decision sustainability is determined by its selection algorithm convergence. From the aspects of selection theory and decision making, principle of optimality is the basis for required and sufficient conditions of decisions optimality. This principle is expressed mathematically as a selection function, which has a nonempty value and represented as follows [100]

$$Y = C(X) \subseteq X \subseteq A,$$

where A — set of all conceivable alternatives or it is a universal set; X —a specific original set of conceivable alternatives, it is a set of presentations; $C(X)$ — set of the most preferable — optimal decisions.

Theory of decision selection was formed, which covers concepts, languages and mechanisms of different extreme tasks solving [99]. Concepts are systems of DM views on the decision statement and selection in particular situations. Formally are presented by selection functions [100—102]. Depending on the completeness and nature of task initial data description, decision-makings are classified [103] as well-structured, unstructured and weakly-structured.

It is obvious that the best results in the area of forest fire prediction and their environmental consequences can be reached using a comprehensive approach, which will combine mathematical modeling methods, technologies of expert systems making [104] and decision making support systems with tools of social ecology. Information and computational basis should become technologies of high-performance computations in the parallel architecture and spatial display systems, and analysis in geoinformation systems.

REFERENCES

1. Concept of establishment and development of spatial data infrastructure of the Russian Federation // Geodeziya i kartografiya. 2006, № 10. P. 1—6. (In Russian)
2. Skvortsov A.V. (2006) Geoinformatics: Textbook. Tomsk: Izd-vo Tom. un-ta, 336 p. (In Russian)
3. Karpik A.P. (2004) Functions of geoinformation support // Geodeziya i kartografiya, 1, 45—48. (In Russian)
4. Sukhinin A.I., Ponomarev E.I. (2003) Mapping and short-term fire danger prediction in forests of Eastern Siberis by satellite data // Sibirskij ekologicheskiy zhurnal, 6, 669—675. (In Russian)
5. Kravtsova V.I. (1995) Space methods of mapping. Moscow: Izd-vo MGU, 240 p. (In Russian)
6. Kronberg P. (1988) Distant study of the Earth / Transl. from German Moscow: Mir, 343 p. (In Russian)
7. Environmental Monitoring and Characterization. / Ed. J. F. Artiola, I. J. Pepper, M. L. Brusseay. Netherlands: Elsevier, 2004. 410 p.
8. Remote Sensing and GIS for site characterization: applications and standards / Eds. V. Singhroy, D. D. Nebert, A. I. Johnson. USA: ASTM International, 1996. 177 p.
9. Grishin A.M. Filkov A.I. (2004) About geoinformation system of forest fire prediction // Ekologicheskie sistemy i pribory, 8, 26—28. (In Russian)
10. Filkov A.I. (2005) Determintate-probability system of forest fire danger prediction. Dissertation … PhD.Phys.Math.Sci. Tomsk: TSU, 163 p. (In Russian)
11. Volokitina A.V., Sofronov M.A. (2002) Classification and mapping of flammable vegetation. Novosibirsk: Izd-vo SB RAS, 314 p. (In Russian)
12. Vakalis D., Sarimveis H., Kiranoudis C. et al. (2004) A GIS based operational system for wildland fire crisis management I. Mathematical modelling and simulation // Applied Mathematical Modelling, 28(4), 389—410.
13. Vakalis D., Sarimveis H., Kiranoudis C., Alexandridis A., Bafas G. (2004) A GIS based operational system for wildland fire crisis management I. System architecture and case studies // Ibid., 411—425.
14. Zadeh L.A. (1965) Fuzzy sets // Information and Control, 8(3), 338—353.
15. Zadeh L.A., Klir G.J., Yuan B. (1996) Fuzzy sets, fuzzy logic and fuzzy systems: Selected Papers. N. J.: World Scientific, 840 p.
16. Bhat N., McAvoy T.J. (1990) Use of neural nets for dynamic modelling and control of chemical process systems // Computers and Chemical Engineering, 14, 573—583.
17. Narendra K.S., Parthsarathy K. (1990) Identification and control of dynamical systems using neural networks // IEEE Transactions on Neural Networks, 1(1), 4—27.
18. Kopylov V.N., Polischuk Yu.M., Khamedov V.A. (2004) Geoinformation technology of of forest fires impact assessment using data of distant probing // Geoiformatics, 2, 56—61. (In Russian)
19. Satellite monitoring of forest fires in Russia. Summary. Problems. Prospects: Analytical review / Edited by BV. V. Belov / GPNTB SB RAS. Novosibirsk, 2003. 135 p. (In Russian)
20. Alekseyeva M.N., Dyukarev A.G., Kopylov V.N., Pologova N.N. (2003) Space-geoinformation method of vegetation layer structure analysis of forest-samp territories // Materials of conference «The 5th Siberian meeting on climate ecological monitoring». Tomsk: Izd-vo IOM SB RAS, P. 197—201. (In Russian)
21. Alekseyeva M.N., Dyukarev A.G., Polischuk Yu.M., Pologova N.N. (2004) Research of forest-swamp complex structure of the Vasygan plain, using GIS, distant and sub-satellite data // Geogr. i prir. Resursy, 2, 71—77. (In Russian)
22. Lee B.S., Alexander M.E., Hawkes B.C. et al. (2002) Information systems in support of wildland fire management decidion making in Canada // Computers and Electronics in Agriculture, 37(1—2), 185—198.

23. Yelanskiy N.F., Novakovskiy B.A., Prasolova A.I., Mikheeva A.I. (2007) Survey of atmospheric air quality of the Moscow regionб using GIS-technologies // Geodeziya i kartografiya, 2, 34—45. (In Russian)
24. Venitsianov E.V., Vinichenko V.N., Guseva T.V. et al. (2003) Ecological monitoring: step by step / Edited by E. A. Zaika. M.: RHTU named after D. I. Mendeleev, 252 p. (In Russian)
25. Pummakarnchana O., Tripathi N., Dutta J. (2005) Air pollution monitoring and GIS modelling: a new use of nanotechnology based solid state gas sensors // Science and Technology of Advanced Materials, 6(3—4), 251—255.
26. Vega Garcia P., Woodard P., Lee B. (1993) Geographic and temporal factors that seem to explain human-caused fire occurrence in Whitecourt Forest, Alberta // Proceedings of Symposium on GIS'93. Vancouver: University of British Columbia, P. 115—119.
27. Ovodkov M.V. (2005) Geoinformation mapping of ecological risks // Geodeziya i kartografiya, 10, 44—46. (In Russian)
28. Hernandez-Leal P.A., Arbelo M., Gonzalez-Calvo A. (2006) Fire risk assessment using satellite data // Advances in Space Res., 37(4), 741—746.
29. Illera P., Fernandez A., Delgado J.A. (1996) Temporal evolution of the NDVI as an indicator of forest fire danger // Int. J. Remote Sensing, 17, 1093—1105.
30. Hardy C.C., Burgan R.E. (1999) Evaluation of NDVI for monitoring live moisture in three vegetation types of western US // Photogrammetric Engineering and Remote Sensing, 65, 603—610.
31. Moran M.S., Clarke T.R., Inque Y. et al. (1994) Estimating crop water deficit using the relation between surface—air temperature and spectral vegetation index // Remote Sensing of Environment, 49, 246—263.
32. Hao X., Qu J.J. (2007) Retrieval of real-time live fuel moisture content using MODIS measurements // Remote Sensing of Environment, 108(2), 130—137.
33. Justice C.O., Giglio L., Korontzi S. et al. (2002) The MODIS fire products // Remote Sensing of Environment, 83(1—2), 244—262.
34. Leblon B., Fernandez Garcia P.A., Oldford S. et al. (2007) Using cumulative NOAA-AVHRR spectral indices for estimating fire danger codes in northern boreal forests // Int. J. Applied Earth Observation and Geoinformation, 9(3), 335—342.
35. Maki M., Ishihara M., Tamura M. (2004) Estimation of leaf water status to monitor the risk of forest fires by using remotely sensed data // Remote Sensing of Environment, 90(4), 441—450.
36. Chuvieco E., Cocero D., Riano D. et al. (2004) Combining NDVI and surface temperature for the estimation of live fuel moisture content in forest fire danger rating //Ibid., 92(3), 322—331.
37. Fraser R.H., Li Z. (2002) Estimating fire-related parameters in boreal forest using SPOT VEGETATION // Ibid., 82(1), 95—110.
38. Afonin S.V., Belov V.V., Gridnev Yu.V. (2000) Space monitoring system organization for in forest fires Tomsk region // Matematicheskoe i fizicheskoe modelirovanie sopryazhennyh zadach mekhaniki i ekologii: Selected reports of International Conference. Tomsk: Izd-vo Tom. un-ta, P. 22—36. (In Russian)
39. Dorrer G.A., Dorrer M.G., Klishta I.N. et al. (2000) Problems of regional information-analytical systems establishing for forest fire proteciton // Mathematical и physical modelling of conjugate problems of mechanics and ecology: Selected reports of International conference. Tomsk: Izd-vo Tom. un-ta, P. 133—159. (In Russian)
40. Sukhinin A.I., Kashkin V.B., Ponomarev E.I. (1999) Monitoring forest fire in eastern siberia from space // Prop. of SPIE, 3983, 206—214.
41. Loboda T.V., Csiszar I.A. (2007) Reconstruction of fire spread within wildland fire events in Northern Eurasia from the MODIS active fire product // Global and Planetary Change, 56(3—4), 258—273.
42. Smith R., Adams M., Maier S. et al. (2007) Estimating the area of stubble burning from the number of active fires detected by satellite // Remote Sensing of Environment, 109(4), 95—106.

43. Zhang Y.-H., Wooster M.J., Tutubalina O., Perry G.L.W. (2003) Monthly burned area and forest fire carbon emission estimates for the Russian Federation from SPOT VGT // Ibid., 87(1), 1—15.
44. Liu J., Drummond J.R., Li Q. et al. (2005) Satellite mapping of CO emission from forest fires in Northwest America using MOPITT measurements // Ibid. 95(4), 502—516.
45. Malyshkin V.E. (1998) Basics of parallel computing: textbook. Novosibirsk: Izd-vo NGTU, 60 p. (In Russian)
46. Korneyev V.V. (1998) Parallel computing systems. Moscow: Nolidzh, 320 p. (In Russian)
47. Baranovskiy N.V. (2001) Hardware and software support of parallel computing: workbook. Tomsk: Izd-vo Tom. un-ta, 29 p. (In Russian)
48. Bogdanov A.V., Korkhov V.V., Mareyev V.V., Stankova E.N. (2004) Architectures and layout of multiprocessor computing systems. Leactures: textbook. M.: INTUIT.RU «Internet-University of Information Technologies», 176 p. (In Russian)
49. Becker D.J., Sterling T., Savarese D. et al. (1995) BEOWULF: A parallel workstation for scientific computation // Prop. Int. Conf. on Parallel Processing, P. 11—14.
50. Warren M.S., Germann T.C., Lomdahl P.S. et al. (1998) Avalon: An Alpha/Linux Cluster Achieves 10 Gflops for $150k // Prop. Int. Conf. «SuperComputing'98». USA, Washington: IEEE Computer Society, P. 1—11.
51. Prokhanov R.A. (2007) Software of SKIF Cyberia computational cluster // Program and summaries of the 4th Siberian workshop on parallel and high-performance computing. Tomsk: Izd-vo Tom. un-ta, P. 59—60. (In Russian)
52. Snir M., Otto S.M., Huss-Lederman S. et al. (1996) MPI: The Complete Reference / Boston: MIT Press, 352 p.
53. Karpov Yu.G. (1996) Correctness analysis of parallel program of sets separation // Programming, 6, 27—33. (In Russian)
54. Korneyev V.D. (2000) Parallel programming in MPI. Novosibirsk: Izd-vo SB RAS, 213 p. (In Russian)
55. Squyrws J.M., Lumsdaino A. (2003) A component architecture for LAM/MPI // Prop. of 10th European PVM/MPI User's Group Meeting. LNCS 2840. Springer-Verlag, P. 379—387.
56. Baranovskiy N.V. (2002) Cluster packet LAM/MPI. Tomsk: Izd-vo Tom. un-ta, 22 p. (In Russian)
57. Dagum L., Menon R. (1998) OpenMP: An Industry-Standard API for Shared-Memory Programming // Computational Science & Engineering, 5(1), 46—55.
58. Hughes C., Hughes T. (2004) Parallel and distributed programming using C++. M.: Williams, 672 p.
59. Nemnyugin R.A., Stesik O.L. (2002) Parallel programming for multiprocessor computing systems. SPb.: BXV-SPb, 400 p. (In Russian)
60. Konovalov N.A., Kryukov V.A. (2000) DVM-system of parallel program developemtn // Works of Russian Scientific conference «High performance computing and their applications» (Chernogolovka, 30 October—2 November 2000). Moscow: Izd-vo MGU, P. 33. (In Russian)
61. Zadyhaylo I.B., Yefimkin K.N. (1996) Meaningful symbols and languages of new generation // Information technologies and computing systems, 2, 46—58. (In Russian)
62. Andrianov A.N., Bugerya A.B., Yefimkin K.N., Zadyhaylo I.B. (1995) Norma. Language description. Working standard. Moscow, 50 p. (Pre-print of IPM named after M. V. Keldysh RAN; № 120). (In Russian)
63. Abramova V.A., Vershubskiy V.Yu., Gorelik D.M. et al. (1997) GNS programming system. Fortran GNS language description. Moscow, 23 p. (Pre-print of IPM named after M. V. Keldysh RAN; № 71). (In Russian)
64. Convex Fortran User's Guide. Order N DSW-038, Richardson, Texas, USA, Convex Press, 1994. 277 p.
65. Andrianov A.N., Yefimkin K.N. (2000) Use of Norma system for solving a problem on multiprocessor systems with distributed memory // Works of Russian Scientific conference «High performance computing and their applications» (Chernogolovka, 30 October—2 November 2000). Moscow: Izd-vo MGU, P. 39—42. (In Russian)

66. Voyevodin Vl.V., Filamofitskiy M.P. (2000) Analysis of parallel programs dynamic features // Same. P. 203—207. (In Russian)
67. Voyevodin Vl.V., Filamofitskiy M.P., Tsereteli P.A. (1999) Analysis of parallel programs features via Internet // Research service on the Internet: Summaries of resports of the Rus.Scientific Conference, Novorossiysk, 21—26 September 1999. P. 134—139. (In Russian)
68. DeRose L., Zhang Y., Reed D.A. (1998) SvPablo: A Multi-Language Performance Analysis System // 10th International Conference on Computer Performance Evaluation—Modelling Techniques and Tools—Performance Tools'98, Palma de Mallorca, Spain, September 1998. P. 352—355.
69. Belikov D.A., Starchenko A.V. (2005) Study secondary pollutants (ozone) generation in Tomsk air // Optika atmosfery i okeana, 18(5—6), 435—443. (In Russian)
70. Belikov D.A. (2006) Parallel realization of mathematical model of atmospheric diffusion for research of distribution of primary and secondary air pollutants above urban territory: Avtoref. diss.. … Phd. Phys.-Mat. Sci. Tomsk: TSU, 20 p. (In Russian)
71. Belikov D.A. (2006) Parallel realization of atmospheric diffusion mathematical mode of for study of primary and secondary pollutants over urban territory. Dissertation … PhD.Phys.Math.Sci. Tomsk: TSU, 177 p. (In Russian)
72. Starchenko A.V. (2007) Parallel computing for weather research and environment protection // Program & Abstracts of Int. Conf. and Young Scientists School on Computational Information Technologies for Environmental Sciences. Tomsk: SCERT, P. 26—26. (In Russian)
73. McDonough J.M., Yang T. (2004) Parallel performance of a new model for wild land fire spread prediction // Prop. of Int. Conf. Parallel CFD'04, Gran Canaria, Canary Island, Spain, May 24—27, 2004. P. 45—51.
74. Jorba J., Margalef T., Luque E. (2001) Simulation of forest fire propagation on parallel & distributed PVM platforms // Recent Advances in Parallel Virtual Machine and Message Passing Interface. LNCS V. 2131. Heidelberg: Springer, P. 386—392.
75. Andre J.C.S., Viegas D.X. (1994) A strategy to model the average fireline movement of a light-to-medium intensity surface forest fire // Prop. of the 2nd Int. Conf. on Forest Fire Research. Portugal, Coimbra, P. 221—242.
76. Rothermel R.C. (1983) How to predict the spread and intensity of forest and range fire. USDA-FS. Tech. Rep. INT-143. 161 p.
77. Anderson H.E. (1983) Predicting wind-driven wildland fire size and shape. USDA-FS. Oregon TU. Tech. Rep. INT-305. 30 p.
78. Baranovskiy N.V. (2007) Landscape parallelization and forest fire danger prediction // Sib. zhurn. vychislitelnoi matematiki, 10(2), 141—152. (In Russian)
79. Project of forestry management and development of Timiryazevskiy forestry of Tomsk forestry territorial production association of the Ministry of RSFSR Forestry. V. III. Mensuraion description of Temiryazevo forestry. B. 3. Quarters 91-145. Inv. № 390 / Gosleskhoz USSR. Vsesoyuznoe obyedinenie “Lesproekt”. Zapadno-Sibirskoe lesoustroitelnoye predpriyatie. Tomsk, 1990. 400 p. (In Russian)
80. Baranovsky N.V., Grishin A.M. (2002) Prediction of forest fire maturity of forest fuel layer using landscape parallelization // Vychislitelnye tekhnologii, 7(1), 37—44. (In Russian)
81. Baranovsky N.V., Grishin A.M. (2002) Landscape parallelization and forest fire maturity of forest fire layer // Prop. of Int. Conf. on Computational Mathematics. P. II/ Ed. G. A. Mikhailov, V. P. Il'in, Yu. M. Laevsky. Russia, Novosibirsk: ICM&MG Publisher, P. 345—349. (In Russian)
82. Baranovskiy N.V. (2007) Landscape parallelization and forest fire danger prediction // Parallel computing technologies: Works of Intl. conference (29 January—2 February 2007, Chelyabinsk). In 2 v. V. 1. Chelyabinsk: Izd-vo YUrGU, 2007. C. 227—236. (In Russian)
83. Baranovskiy N.V. (2002) Landscape parallelization technology and its application to forest fire prediction: textbook. Tomsk: Izd-vo Tom. un-ta, 34 p. (In Russian)
84. Avetisyan A.I., Gaisaryan R.R., Samovarov O.I. (2002) Capabilities of optimal execution of parallel programs, containing simple and iterated cycles, in heterogeneous parallel computing systems with distributed memory // Programming, 1, 38—54. (In Russian)

85. Lipayev V.V. (2003) Methods of large-scale software quality support. Moscow: SINTEG, 520 p. (In Russian)
86. Ulyanov M.V. (2004) Method of time estimates of program algorithm realizations based on labor-intensity funcitons // Information technologies, 5, 54—62. (In Russian)
87. Ulyanov M.V. (2003) Algorithm classification for practical analysis // Same. 11, 29—36. (In Russian)
88. Mikhaylov B.M., Ulyanov M.V. (2005) Instruments for algorithm efficiency study: concept and basic principles of building // Same, 2, 54—57. (In Russian)
89. Tanenbaum E., M. van Steen. (2003) System distribution. Examples and paradigms. SPb.: Piter, 877 p. (In Russian)
90. Neuman B. (1994) Scale in distributed systems // Readings in Distributed Computing Systems / Eds. T. Casavant, M. Singhal. Los Alamos, CA: IEEE Computer Society Press, P. 463—489.
91. Carlett C., Smarr L. (1992) Metacomputing // Communications of the ACM, 35, 44—52.
92. Foster I., Kesselman C. (1998) The Globus Project: A Status Report // Prop. IPPS/SPDP '98 Heterogeneous Computing Workshop, P. 4—18.
93. Foster I., Kesselman C. (1997) Globus: A metacomputing infrastructure toolkit // Int. J. Supercomputer Applications, 11(2), 115—128.
94. Khaikin R. (2006) Nueral networks: full course. 2-nd edition, rev. Transl. from Eng.. Moscow: Williams, 1104 p. (In Russian)
95. Gelovani V.A., Bashlykov A.A., Britkov V.B., Vyazilov E.D. (2001) Intellectual systems of decision making support in emergency situations, using information about environmental conditions. Moscow: Editorial URSS, 304 p. (In Russian)
96. Britkov V.B., Vasilyev A.A., Golosov A.O. (1987) Intellectualization of input process in information systems // Programming mathematical methods of information science in system modelling / VNIISI. Moscow, Issue 15. P. 64—68. (In Russian)
97. Britkov V.B. (1988) Architecture of intellectual information systems for decision making // Problems and methods of decision making in organizational management systems / VNIISI AN USSR. Moscow, P. 31—32. (In Russian)
98. Aizerman M.A., Alekserov F.T. (1990) Selection of options: theoretical basis. Moscow: Nauka, 240 p. (In Russian)
99. Katulev A.N., Severtsev N.A. (2003) Mathematical methods in decision making support systems: textbook. Tver: Izd-vo Tver Gor. Un-ta, 327 p. (In Russian)
100. Levchenkov V.R. (2002) Two priniples of rationality theory of selection: Borda vs. Condorcet. Moscow: Izd-vo Mosk. Un-ta, 264 p. (In Russian)
101. Makarov I.M., Vinogradskaya T.M., Rubchinskiy A.A., Sokolov V.B. (1982) Theory of selection and decision making. Moscow: Nauka, 342 p. (In Russian)
102. Mulen E. (1971) Cooperative decision making: Axioms and models. Moscow: Nauka, 464 p. (In Russian)
103. Larichev O.I., Moshkovich E.M. (1996) Qualitative methods of decision making. Moscow: Nauka. (In Russian)
104. Giarratano J., Riley G. (2007) Expert systems: Principles and Programming, 4-th Edition / Transl. Moscow: Williams, 1152 p. (In Russian)

ANNEX 1
METHODS FOR LIFE QUALITY ASSESSMENT

The most important factor of human health condition is a self-assessment of a health condition for certain diseases [1-11]. There are different definitions for life quality. Let us move away from the term “patient” and widen and somewhat expand the meaning of life quality. Human life quality is described by how physical, emotional and social well-being varies under external and internal factors (including, diseases and their treatment).

Life quality survey, related to health, makes it possible to assess the impact of disease and treatment on all human life quality factors, considering all health components — physical, psychological and social activity. Notion of life quality is the foundation of a new concept of disease comprehension and determining of its treatment methods. This concept was developed by experts of the Multinational Center for Quality of Life Research. Main elements: 1) definition of life quality; 2) life quality concept components; 3) methodology of life quality survey; 4) main scope of application in medicine.

Life quality is an integral feature of physical, psychological, emotional and functioning of patients, based on their subjective perception. At present life quality survey is carried out practically in all medicine areas. A reasonable step will be application of the life quality concept in researches of forest fires effect on human health.

Scope of life quality survey application in practice of health care system is quite broad. The most important are the following:

1) Standardization of treatment methods;

2) Expert review of new treatment methods, using international criteria, adopted in majority of developed countries;

3) Provision for a full individual monitoring of patients’ health with assessment of early and long-term results of treatment;

4) Development of prognostic models of disease progress and outcome;

5) Social and medical population surveys with identification of risk groups;

6) Development of fundamental principles of palliative medicine;

7) Provision for a dynamic observation over risk groups and assessment of preventive programs effectiveness;

8) Increase of expert examination quality for new medications;

9) Feasibility study of treatment methods, considering such factors as, price—quality, cost—effectiveness, and other pharmacoeconomic criteria.

Life quality survey is based on a multicomponent methodology, which includes the following major components:

1. Development of survey protocol.
2. Selection of survey tools.
3. Examination of patients.
4. Data acquisition.
5. Database development.
6. Selection of data scale for a questionnaire.
7. Statistical data processing.

8. Results analysis and interpretation.

Depending on the area of application, questionnaires are divided into two groups.

1. General questionnaires (for children and adults).

2. Special questionnaires:

By areas of medicine (oncology, neurology, etc.);

By nosology (breast cancer, gastric ulcer, etc.);

Questionnaires, specific for a particular condition.

Depending on the, there are:

1. Profile questionnaires — several numerical values, which present a profile, formed by several scales values.

2. Indices — a single numerical value.

An important feature of questionnaire is its validity (reliability) —a questionnaire capability to measure reliably that main feature, on which it is based. Validation is an examination of psychometric properties of questionnaire. Validation procedure includes evaluation of reliability, validity and sensitivity.

Scaling (conversion) of questionnaire data — is a procedure of questionnaire unprocessed data translation into points of life quality by questionnaire scales. Methods of statistical analysis, processing and subsequent data interpretation have a number of peculiarities. Sometimes a question arises whether we deal with qualitative or quantitative data? Unprocessed answers to questions are qualitative, but after a scaling procedure they become quantitative in a range of questionnaires.

Life quality assessment for one person, group of people, different population layers and society in general is possible. Valuable information can be acquired from screening polls of population in different regions with monitoring of during a required time interval. Standard life quality indices are available in all developed countries.

Information about standards can be used in different sectors of society life:

1) For comparing life quality indices of specific population groups from different regions with the population standard;

2) For monitoring of life quality of different population layers during a required observation period;

3) For comparing of life quality indices of a particular patients group with the population standard;

4) For a complex assessment of health care programs efficiency;

5) For development of rehabilitation programs, social adaptation measures for different population categories.

Life quality survey can be correct and informative, if it is based on standard international survey methods. Methodically a competent survey is possible if the following is available:

1) Survey protocol;

2) Approved national questionnaire version;

3) Trained researcher;

4) Team, performing database maintenance, scaling of questionnaire and statistical processing of results.

Data bank, including information about quality of life research tools in the Russian language, which passed all required stages of psychometric testing, approved for

use in the territory of Russia, was developed by the Multinational Center for Quality of Life Research. Currently the Center coordinates majority of national educational and research programs for quality of life research, providing methodological assistance to specialists in over 30 cities of Russia.

REFERENCES

1. Guidelines for life quality survey in medicine. 2-nd edition / Rev. acad. RAMN Yu. L. Shevchenko. M.: ZAO «OLMA Media Group», 2007. 320 p. (In Russian)
2. Bowling A. (1996) Measuring Disease: A Review of Disease-specific Quality of Life Measurement Scales. Philadelphia: Open University Press, 374 p.
3. Quality of life and pharmacoeconomics in clinical trials. 2nd Ed./ Eds. B. Spilker. Philadelphia: New York Lippincott-Raven, 1996. 1259 p.
4. Quality of life assessment in clinical trials / Eds. M. J. Staquet. Oxford: Oxford University Press, 1998. 360 p.
5. Novik A.A., Ionova T.I., Kaynd P. (1999) Concept of life quality survey in medicine. SPb.: Elbi, 140 p. (In Russian)
6. Shevchenko Yu.A. (2000) Life qulity in cardiology // Vestnik RVMA, 9, 5—15. (In Russian)
7. Bone M.R. (1992) International efforts to measure health expectancy // J. Epidemiol. and Community Health, 46, 555—558.
8. Andrews F.M., Withey S.B. (1976) Social Indicators of Well-being: Americans Perceptions of Life Quality. New York: Plenum Press, 220 p.
9. Gandek B., Ware J. (1998) Methods for validating and norming translations of health status questionnaires: The IQOLA Project approach // J. Clinical Epidemiology, 51(11), 953—959.
10. Baranovskiy N.V., Baranovskaya S.V. (2006) Probability of asthma-like symptoms due to forest fires // Izv. vuzov. Fizika, 49(3). Annex. 214—215. (In Russian)
11. Baranovskiy N.V., Baranovskaya S.V., Isakova A.V. (2007) Asthma-like symptoms among population due to forest fires in the settlement surroundings // Health —the basis of human potential: problems and ways to solutions. Works of 2nd Rus. sci.-pract. conference with international participants. SPb.: Izd-vo Polytech. University, P. 24—30. (In Russian)

ANNEX 2
PRESCRIBED BURNING AS A TOOL OF FOREST FIRE FIGHTING

In some regions the so-called prescribed burnings are used to fight against forest fires. A vast material of methods for such burnings procedure is given in the book [1]. However, the monograph will not be complete without a brief consideration of this technology.

Interrelation of Controlled Forest Fires and Prescribed Burning Strategy

Currently the controlled forest fires strategy is suggested [2]. This concept is applicable to fires planning, arrangement and effective management, executed by an organization. The strategy includes an entire range of fire control activities – from prevention, early warning, detection, mobilization and fighting the extinguishing of undesirable and destructive fires. Use of natural or man-induced fire serves as a tool in conservation of environmental values and integrity of certain ecosystems and prior to fire application in order to reduce accumulation of natural combustible materials, industrial and non-industrial wastes and restoration of fire-damaged or fire-dependent ecosystems [3].

According to [3], a concept of a "good fire" existence is suggested. A fire can be useful for habitats, resources, for mitigating the threat of losses and cultural values preservation. From the aspect of fire control, there is no difference in using a fire for planted crops or creation of favorable growth conditions for natural sources of food, consumed by people and animals. It is also fair in fire application for preservation of traditional or cultural landscapes or vegetation composition [3].

Fire can serve as a tool for land clearing and conversion. Felling or transfer of live plants into wastes, left for drying when it can spread fire, is relatively easy in many ecosystems. The vegetation is burned at this very moment. Fire prevention can be one of the most economical and effective programs, which an organization or community are able to execute [3]. Prevention of undesirable destructive fires is always more cost-effective than their extinguishing. Fire prevention programs, adopted and advocated in the community, do not only reduce costs and damage to resources, but also promote the understanding of fires role and impact on the ecosystem. Fires prevention is used for controlled man-induced burning, and requires a united community training, effective prevention programs and strengthening of laws and regulations. In fire-dependent ecosystems and zones of a cultural value, allowance of some fires in certain conditions can be useful, although man-induced fires for ecosystem support can complicate the prevention efforts improvement. In many parts of the world the controlled fire is used as a fire prevention component [1]. Fire can have a highly important and favorable impact on reduction of fires severity and damage, as well as facilitate the firefighters in fire extinguishing. Moreover, fire has many other useful properties for provision of ecosystems sustainability, conservation and restoration.

The term “combustible materials management” refers to all methods for combustible materials processing and conversion for any purpose [3]: fire risk mitigation, community protection, ecosystem restoration, disposal of wastes after logging or any other activities. Any activity that changes location or composition of combustible materials shall be considered in the program of combustible materials processing. Application of chemicals and resources management activities, including cattle pasturing and logging, result in changes of combustible materials layer. These activities should be planned in advance and performed with account for potential change of fire intensity, distribution and damage.

One more example where combustible materials processing activities can be an important part of the program, are territories in which houses or other buildings are adjacent to the vegetation, subject to fires [3]. House owners can use different methods for shrubbery elimination and wastes disposal from the territory around the house, including properly planned and executed burnings. Removal of this combustible material increases chances that fire will not destroy households. Although measures on combustible materials processing might not reduce the fires frequency, they will certainly reduce intensity of burning, and thus, will improve the fire-fighting strategy efficiency.

Planned fire means its intentional use for specific goals of control [3]. Combustible materials can be either live or dead. In some territories the planned burning for community protection are referred to preventive measures.

Planned fire use is a fairly effective method for removing the undesirable vegetation for various purposes. Fire is used in agriculture, animal breeding, forestry, and soil cleanup all over the world. Fire is also important for preservation of healthy fire-dependent ecosystems. Natural fires have a positive effect on such ecological systems, and they should be supported and controlled as a part of the entire fire control program [3].

Ecosystems and territories of cultural importance where fires are common can be very resistant to fire effect. Flora may rather be rejuvenated by fire than replaced or destroyed, and, consequently, the fauna which also depends on it. If the goal is to preserve or restore sustainable ecological systems and territories of cultural importance, then the program allows burnings for restoration and rehabilitation as a part of the entire fire control plan. One of the most important program components for prescribed fire use is minimizing the smoke effect [4]. An effective program for smoke formation control will be very important in the territories where legal requirements on providing air purity and population protection from respiratory disease threat are effective.

Interacting with the meteorological service may be useful because this service provides the probable impact forecasts for specific burnings, which are especially developed for management. Such instructions may facilitate the supervisors, responsible for burnings.

Prescribed Burnings in Russia

The strategy consists in active regulation of forest flammability (including prescribed burnings) so to preserve and restore an effective interchange of areas, referred to different succession stages, for maintaining a natural biodiversity [5]. Regarding human settlements, the burnings are rarely used for their protection [6]. However, this method is viewed as effective in practical recommendations, developed in the Institute of Forest named after N. V. Sukachev, SB RAS [7]. At present, burnings are widely used by "Avialesookhrana" ("Aviation Fire Protection of Forests") for forest fire extinguishing [6]. However, in the regions of ground protection where settlements are located, burnings are scarcely used, including cases of settlement protection [6]. The burning method consists in eliminating combustibles before the fire margin, burning of litter and ground cover with a low windward fire, due to which it is possible to stop a surface fire spreading. Here a crown fire spreading also ceases, because a crown fire cannot spread for more than 200 m at non-storm wind conditions without surface fire support [8]. It is worth mentioning that there are few specialists among ground forest fire-fighting service, familiar with the burnings in practice [6].

The task fulfilled during settlement protection is to prevent fire approaching at a dangerous distance (less than 500 m), that is why firebreaks are usually made at about 500 m distance [6]. The main task of settlement protection burnings is not a fire extinguishing, but prevention of its approach at a dangerous distance.

Prescribed Burnings in Other Countries

Prescribed burnings are used more frequently in other countries than in Russia. A research [9], conducted in North-West Portugal, is illustrative. Many forest areas consist of pinetums [10]. It is known that pines can withstand fires of weak intensity without serious consequences, which makes such forests the first candidate for prescribed burnings use [11]. Prescribed burnings pursue clear objectives within a specific fire area (prescription) and follow accurate procedures (a burning plan) [12]. The main reason for prescribed burnings is to reduce fire frequency.

A typical scenario of prescribed burning should be described [9]. The blocks that are prescribed for burning are usually separated by forest roads, fireproof breaks and are complemented by fire control lines. Burning starts from the ignition line (that rarely exceeds 200 meters length) and is done in reverse fire mode (i.e. upwind and downhill). Downwind and uphill burnings are made if moisture content is too high for reverse burning, usually in a succession of fire lines separated by small distances. A team of burners is staffed with a supervisor and 4-10 firemen that could extinguish a fire if it goes out of control.

A systematic monitoring and registration of significant variables prior to, during and after the fire are key actions to determine whether the results planned have been achieved [9].

REFERENCES

1. Weir J.R. (2009) Conducting Prescribed Fires: A Comprehensive Manual. USA, Texas: Texas A&M University Press, College Station, 194 P.
2. Gundar S.V., Podgrushnyi A.V. (2006) Forest fires management // Pozharovzryvobezopasnost, 4, 74 – 80. (In Russian)
3. Holmgren P., Karl G. (2007) Voluntary Guidelines for Fire Management. Principles and Strategic actions. Italy, Rome: FAO. 56 p.
4. Reisen F., Hansen D., Meyer C.P. (2011) Exposure to bushfire smoke during prescribed burning and wildfires: Firefighters' exposure risk and options // Environmental International, 37(2), 314 – 321.
5. Redkin A.Yu., Volokitina A.V., Sofronov M.A. (2009) Mapping of vegetation combustible materials during forest reserves management // Journal of Siberian Federal University. Engineering & Technologies, 2, 368 – 375. (In Russian)
6. Volokitina A.V., Sofronova T.M. (2011) Protection of human settlements against natural fires // Pozharovzryvobezopasnost, 3, 22 – 31. (In Russian)
7. Volokitina A.V. (2002) Protection of human settlements against emergencies related to natural fires: Practical guidelines, developed under financial support of MacArthur Foundation, Ind. Grant No. 01-68116-000. Krasnoyarsk: IL SB RAS, 63 P. (In Russian)
8. Kurbatskiy N.P. (1959) Containment of severe forest fires by surface backfire // Lesnoye khozyaistvo, 3, 52 – 55. (In Russian)
9. Fernandes P., Botelho H. (2004) Analysis of the prescribed burning practice in the pine forest of northwestern Portugal // Journal of Environmental Management, 70, 15 – 26.
10. Brower R., (1993) The Forestry Services and the Commons in Portugal. Forest and Conservation History 37, 160–168.
11. de Ronde, C., Goldammer, J.G., Wade, D., Soares, R.V. (1990) Prescribed fire in industrial pine plantations. In: Goldammer, J., (Ed.), Fire in the Tropical Biota: Ecosystem Processes and Global Challenges, Springer, Berlin, pp. 216–272.
12. Pyne, S.J., Andrews, P.L., Laven, R.D. (1996) Introduction to Wildland Fire, second ed., Wiley, New York, 769 pp.

NIKOLAY V. BARANOVSKIY, GENIY V. KUZNETSOV

FOREST FIRE OCCURRENCES AND ECOLOGICAL IMPACT PREDICTION

Monograph

Н.В. Барановский, Г.В.Кузнецов
Прогноз возникновения лесных пожаров и их экологических последствий
(на английском языке)

Electronic online scientific publication
Text edition

Date of signing for use 24.03.2017
Volume of the edition 23,88 Мб

PUBLISHING HOUSE OF THE SIBERIAN BRANCH
OF THE RUSSIAN ACADEMY OF SCIENCES
Morskoy pr. 2, Novosibirsk 630090, Russia
Tel.: +7 (383) 330-80-50 / Fax: +7 (383) 330-86-49
http://www.sibran.ru e-mail: psb@sibran.ru